Florian J. ARBEITER

Dissertation

“Ninety percent of most magic merely
consists of knowing one extra fact.”

- Sir Terence David John "Terry" Pratchett, OBE, *Night Watch*

Florian J. ARBEITER

Dissertation

Evaluation of long-term properties of polymeric pipe grade materials using fatigue tests and fracture mechanics

August 2015

Institute of Materials Science and Testing of Polymers
Department Polymer Engineering and Science, Montanuniversitaet Leoben

About the Dissertation

This cumulative Dissertation was authored by

DI Florian Josef Arbeiter
born 05. January 1988
in Linz (Oberösterreich, Austria)

Conducted at

Institute of Materials Science and Testing of Polymers
Department Polymer Engineering and Science
Montanuniversitaet Leoben

Submitted to

Institute of Materials Science and Testing of Polymers
Department Polymer Engineering and Science
Montanuniversitaet Leoben

Academic Supervisor

Univ.-Prof. Dr. Gerald PINTER
Chair of Materials Science and Testing of Polymers
Department Polymer Engineering and Science
Montanuniversitaet Leoben

Part I.

Preamble

Affidavit

I declare in lieu of oath, that I wrote this thesis and performed the associated research myself, using only literature cited in this volume.

Florian J. Arbeiter

Leoben, August 2015

Acknowledgement

I would like to use this chance to express my appreciation and gratitude to all persons who helped and inspired me during the course of this thesis.

Foremost, I thank my supervisor Univ.-Prof. Dr. Gerald PINTER (Institute of Materials Science and Testing of Polymers, Department Polymer Engineering and Science, Montanuniversitaet Leoben) for the chance to perform this thesis at his institute. Thanks to his support and guidance working on this thesis went along quite smoothly. I would also like to express my gratitude for all the scientific discussions and support. I'm also thankful for the chances to visit interesting conferences and Gerald's help to eventually join the scientific community.

Special thanks also go to Dr. Andreas FRANK (Polymer Competence Center Leoben GmbH) who was always willing to discuss results and theories. Furthermore, he was also kind enough to share his knowledge in the area of the cracked round bar test and experimental procedures which was crucial for this thesis.

I would also like to thank Dr. Alicia SALAZAR (Grupo de Durabilidad e Integridad Mecánica de Materiales Estructurales, Universidad Rey Juan Carlos) who got me interested in the thrilling world of notching procedures and their influence on the micro-mechanical fracture behaviour of polymers.

It is also very important to me, to thank my colleagues at the institute, who accompanied me on this interesting and challenging journey. I would like to especially thank my office colleagues Dr. Julia MAIER and Jürgen GROSSER, who managed to keep my shenanigans to a minimum. I would also like to thank Dr. Steffen STELZER, DI Peter GUTTMANN, DI Alexander

MAIER, DI Wolfgang ZIEGLER, DI Katharina BRUCKMOSER, DI Andrea KLEIN and Mag. Andreas POMPENIG for the interesting scientific and private conversations. Overall, I would like to thank the whole Institute for the warm and almost family like atmosphere during the last years, which eased potential difficulties immensely.

During the time of this thesis I also had the immense pleasure of guiding two academic works. Hereby I would also like to thank Silvia BRUNBAUER and Manuel SCHWAB who helped me not only covering certain scientific topics, but also were kind enough to provide me with my first experience in leading young researchers.

Last but not least, I would like to express my deepest gratitude to my family. Without the support of my parents, Christa and Josef, and my sister Michaela I would not be who and where I am today. Their unconditional love and support during the last years encouraged me to take risks and strive for more and more challenging tasks.

Kurzfassung

Zur Sicherstellung von Langlebigkeit und Langzeiteigenschaften von Rohrleitungssystemen aus polymeren Werkstoffen existieren strenge und umfassende Regelwerke. Rohre aus Kunststoff müssen mindestens 50, oft 100 Jahre Lebensdauer in ihren Anwendungsgebieten garantieren können. Da es nicht zweckmäßig wäre diese Lebensdauern unter realen Anwendungen zu überprüfen, ist es notwendig beschleunigte aber aussagekräftige Prüfverfahren für diese Materialien zu entwickeln. Aufgrund stetiger Verbesserungen in der Materialqualität im Laufe der letzten Jahre, können klassische, etablierte Methoden nur noch bedingt eingesetzt werden um Eigenschaften zu charakterisieren. Eine neu entwickelte und vielversprechende Methode ist der zyklische „Cracked Round Bar“ Versuch, der sich derzeit im letzten Stadium der ISO-Standardisierung für Polyethylen-Rohrwerkstoffe im Gas- und Wasserbereich befindet. Für andere Kunststoffe im Rohrbereich, wie Polypropylen oder Polyamid, werden nun ebenfalls neue, schnellere und selektive Prüfmethoden benötigt.

Im Zuge dieser Arbeit konnte gezeigt werden, dass der oben erwähnte, auf bruchmechanischen Methoden basierende und für PE entwickelte zyklische Test prinzipiell auch auf andere Kunststoffe in Rohranwendungen, wie Polypropylen, Polyvinylchlorid, Polyamid und Polybutylen, anwendbar ist. Speziell für Polypropylen, das sehr vielseitig eingesetzt wird (mit oder ohne Innendruck, Raumtemperatur oder bei erhöhter Einsatztemperatur) brachte der Test interessante Ergebnisse. Bei Untersuchungen unter verschiedenen Last- und Temperaturbedingungen zeigte sich, dass für das Ermüdungsverhalten von PP vor allem die Rissinitiierungs-Phase von enormer Bedeutung ist. Da diese bis zu 80% der Gesamtversagensdauer der Versuche ausmachte, wurde auch der Kerbprozess selbst untersucht.

Zusätzlich wurde auch der Einfluss von Verstärkungsstoffen und der Material-Morphologie auf die Ergebnisse untersucht. Dabei konnten im konkreten Fall die Unterschiede zwischen Block-, Random-, und Homopolymer belegt werden.

Es konnte weiters gezeigt werden, dass der Test nicht nur großes Potential für die Differenzierung von Materialien, sondern auch verschiedener Versagensmechanismen besitzt. Bei Kurzzeitprüfungen unter hohen Lasten wurden Materialien im duktilen Versagensbereich innerhalb weniger Stunden bis Tage untersucht und verglichen. Im Versagensbereich unter niedrigeren Lasten, der oft als „quasi-spröd“ bezeichnet wird, konnten Materialien innerhalb weniger Tage bis Wochen gegenübergestellt werden. Im Vergleich zu klassischen Prüfmethoden, bei denen selbst nach mehr als 10.000 Stunden keine Unterscheidung möglich ist, zeigt sich eindeutig das große Potential dieser Prüfmethode für die untersuchten Werkstoffe. Zusätzlich zu den technologischen Versagenskurven, wurden weitergehend Bruchflächen, Hysterese-Entwicklungen und Nachgiebigkeitsverläufe zur genaueren Untersuchung der Versagensmechanismen der einzelnen Materialien herangezogen.

Neben mechanischer Belastung, kann es bei Rohrwerkstoffen auch aufgrund der extrem langen Anwendungszeiträume zu Alterungsprozessen und Materialabbau, und damit zu Einschränkungen in der Lebensdauer kommen. Zur Charakterisierung des Einflusses von physikalischer und chemischer Alterung auf Materialeigenschaften wurde ein Material künstlich beschleunigt gealtert. Es konnte gezeigt werden, dass durch die Kombination primärer und sekundärer Antioxidantien chemische Alterungsprozesse über die gesamte Auslagerungsdauer von mehr als 18 Monaten bei 80°C verhindert wurden. Die Untersuchungen ergaben ebenfalls, dass durch die künstliche Alterung Prozesse stattfinden, die unter realen Bedingungen nicht auftreten. Konkret wurden Eigenspannungen stark abgebaut, wodurch es zu einer scheinbaren Verbesserung der untersuchten Materialeigenschaften kam. Derartige Einflüsse müssen beachtet und untersucht werden, um zu verhindern, dass sie zu nicht konservativen Ergebnissen in Lebensdauerabschätzungen führen.

Abstract

To increase the effectiveness and durability of pipe systems, there are rigorous regulations with regard to expected lifetimes. Pipe materials have to withstand at least 50, or sometimes 100 years in application. Seeing that testing under real conditions cannot be done within feasible amounts of time and due to vast improvements in quality of polymer materials over the last years, the necessity for new, faster and more selective test methods has arisen. One of these faster methods is the cyclic cracked round bar test, which is currently under ISO standardization for polyethylene pipe grade materials used in gas and water supply pipes. However, other materials, such as polypropylene or polyamide are also in dire need of faster and more selective tests, in order to remain competitive.

The newly developed cyclic method, which is based on fracture mechanics and was developed for PE only, has been applied to different polymer pipe materials, to examine the feasibility as a tool for long-term property screening. It was found, that the test can be applied to pipe materials such as polypropylene, polyvinylchloride, polyamide and polybutylene. Especially for polypropylene, which has been the focus of this thesis and is very diversely used both in pressurized and unpressurized applications, at ambient and elevated temperatures, the test showed promising results. Experiments conducted under various load and temperature conditions showed the enormous importance of the crack initiation phase during fatigue testing for PP. Initiation accounted for up to 80% of total fatigue lifetime. Therefore, influence of notching procedures has been investigated. Additionally, the influences of reinforcement and morphology have been investigated in depth during this study. Specifically, the differences in properties of polypropylene block-, random-, and homopolymer were investigated.

It showed that the cyclic cracked round bar test possesses vast potential to rank materials in the different failure modes. For example, in the short term failure region materials can be compared within hours to days of testing. Even long-term failure, which is referred to as “quasi-brittle”, could be achieved for most materials within days or weeks of testing. Compared to more than 10,000 hours of testing using classical methods, this is an enormous improvement. Fracture surfaces, hysteresis analysis and compliance development have also been used to further investigate the specific damage mechanisms of individual materials.

Besides mechanical failure mechanisms, also ageing of the material can play a major role with regard to the lifetime of pipe systems made from polymers. To characterize the influence of physical and chemical ageing, one of the examined polypropylene materials, has been investigated after severe artificially accelerated ageing at elevated temperatures. It was found, that the used combination of primary and secondary antioxidants could delay chemical ageing over a period of more than 18 months at 80°C. Results of the ageing study also clearly showed that additional physical processes which only occur due to the accelerated ageing itself can significantly influence material performance. In this case, annealing lead to a significant decrease in residual stress in the material. Due to this decrease, fracture mechanical properties seemingly improved with ageing time. However, this physical ageing process does not occur in real application, and could lead to non-conservative results in lifetime estimations if ignored.

Contents

Part II.

Introduction and motivation of the thesis

1. Motivation and background

1.1. Polymer pipes as an essential economic and ecological factor in infrastructural applications

Providing stable and reliable infrastructure is now more important than ever. With a fast growing population around the globe and cities which increase its size by the day, more and more building sites have to be opened up. To supply new sites with its necessities, such as water, gas or electricity, dynamic and versatile solutions are necessary. Due to the broad spectrum of applications, polymer pipes have been on the rise for decades now, without signs of slowing down.

In Germany alone more than 50,000 km of new pipes were installed in public domain between 2009 and 2013 and more than 40% of these pipes were made from polymers [1]. In Austria, a quite small country in comparison, more than 50 billion € were spent on the rejuvenation and extension of sewer and water transportation within the last 50 years [2]. Furthermore, annual growth of polymer pipes is expected to be in the double digits over the next years [3]. Also the polymer pipe and its support industry are expected to reach global sales turnover of more than 500 billion USD until 2024 [3].

Besides impressive numbers from economical aspects, polymer pipes can also contribute to ecological aspects in infrastructural applications. Over the last years, ecological conscience has arrived at a point, where also usable and clean water is seen as a valuable natural resource. All the more shocking, that 10 to 15% of water loss is still considered as normal business practice for new pipe systems [4]. Leakage, which is mainly responsible for this vast amount of water loss, can also impair the effectiveness of other pipe systems, such as storm water, drainage or sewer pipes. When sewer pipes are affected, the issue of groundwater pollution can arise [5,6]. Therefore, not

only the question of costs for repair or renewal arises, but also the impact on the environment and health has to be considered.

To avoid leakage of valuable resources or of waste polluting groundwater, it is necessary to keep pipe system failures to a minimum. Assuming a “bathtub-curve” like failure behaviour, as is common for many engineering applications, consisting of the “early failure period”, the “intrinsic failure period” and the “wear out failure period”, it is quite obvious that especially the last part is of high interest with regard to durability of pipe systems. Whereas failure in the “early failure period” is commonly detected immediately, for example during pressure testing after trenching, the wear-out failure period could go unnoticed for quite some time. In the case of pressurized systems, small cracks could be disregarded, since a certain amount of pressure drop is always experienced in these systems. Nevertheless, leakage would occur, which decreases the effectiveness of the system. In the case of unpressurized sewer pipe systems, failures are usually only detected via camera-inspections or if the damage caused by the failure is already affecting the bordering environment. Therefore, it is important to precisely know the long-term properties and lifetimes which can be expected before failure, to keep costs and damages to a minimum and set correct intervals for pipe systems repair and rejuvenation.

Emanating from aforementioned points, durable and leakage minimized pipe systems are of highest interest to grid operators, city councils and in the long run whole governments and countries.

1.2. Lifetime assessment of polymer pipe materials

The subject of assessing lifetimes of polymer pipes has been a topic of interest for many years now. However, to assess the whole lifetime of pipe systems which spans several decades, accelerated testing methods are necessary. There are several methodologies described in literature on this topic. Most of them are either based on activation energy calculations [7,8], fracture mechanical methods or a combination of both, to induce accelerated slow crack growth [8–12]. Holistic approaches have been made available in the last years, by combining these approaches with finite element analysis. Using this combination, it is now not only possible to characterize the base

materials which are used, but actually whole pipe systems, including residual stress from processing, branching symmetries in grid systems, point loads from trenching, etc.

A detailed description of polymer pipe failures and fracture mechanical approaches for lifetime estimation is given in Part III. Further work presented in this thesis can be seen as an extension starting from the state of the art presented there.

1.3. Pushing established concepts to new frontiers

Seeing, that most traditional concepts for polymer pipe lifetime assessment are not feasible any longer, aforementioned accelerated methods are necessary. However, most of the concepts which were developed over the last years have only been applied to water or gas transportation pipes, which are mainly made from polyethylene (PE). Due to high pressures of up to 10 bar in these applications and associated safety requirements, the immediate need for these models is self-explanatory. Nevertheless, seeing as PE covers only about 28 to 45% (depending on region) of polymer pipe demands [13] there is still a vast field of applications where no such holistic models for lifetime estimations are available. Whilst there is still work to be done in the field of PE pipes, for example in the area of the influence of exact specimen preparation, it is past time to additionally focus on other polymeric pipe materials as well.

For example, there have been interesting developments in the field of polypropylene (PP). The appearance of 2nd generation random-PP (PP-R) has led to a similar problem compared to very tough PE pipe grades. Pipes made from this material show no brittle fracture in classical ISO 9080 tests [14] at any temperatures. While this testifies to the extraordinary properties of the material it also implies, that these materials cannot be compared to each other using this test method. Another example of new arising pipe applications is the discussion about using polyamide for high pressure gas applications at 16 bar [15]. Whereas higher pressure levels would allow for a better performance, there is nowhere near as much experience using this material in pipe applications, compared to PE or PP.

While the list of reasons continues the dire need for newer and faster test methods and possibilities to assess lifetimes or long-term properties of these materials is already obvious. Therefore, the clear aim of this thesis is to develop feasible methods for long-term property material characterization of both established pipe materials, as well as materials for new and emerging applications.

1.4. References

[1] Kunststoffrohrverband e.V. Jahresbericht 2014. Bonn; 2014.

[2] Bundesministerium für Land- und Forstwirtschaft, Umwelt und Wasserwirtschaft. Vorsorgen!: Für den Erhalt unserer Trinkwasser- und Abwassernetze; 2014.

[3] The European Plastic Pipes & Fittings Association. DOUBLE DIGIT GROWTH EXPECTED IN GLOBAL PLASTIC PIPE MARKET. Press Release. Brussels; 2014.

[4] Plastics Pipe Institute. Spotlight on water conservation. Irving, TX; 2014.

[5] Eiswirth M, Hötzl H. The impact of leaking sewers on urban groundwater.

[6] Wolf L, Held I, Eiswirth† M, Hötzl H. Impact of Leaky Sewers on Groundwater Quality. Acta hydrochim. hydrobiol. 2004;32:361–73.

[7] Hoàng EM, Lowe D. Lifetime prediction of a blue PE100 water pipe. Polymer Degradation and Stability 2008;93:1496–503.

[8] Brown N. Intrinsic lifetime of polyethylene pipelines. Polym. Eng. Sci. 2007;47:477–80.

[9] Pinter G, Arbeiter F, Berger I, Frank A. Correlation of Fracture Mechanics Based Lifetime Prediction and Internal Pipe Pressure Tests. In: Proceedings Plastic Pipes XVII 2014; 2014.

[10] Chudnovsky A, Zhou Z, Zhang H, Sehanobish K. Lifetime assessment of engineering thermoplastics. International Journal of Engineering Science 2012;59:108–39.

[11] Hutař P, Ševčík M, Náhlík L, Pinter G, Frank A, Mitev I. A numerical methodology for lifetime estimation of HDPE pressure pipes. Engineering Fracture Mechanics 2011;78:3049–58.

[12] Pinter G, Lang RW, Haager M. A Test Concept for Lifetime Prediction of Polyethylene Pressure Pipes. Monatsh. Chem 2007;138:347–55.

[13] Ceresana Research. Market Study: Plastic Pipes; 2011.

[14] EN ISO 9080. Plastics piping and ducting systems - Determination of the long-term hydrostatic strength of thermoplastics materials in pipe form by extrapolation; 2003.

[15] Frans S, M. W. PA Pipes for 16 Bars Gas Pipelines. In: Proceedings Plastic Pipes XIV 2010; 2010.

2. Objectives

As indicated in the introduction above, estimation of long-term properties of polymer pipes is both necessary and complex. Experimental studies were mainly dedicated to the group of PP materials in order to make reasonably detailed scientific research possible. Even though polymer pipe systems may fail in different modes, focus was put on the quasi-brittle failure, which can be seen as the most critical in real application. Polypropylene was found to be much more dependent on crack initiation, compared to PE. Therefore, the respective contributions of crack initiation and propagation were examined closely. After assessing the applicability of fatigue tests as means to understand long-term properties of polymer pipe grade materials in principle, it was important to also characterize the influence of molecular structure and morphology on the fatigue behaviour. Besides mechanical loading, also ageing-mechanisms influence the overall performance of pipe systems. Therefore, depletion of stabilizers and its influence on pipe material was studied in depth.

To fulfil the aspects described above, following objectives were set as the goals of this thesis:

1. Extensive literature review, to understand the influences, pit falls and uncertainties of accelerated test methods.
2. Understanding the influence of specimen preparation.
    - Examination of the influence of different notching procedures used in fracture mechanical tests on resulting fracture

properties (e.g. razor pressing, broaching, femtolaser ablation and fatigue).

3. Applicability of accelerated test method to the materials in question.
    - Screening of materials which can be examined using this method.
    - Identification of applicable specimen dimensions, load levels, frequencies and temperature for fatigue tests.
4. In-depth fatigue tests on tough high molecular weight PP pipe materials.
    - Influence of molecular structure and morphology on the fatigue behaviour of PP
    - Impact of temperature and load level on damage initiation and propagation in PP
    - Influence of reinforcement on the fatigue behaviour of PP
    - Development of evaluation techniques to distinguish between failure modes of tough PP materials
5. Examination of the influence of stabilization and ageing on long-term properties
    - Characterization of artificially aged reinforced PP with regards to stabilizer depletion, mechanical, fracture mechanical and fatigue properties

3. Structure of the Thesis

In accordance to aforementioned motivation and objectives this thesis is divided into seven parts:

I. Preamble
II. Introduction and motivation of the thesis
III. State of the art in polyolefin pipe lifetime assessment
IV. Notching induced pre-damage in polyolefins
V. Fatigue damage behaviour of polyolefin pipe grade materials
VI. Influence of thermal ageing on the performance of reinforced pipe grade polypropylene
VII. Summary, conclusions and outlook

In the first part all mandatory sections and contents for the thesis are collected (affidavit, table of content, acknowledgement, etc.).

The second part deals with the introduction and the basic motivation for this thesis. The main objectives which act as a guide of the thesis are also stated. In the third part, which also consists of the first publication, the state of the art in polyolefin pipe lifetime assessment is presented. This chapter is used to offer an insight into relevant literature and established procedures. It also highlights the most important problems of this topic and explains the pressing necessity for further development.

Part IV deals with the influence of specimen preparation on fracture mechanics based tests. Seeing that approaches for lifetime assessment, are often based on fracture mechanics [1–11] this topic has to be addressed in

detail. As shown in literature [12–17], obtained values from fracture mechanical tests can be influenced significantly by the notching procedure itself. In order to attain valid information for lifetime calculations, it is of utmost importance to understand this influence of specimen preparation. Various notching procedures, apparatuses and their influence on fracture behaviour have been studied using linear elastic- and elastic plastic fracture mechanics. Two of the apparatuses used have also been developed and tested over the course of this thesis.

Part five deals with the fatigue behaviour of various polymeric materials which can be used in piping applications. A big focus has been put on the experimental investigation of the fatigue behaviour of different PP pipe grade materials used for non-pressure and pressure applications. Also the influence of non-organic reinforcement has been studied. For lifetime estimation of polymer pipe systems, it is essential to know the quasi-brittle failure regime of pipe grade materials, which is practically impossible to measure with established methods. Therefore, the recently for PE pipe materials developed and standardized cracked round bar test [18–21] has been studied as means to induce this type of fracture in various polymers. Besides the big focus on PP, other materials that can be interesting for pipe applications, such as poly vinyl chloride (PVC), polybutylene (PB), polyamide (PA), etc. have been studied. Whereas the test could be successfully applied to almost all materials, especially tough PP materials still pose a challenge. To further investigate these materials additional methods, such as hysteresis or compliance analysis has been used.

The sixth part of this thesis also deals with the influence of artificially accelerated ageing of reinforced PP pipe material. Since polymeric materials can degrade over time, it is important to assure sufficient material quality over time periods of 50 to 100 years in applications. Due to the inadequacy of suchlike testing times it is important to find other means for verification. To accelerate ageing, material has been stored at elevated temperatures for one and a half year. Afterwards, the aged material has been screened with regards to the most important properties for pipe applications. Thermic analysis, infrared spectroscopy and chromatography have been used to verify material and stabilizer degradation. Tensile tests, fracture mechanical

tests based on elastic plastic fracture mechanics, fatigue tests based on linear elastic fracture mechanics and residual stress have been used to study mechanical properties after ageing.

The last part of the thesis offers a short summary and conclusions of the findings in this study. Furthermore, an outlook for possible future work is presented.

3.1. References

[1] Andena L, Rink M, Frassine R, Corrieri R. A fracture mechanics approach for the prediction of the failure time of polybutene pipes. Engineering Fracture Mechanics 2009;76(18):2666–77.

[2] Frank A, Hartl AM, Pinter G, Lang RW. Validation of an accelerated fracture mechanics extrapolation tool for lifetime prediction of PE pressure pipes. In: Society of Plastics Engineers, editor. ANTEC; 2010, p. 1638–43.

[3] Frank A, Pinter G, Lang RW. Fracture Mechanics Lifetime Prediction of PE 80 and PE 100 Pipes under Complex Loading Conditions. In Proceedings Plastics Pipes XV Vancouver (Cdn) 2010.

[4] Pinter G, Arbeiter F, Berger I, Frank A. Correlation of Fracture Mechanics Based Lifetime Prediction and Internal Pipe Pressure Tests. In: Proceedings Plastic Pipes XVII 2014, Chicago; USA.

[5] Hutař P, Ševčík M, Náhlík L, Pinter G, Frank A, Mitev I. A numerical methodology for lifetime estimation of HDPE pressure pipes. Engineering Fracture Mechanics 2011;78(17):3049–58.

[6] Anderson U. Which factors controls the lifetime of plastic pipes and how can the lifetime be extrapolated. In Proceedings Plastics Pipes XI, Munich (Ger) 2001:311–20.

[7] Lang RW, Pinter G, Balika W, Haager M. A Novel Qualification Concept for Lifetime and Safety Assessment of PE Pressure Pipes for Arbitrary Installation Conditions. In: Proceedings Plastic Pipes XIII, Washington D.C; USA.

[8] Chudnovsky A, Zhou Z, Zhang H, Sehanobish K. Lifetime assessment of engineering thermoplastics. International Journal of Engineering Science 2012;59:108–39.

[9] Pinter G, Lang RW, Haager M. A Test Concept for Lifetime Prediction of Polyethylene Pressure Pipes. Monatsh. Chem 2007;138(4):347–55.

[10] Brown N. Intrinsic lifetime of polyethylene pipelines. Polym. Eng. Sci. 2007;47(4):477–80.

[11] Lang RW, Stern A, Dörner GF. Applicability and limitations of current lifetime prediction models for thermoplastics pipes under internal pressure. Die Angewandte Makromolekulare Chemie 1997(247):131–45.

[12] Lu X, Qian R, Brown N. Notchology-the effect of the notching method on the slow crack growth failure in a tough polyethylene. Journal of Materials Science 1991;26(4):881–8.

[13] Goolsby RD, Chatterjee AM. Notch sensitivity and fractography of polyolefins. Polym. Eng. Sci. 1983;23(3):117–24.

[14] Salazar A, Rodríguez J, Segovia A, Martínez AB. Relevance of the femtolaser notch sharpening to the fracture of ethylene–propylene block copolymers. European Polymer Journal 2010;46(9):1896–907.

[15] Salazar A, Rodríguez J, Martínez AB. The role of notch sharpening on the J-fracture toughness of thermoplastic polymers. Engineering Fracture Mechanics 2013;101:10–22.

[16] Salazar A, Rodríguez J, Arbeiter F, Pinter G, Martínez AB. Fracture toughness of high density polyethylene: Fatigue pre-cracking versus femtolaser, razor sharpening and broaching. Engineering Fracture Mechanics 2015.

[17] Stern A. Fracture mechanical characterization of the long-term behavior of polymers under static loads. Leoben, Montanuniv., Diss., 1995; 1995.

[18] Kratochvilla TR, Frank A, Pinter G. Determination of slow crack growth behaviour of polyethylene pressure pipes with cracked round bar test. Polymer Testing 2014;40:299–303.

[19] Frank A, Pinter G, Lang RW. Lifetime prediction of polyethylene pipes based on an accelerated extrapolation concept for creep crack growth with fatigue tests on cracked round bar specimens. In: Society of Plastics Engineers, editor. ANTEC; 2009, p. 2169–74.

[20] ISO. Polyethylene (PE) materials for piping systems — Determination of resistance to slow crack growth under cyclic loading — Cracked Round Bar test method(18489); 2015.

[21] Frank A, Lang RW, Pinter G. Accelerated Investigation of creep crack growth in polyethylene pipe grade materials by the use of fatigue tests on cracked round bar specimens: Proceedings Annual Technical Conference - ANTEC, Society of Plastics Engineers, Milwaukee, Wisconsin, USA 2008:2435–9.

Part III.

State of the art in polyolefin pipe lifetime assessment

4. Introduction to Publication 1

To assess the service lifetime of polymer pipes there are several established methods. For example, internal pressure tests have been standardized (e.g. [1,2]) and conducted for several decades. However, due to improvement in material properties, established test methods cannot deliver the desired information within feasible amounts of time anymore. Even after 10,000 hours of testing, which is the maximum testing time in tests such as internal pipe pressure test (ISO 9080 [2]) or full notch creep test (ISO 16770 [3]), there is no possibility to further distinguish between different tested materials. Therefore, newer, faster and more selective test methods are necessary.

Tests based on fracture mechanics have become the method of choice over the last years. Not only do they accelerate tests, but they also offer the possibility for actual lifetime estimation [4–7] based on Paris-Erdogan crack kinetic curves [8]. However, accelerated tests are always in danger of changing the failure mechanism compared to the actual application. Therefore, it is necessary to take into account differences between application and testing conditions, such as temperature, media, loading, etc.

As a first step before going into material testing, an extensive literature review of existing methods and their specific requirements and benefits was conducted. Since the intended method for characterization of long-term properties of materials in this thesis is based on cyclic tests, special focus was put on influences such as frequency and hysteretic heating [9–11], applied load and also the extrapolation from fatigue tests to actual pipe applications [12–16].

Besides the publication shown in the following part, several more contributions have been made by the author in this field. In order to maintain

the systematic focus of this thesis and not go too far beyond the scope, they have not been included directly, but are listed below for further inquiries:

Journal Publication: Sevcik, M.; Arbeiter, F.; Hutar, P.; Pinter, G.; Lubos, N.; “The effect of soil load on fracture behaviour of three-layer polymer pipe for non-pressurised applications”, Key engineering materials (627), 197-200, 2014 (DOI: 10.4028/www.scientific.net/KEM.627.197)

Journal Publication: Mikula, J.; Hutar, P.; Nezbedova, E.; Lach, R.; Arbeiter, F.; Sevcik, M.; Pinter, G.; Grellmann, W.; Nahlik, L.; „On crack propagation in the welded polyolefin pipes with and without the presence of weld beads”, Materials & Design (87), 95-104, 2015 (DOI: 10.1016/j.matdes.2015.07.131)

Conference contribution: Pinter, G.; Arbeiter, F.; Berger, I.; Frank, A.; “Correlation of Fracture Mechanics Based Lifetime Prediction and Internal Pipe Pressure Tests”, in Proceedings Plastic Pipes XVII, Chicago, USA, 2014

Conference contribution: Arbeiter, F.; Berer, M.; Pinter, G.; Frank, A.; “Linear elastic fracture mechanics: a useful tool for lifetime estimation of structures made from thermoplastic polymers”, Poster at 16th International Conference on Deformation, Yield and Fracture of Polymers, Kerkrade, NL, 2015

Conference contribution: Arbeiter, F.; Sevcik, M.; Hutar, P.; Pinter, G.; Frank, A.; “Definition of stress intensity factor development and determination of crack growth kinetics in multi layer polypropylene pipes”, 7th International Conference on Fracture of Polymers, Composites and Adhesives, Les Diablerets, CH, 2014

Conference contribution: Arbeiter, F.; Sevcik, M.; Hutar, P.; Feuchter, M.; Bruckmoser, K.; Pinter, G.; “Optimization of the Long-term Performance of Pipes by Multilayer Build Ups”, Polymer Processing Society Conference - PPS2015”, Graz, AUT, 2015

4.1. References

[1] ASTM International. Standard Test Method for Obtaining Hydrostatic Design Basis for Thermoplastic Pipe Materials or Pressure Design Basis for Thermoplastic Pipe Products; 2011.

[2] EN ISO 9080. Plastics piping and ducting systems - Determination of the long-term hydrostatic strength of thermoplastics materials in pipe form by extrapolation; 2003.

[3] ISO 16770. Plastics -- Determination of environmental stress cracking (ESC) of polyethylene -- Full-notch creep test (FNCT); 2004.

[4] Andena L, Rink M, Frassine R, Corrieri R. A fracture mechanics approach for the prediction of the failure time of polybutene pipes. Engineering Fracture Mechanics 2009;76:2666–77.

[5] Frank A, Pinter G, Lang RW. Fracture Mechanics Lifetime Prediction of PE 80 and PE 100 Pipes under Complex Loading Conditions. In Proceedings Plastics Pipes XV Vancouver (Cdn) 2010.

[6] Pinter G, Arbeiter F, Berger I, Frank A. Correlation of Fracture Mechanics Based Lifetime Prediction and Internal Pipe Pressure Tests. In: Proceedings Plastic Pipes XVII 2014; 2014.

[7] Lang RW, Stern A, Dörner GF. Applicability and limitations of current lifetime prediction models for thermoplastics pipes under internal pressure. Die Angewandte Makromolekulare Chemie 1997:131–45.

[8] Paris P, Erdogan F. A critical analysis of crack propagation laws. Transactions of the ASME. Journal of Basic Engineering;1963:528–34.

[9] Janssen, Roel P. M., Govaert LE, Meijer, Han E. H. An Analytical Method To Predict Fatigue Life of Thermoplastics in Uniaxial Loading: Sensitivity to Wave Type, Frequency, and Stress Amplitude. Macromolecules 2008;41:2531–40.

[10] Hertzberg RW, Manson JA, Skibo MD. Frequency sensitivity of fatigue processes in polymeric solids. Polym. Eng. Sci. 1975;15:252–60.

[11] Frank A, Redhead A, Pinter G. The influence of test frequency and eccentric crack growth on cyclic CRB tests. In: Society of Plastics

Engineers (Hg.) 2012 – 70th Annual Technical Conference, p. 1899–1904.

[12] Parsons M, Stepanov EV, Hiltner A, Baer E. Correlation of stepwise fatigue and creep slow crack growth in high density polyethylene. Journal of Materials Science 1999;34:3315–26.

[13] Zhou Z, Hiltner A, Baer E. Predicting long-term creep failure of bimodal polyethylene pipe from short-term fatigue tests. J Mater Sci 2011;46:174–82.

[14] Ayyer R, Hiltner A, Baer E. A fatigue-to-creep correlation in air for application to environmental stress cracking of polyethylene. J Mater Sci 2007;42:7004–15.

[15] Parsons M, Stepanov EV, Hiltner A, Baer E. Correlation of fatigue and creep slow crack growth in a medium density polyethylene pipe material. Journal of Materials Science 2000;35:2659–74.

[16] Pinter G, Balika W, Lang RW. A correlation of creep and fatigue crack growth in high density poly(ethylene) at various temperatures 2002;29:267–75.

5. Publication 1

5.1. Bibliographic information

- Title: Fracture mechanics methods to assess the lifetime of thermoplastic pipes
- Authors and relevant contributions to this publication:
  - Florian Arbeiter[1]
    Preparation of the publication
  - Gerald PINTER[1,3]
    Discussion and scientific guidance
  - Reinhold W. LANG[2]
    Discussion and scientific guidance
  - Andreas FRANK[3]
    Discussion and scientific guidance
- Affiliation:
  1. Institute of Materials Science and Testing of Polymers, Montanuniversitaet Leoben, Otto Glöckel-Strasse 2, 8700 Leoben, Austria
  2. Institute of Polymeric Materials and Testing, Johannes Keppler Universitaet Linz, Altenberger Straße 69, 4040 Linz, Austria
  3. Polymer Competence Center Leoben GmbH, Roseggerstr. 12, 8700 Leoben, Austria
- Book Chapter in: Deformation and Fracture Behaviour of Polymer Materials (Wolfgang Grellmann and Beate Langer (Eds.))
- Status: in press (publication early 2016)

Statement with regard to this publication: The manuscript presented here is an adapted accepted manuscript in order to fit the formatting of the thesis and does not necessarily reflect exactly the actually published version.

5.2. Failure behaviour of polymer pipes

The long-term failure of pressurized pipes made from high density polyethylene (PE-HD) can be characterized by the determination of the long-term hydrostatic strength with internal pressure tests, which is regulated in EN ISO 9080 [1] or ASTM D2837 [2]. Total testing time of pipes using this method is usually about 1 year. However, pipes that do not fail are removed from testing after a time period of 10^4 hours. This means that for modern PE types of the classification of PE 80, PE 100 and PE 100-RC (acc. to PAS 1075) almost no quantitative information concerning the long-term relevant quasi-brittle failure region can be measured as only the ductile failure regime is characterized within testing times. This presents a problem for material developers and grid operators, since no quantitative information regarding failure times of modern material grades can be determined. Therefore, new and faster testing procedures are necessary to provide this vital information.

The typical failure behaviour of PE pipes of internal pressure tests has been well investigated [3–8] and can typically be divided into three different failure regimens depending on the stress level. The regimens are illustrated in Figure 5.1 [8,9].

In Region A, at high internal pressures, the failure is dominated by ductile deformation with the formation of large plastic zones after rather short testing times. This region is mainly controlled by the yield stress of the material and failure usually occurs at the smallest wall thickness or at defects [10].

With decreasing stresses the failure mechanism passes a ductile brittle transition knee into the quasi-brittle failure (Region B), which exhibits a different slope, compared to Region A. In this region the failure is determined by a combination of crack growth initiation (CGI) and slow crack growth (SCG) with only small scale plastic deformations adjacent to the crack tip. Due to stress concentrations at small defects in the material, cracks initiate and propagate continuously through the pipe wall until failure. The failure time of the pipe is comprised of both, CGI and SCG time [8,11–13]. Slow crack growth is significantly influenced by the chemical structure of the

polymer, such as the molecular mass as well as the concentration and length of short chain branches [5,10,13–18].

The third failure Region C, where pipes fail nearly independent from the load, becomes essential after very long testing or operational times. It is the result of material aging and polymer degradation processes. The effect of global aging of the material leads to the formation of a vast quantity of cracks and small stresses may already cause brittle failure of the pipe. The resistance against failure in Region C is mainly controlled by stabilizers [4,12,19,20] which prolong the time before material deterioration.

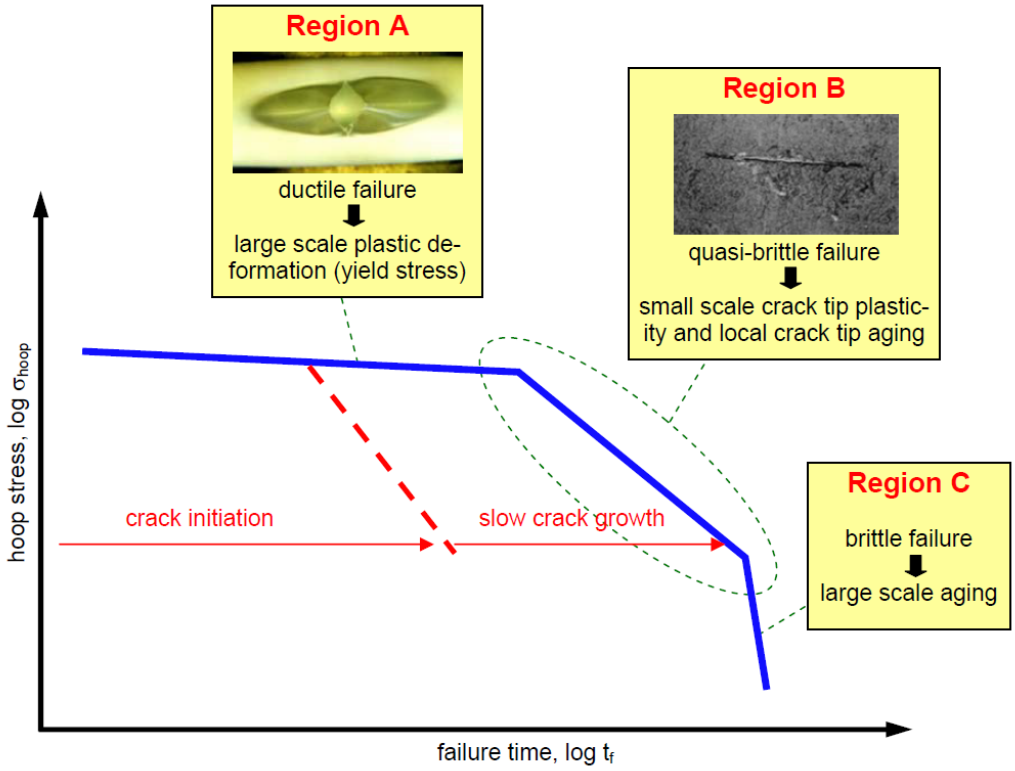

Figure 5.1: Characteristic failure behaviour Regions A, B and C of PE pressure pipes [9]

For long-term application of pressurized pipes (e.g. gas or water distribution) it is an accepted fact, that failure according to Region B is the critical failure mechanism. Slow crack growth usually starts at an initial defect located close to or at the inner pipe wall surface [11–13]. This initial defect creates a stress concentration in which micro-deformations start to nucleate micro-voids. These simultaneously originate crazes. During the formation of crazes a

combination of shearing in the amorphous phase and a transformation of the crystalline phase finally lead to highly drawn fibrils. Ensuing quasi-brittle crack growth initiates. Through the rupturing of the highly drawn fibrils a prolonged crack is formed. Simultaneously the stress at the tip of the craze zone increases initiating the formation of new micro-voids and crazes. This ongoing procedure of craze formation and breakdown of drawn fibrils is characteristic for quasi-brittle SCG and has been investigated in numerous studies [5,21–25]. Chain disentanglement and chain rupture may be assumed to have a contribution to the failure of fibrils [26,27]. Also local crack tip aging can affect the mechanisms of SCG [8,13,28,29]. Concluding that the most important failure mechanism for lifetime of thermoplastic pipes is the Region B failure, this Region has been examined closely.

Accelerated test methods, such as internal pipe pressure tests, notched pipe tests (NPT), Full-notch creep test (FNCT), Pennsylvania Edge Notch Test (PENT) etc., were developed to characterize this failure behavior. For newer materials, these tests are no longer feasible anymore. To estimate long-term behavior, faster methods are required. Consequently, alternative methods, such as the cyclic cracked round bar (CRB [30]), or the strain hardening (SH [31]) test have emerged as promising methodologies to rank materials in regard to their resistance against SCG.

Besides quality control and ranking of materials it is of high interest to estimate actual lifetimes of pipes under application conditions, to schedule service or replacement intervals. For this goal, fracture mechanical concepts such as the linear elastic fracture mechanic (LEFM), on which also aforementioned ranking tests like NPT, FNCT, PENT and CRB are based, provide promising prospects.

5.3. Fracture mechanics approach for pipe lifetime calculations

The LEFM approach used to estimate lifetimes of PE pipe systems is explained in the following chapter. Alongside, chapter 3 provides the necessary material specific limitations which have to be considered when using LEFM with thermoplastic pipe grade materials.

The basic idea behind this approach is to use material specific constants, which can be measured with rather simple experiments, in combination with crack propagation laws based on the stress intensity factor K_I [32] to describe the advance of a crack through any arbitrary structure. A well-known crack propagation law in LEFM is the approach described by Paris and Erdogan in 1963 for cyclic loads [33] and is shown in Equation 5.1, adapted for a static loading case. Even though A and m are material constants, they are dependent on the loading situation and temperature. They have to be measured for the respective loading case and environmental conditions of the actual application. Buried PE-pipes are mainly subjected to static internal pressure. Therefore, A and m are measured using fracture mechanics specimens under static loading. Due to the principle of crack tip similitude they can then be used for other structures made from the same material subjected to the same loading conditions. For this situation, Equation 5.1 can be applied, where K_I is the stress intensity factor of the examined structure and da/dt the crack extension over a period of time.

$$\frac{da}{dt} = AK_I^m \tag{5.1}$$

By Integration of this crack propagation law, failure times due to SCG can be estimated. The stress intensity factor K_I used in Equation 5.1 is mainly dependent on the applied stress (σ_I) and the actual crack length (a) (compare Equation 5.2). Since cracks propagate during the lifetime of pipes, the respective values of K_I have to be calculated for each crack length during lifetime. For simple cases, the development of K_I as a function of crack length a and remaining ligament (f(a/W)) can be derived via analytical analysis (e.g. [34]). More complex situations or geometries require finite element analysis (FEA) to determine the respective stress field adjacent to the crack tip ([35,36] et. seq.).

$$K_I = \sigma\sqrt{a}f\left(\frac{a}{W}\right) \tag{5.2}$$

A schematic illustration of the relationship between crack length a_1 to a_3 in an internally pressurized pipe and the development of K_I is depicted in Figure 5.2. It can be seen, that K_I usually increases with advances in crack growth through the pipe wall (a/W).

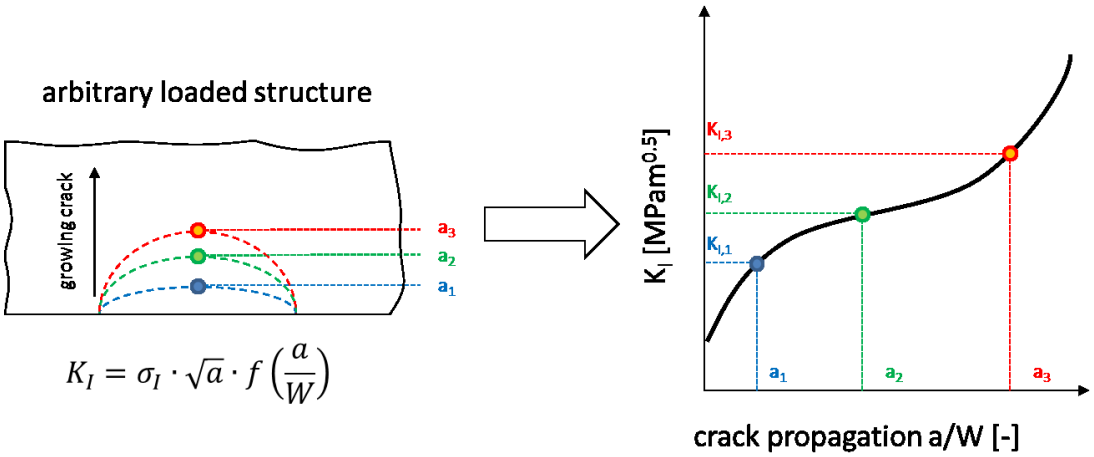

Figure 5.2: Relation between growing crack length in an arbitrary loaded structure and resulting K_I-values

Subsequently, the time for a crack to grow through a component can be calculated by re-arranging Equation 5.1 to the form shown in Equation 5.3. The slow crack growth time (t_{SCG}) is expressed as a function of the parameters A and m, the load dependent stress intensity factor K_I of the structure and the distance of the growing crack in the component starting from the initial crack length a_{ini} to the final crack length a_f.

$$t_{SCG} = \frac{1}{A}\int_{a_{ini}}^{a_f} \frac{1}{K_I^m} da \tag{5.3}$$

The total amount of time to failure t_f consists of t_{SCG} and also of the time to crack initiation t_{ini} which can be approximated for PE by the formula given in Equation 5.4 [12], where B and n are again material constants, which are dependent on the test conditions such as temperature, pre-notching or environment [12,37]. Therefore, the total amount of time to fracture can be summarised as stated in Equation 5.5 [37].

$$t_{ini} = BK_{I,ini}^{-n} \tag{5.4}$$

$$t_f = t_{ini} + t_{SCG} = BK_{I,ini}^{-n} + \frac{1}{A}\int_{a_{ini}}^{a_f} \frac{1}{K_I^m} da \tag{5.5}$$

Using this approach, it is possible to estimate lifetimes of pipes as long as the application and loading situation of the pipe, the development of K_I as a function of crack length and the material constants A, m, B and n are known.

The development of K_I as a function of a growing crack in a pipe wall is important for correct estimation of failure times. Literature provides different solutions of K_I under internal pressure [34,38,39]. Also FEA can be applied to estimate K_I. In Figure 5.3 a comparison between different solutions from literature and from FEA is shown. The calculations for the FEA solutions were performed for a semi-elliptical surface crack with the width (b) of the crack being twice as long as the depth (a) [12]. The formulations proposed by Anderson and Murakami converge with results of FEA. However, the solution proposed my Krishnamachari delivers significantly different results.

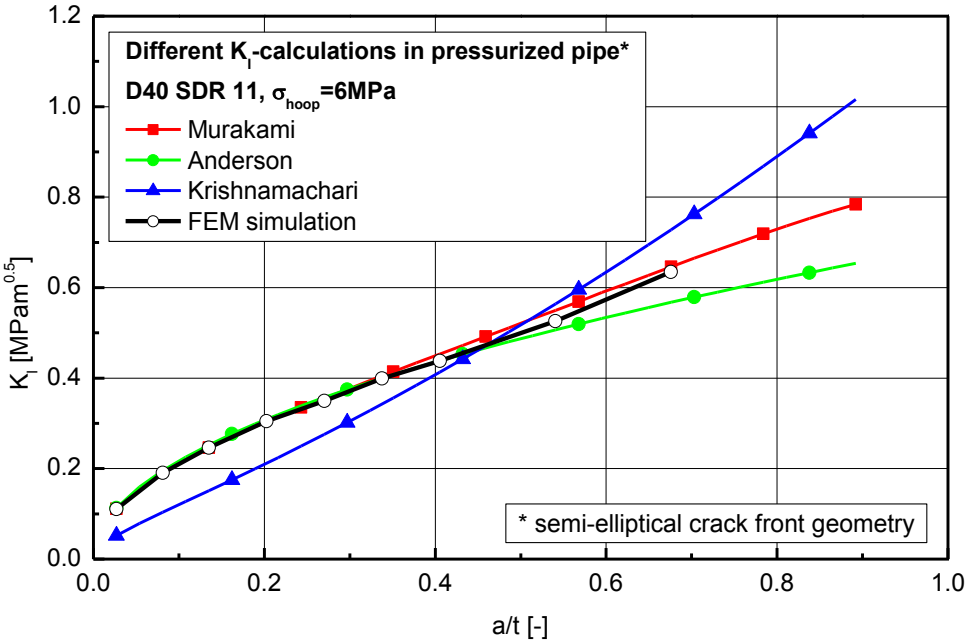

Figure 5.3: Differences in stress intensity factor development of a crack growing through the pipe wall of an internal pressurized pipe with a semi-elliptical crack front [40,41].

For correct estimation of K_I during a test, not only changes in crack length but also in the actual shape of the crack, which might change the stress field significantly, has to be considered [42–47]. As an example, the difference between a semi-circular and a semi-elliptical crack front is shown in Figure 5.4 [40]. Even though both cracks have the same initial crack length (a_{ini}), stress distribution around the crack differs quite significantly. For the semi-elliptical crack shape, K_I in point A is significantly higher compared to point C_e which results in a shift to a semi-circular crack front as the crack

advances through the pipe wall [13]. If the crack starts out with a semi-circular crack front, K_I is only slightly higher in point C_c than in A. Therefore there is only a small tendency of the crack to change the crack front geometry to a semi-elliptical shape.

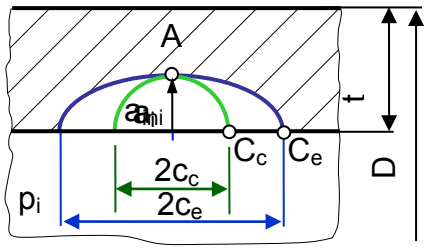

t…….. pipe wall thickness
D……... pipe diameter
a_{ini}…….. initial crack length
$2c_e$, $2c_c$……. crack width

Figure 5.4: Difference between semi-elliptical and semi-circular crack front for the same initial crack length aini in an internal pressurized pipe [40].

Due to the discontinuous crack growth in PE, which consists of a continuous formation of crazes with highly oriented fibrils at the crack tip and their stepwise breakdown [11,13,48–51] it is possible to estimate crack front shapes at various testing times from striations on fracture surfaces. In Figure 5.5 a pipe, which fractured during internal pressure testing, with changing front shape from a semi-circular to a semi-elliptical crack can be seen [40].

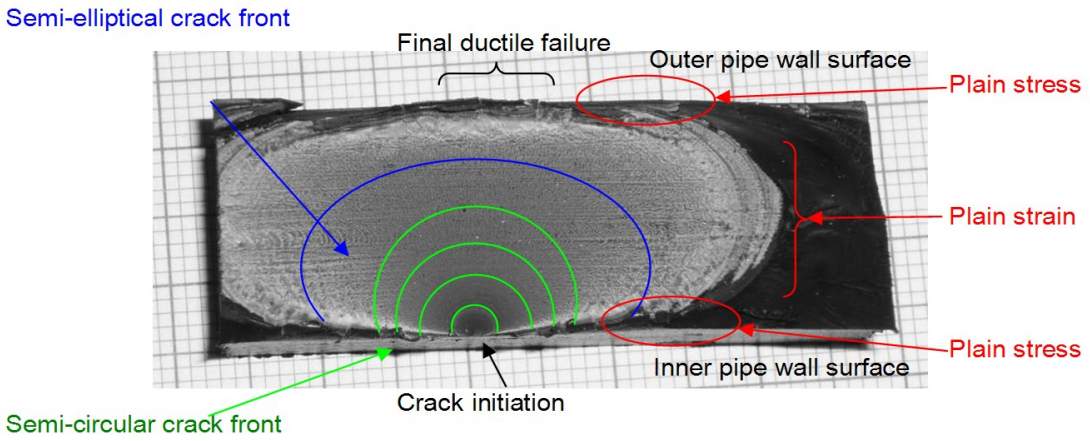

Figure 5.5: Fracture surface of an internal pressure test with a changing crack front shape from semi-circular to semi-elliptical [40].

Therefore, changes in crack front shape have to be taken into account, when calculating stress intensity factor development for lifetime extrapolation. FEA has proven to be a valid tool in this endeavour, especially since additional influences of outside loads [52] or residual stresses in the material can be included [44].

5.3.1. Crack Growth in polyethylene

When using a lifetime concept based on LEFM, applicability and general limitations of the used material have to be verified. The following chapter focuses on the behavioural details and restrictions of CGI and SCG in polyethylene under similar conditions as in pressurized pipes.

Slow crack growth in polyethylene usually starts due to stress concentrations (e.g. around inclusions, defects, material-inhomogeneity, etc.) or in the case of fracture mechanical tests around notches. Stress concentrations lead to the formation of small plastic zones, which are characterized by the typical properties of crazes in PE [23,53]. Due to local flow in the amorphous area of the polymer, small voids are created which start to grow, coalesce and form fibrils. Initial crazes start to grow under stress by dragging neighbouring uninfluenced material into the process zone and by disentanglement of tie-molecules between lamellas. Local creep processes can also influence craze formation and propagation (e.g.[54]). As soon as first fibrils start to fracture, CGI followed by SCG takes place. The process of SCG is mainly governed by disentanglement of tie-molecules [13] and up to a certain amount by fracture of covalent bounds [55]. After first crack initiation and propagation the crack starts to grow by further formation and breakdown of fibrillated zones in front of the crack tip. In PE pipe materials this failure occurs in a step-wise mode, which leads to the formation of discernible markings on the fracture surface of test specimens. These striations were reported for test specimens under constant [13,56–58] and fatigue load [48,51,56,59–65], as well as internally pressurized pipes [13,40,58]. However, this seemingly rather simple process of build-up and break down of material in front of a crack tip is dependent on different aspects which have to be addressed before lifetime estimations can be performed.

Methods based on LEFM are restricted to linear elastic or linear elastic material including small scale yielding [32,66]. It was found for polymeric

materials that the global loading situation also has to be within the region of linear-viscoelasticity [24]. For PE used in pressurized pipes, this level is usually surpassed [37]. Nevertheless, several authors have successfully shown that failure by SCG in PE pipe materials and several other polymers can be described using LEFM (e.g. [13,15–17,56,57,67–74]). The group around Brown and Lu was among the first to thoroughly investigate this specific topic from different angles. Influences, such as the transition between ductile and SCG failure [75,76] as well as the main parameters that govern SCG in polyethylene, like molecular weight [77], density of side branches in copolymers [78,79], notching [80], stress cracking agents [81] and test temperature and morphology [82] were addressed. Nevertheless, by using the concept of LEFM for lifetime estimations, several simplifications or assumptions have to be made. For example, the size and shape of intrinsic defects in the pipe wall influences calculated lifetimes significantly [12,37,40]. A study of fractured pipes from internal pipe pressure tests provided a range between 100 to 400 µm for initial crack length [83]. This margin signifies differences of more than a decade of years for calculated lifetimes. Furthermore, fracture mechanical tests are usually performed at much higher initial K_I values compared to pipes. The power-law correlation between crack kinetic and applied stress level found in experiments is then simply extrapolated to lower values, neglecting changes of the relation due to short-crack effects or a possible threshold value [37]. Also material deterioration, which is significantly enhanced close to crack tips can influence the behaviour of SCG in PE [19] which is not addressed in a classical LEFM calculation.

Remarkable advances in material development over the last decades also lead to modern PE pipe materials with significantly improved resistance to SCG. While opening up new possibilities for pipe manufacturers and grid operators in regards to service time and applied pressure levels in pipe systems it poses a great challenge for material testing and lifetime estimations using a LEFM approach. The high resistance to SCG has made it virtually impossible to measure the necessary material parameters (e.g. A and m for SCG) without either invalidating the requirements of LEFM, testing at highly elevated temperatures which are far from actual application, using stress cracking agents or resulting in testing times of several years. To

accelerate tests without using chemicals or going to elevated temperatures, several authors suggested using cyclic instead of static loads. This proposition was supported by good correlations between results from cyclic- and static tests [11,18,24,48,61–65,72,73,84,85]. By changing the load situation during tests, material constants used for the LEFM approach do not describe the same process as in a pipe under static load. Therefore, they cannot directly be used for lifetime estimation. To calculate correct CGI and SCG times, material parameters have to be extrapolated to the loading case of the actual application. Additional influences of the cyclic loading also have to be examined in order to produce valid results.

5.3.2. Extrapolation to static crack growth behaviour from fatigue tests

The basic idea behind this procedure is to calculate synthetic creep crack growth (CCG) curves from tests at different loading conditions (R-ratio = $\sigma_{min}/\sigma_{max}$) with short term tests and extrapolate to a static loading case which would require considerably longer testing times. This approach has been investigated by several authors for PE [48,56,86–90] over the last years. Even though different focuses and approaches were chosen in the respective works, authors agree in general that an extrapolation to a static loading case from fatigue tests seems possible as long as several additional influences are considered. For example, whereas static tests are driven by CCG alone, fatigue tests are a combination of creep and fatigue crack growth with different ratios, depending on the specific test configuration. Studies have shown that fatigue tests at R-ratios close to 1 are dominated by creep crack growth than ratios close to 0 where fatigue failure mechanisms are much more dominant [48,86,87,91]. Similar results were found for the influence of testing temperature. For testing temperatures around 23°C creep crack growth was less pronounced, compared to tests at higher temperatures (e.g. 80°C) [70,86,87]. Furthermore, choice of frequency can also significantly influence results if not chosen adequately [91–94]. To account for different contributions to failure, Hertzberg et.al.[94], Wyzgoski et.al.[95] and Pegoretti [96] amongst others proposed a combination of fatigue and creep to describe crack growth behaviour of thermoplastic materials.

However, it has been shown, that for frequencies around 5 Hz or higher, the influence of creep contributions is not as significant for specimen failure in PE, as it is for rather low frequencies (<0.1 Hz) [91,97], as long as no significant hysteretic heating takes place. For PE-HD materials frequencies of up to 10 Hz at moderate loading were found to impose only minor influence in this regard [93,97]. Similar trends were found for polycarbonate [98] and glass fibre reinforced polyamide [95]. However, the contribution of creep is mainly addressed at either high R-ratios and/or rather low frequencies (mostly below 1Hz), where the pronounced creep damage contribution leads to lower cycles to failure. Frank et. al [97] tested PE-HD under the conditions of R=0.1 and frequencies between 5 and 20 Hz. In this study, only minor differences in total cycle number to failure was observed. Contrary to findings at very low frequencies, in this study higher frequencies (20 Hz) lead to a minor decrease in total cycle number, which may be attributed to some hysteretic heating in the specimen (ΔT around 7°C).

Pegoretti et.al. [96] showed in their work for glass fibre reinforced PP, that if crack growth da/dN for a constant ΔK_I (at R=0.4) is plotted as a function of different fatigue time period (=frequency^{-1}) the contribution of viscoelastic creep and amount of “true fatigue” can be estimated. For the examined material with 10 wt% glass fibre the contribution creep was about 140 times higher to failure than fatigue induced damage at 0.1 Hz. Contrary, at 10 Hz fatigue and creep were on par. Besides frequency, hysteretic heating, loading levels, etc. there have also been discussions about changes of fibrillary movement in crazes during fatigue tests due to different R-ratios. At higher R-ratios close to 1, fibrils in crazes are constantly loaded in a tensile mode for both σ_{max} and σ_{min}. For low R-ratios close to 0 a change to tensile mode at σ_{max} and bending at σ_{min} has been envisaged (compare [60,90] for PE or [99] for polystyrene). As pointed out in [86] and described above, there are several processes running simultaneously during crack propagation in PE and establishing a generalized model which accounts for all factors is still challenging.

Nevertheless, for PE-HD at reasonable temperatures it was found, that the cyclic part was dominant during fatigue tests. The transition from fatigue dominated damage at low R-ratios to the purely creep crack growth dominated failure at R=1 was found to be reflected in the micromorphology of

the fracture surfaces. In Figure 5.6 this transition is depicted for PE-HD tested at 60°C and fatigue loads with R-ratios of 0.1, 0.3, 0.5 and the static case of R=1 at K_{Imax}=0.45 $MPam^{0.5}$ and equal crack growth rates. With increasing R-ratio appearances of fractographs under fatigue load are alike those of tests under constant loads [86].

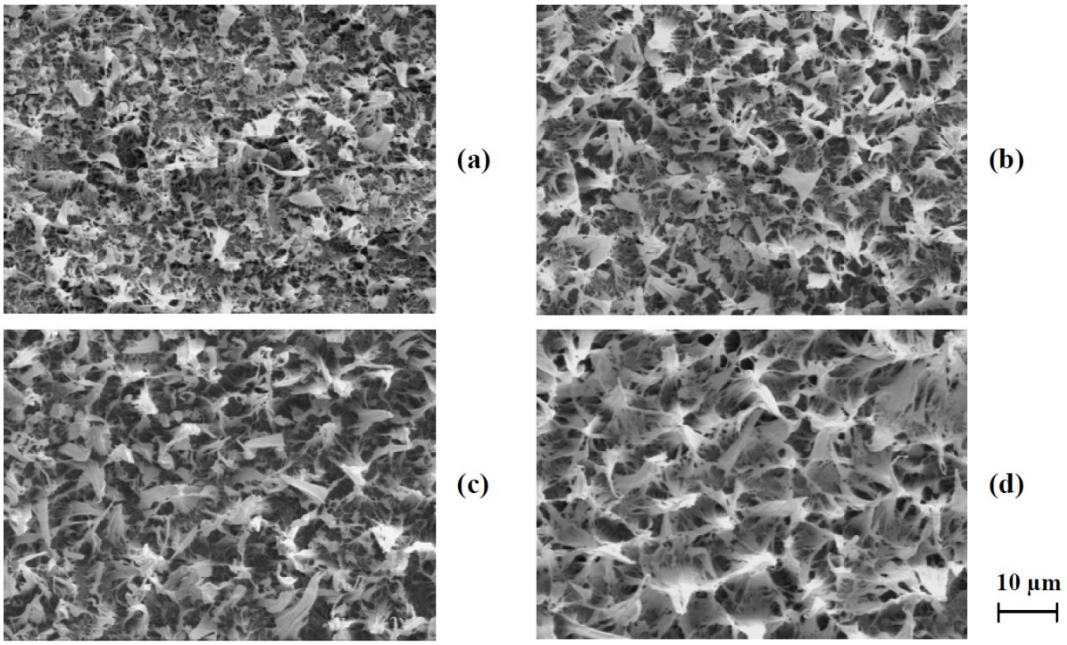

Figure 5.6: Changes in micromorphology of fracture surfaces of PE-HD tested at T=60°C and R-ratios of (a) 0.1, (b) 0.3, (c) 0.5 and (d) 1 [86]

Therefore, it seems to be an acceptable hypothesis that the variation of R-ratio, taking into account that at a testing frequency of 10 Hz the influence of frequency itself is highly reduced, can be used to extrapolate to static loading of R=1 from fatigue tests at lower R-ratios. This extrapolation procedure is depicted below in Figure 5.7.

5.3.3. Lifetime calculation of PE pipe grades

Using the approach described in the chapters above, it should be possible to calculate lifetimes for modern PE pipe systems using LEFM and fatigue tests. However, resin manufacturers have been diligently improving pipe grade materials as well. Compared to a few decades back, resistance of modern PE pipe grades has improved remarkably.

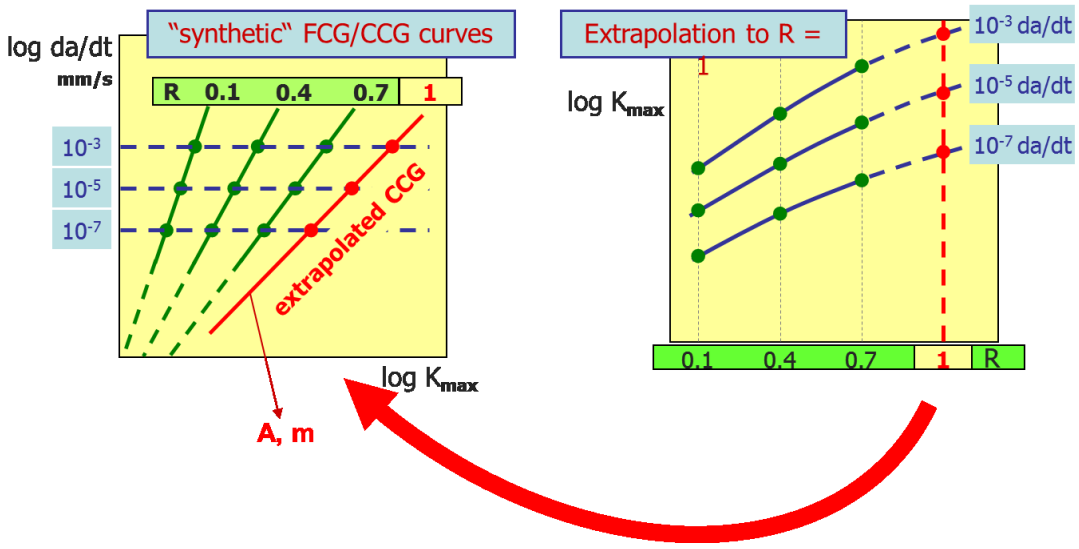

Figure 5.7: Extrapolation procedure from fatigue tests at various R-ratios to the "synthetic" creep crack growth curve under static loading of R=1 [40,100–102]

Due to the high resistance against crack growth, even with cyclic loading either long testing times have to be endured or higher loads have to be chosen. Unfortunately, due to the rather ductile behaviour of modern PE grades, plastic zones develop rather easy at higher loads (compare Equation 5.6). This inevitably invalidates the limitations of LEFM, rendering the whole method unusable. Therefore, new specimen geometries compared to the classical compact tension (CT), wedged open loading (WOL), etc. specimens have to be used, where formation of plastic zone sizes is restricted. Since the size of a plastic zone is significantly influenced by the stress state (either plane stress or strain, see Equation 5.6) specimen geometry with significant amount of plane strain would be preferable. Plane stress mainly forms at free surfaces. Therefore, a round specimen with a circumferential notch without a free surface perpendicular to the notch seems promising (Figure 5.8).

$$r_p = \frac{1}{m\pi}\frac{K_I^2}{\sigma_{ys}^2} \tag{5.6}$$

m = 1 for plane stress; 3 for plane strain [66]

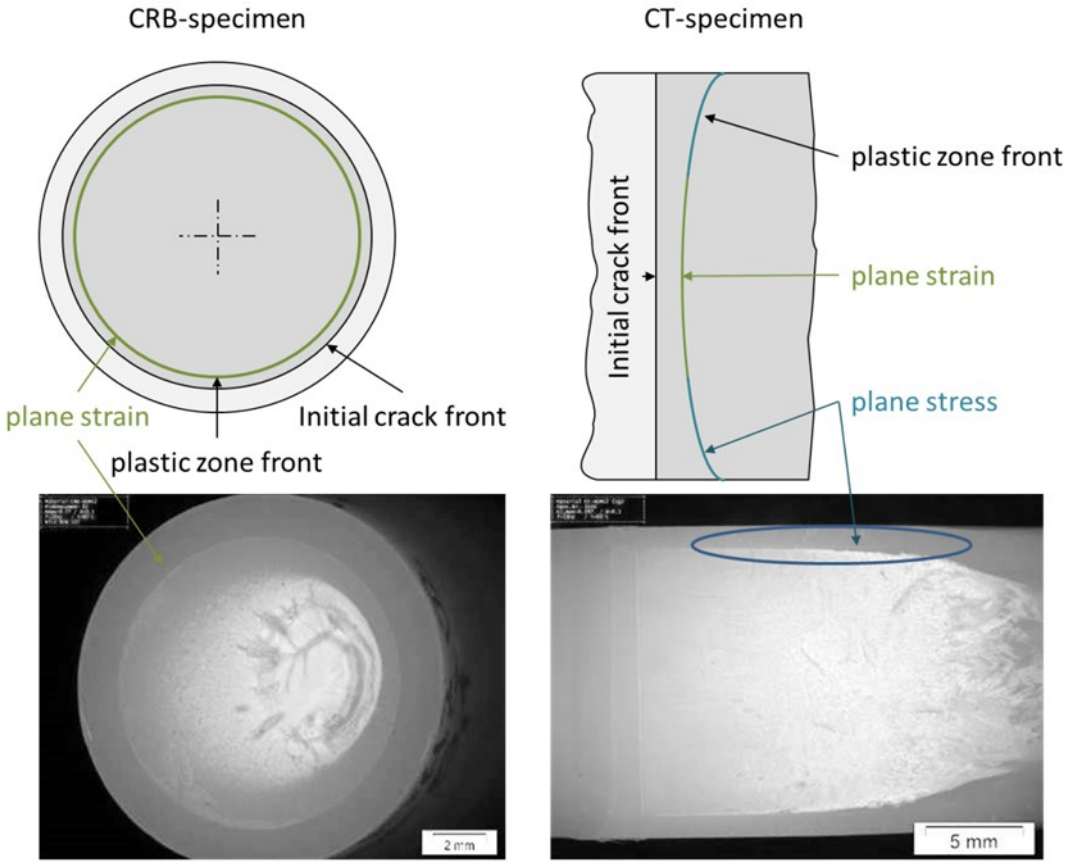

Figure 5.8: Areas of different stress states and their impact on the fracture surface of compact tension and cracked round bar specimen [103]

The impact of different stress states for crack kinetics of the same PE material tested at 80°C is shown in [103]. In this work significantly different values for crack growth kinetics for CT and CRB specimens were measured for different R-ratios which are necessary for the extrapolation to the static case. This might be an indication that for this material and chosen load levels CT specimens are not usable within the limitations of LEFM.

The downside of CRB specimens is that crack initiation and propagation cannot be monitored directly using optical methods. Therefore, a compliance calibration with pre-notched specimens and extensometers around the specimens is necessary to monitor crack kinetics. The exact procedure for this calibration is described in [89,104]. Also crack initiation can be calculated with the approach described in [105]. However, since this approach is rather

time consuming an assessment of accuracy and feasibility has to be made individually. When neglecting crack initiation times in lifetime estimations of PE pipe systems they can be seen as an additional safety margin.

5.4. Lifetime calculation of a PE pipe grade at 80°C using cyclic CRB tests

The following chapter will present PE pipe lifetime calculations as a matter of validation for the approach presented. Since failure time-data of real PE pipe systems under application conditions are scarce and not broadly available, all measurements were carried out at 80°C and compared to internal pipe pressure tests at 80°C. Contrary to classical ISO 9080 [1] tests, the pipes subjected to internal pressure were provided with sharp axial razor blade notches (a_{ini}=0.8 mm and a width of 2b=10 mm) on the inside pipe wall. This special preparation method was chosen to be able to calculate the exact K_I values at the position of CGI using FEA. Additionally, testing times are significantly shorter compared to classical ISO 9080 tests, while still producing quasi-brittle cracks.

The tested material was a commercially available PE-HD for pipe applications. As a first step, compliance calibration according to [89] was performed for CRB specimens. The data was fitted with a 2nd order polynomial for crack length calculation. The fit is shown in Figure 9. Afterwards, cyclic CRB tests were performed at several different load levels to ensure failure in quasi-brittle failure mode and to measure crack kinetics for the loading cases of R=0.1; 0.3 and 0.5 (compare Figure 5.10). The data was extrapolated to the “synthetic” CCG curve of R=1 according to [40] using a logarithmic fit.

For comparison, the same method was applied to CT-specimens. The results for crack kinetics at R=1 after extrapolation are shown in Table 5.1. The next step for the lifetime estimation is the development of the stress intensity factor K_I of the component in question. As previously mentioned and shown in Figure 5.3 FEA provides the necessary data for this step.

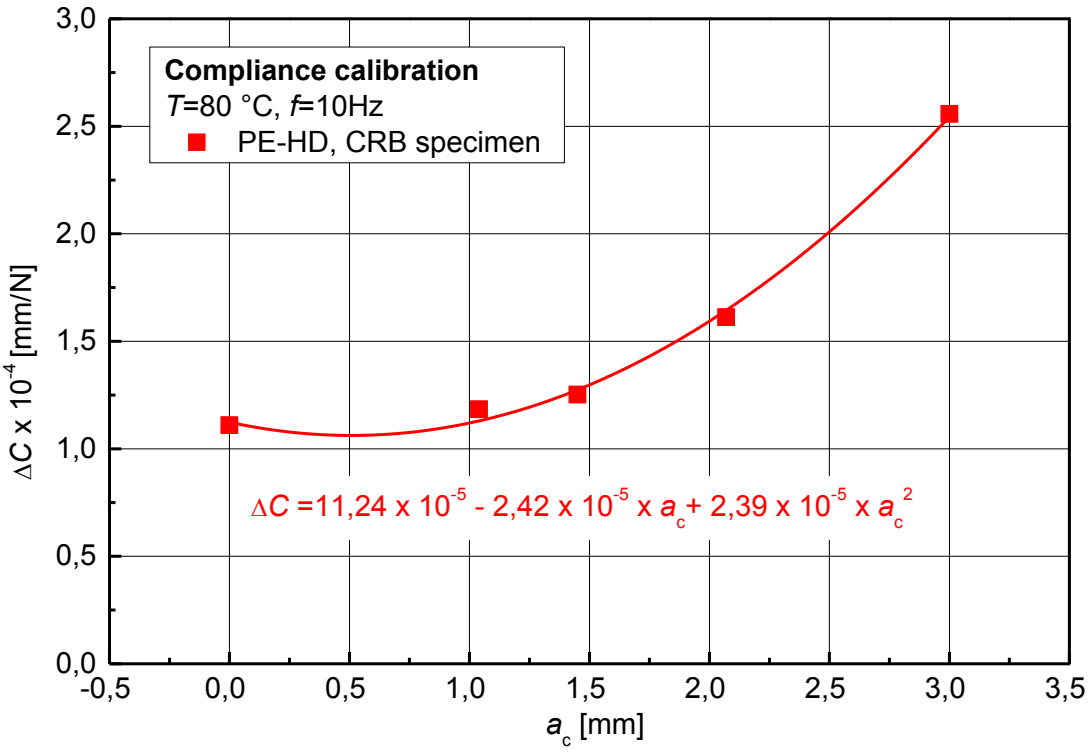

Figure 5.9: Compliance calibration curve ΔC as a function of the crack length ac for CRB specimens of the investigated PE-HD at a temperature of T=80°C [103].

Table 5.1: Fracture mechanics material parameter A and m for SCG at static loading in PE-HD at a temperature of T=80°C determined with CRB, CT and SCK specimens [103].

Specimen geometry	A	m
CRB	59.2×10^{-4}	5.8
CT	1.5×10^{-4}	4.5

Values in Table 5.1 were taken from Figure 5.10 [103]. In this diagram the big differences in crack kinetics due to different specimen configuration is shown. It is quite noticeable, that besides different slopes at K_I values the impact of the R-ratio is much less distinctive in CRB specimens compared to the classical CT specimen.

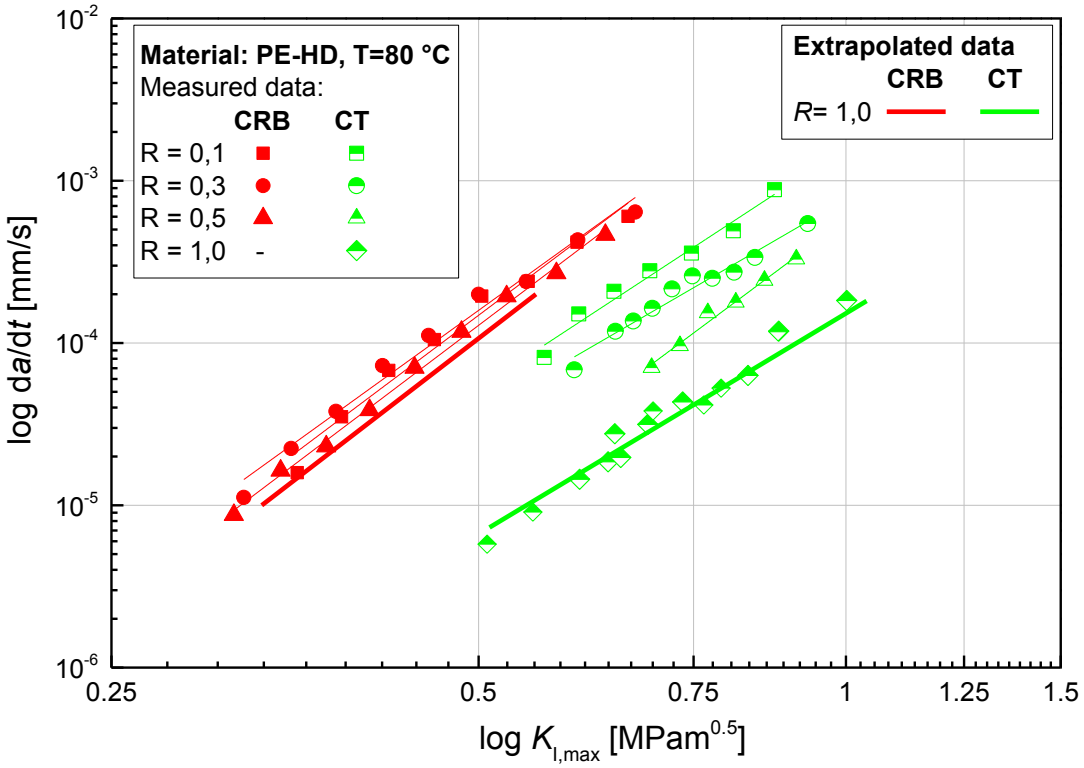

Figure 5.10: Influence of specimen geometry on crack growth kinetics [103] at different R-ratios, Data reprinted with permission of Frank et.al. 2014.

The final step, after estimation of crack growth kinetics and K_I development is the integration according to Equation 5.3. The overlap of the extrapolated data with measured crack kinetics at R=1.0 for CT-specimens generally confirmed the validity of the used extrapolation procedure [103].

From previous studies it is known, that in internal pipe pressure tests with un-notched pipes typical initial defect sizes are within the range of 100 to 400 µm [37]. As mentioned before, the broad range of initial defect sizes leads to high scatter in the results of internal pipe pressure tests. The precise pre-notching of the pipes to an initial defect size depth of a_{ini}=0.8 mm in this case resulted in a well-defined initial K_I. Due to the knowledge of the exact initial crack length a significant decrease of scatter and also a reproducible reduction of failure times was achieved [103].

Calculated lifetimes and measured lifetimes due to SCG of internal pressurized pre-notched pipes are shown in Figure 5.11. In this figure the

logarithmic failure time t_f is shown as a function of the applied hoop stress (σ_{hoop}). In the diagram a clear linear correlation between σ_{hoop} and t_f can be seen for the internally pre-notched pipes. All data points in the diagram from pipe pressure tests failed in quasi-brittle mode with cracks initiating at one of the internal pre-notches. In comparison to the included reference point from ISO 9080 it can be seen, that the lifetimes were about one decade shorter due to the internal pre-notching.

The parameters for crack growth kinetics determined via CRB specimen provide a very good correlation with real failure times. The agreement of predicted pipe lifetimes based on CRB extrapolation with experimental life times was also confirmed in several previous studies [40,106,107]. Considering, that CGI was neglected in this study for both CRB and CT specimens which would shift the curves of total lifetime to the right, it can be seen, that crack kinetics taken from CT-specimen tests tend to overestimate lifetimes of pipes. This can mainly be attributed to the formation of significant plastic zones during testing, which restrict crack growth and can undermine limits of LEFM.

5.5. Conclusion and outlook

When performing lifetime estimations using extrapolation concepts, it is vital to estimate the uncertainties which always accompany accelerated testing methods. Uncertainties may arise from deviating parameters such as changes in environmental conditions, temperature, different loading ratios, chemicals such as stress cracking agents, etc. Only when these influences are known it is justifiable to go into lifetime calculations.

Recent studies of Pinter et. al. [103] showed, that fracture mechanics extrapolation concepts for accelerated prediction of PE pressure pipes using short time fatigue tests provide valid results when compared to pre-notched internal pipe pressure tests. The use of a CRB specimen for LEFM tests improves the results compared to classical CT specimens, which tend to overestimate lifetimes. This can mainly be attributed to bigger plastic zone sizes which restrict SCG in CT specimens. Another advantage is the similarity of constraint and K_I-development between a pipe and CRB specimens. Summarising, the extrapolation concept using short term fatigue

tests on CRB specimens provides a valuable and valid tool to perform lifetime estimations for pipe systems made from PE-HD pipe materials.

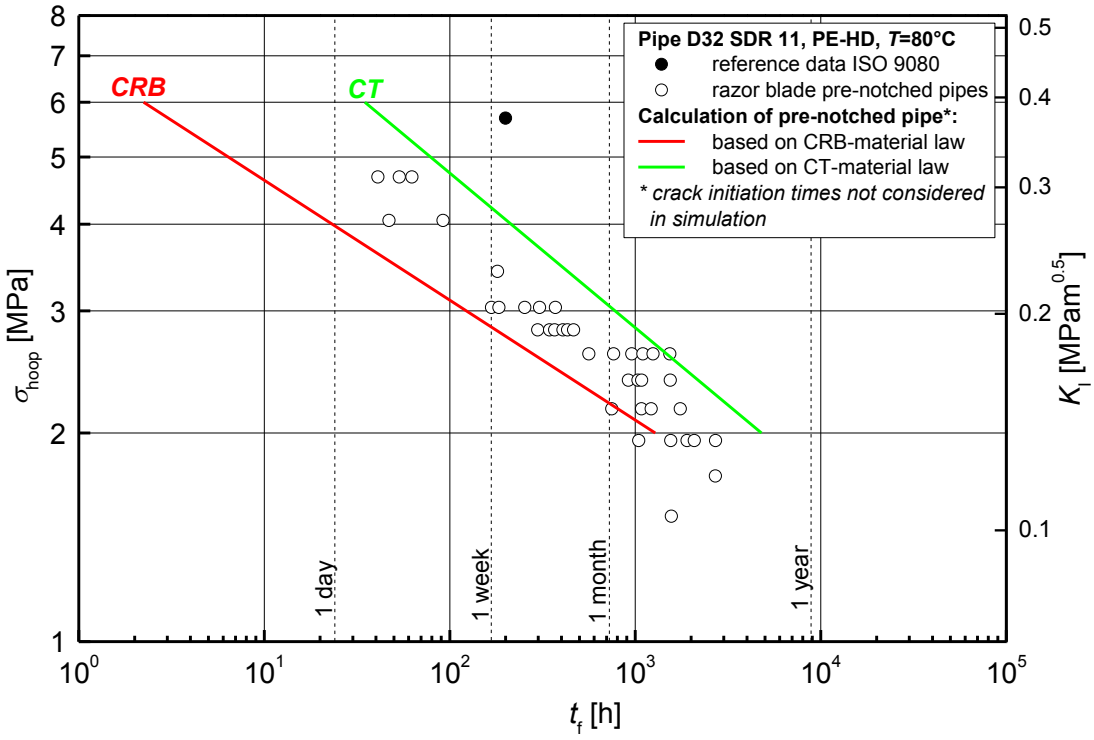

Figure 5.11: Comparison of lifetimes according to calculated CCG of CT- and CRB-specimens with failure times from internal pipe pressure tests performed at 80°C.

Further steps in the development of the approach using cyclic CRB tests are currently under evaluation. For example, the implementation of influences due to media [108,109] is an important addition, to be able to cover the area of media and crude oil transportation. The impact of CGI is also a topic which has yet to be addressed. So far it has often been neglected in lifetime estimations due to complex testing procedures [105]. Also the use of the cyclic CRB test for different polymeric pipe materials [110] is currently examined. Seeing that only about a third of all thermoplastic pipes is produced from PE-HD material [111,112] this is a logical next step.

Besides lifetime estimation, the use of the cyclic CRB tests at R=0.1 is also discussed for ISO-standardization for material quality control [30,110,112,113]. Good correlations with established methods support its claim as a precise and fast ranking tool for PE-HD pipe grades [114,115].

5.6. References

[1] EN ISO 9080. Plastics piping and ducting systems - Determination of the long-term hydrostatic strength of thermoplastics materials in pipe form by extrapolation; 2003.

[2] ASTM International. Standard Test Method for Obtaining Hydrostatic Design Basis for Thermoplastic Pipe Materials or Pressure Design Basis for Thermoplastic Pipe Products; 2011.

[3] Richard K, Gaube E, Diedrich G. Trinkwasserrohre aus Niederdruckpolyäthylen. Kunststoffe;1959:516–25.

[4] Gaube E, Gebler H, Müller W, Gondro C. Zeitstandfestigkeit und Alterung von Rohren aus HDPE. Kunststoffe;1985:412–5.

[5] Lustiger A. Environmental stress cracking: the phenomenon and its utility. Carl Hanser Verlag, Failure of Plastics 1986:305–29.

[6] Kausch HH. Polymer fracture. Berlin/Heidelberg: Springer-Verlag, Berlin; 1987.

[7] Ifwarson M, Tränkner T. Gebrauchsdauer von Polyethylenrohren unter Temperatur und Druckbelastung. Kunststoffe 1989:525–9.

[8] Lang RW. Polymerphysikalische Ansätze zur Beschreibung des Deformations- und Versagensverhaltens von PE-Rohren. 3R International 1997:40–4.

[9] Lang RW, Pinter G, Balika W. Konzept zur Nachweisführung für Nutzungsdauer und Sicherheit von PE-Druckrohren bei beliebiger Einbausituation. 3R International 2005:32–41.

[10] Krishnaswamy RK. Analysis of ductile and brittle failures from creep rupture testing of high-density polyethylene (HDPE) pipes. Polymer 2005;46:11664–72.

[11] Barker MB, Bowman J, Bevis M. The performance and causes of failure of polyethylene pipes subjected to constant and fluctuating internal pressure loadings. J Mater Sci 1983;18:1095–118.

[12] Stern A. Fracture mechanical characterization of the long-term behavior of polymers under static loads. Leoben, Montanuniv., Diss., 1995; 1995.

[13] Pinter G. Rißwachstumsverhalten von PE-HD unter statischer Belastung. Dissertation. Leoben, Austria; 1999.

[14] Böhm LL, Enderle HF, Fleissner M. High-density polyethylene pipe resins. Adv. Mater. 1992;4:234–8.

[15] Brown N, Lu X, Huang Y. The fundamental material parameters that govern slow crack growth in linear polyethylene. Plastics, Rubber and Composites Processing and Applications 1992:255–8.

[16] Egan BJ, Delatycki O. The morphology, chain structure and fracture behaviour of high-density polyethylene: Part I: Fracture at a Constant Rate of Deflection. Journal of Materials Science 1995;30:3307–18.

[17] Egan BJ, Delatycki O. The morphology, chain structure and fracture behaviour of high-density polyethylene: Part II: Static Fatigue Fracture Testing. Journal of Materials Science 1995;30:3351–7.

[18] Pinter G, Lang RW. Creep Crack Growth in High Density Polyethylene. The Application of Fracture Mechanics to Polymers, Adhesives and Composites 2004:47–54.

[19] Dörner GF. Stabilisatoreinflüsse auf das Alterungs- und Zeitstandverhalten von Rohren aus PE-MD. Leoben, Montanuniv., Diss., 1994; 1994.

[20] Choi B, Chudnovsky A, Paradkar R, Michie W, Zhou Z, Cham P. Experimental and theoretical investigation of stress corrosion crack (SCC) growth of polyethylene pipes. Polymer Degradation and Stability 2009;94:859–67.

[21] Dugdale D. Yielding of steel sheets containing slits. Journal of the Mechanics and Physics of Solids 1960;8:100–4.

[22] Barenblatt GI. The mathematical theory of equilibrium cracks in brittle fracture. Advances in applied mechanics 1962;7:55–129.

[23] Friedrich K. Crazes and shear bands in semi-crystalline thermoplastics. In: Crazing in Polymers: Springer; 1983, p. 225–274.

[24] Lang RW. Applicability of linear elastic fracture mechanics to fatigue in polymers and short-fiber composites. Dissertation. Bethlehem, Pennsylvania; 1984.

[25] Kausch H, Gensler R, Grein C, Plummer, C. J. G., Scaramuzzino P. Crazing in semicrystalline thermoplastics. Journal of Macromolecular Science, Part B 1999;38:803–15.

[26] Kausch H. Polymer fracture. 2nd ed. Berlin, Heidelberg: Springer-Verlag; 1987.

[27] Lustiger A, Ishikawa N. An analytical technique for measuring relative tie-molecule concentration in polyethylene. J. Polym. Sci. B Polym. Phys. 1991;29:1047–55.

[28] Pinter G, Lang RW. Effect of stabilization on creep crack growth in high-density polyethylene. Journal of Applied Polymer Science 2003:3191–207.

[29] Haager M, Pinter G, Lang RW. Estimation of Slow Crack Growth Behavior in Polyethylene after Stepwise Isothermal Crystallization. Macromol. Symp 2004;217:383–90.

[30] Frank A, Pinter G. Evaluation of the applicability of the cracked round bar test as standardized PE-pipe ranking tool. Polymer Testing 2014;33:161–71.

[31] van der Stok E, Scholten F. STRAIN HARDENING TESTS ON PE PIPE MATERIALS. In Proceedings Plastics Pipes XVI;2012.

[32] Irwin GR. Analysis of stresses and strains near the end of a crack traversing a plate. J. Appl. Mech. 1957:361–4.

[33] Paris P, Erdogan F. A critical analysis of crack propagation laws. Transactions of the ASME. Journal of Basic Engineering;1963:528–34.

[34] Murakami Y. Stress intensity factors handbook. Oxford: Pergamon Pr; 1990.

[35] DIXON JR, POOK LP. Stress intensity Factors calculated generally by the Finite Element Technique. Nature 1969;224:166–7.

[36] Yamamoto Y, Tokuda N. Determination of stress intensity factors in cracked plates by the finite element method. Int. J. Numer. Meth. Engng. 1973;6:427–39.

[37] Lang RW, Stern A, Dörner GF. Applicability and limitations of current lifetime prediction models for thermoplastics pipes under internal pressure. Die Angewandte Makromolekulare Chemie 1997:131–45.

[38] Anderson TL. Fracture mechanics: Fundamentals and applications. 3rd ed. Boca Raton [u.a.]: CRC, Taylor & Francis; 2005.

[39] Krishnamachari SI. Applied stress analysis of plastics: A mechanical engineering approach. New York: Van Nostrand Reinhold; ©1993.

[40] Frank A. Fracture Mechanics Based Lifetime Assessment and Long-term Failure Behavior of Polyethylene Pressure Pipes: Dissertation. Disseratation. Leoben, Austria; 2010.

[41] Frank A, Hutař P, Mitev I, Náhlík L, Pinter G, Ševčík M (eds.). NUMERICAL SIMULATION OF THE FAILURE BEHAVIOR OF PE PRESSURE PIPES WITH ADDITIONAL LOADS: 67th Annual Technical Conference of the Society of Plastics Engineers 2009, (ANTEC 2009), 22-24 June 2009, Chicago, Illinois, USA. Brookfield, Conn: The Society; 2009.

[42] Ševčík M, Hutař P, Zouhar M, Náhlík L. Numerical estimation of the fatigue crack front shape for a specimen with finite thickness. International Journal of Fatigue 2011.

[43] Portch DJ. An investigation into the change of shape of fatigue cracks initiated at surface flaws; 1979.

[44] Hutař P, Ševčík M, Zouhar M, Náhlík L, Kučera J. The effect of residual stresses on crack shape in polymer pipes. In: Carpinteri A, editor. Proceedings of the 4th International conference on Crack paths (CP 2012), Gaeta (Italy), 19-21 September, 2012. [Gaeta: s. n.]; 2012, p. 489–496.

[45] Broek D. Elementary engineering fracture mechanics. 3rd ed. The Hague, Boston, Hingham, Mass: Martinus Nijhoff; Distributed by Kluwer Boston; 1982.

[46] Broek D. The practical use of fracture mechanics. 2nd ed. Dordrecht, Boston: Kluwer Academic Publishers; 1989.

[47] Hertzberg RW. Deformation and fracture mechanics of engineering materials. 4th ed. New York: J. Wiley & Sons; 1996.

[48] Parsons M, Stepanov EV, Hiltner A, Baer E. Correlation of fatigue and creep slow crack growth in a medium density polyethylene pipe material. Journal of Materials Science 2000;35:2659–74.

[49] Favier V, Giroud T, Strijko E, Hiver J, G'Sell C, Hellinckx S et al. Slow crack propagation in polyethylene under fatigue at controlled stress intensity. Polymer 2002;43:1375–82.

[50] Pinter G, Haager M, Balika W, Lang RW. Fatigue crack growth in PE-HD pipe grades. Plas. Rub. Compos 2005;34:25–33.

[51] Balika W, Pinter G, Lang RW. Systematic investigations of fatigue crack growth behavior of a PE-HD pipe grade in through-thickness direction. J. Appl. Polym. Sci 2007;103:1745–58.

[52] Ševčík M, Hutař P, Náhlík L, Pinter G. Pressure Pipes - Effect of the point loads.

[53] Bhattacharya SK, Brown N. Micromechanisms of crack initiation in thin films and thick sections of polyethylene. J Mater Sci 1984;19:2519–32.

[54] O'Connell PA, Bonner MJ, Duckett RA, Ward IM. The relationship between slow crack propagation and tensile creep behaviour in polyethylene. Polymer 1995;36:2355–62.

[55] Kausch HH. Energy considerations for crack growth in thermoplastics. Kunststoffe 1976:538–44.

[56] Balika W. Rissausbreitung in Kunststoff-Rohrwerkstoffen unter statischer und zyklischer Belastung: Vergleich kommerzieller Rohrwerkstoffklassen und Einfluss der Werkstoffmikrostruktur. Dissertation. Leoben, Austria; 2003.

[57] Chan M, Williams JG. Slow stable crack growth in high density polyethylenes. Polymer 1983;24:234–44.

[58] Hamouda HBH, Simoes-betbeder M, Grillon F, Blouet P, Billon N, Piques R. Creep damage mechanisms in polyethylene gas pipes. Polymer 2001:5425–37.

[59] Choi B, Balika W, Chudnovsky A, Pinter G, Lang RW. The use of crack layer theory to predict the lifetime of the fatigue crack growth of high density polyethylene. Polym. Eng. Sci 2009;49:1421–8.

[60] Parsons M, Stepanov EV, Hiltner A, Baer E. Correlation of stepwise fatigue and creep slow crack growth in high density polyethylene. Journal of Materials Science 1999;34:3315–26.

[61] Shah A, Stepanov EV, Capaccio G, Hiltner A, Baer E. Stepwise fatigue crack propagation in polyethylene resins of different molecular structure. J. Polym. Sci. B Polym. Phys. 1998;36:2355–69.

[62] Parsons M, Stepanov EV, Hiltner A, Baer E. Effect of strain rate on stepwise fatigue and creep slow crack growth in high density polyethylene. Journal of Materials Science 2000;35:1857–66.

[63] Shah A, Stepanov EV, Hiltner A, Baer E, Klein M. Correlation of fatigue crack propagation in polyethylene pipe specimens of different geometries. International Journal of Fracture 1997;84:159–73.

[64] Shah A, Stepanov EV, Klein M, Hiltner A, Baer E. Study of polyethylene pipe resins by a fatigue test that simulates crack propagation in a real pipe. JOURNAL OF MATERIALS SCIENCE 1998;33:3313-3319.

[65] Hertzberg RW, Manson JA. Fatigue of engineering plastics. New York: Academic Press; 1980.

[66] Irwin GR. Plastic Zone Near a Crack and Fracture Toughness. Proceedings, Seventh Sagamore Ordnance Materials Research Conference 1960.

[67] Brown N. A fundamental theory for slow crack growth in polyethylene. Polymer 1995;36:543–8.

[68] Braga M, Rink M, Pavan A. Variations in the fracture behaviour of polyethylene pipe materials induced by thermal treatments. Polymer 1991;32:3152–61.

[69] Brown N, Lu X, Huang Y, Qian R. Slow crack growth in polyethylene - a review. Makromolekulare Chemie. Macromolecular Symposia 1991;41:55–67.

[70] Haager M, Zhou W, Pinter G, Chudnovsky A. Studies of Creep and Fatigue Crack Growth in HD-PE pipe materials. In: Society of Plastics Engineers, editor. ANTEC. Brookfield, USA: Society of Plastics Engineers; 2005, p. 3538–3542.

[71] Reynolds PT, Lawrence CC. Mechanisms of deformation in the fatigue of polyethylene pipe. Journal of Materials Science 1993;28:2277–82.

[72] Haager M. Bruchmechanische Methoden zur beschleunigten Charakterisierung des langsamen Risswachstums von Polyethylen-Rohrwerkstoffen. Dissertation. enLeoben, Austria; 2006.

[73] Lang RW, Balika W, Pinter G. Applicability of linear elastic fracture mechanics to fatigue in amorphous and semi-crystalline polymers. The Application of Fracture Mechanics to Polymers, Adhesives and Composites 2004:83–92.

[74] Pinter G. Slow crack growth in PE-HD under static and cyclic loads. Habilitation. Leoben; 2008.

[75] Brown N, Donofrio J, Lu X. The transition between ductile and slow-crack-growth failure in polyethylene. Polymer 1987;28:1326–30.

[76] Lu X, Brown N. The transition from ductile to slow crack growth failure in a copolymer of polyethylene. J Mater Sci 1990;25:411–6.

[77] Huang Y, Brown N. The effect of molecular weight on slow crack growth in linear polyethylene homopolymers. J Mater Sci 1988;23:3648–55.

[78] Huang Y, Brown N. The dependence of butyl branch density on slow crack growth in polyethylene: Kinetics. J. Polym. Sci. B Polym. Phys. 1990;28:2007–21.

[79] Huang Y, Brown N. Dependence of slow crack growth in polyethylene on butyl branch density: Morphology and theory. J. Polym. Sci. B Polym. Phys. 1991;29:129–37.

[80] Lu X, Qian R, Brown N. Notchology-the effect of the notching method on the slow crack growth failure in a tough polyethylene. Journal of Materials Science 1991;26:881–8.

[81] Ward AL, Lu X, Huang Y, Brown N. The mechanism of slow crack growth in polyethylene by an environmental stress cracking agent. Polymer 1991;32:2172–8.

[82] Lu X, Mcghie A, Brown N. The dependence of slow crack growth in a polyethylene copolymer on test temperature and morphology. J. Polym. Sci. B Polym. Phys. 1992;30:1207–14.

[83] TGM. Gutachten Nr. K 14 450. Wien, Austria; 1993.

[84] Chudnovsky A, Moet A, Bankert RJ, Takemori MT. Effect of damage dissemination on crack propagation in polypropylene. J. Appl. Phys. 1983;54:5562.

[85] Pinter G, Haager M, Balika W, Lang RW. Cyclic crack growth tests with CRB specimens for the evaluation of the long-term performance of PE pipe grades. Polymer Testing 2007;26:180–8.

[86] Pinter G, Balika W, Lang RW. A correlation of creep and fatigue crack growth in high density poly(ethylene) at various temperatures 2002;29:267–75.

[87] Zhou Z, Hiltner A, Baer E. Predicting long-term creep failure of bimodal polyethylene pipe from short-term fatigue tests. J Mater Sci 2011;46:174–82.

[88] Frank A, Lang RW, Pinter G. Accelerated Investigation of creep crack growth in polyethylene pipe grade materials by the use of fatigue tests on cracked round bar specimens: Proceedings Annual Technical Conference - ANTEC, Society of Plastics Engineers, Milwaukee, Wisconsin, USA 2008:2435–9.

[89] Frank A, Freimann W, Pinter G, Lang RW. A fracture mechanics concept for the accelerated characterization of creep crack growth in PE-HD pipe grades. Engineering Fracture Mechanics 2009;76:2780–7.

[90] Ayyer R, Hiltner A, Baer E. A fatigue-to-creep correlation in air for application to environmental stress cracking of polyethylene. J Mater Sci 2007;42:7004–15.

[91] Nishimura H, Narisawa I. Fatigue behavior of medium-density polyethylene pipes. Polym. Eng. Sci. 1991;31:399–403.

[92] Zhou Y, Brown N. The mechanism of fatigue failure in a polyethylene copolymer. J. Polym. Sci. B Polym. Phys. 1992;30:477–87.

[93] Janssen, Roel P. M., Govaert LE, Meijer, Han E. H. An Analytical Method To Predict Fatigue Life of Thermoplastics in Uniaxial Loading: Sensitivity to Wave Type, Frequency, and Stress Amplitude. Macromolecules 2008;41:2531–40.

[94] Hertzberg RW, Manson JA, Skibo MD. Frequency sensitivity of fatigue processes in polymeric solids. Polym. Eng. Sci. 1975;15:252–60.

[95] Wyzgoski MG, Novak GE, Simon DL. Fatigue fracture of nylon polymers. J Mater Sci 1990;25:4501–10.

[96] Pegoretti A, Ricco T. Fatigue crack propagation in polypropylene reinforced with short glass fibres. Composites Science and Technology 1999;59:1055–62.

[97] Frank A, Redhead A, Pinter G. The influence of test frequency and eccentric crack growth on cyclic CRB tests. In: Society of Plastics Engineers (Hg.) 2012 – 70th Annual Technical Conference, p. 1899–1904.

[98] Moskala EJ. Effects of mean stress and frequency on fatigue crack propagation in rubber-toughened polycarbonate/copolyester blends. J. Appl. Polym. Sci. 1993;49:53–64.

[99] Brown HR, Kramer EJ, Bubeck RA. Studies of craze fibril deformation during fatigue in polystyrene. J. Polym. Sci. B Polym. Phys. 1987;25:1765–78.

[100] Lang RW, Pinter G, Balika W, Haager M. A Novel Qualification Concept for Lifetime and Safety Assessment of PE Pressure Pipes for Arbitrary Installation Conditions. In: Proceedings Plastic Pipes XIII; 2006.

[101] Pinter G, Lang RW, Haager M. A Test Concept for Lifetime Prediction of Polyethylene Pressure Pipes. Monatsh. Chem 2007;138:347–55.

[102] Pinter G, Haager M, Lang RW. Lifetime and safety assessment of PE pressure pipes based on fracture mechanics fatigue tests. Proceedings of Antec;2007:2921–5.

[103] Pinter G, Arbeiter F, Berger I, Frank A. Correlation of Fracture Mechanics Based Lifetime Prediction and Internal Pipe Pressure Tests. In: Proceedings Plastic Pipes XVII 2014; 2014.

[104] Freimann W. Charakterisierung des Risswachstumsverhaltens von Cracked Round Bar (CRB) Prüfkörpern auf Basis der Materialnachgiebigkeit. Masterarbeit. Leoben, Austria; 2008.

[105] Redhead A, Frank A, Pinter G. Investigation of slow crack growth initiation in polyethylene pipe grades with accelerated cyclic tests. Engineering Fracture Mechanics 2013;101:2–9.

[106] Frank A, Pinter G, Lang RW. Lifetime prediction of polyethylene pipes based on an accelerated extrapolation concept for creep crack growth with fatigue tests on cracked round bar specimens. In: Society of Plastics Engineers, editor. ANTEC; 2009, p. 2169–2174.

[107] Frank A, Hartl AM, Pinter G, Lang RW. Validation of an accelerated fracture mechanics extrapolation tool for lifetime prediction of PE pressure pipes. In: Society of Plastics Engineers, editor. ANTEC; 2010, p. 1638–1643.

[108] Schoeffl PF, Bradler PR, Lang RW. Yielding and crack growth testing of polymers under severe liquid media conditions. Polymer Testing 2014;40:225–33.

[109] Schoeffl PF, Lang RW. Effect of liquid oilfield-related media on slow crack growth behavior in polyethylene pipe grade materials. International Journal of Fatigue 2015;72:90–101.

[110] Arbeiter F, Pinter G, Frank A. Characterisation of quasi-brittle fatigue crack growth in pipe grade polypropylene block copolymer. Polymer Testing 2014.

[111] Ceresana Research. Market Study: Plastic Pipes; 2011.

[112] Frank A, Berger I, Arbeiter F, Pinter G. Characterization of crack initiation and slow crack growth resistance of PE 100 and PE 100 RC pipe grades with Cyclic Cracked Round Bar (CRB) Tests. In: Proceedings Plastic Pipes XVII 2014; 2014.

[113] ISO/DIS. Polyethylene (PE) materials - Determination of resistance to slow crack growth under cyclic loading - Cracked Round Bar test method(18489); 2014; Available from: http://www.iso.org/iso/catalogue_detail.htm?csnumber=62593.

[114] Kratochvilla TR, Frank A, Pinter G. Determination of slow crack growth behaviour of polyethylene pressure pipes with cracked round bar test. Polymer Testing 2014;40:299–303.

[115] Frank A, Redhead A, Kratochvilla T, Dragaun H, Pinter G. Accelerated Material Ranking with Cyclic CRB Tests. In: Proceedings Plastic Pipes XIV 2010; 2010.

Part IV.

Notching induced pre-damage in polyolefins

6. Introduction to Publication 2

As mentioned in the previous chapters and introduction, not only testing parameters can influence the results from lifetime estimation procedures. Also specimen preparation, in this case the notching of fracture mechanical specimens, can have a big impact on fracture properties. Usually this topic is of high interest for polymeric resins, but there has also been done a lot of work for heterogeneous ethylene-propylene block copolymers [1–4] and polycarbonate [5]. However, the influence on materials used in this thesis, such as very tough PE-HD, reinforced PP or PVC, has not been sufficiently covered in literature yet.

A preliminary series of test conducted on various polymeric pipe materials used later on in this thesis showed that, depending on the notch sharpening technique, different types of notch roots can be found in the material [6]. For example, in Figure 6.1 resulting characteristics of different notching procedures on PE-HD are shown. It is quite visible, that the notches differ significantly. Similar differences were found for unreinforced and reinforced PP as well as for PVC-U.

Furthermore, material in front of the notch tip itself is influenced by the notching procedure. This resulting “pre-damage” due to notching can influence fracture parameters, such as fracture toughness, or crack initiation time during fatigue tests. In Figure 6.2, there is an example of pre-damage in front of a crack tip due to razor-pressing in unreinforced PP using a commercial 0.3 mm razor blade. It can be seen, that material in front of the notch-tip is already significantly damaged even though the specimen has not been loaded yet. In order to correctly perform lifetime estimation of pipe materials, also this influence has to be examined in detail. The following chapter focuses on the impact of different notching techniques to fracture

parameters such as critical stress intensity factor (K_{IC}) and J-Integral (e.g. $J_{0.2}$) of PE-HD pipe grade material used for pressurized piping applications.

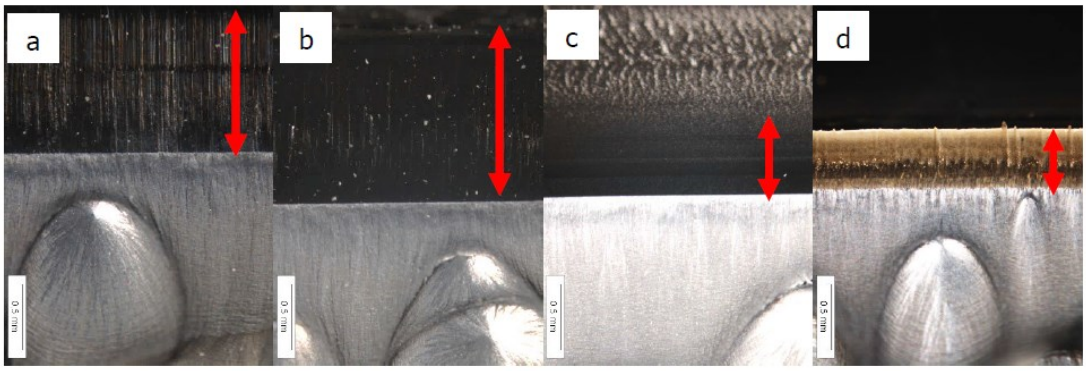

Figure 6.1: Characteristic notch roots of PE-HD depending on notching technique: (a&b) razor pressing with different razor blades, (c) broaching and (d) femtolaser ablation [6].

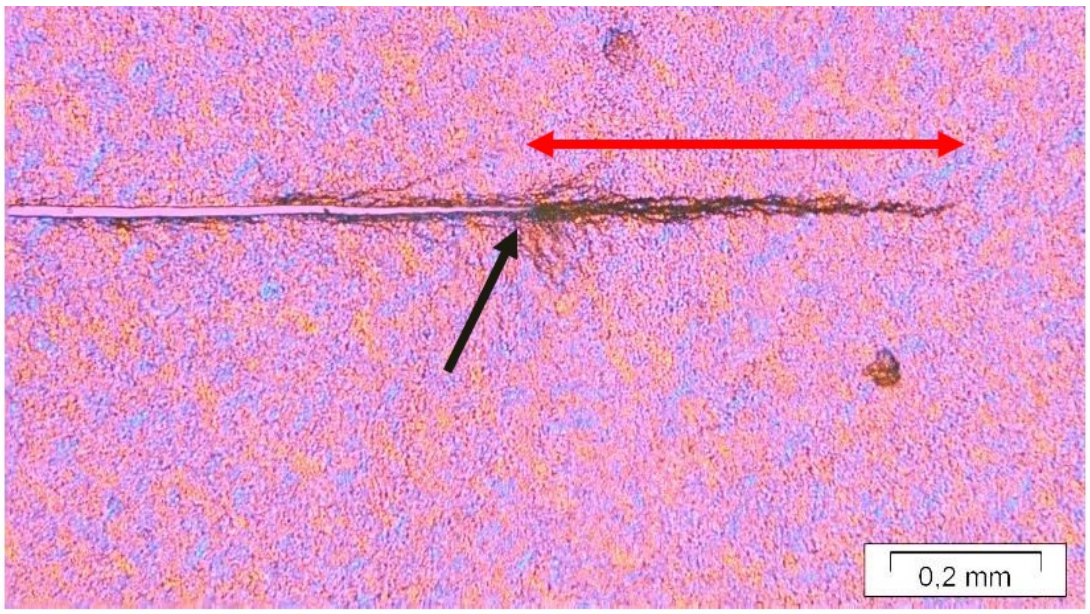

Figure 6.2: Pre-damage in unreinforced PP due to razor pressing with a 0.3 mm razor blade, a penetration speed of 10 mm/min and a notching depth of 1.5 mm [6].

Besides the publication shown in the following part, another contribution has been made by the author in this field. In order to maintain the systematic

focus of this thesis and not go too far beyond the scope, they have not been included directly, but are listed below for further inquiries:

Bachelor's Thesis of Brunbauer S.; "Influence of notching techniques on pre-damage and plastic deformation for tough pipe materials" (in German); Montanuniversitaet Leoben, 2015

6.1. References

[1] Salazar A, Rodríguez J, Segovia A, Martínez AB. Influence of the notch sharpening technique on the fracture toughness of bulk ethylene–propylene block copolymers. Polymer Testing 2010;29:49–59.

[2] Salazar A, Rodríguez J, Segovia A, Martínez AB. Relevance of the femtolaser notch sharpening to the fracture of ethylene–propylene block copolymers. European Polymer Journal 2010;46:1896–907.

[3] Salazar A, Rodríguez J, Martínez AB. The role of notch sharpening on the J-fracture toughness of thermoplastic polymers. Engineering Fracture Mechanics 2013;101:10–22.

[4] Salazar A, Segovia A, Martínez AB, Rodríguez J. The role of notching damage on the fracture parameters of ethylene-propylene block copolymers. Polymer Testing 2010;29:824–31.

[5] Salazar A, Rodríguez J, Martínez AB. Fracture Toughness Reliability in Polycarbonate: Notch Sharpening Effects. Indian Journal of Materials Science 2013;2013:1–4.

[6] Brunbauer S. Einfluss der Kerbeinbringung auf plastische Zonenbildung und monotonen Zugversuch. Bachelor's Thesis. Leoben; 2015.

7. Publication 2

7.1. Bibliographic information

- Title: Fracture toughness of high density polyethylene: Fatigue pre-cracking versus femtolaser, razor sharpening and broaching
- Authors and relevant contributions to this publication:
  - Alicia SALAZAR[1]

    Experimental testing, microscopic investigation, preparation of publication
  - Jesus. RODRÍGUEZ[1]

    Discussion and scientific guidance
  - Florian ARBEITER[2]

    Development of broaching and pressing procedure
  - Gerald PINTER[2]

    Discussion and scientific guidance
  - Antonio MARTÍNEZ[3]

    Discussion and scientific guidance
- Affiliation:

  1. DIMME, Grupo de Durabilidad e Integridad Mecánica de Materiales Estructurales, Universidad Rey Juan Carlos, C/ Tulipán s/n, 28933 Móstoles, Madrid, Spain
  2. Institute of Materials Science and Testing of Polymers, Montanuniversitaet Leoben, Otto Glöckel-Strasse 2, 8700 Leoben, Austria
  3. Centro Catalán del Plástico, Colom 114, 08222 Terrasa, Spain

- Periodical: Engineering Fracture Mechanics
- DOI: doi:10.1016/j.engfracmech.2015.07.016 (in press)

Statement with regard to this publication: The manuscript presented here is an adapted accepted manuscript in order to fit the formatting of the thesis and does not necessarily reflect exactly the actually published version.

7.2. Abstract

This work analyses the fracture toughness under LEFM and EPFM conditions of high density polyethylene specimens sharpened via contact procedures such as razor pressing and broaching and non-contact procedures such as femtolaser and fatigue. The fatigue notch sharpening was accomplished following the guidelines for fatigue pre-cracking in metals. Under LEFM conditions, there was no influence of the notch sharpening technique on the fracture toughness but under EPFM conditions, the fracture toughness values of the fatigue sharpened specimens were the smallest. The analysis of the crack front of the non-tested specimens after sharpening allowed the explanation of these results.

7.3. Keywords

High density polyethylene; Fatigue pre-cracking; Femtolaser; Razor sharpening; Broaching; Pressing; Fracture toughness

7.4. Introduction

The influence of crack sharpness on the fracture toughness values of polymeric materials is still an unsolved problem. Several publications have appeared in the literature highlighting the role of the notch sharpening technique on the fracture parameters of thermoplastic polymers like semi crystalline heterogeneous materials such as ethylene-propylene block copolymers [1], [2], [3], [4], [5] and [6], amorphous polymers such as glycol-modified poly (ethylene terephthalate) (PETG) [7] or polycarbonate [5] and [8], as well as thermoset epoxy resins [9]. In all these studies, which have been conducted by the author of the present paper and his co-workers, fracture data were obtained from samples that notch was prepared by two distinct procedures: either by a non-contact technique based on femtosecond

laser ablation or by the traditional contact methods using a razor blade such as tapping, sliding, pressing or broaching. The data gathered revealed that the lowest fracture toughness values were obtained for specimens with sharp cracks and no damage at the crack front. Especially for the thermoset polymers, natural cracks could be obtained via tapping and specimens sharpened via this technique yielded the lowest fracture toughness values [9]. Conversely, for the thermoplastic polymers investigated, natural cracks could not be obtained via any of the contact techniques applied and the fracture toughness determined from the samples sharpened via the femtosecond laser ablation technique showed the lowest values independent of the fracture mechanics approach. Both the non-contact procedure and the contact techniques gave rise to the very same crack tip radii and the reason for attaining the lowest values of fracture toughness in specimens sharpened via femtolaser ablation is because the femtosecond pulsed laser ablation can create vapor and plasma phases at negligible heat conduction and the absence of a liquid phase [10] and [11]. Thus, this technique can remove material at the notch tip by ablation with almost no heat dissipation, preventing melting and thermal deformations of the surrounding area. However, the specimens sharpened using razor blades always showed damage ahead of the crack tip in the form of plastic deformation which seems to be the reason for the higher fracture toughness values. Moreover, these investigations indicate not only that the sharpening method influences significantly the fracture parameters of thermoplastic polymers, but also that these differences were more noticeable under elastic–plastic and fully plastic conditions. For multiphase semicrystalline ethylene-propylene copolymers, the differences were approximately ∼10% under Linear Elastic Fracture Mechanics (LEFM) conditions [2], [4] and [6], of ∼25–75% under elastic–plastic conditions [2], [3], [4] and [5] and up to ∼90% for fully plastic conditions [1] and [4]. For the amorphous polycarbonate, the differences reached ∼40% under LEFM conditions [8] and up to ∼400% under elastic–plastic situations [5]. In turn, for the amorphous PETG the differences ranged from 10% to 20% under LEFM application [7].

All these discoveries have raised questions concerning the well-established criteria of the quality of the notch and above all, they have shown that the specimens with notches sharpened via the contact procedures

recommended by both ESIS (European Structural Integrity Society) [12], [13], [14] and [15] and ASTM (American Society for Testing and Materials) [16] and [17] based on razor blades do not provide the lowest fracture toughness values, at least for the thermoplastic polymers under study as described above. All these contact procedures created damage at the crack front inducing plastic deformation. The only way to avoid this type of damage, or at least to reduce it, is by employing a non-contact procedure. Although femtosecond pulsed laser ablation produces notch sharpened specimens with no damage at the crack front hence providing the lowest fracture toughness values in the thermoplastic polymers mentioned above, this technique does not seem to be the solution as it will be inaccessible for many laboratories. All this leads to the alternative contactless procedure which is based on fatigue. For metals, it is unquestionable that the most efficient way to produce a natural crack with an infinitely sharp tip is by cyclic loading [18]. Although fatigue pre-cracking is also recommended for polymers by ESIS [12] and [13] and ASTM [17], from an experimental point of view the razor sharpening technique is in favor over fatigue to produce “sufficiently” sharp cracks since fatigue is considered to be a very time consuming practice as the frequency must be kept low (<4 Hz) [12], [13] and [17] to avoid hysteretic heating and in some cases, it is difficult to apply because of unstable fatigue crack growth [12].

In the light of the previous results, the aim of the present work is to investigate fatigue pre-cracking as an alternative non-contact sharpening technique for thermoplastic polymers. The polymer chosen for this study has been a semicrystalline high density polyethylene, especially utilized for pressurized pipes in the field of gas and water distribution. Sharp cracks by fatigue crack growth should be attained following strictly the guidelines of the ASTM E1820–06 standard [18] for fatigue pre-cracking in metals. Fracture toughness of these samples will be evaluated at different temperatures to guarantee LEFM and Elastic-Plastic Fracture Mechanics (EPFM) conditions. The values will be compared with those obtained by traditional contact techniques such as razor pressing or broaching and also the non-contact techniques such as femtolaser ablation. Prior to the fracture toughness tests and after the sharpening process, the crack front of the virgin specimens was inspected to check the quality of the sharpened notch.

7.4.1. Experimental procedure

The material under study was a high density polyethylene, PE, commercially named PE100. Parallelepipedic bars with 17.5 mm × 10 mm × 1 mm in size were used for Dynamic Mechanical Thermal Analysis (DMTA). The tests were conducted on a dual cantilever beam configuration and at 30 μm of displacement amplitude under multifrequency strain mode conditions. Data were collected from −130°C to 150°C at a scanning rate of 5°C/min. The resulting glass transition temperature, T_g, here defined by the temperature at the maximum of tan(δ) was found at −107.6°C.

ISO 3167 [19] dumbbell tensile specimens were tested in a universal electromechanical testing machine (MTS Alliance RF/100) with a load cell of ±5 kN equipped with a contact extensometer (MTS 634-12F-54) and also with a video extensometer (LIMESS). Tests were carried out at a crosshead rate of 10 mm/min and at the testing temperatures of the fracture tests, that is, at 23°C, −60°C and −120°C. For the low temperature tests, the load train (hinges, grips and specimen) was placed into an environmental chamber (MTS 651.06E-03) connected to a Dewar flask. The cooling process was conducted till the load frame ceased to move to balance the thermal contractions and maintained a constant load of +50 N on the specimen. Once the target temperature (either −60°C or −120°C) was reached the specimen was kept for further 30 min at this temperature before starting the test to ensure thermal equilibrium. Three tensile tests were carried out for each testing condition to determine the Young's modulus, E, the yield stress, σ_Y, and the Poisson's ratio, ν, following the guidelines given in the ISO 527 standard [20] (Table 7.1).

Table 7.1: Mechanical properties of PE100 determined by tensile tests at various testing temperatures.

Temperature [°C]	*E* [GPa]	σ_Y [MPa]	ν *[-]*
23	1.05 ± 0.09	22.0 ± 0.2	0.46 ± 0.01
−60	3.2 ± 0.2	51.0 ± 0.9	0.38 ± 0.04
−120	5.1 ± 0.4	87.4 ± 0.2	0.37 ± 0.03

The effect of the notch sharpening procedure on fracture toughness values evaluated by different approaches such as LEFM and EPFM was investigated. To guarantee the adherence to the LEFM and EPFM requirements, fracture tests were performed at different testing temperatures: at −120°C, below the T_g of PE, for the application of the LEFM approach; and at −60°C and 23°C, above the T_g of PE, for the evaluation of fracture parameters under EPFM conditions. The crosshead speed for the tests at −120°C was 10 mm/min and the critical stress intensity factor, K_{IC}, and the critical energy release rate, G_{IC}, were computed from 3 repeats for each testing condition following the guidelines of the ISO 13586 standard [15]. In turn, for the tests under EPFM conditions, the crosshead rate was at 1 mm/min and J–R curves were determined from 2 to 3 repeats by the normalization method following the ASTM E1820 standard [18]. Fracture toughness at crack initiation, J_{IC}, was computed following the guidelines described by Hale et al. [13], where this critical value was replaced by a pseudo-initiation value $J_{0.2}$, which defines crack resistance at 0.2 mm of total crack growth.

The chosen configuration was compact tension (CT). The overall nominal dimensions of the specimens were 50 mm × 48 mm × 15 mm. Side grooves were inserted to promote straighter crack fronts during testing with a total reduction in thickness of 2 mm. An initial straight-through slot with a length to width ratio of 0.45 that terminated in a Charpy type A V-notch [21], with 0.25 ± 0.05 mm in root radius and 45° ± 1° in notch angle, was machined in all the samples. The sharp crack was introduced by contact methods such as razor pressing and razor broaching and non-contact methodologies such as femtolaser ablation and fatigue crack growth. The following notch sharpening procedures were used:

7.4.1.1. Pressing:

The notch sharpening was attained by pressing a fresh razor blade into the machined prenotch. To avoid effects by operatoŕs expertise [7], the notch sharpening via pressing was performed in a controlled and automatized manner employing a servo-hydraulic testing machine MTS 858 Table Top equipped with a load cell of ±15 kN. The new razor blade was mounted on the load train by an adaptor rig and placed into the root of the notch. The

razor blade was inserted into the specimen at a displacement rate of 1 mm/min till achieving the desired notch sharpening length.

7.4.1.2. Broaching:

The notch sharpening via broaching employs of a sharp tool that is repeatedly drawn across the machined prenotch to extend the notch by a small increment on each pass until fulfilling the notch extension criterion. This notch sharpening technique is similar to that employed by CEASŤs notching machines for the preparation of notches in Izod and Charpy impact testing specimens, but in this case a triangular industrial blade with a thickness of 0.2 mm is used, which is replaced regularly to prevent wear.

7.4.1.3. Femtolaser:

The prenotch sharpening was carried out by a femtosecond pulsed laser [10] and [11], using a commercial Ti:sapphire oscillator (Tsunami, Spectra Physics) plus a regenerative amplifier system (Spitfire, Spectra Physics) based on the chirped pulse amplification (CPA) technique. Linearly polarized 120 fs pulses of 395 nm wavelength with a repetition rate of 1 kHz were produced. The scanning speed was 130 μm/s. Three passes were carried out with a pulse energy of 0.050 mJ. The sharpening length inserted by the femtolaser was ca. 500 μm. The specimens were sharpened by Servicio Láser of the University of Salamanca.

7.4.1.4. Fatigue:

The notch sharpening was carried out via fatigue pre-cracking following the procedure described in ASTM E1820 for the measurement of fracture toughness of metallic materials [18]. The fatigue pre-cracking was carried out at −60°C, at a frequency of 10 Hz and a force ratio $R = P_{min}/P_{max}$ of 0.1. The fatigue pre-cracking was performed at low temperature to minimize the effect of adiabatic heating and/or viscoelastic behavior of the material. Regarding the frequency, Frank et al. [22] proved that the test frequency had minimal effect on the crack growth in Cracked Round Bar (CRB) fatigue tests for the determination of the fatigue resistance. The measurements of the relative temperature change at the crack tip of CRB specimens revealed that at a frequency of 10 Hz the temperature increase only amounts to 3 K in a cyclic test at 23°C.

The length of the fatigue precrack extension was higher than 1.3 mm and the fatigue pre-cracking was accomplished in two steps. The load conditions during fatigue notch sharpening varied depending on the fracture test temperature as follows:

The first step covered the crack growth initiation and the first 50% of the total fatigue crack length. The maximum load, P_{max}, was calculated taking into account that the corresponding stress intensity factor was 70% of K_{max}, with:

$$K_{max} = (\frac{\sigma_Y^f}{\sigma_Y^t})(0.063\sigma_Y^f) \quad (7.1)$$

where σ_Y^f is the yield stress at the fatigue pre-cracking temperature, that is, at −60°C and σ_Y^t is the yield stress at the temperature of the fracture test.

The second step included the final 50% of the fatigue crack extension and in any case the maximum stress intensity factor must be higher than:

$$K_{max} = 0.6(\frac{\sigma_Y^f}{\sigma_Y^t})K_{IC} \quad (7.2)$$

where K_{IC} is the fracture toughness at the corresponding testing temperature. The stress intensity factor, K, for CT specimens is given by:

$$K = \frac{P}{\sqrt{BB_N W}} \frac{2+x}{(1-x)^{\frac{3}{2}}}(0.866 - 4.64x - 13.32x^2 - 14.72x^3 - 5.60x^4 \quad (7.3)$$

where α = a/W, with a the crack length and W the width; B the thickness; B_N the net specimen thickness and P the applied load.

The fatigue notch sharpening tests were carried out in a servo-hydraulic testing machine MTS 810 with a load cell of ± 5 kN and a Crack Opening Displacement (COD) extensometer MTS 632.02F-20 with a displacement range of + 3.9 mm to -2 mm. The load train (hinges, clevis grips, sample and COD extensometer) was placed inside an environmental chamber (MTS 651.06E-03) connected to a Dewar flask. The cooling process was conducted until the load frame ceased to move to balance the thermal contractions and maintained a constant load of + 50 N on the specimen. Once the fatigue pre-cracking temperature (−60°C) was reached in the specimen was kept for further 30 min at this temperature before starting the test to ensure thermal equilibrium.

To determine the crack growth during fatigue tests, compliance and visual methods were used. For the optical procedure, images of the crack tip front were taken during the test at a certain frequency (every five minutes) and the crack growth length was measured on the fracture surface after complete fracture. For the compliance method the crack growth was inferred from the flexibility of the specimen using a polynomial that relates the normalized crack length, a/W, while knowing the current compliance of the CT specimens. These Equations have been determined for metals and have also been validated for polymeric materials [23]:

$$\frac{a}{W} = 1.001 - 4.6695U + 18.460U^2 + 236.82U^3 + 1214.9U^4 - 2143.6U^5 \quad (7.4)$$

with

$$U = \frac{1}{(\frac{BEv}{P})^{\frac{1}{2}} - 1} \quad (7.5)$$

where v is the COD reading and E is the elastic modulus. The compliance method was validated via two procedures. Firstly, by comparing the crack length at any instant of the test with that obtained from the optical method, and secondly, by comparing the calculated final crack length with the measured fatigue crack length on the fracture surface of the tested specimens. Data from both procedures differed by less than 10%.

Independent of the sharpening procedure, the ratio of total initial crack length after sharpening, a_0, over width, W, ratio was within 0.45–0.55 and 0.55–0.65 for the tests under LEFM and EPFM conditions, respectively.

For the fracture tests performed at low temperatures, the same procedure was applied as described for the tensile tests or fatigue pre-cracking procedure at −60°C, that is, after reaching the target temperature of the fracture test, either −60°C or −120°C, conditioning was extended for 30 min to ensure that the specimen was in thermal equilibrium before starting the fracture test.

Morphology and dimensions of the crack tip after sharpening and the area beneath the crack front of virgin specimens were analysed via light microscopy and scanning electron microscopy (Hitachi S-3400 N). For

microscopic inspections sections with 15 µm to 20 µm in thickness were cut off from bulk PE with a microtome (Rotary Microtome Leica RM2255). Both the sections cut off as well as the polished bulk surface left behind were analysed. Specifically, the thin films were picked up and either mounted on microscope slides to be inspected via transmitted light microscopy or sputter coated with platinum for scanning electron microscopy.

Finally, the fracture surfaces of the broken specimens were analysed by scanning electron microscopy (Hitachi S-3400N) to detect possible differences caused by the notching technique and the temperature.

7.5. Results and discussion

7.5.1. Fracture characterization under LEFM approach

Figure 7.1 depicts a representative collection of the load–displacement records at −120°C and 10 mm/min of the PE100 specimens precracked by pressing, broaching, femtolaser, and fatigue. The differences found among the curves are due to slight deviations in the initial crack lengths. The mechanical response is initially semibrittle and becomes unstable just having passed the maximum load. Nonetheless, the linearity criterion of LEFM ($P_{max}/P_{5\%} < 1.1$) is fulfilled in 70% of the specimens (Table 7.2) and the critical stress intensity factor, K_{IC}, and the critical energy release rate, G_{IC}, were computed in accordance with the ISO13856 standard [15]. The average values, together with their corresponding standard errors, are shown in Table 7.2. All specimens have satisfied the size criteria for plane strain conditions [12]:

$$B, a, W - a > 2.5(\frac{K_{IC}}{\sigma_Y})^2 \tag{7.6}$$

Under these testing conditions, there were hardly any differences between the values obtained from specimens sharpened via the contact techniques such as pressing and broaching and those from specimens precracked via the non-contact procedures such as femtolaser ablation. However, the specimens sharpened via fatigue tend to give slightly higher values, around 8% and 3% higher when evaluated in terms of the energy release rate and the stress intensity factor, respectively.

Table 7.2: Fracture data, G_{IC} and K_{IC}, and the linearity criterion, $P_{max}/P_{5\%}$, of PE100 at − 120°C of pressing, broaching, femtolaser and fatigue sharpened specimens.

	G_{IC} [kJ/m^2]	K_{IC} [MPa m$^{1/2}$]	$P_{max}/P_{5\%}$ [-]
Pressing	6.0 ± 0.7	5.96 ± 0.03	1.13 ± 0.05
Broaching	6.0 ± 0.8	5.94 ± 0.08	1.10 ± 0.04
Femtolaser	6.1 ± 0.7	6.01 ± 0.05	1.07 ± 0.07
Fatigue	6.5 ± 0.9	6.2 ± 0.1	1.07 ± 0.09

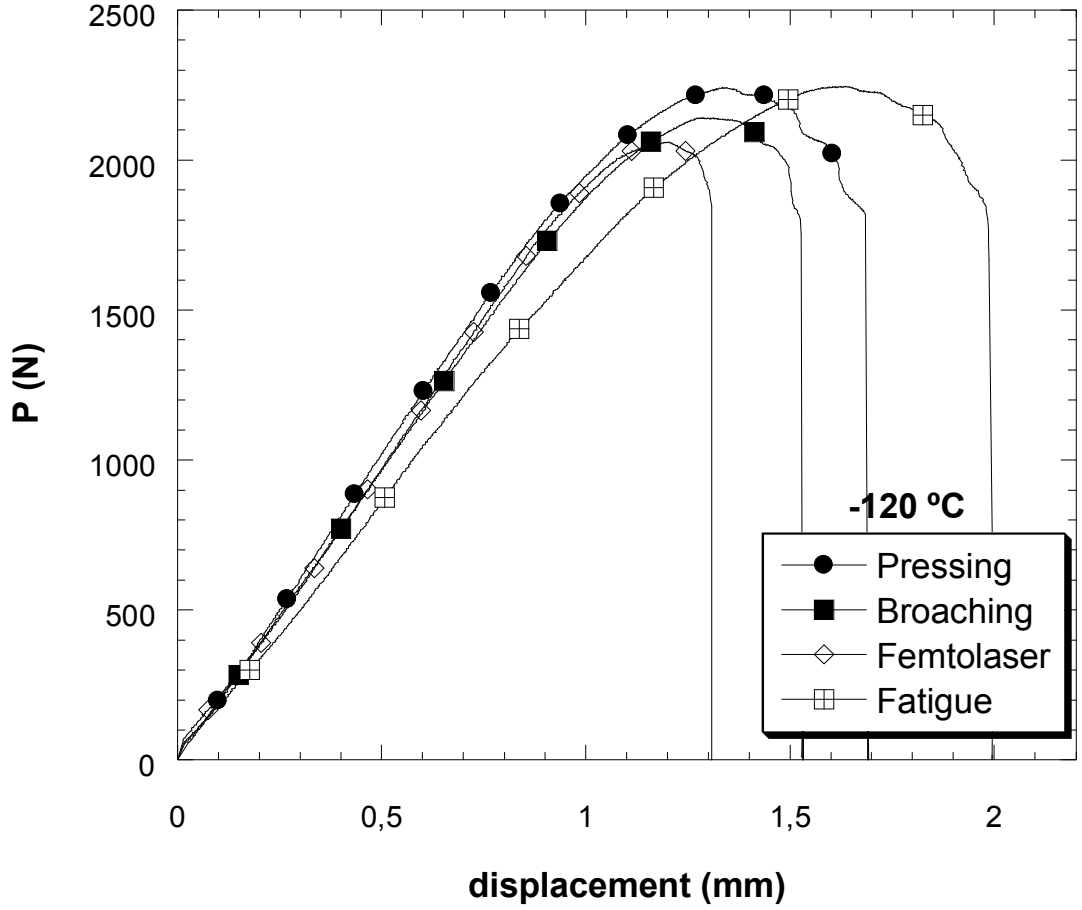

Figure 7.1: Load, P, versus displacement at −120°C and cross head rate of 10 mm/min of PE100 specimens sharpened by pressing, broaching, femtolaser and fatigue.

Figure 7.2 shows the morphology of the fracture surfaces ahead of the crack tip of the specimens sharpened via different procedures. Independent of the

sharpening method, all samples exhibited stable crack growth after initiation but prior to instability and this explains the non-linearity in the load–displacement diagrams (Figure 7.1). The morphology of the stable crack growth region close to the notch of the pressing (Figure 7.2a), broaching (Figure 7.2b) and femtolaser (Figure 7.2c) samples was identical. By contrast, the fracture surface of the area immediately after the crack tip introduced via fatigue and delimited by a dashed line in Figure 7.2d is wavier (Figure 7.3b) and with a microstructure much finer than those of the pressing, broaching and femtolaser samples (Figure 7.3a). The presence of this wavy zone, which extends 100–200 µm in depth, in front of the crack tip in the fatigue sharpened specimens seems to be the reason for the slightly higher values in the fracture toughness values at −120°C in comparison with the razor blade and femtolaser sharpened samples (Table 7.2).

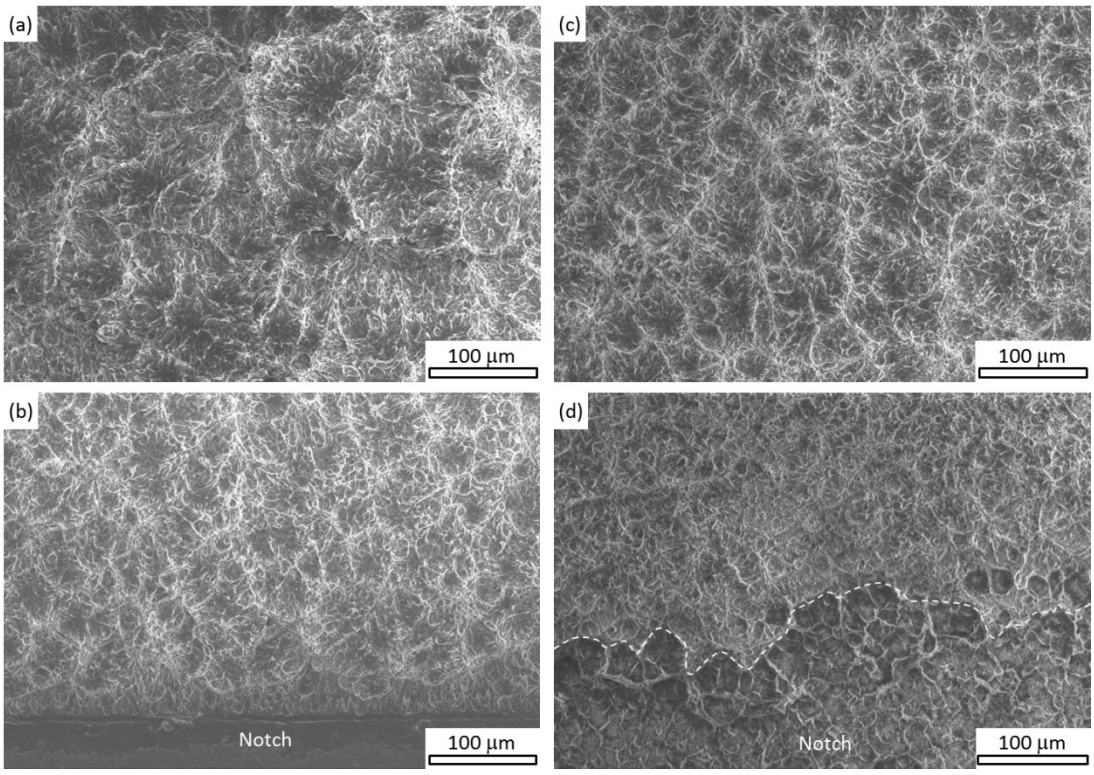

Figure 7.2: SEM micrographs of fracture surfaces of PE100 tested at −120°C of (a) pressing, (b) broaching, (c) femtolaser and (d) fatigue sharpened PE100 samples. The dashed line in (d) delineates the boundary between the fatigue crack tip and the fracture surface.

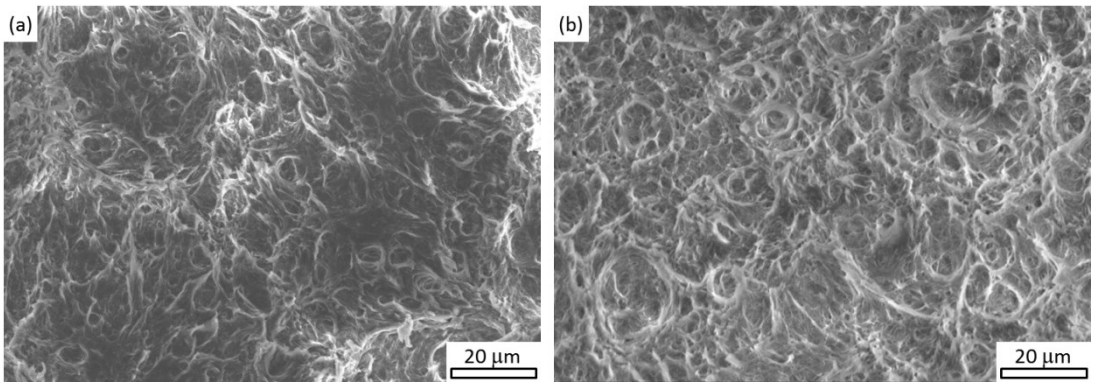

Figure 7.3: Close-up of the fracture surfaces immediately after of the crack tip obtained from the broken specimens tested at −120°C: (a) pressing and (b) fatigue samples.

7.5.2. Fracture characterization under EPFM approach

At −60°C and 23°C, above the T_g of PE, the EPFM assumptions are ensured as evidenced by the load–displacement curves (Figure 7.4). The differences found among the curves are due to the slight difference in the initial crack lengths. J–R curves were determined by the normalization method [18], and Figure 7.5a and b combine the R-curves of the pressing, broaching, femtolaser and fatigue specimens computed from the fracture tests at −60°C and 23°C, respectively. These plots also include the fit of the J-crack growth resistance curve to the power law $J = C \cdot a^N$, with $N < 1$. Independent of the testing temperature, the resistance curves of the fatigue sharpened specimens are below the set of curves formed by either the specimens sharpened by contact procedures such as razor pressing and broaching or non-contact methods such as femtolaser ablation. These differences were more accentuated at the higher temperature.

Table 7.3 collects the fracture toughness, $J_{0.2}$, obtained from the resistance curves of pressing, broaching, femtolaser and fatigue specimens tested at −60°C and 23°C. The average values, together with the corresponding standard errors, are also included. The application of the size requirements for plane strain at $J_{0.2}$, given by [24]

$$B, a, W - a > 25\frac{J_{0.2}}{\sigma_Y} \tag{7.7}$$

revealed that at −60°C all specimens failed in plane strain state whereas at 23°C none of the plane strain criteria were satisfied, i.e. the deformation was not sufficiently localized. Consequently, the fracture toughness values at crack initiation of the fatigue specimens differed much more from those of the pressing, broaching and femtolaser samples. These differences were of 20% at −60°C and arouse to 50% at 23°C.

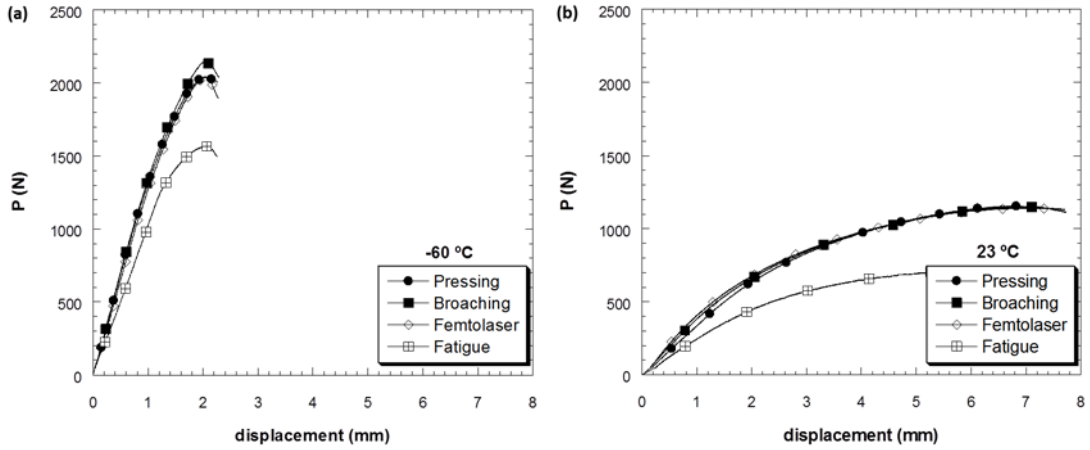

Figure 7.4: Load, P, versus displacement curves of PE100 specimens sharpened by pressing, pressing, broaching, femtolaser and fatigue, obtained from fracture tests at a loading rate of 1 mm/min and at −60°C (a) and at 23°C (b).

Table 7.3: Fracture toughness values, $J_{0.2}$, obtained from pressing, broaching, femtolaser and fatigue sharpened PE100 specimens at −60 C and 23 C.

$J_{0.2}$ [kJ/m^2]	Pressing	Broaching	Femtolaser	Fatigue
−60°C	17 ± 1	18 ± 2	18 ± 2	15 ± 1
23°C	31 ± 5	31 ± 3	30 ± 2	19.5 ± 0.5

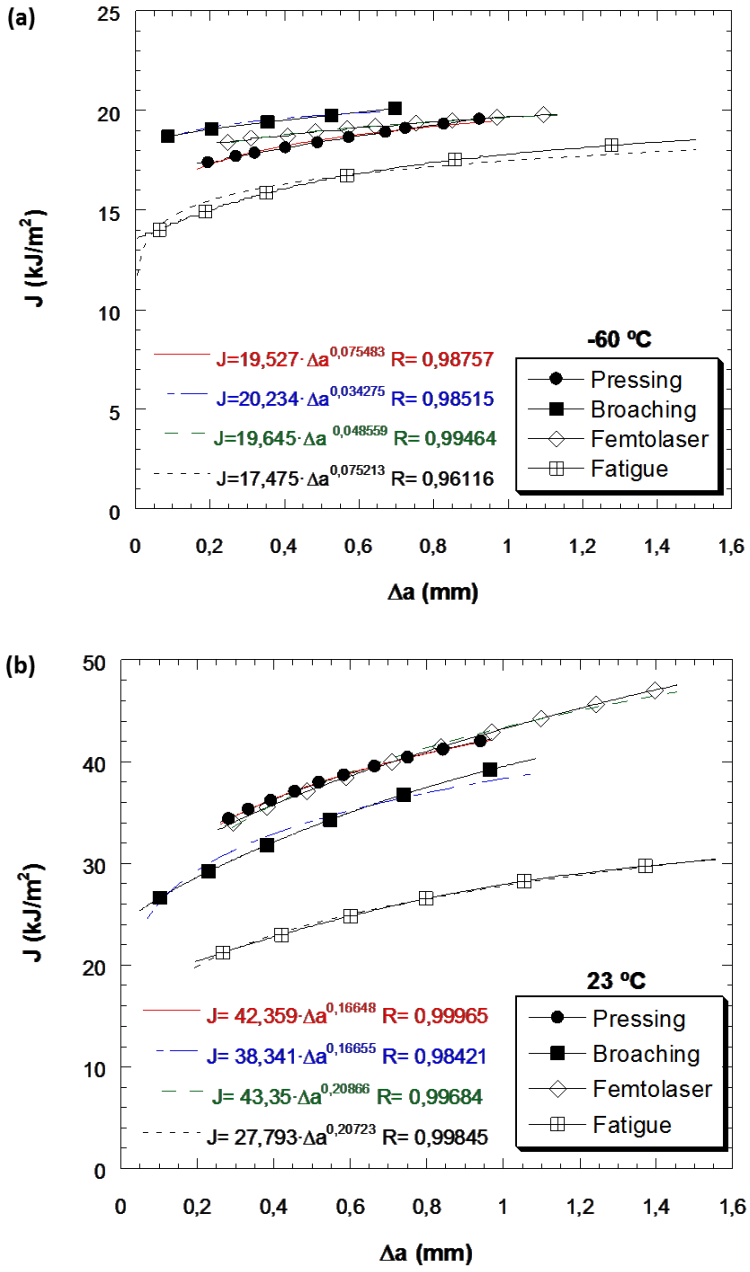

Figure 7.5: J–R curves of pressing, broaching, femtolaser and fatigue specimens determined from tests at −60°C (a) and at 23°C (b).

Figure 7.6 and Figure 7.7 show the morphologies of fracture surfaces in the vicinity of the crack tip obtained at broken specimens tested at −60°C and 23°C, respectively.

For the pressing (Figures 7.6a and 7.7a), the broaching (Figures 7.6b and 7.7b) and femtolaser specimens (Figures 7.6c and 7.7c) two types of morphology are observed: one localized at the root of the notch tip, the other one in the area of stable crack growth. The near crack tip zone is characterized by PE highly oriented along the crack growth direction (Figure 7.8). This area is assigned to the blunting process the initial sharp crack undergoes during the loading process. The areas associated with blunting have a width of 100–200 µm and 300–500 µm for specimens tested at −60°C and at 23°C, respectively. Interestingly, this blunting region morphology was not observed in any of the fracture surfaces obtained from fracture tests performed at −60°C and 23°C and specimens which notches were sharpened by fatigue crack growth (Figures 7.6d and 7.7d).

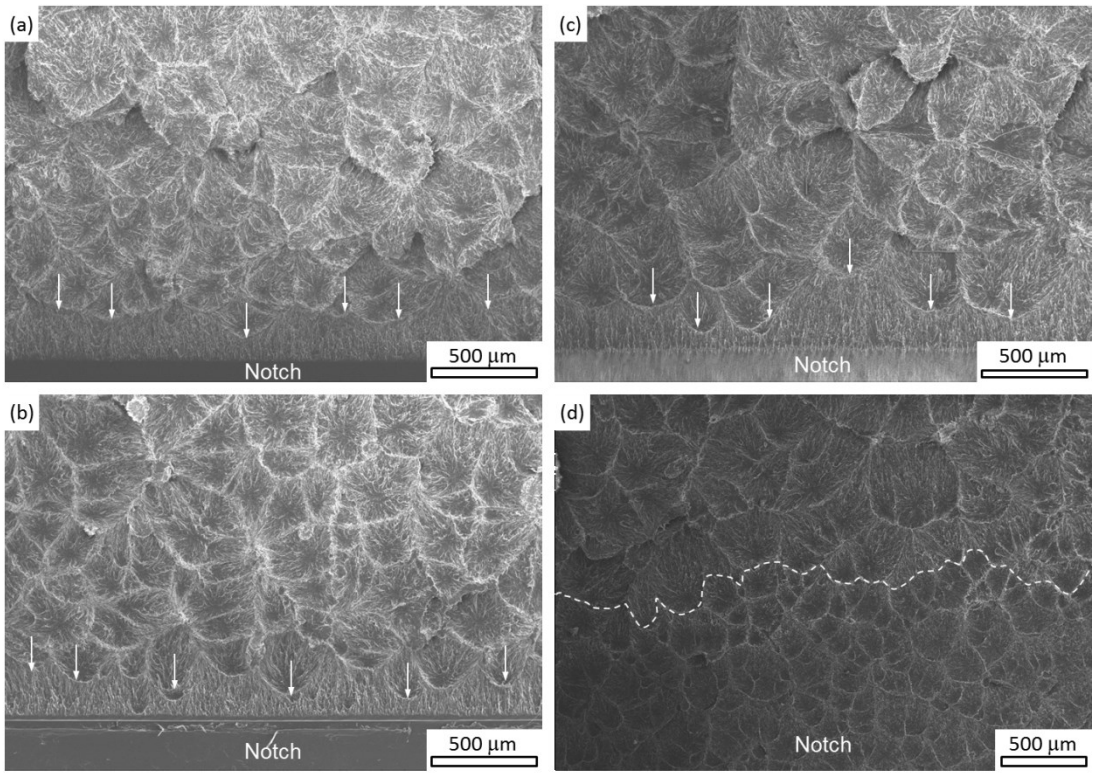

Figure 7.6: SEM fractograms of PE100 tested at −60°C with (a) pressing, (b) broaching, (c) femtolaser and (d) fatigue sharpened notches. The dashed line in (d) delineates the boundary between the fatigue crack tip and the fracture surface. The boundary of the blunting zone is indicated by arrows.

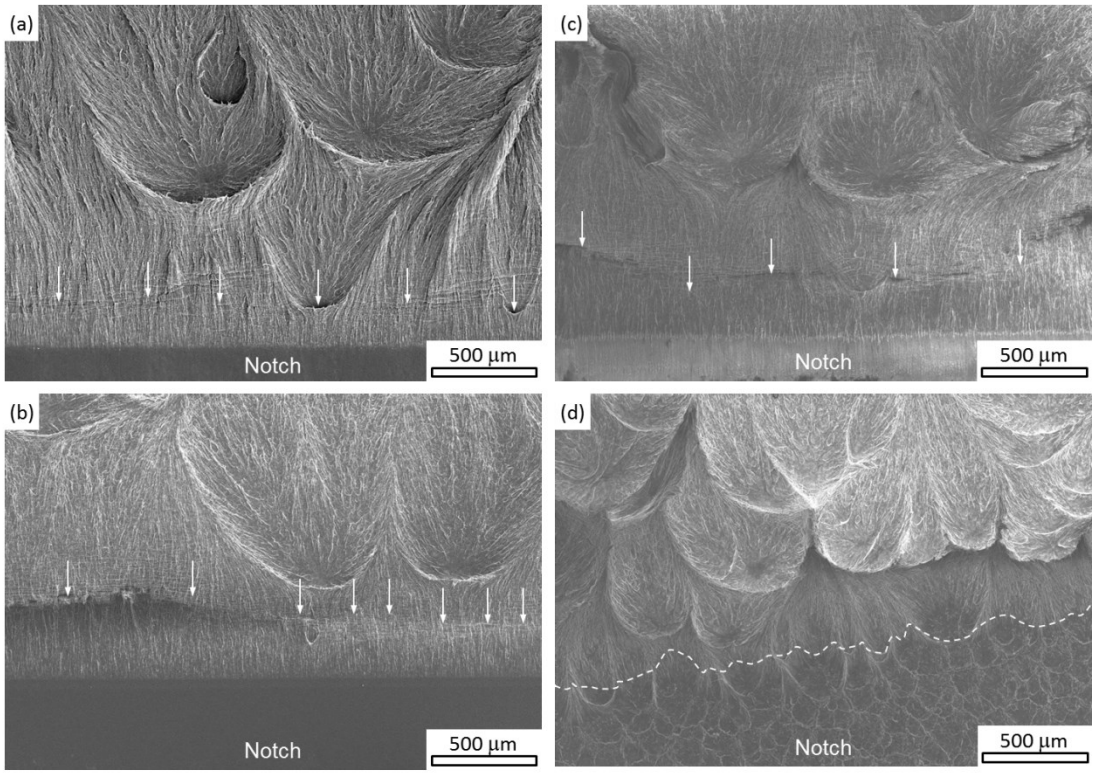

Figure 7.7: SEM fractograms of PE100 tested at 23°C with (a) pressing, (b) broaching, (c) femtolaser and (d) fatigue sharpened notches. The dashed line in (d) delimitates the boundary between the fatigue crack tip and the fracture surface. The boundary of the blunting zone is pointed out by arrows.

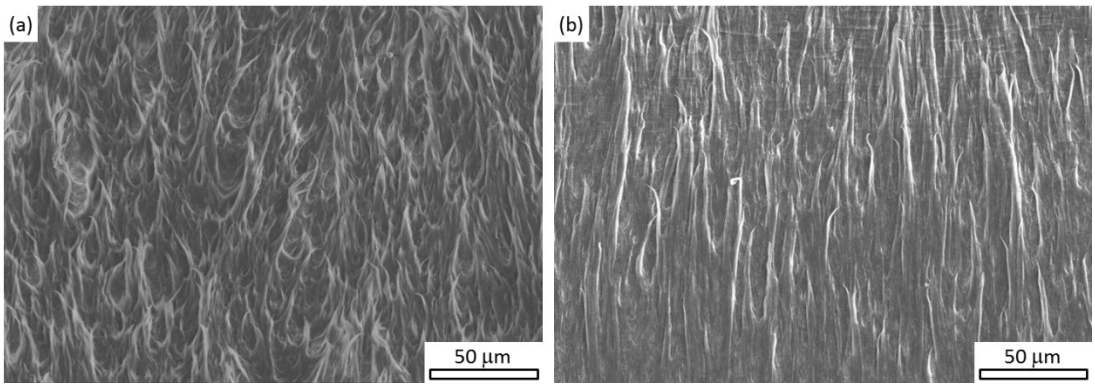

Figure 7.8: Representative micrographs of the blunting zone ahead of the crack tip in the pressing, broaching and femtolaser specimens tested (a) at −60°C and (b) 23°C.

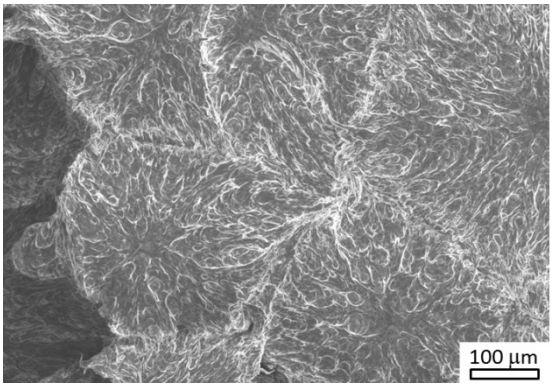

Figure 7.9: Micrograph of the zone of stable crack growth that developed during the fracture process at −60°C. The arrow points out the stable crack growth direction.

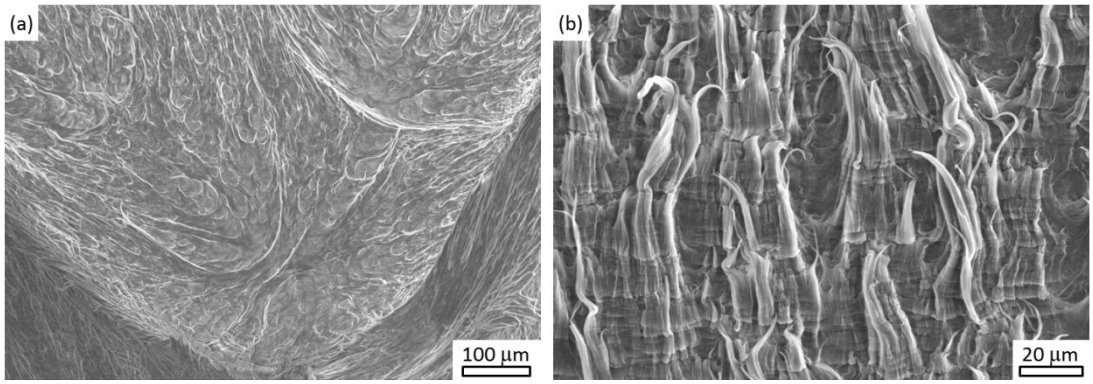

Figure 7.10: (a) Micrograph of the zone of stable crack growth that developed during the fracture process at 23°C. (b) Periodically spaced striations indicating the formation and subsequent coalescence of crazes which terminates when turning into a crack.

This seems to be one of the reasons why the fracture toughness of fatigue precracked specimens is the lowest at −60°C and 23°C. Regarding the morphology in the area of stable crack growth, no differences were observable among specimens with distinctly sharpened notches for a given testing temperature, but the fracture process and hence, the characteristic size of the morphology that developed was temperature dependent. At −60°C, the fracture surface was mainly flat and formed by a patchwork-like pattern (Figure 7.9), while at 23°C the fracture surface was much rougher with qualitatively the same patchwork-like pattern as at −60°C but with

patches much bigger in size (Figure 7.10a). Moreover, in the area just behind the blunting region of the fracture surfaces of specimens broken at 23°C (Figure 7.10b) some striations are observable at high magnifications which are periodically spaced and perpendicularly oriented to the crack growth direction, showing the formation and coalescence of crazes, which propagation terminates when turning into a crack [25] and [26].

Figure 7.11 displays the dependence of fracture toughness of PE100 on temperature and its variation with the notch sharpening technique employed. The material obeys the general trend to be brittle in the glassy state, i.e. below T_g, and becoming increasingly ductile with the distance from T_g in the rubbery state. The values for the pressing, broaching and femtolaser specimens were at 23°C 6 times higher than at −120°C; for the fatigue samples, the values were 3 times higher when going from −120°C to 23°C.

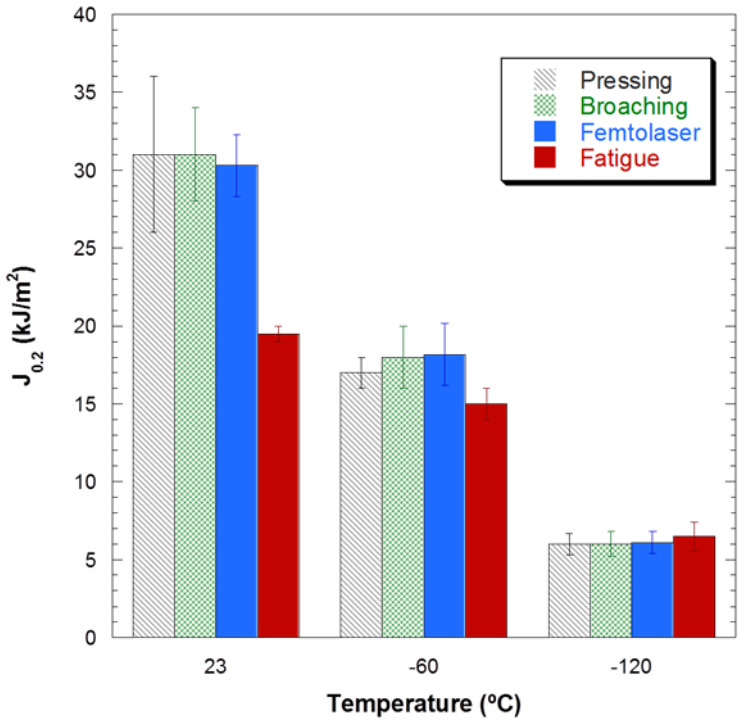

Figure 7.11: Fracture toughness vs. testing temperature for the pressing, broaching, femtolaser and fatigue specimens. The tests at −120°C were conducted at a crosshead speed of 10 mm/min while those at −60°C and 23°C at a loading rate of 1 mm/min.

Figure 7.11 shows several striking features. Firstly, the traditional contact notch sharpening techniques based on the usage of razor blades did not generate the smallest fracture toughness values. This result is in accordance with those reported by Martinez et al. [1], [6] and [7] and Salazar et al. [2], [3], [4], [5] and [8] for thermoplastic polymers. Secondly, for the high density polyethylene, PE100, investigated the non-contact procedure femtolaser ablation gave fracture toughness values identical to those given by the traditional notching techniques such as razor pressing and razor broaching independent of the applied testing temperature. Thirdly, specimens sharpened via fatigue at low temperature, following the guidelines of fatigue notch sharpening for metallic materials [18], exhibited fracture toughnesses similar to pressing, broaching and femtolaser specimens when evaluated under LEFM conditions and the smallest values when determined under EPFM conditions.

In order to shed more light on these results, the crack front of virgin specimens was examined after sharpening and prior to testing. Figure 7.12 displays a low magnification view of the crack front of the pressing, broaching, femtolaser and fatigue samples. Firstly, the sharp cracks introduced via either razor pressing, razor broaching or femtolaser ablation are extremely straight, formed by the track left behind after having inserted or pushed the razor blade into the pressing (Figure 7.12a) and broaching (Figure 7.12b) specimens, or the trace after having passed the laser beam across the femtolaser samples (Figure 7.12c). However, the crack introduced via fatigue resembles more a natural crack. The fatigue crack path is wavy and seems to propagate through the weakest sites in the microstructure especially attenuated during the cycling process (Figure 7.12d).

Table 7.4 gives the crack radii of specimens sharpened via the different techniques. The contact procedures such as razor pressing and broaching together with the fatigue pre-cracking presented crack tip radii smaller than 1 μm. The smallest crack tip radii are achieved by fatigue crack growth. By contrast, the non-contact procedure femtolaser ablation produced the biggest crack tip radii in PE100, ~2.2 μm. This value is four to five times larger than any radius obtained with the rest of the sharpening techniques under study.

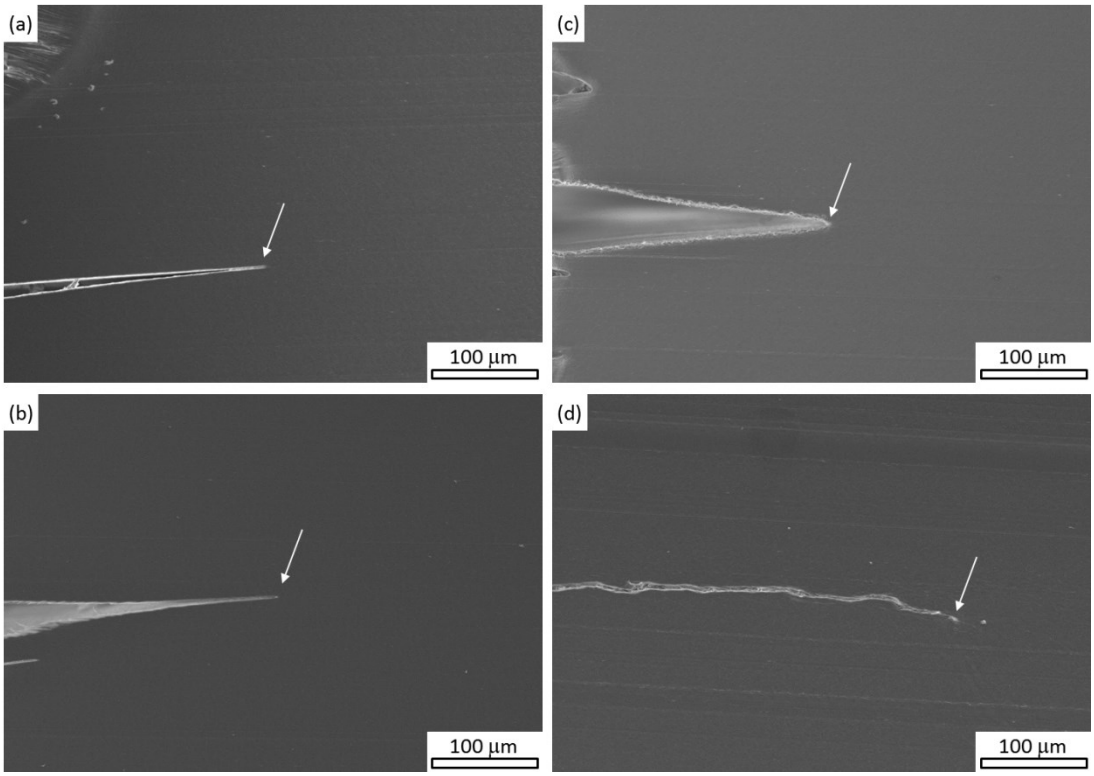

Figure 7.12: Panoramic view of the crack front of the virgin fracture specimens after notch sharpening by the (a) pressing, (b) broaching, (c) femtolaser and (d) fatigue method. The arrow points out the crack tip.

Table 7.4: Crack tip radii in virgin PE100 specimens after sharpening the notch tip by razor pressing, razor broaching, femtolaser ablation and fatigue crack growth.

	Pressing	Broaching	Femtolaser	Fatigue
Crack tip radius [µm]	0.5 ± 0.2	0.4 ± 0.2	2.2 ± 0.3	0.3 ± 0.1

The analysis of the crack front of the non-tested specimens revealed some type of damage ahead of the crack tip independent of the notch sharpening technique. The specimens sharpened via razor pressing and broaching showed a similar morphology in the area beneath the crack tip which is particularly affected by the sharpening procedure (Figure 7.13). The damage zone is about 100 µm to 200 µm wide and appears similar to that observed in other polyolephines such as polypropylenes, PP, when using razor blade

techniques for notch sharpening [3] and [4] (Figure 7.13b). The local deformation induced by the razor blade may be close to or even higher than the yield strain giving rise to this damaged area.

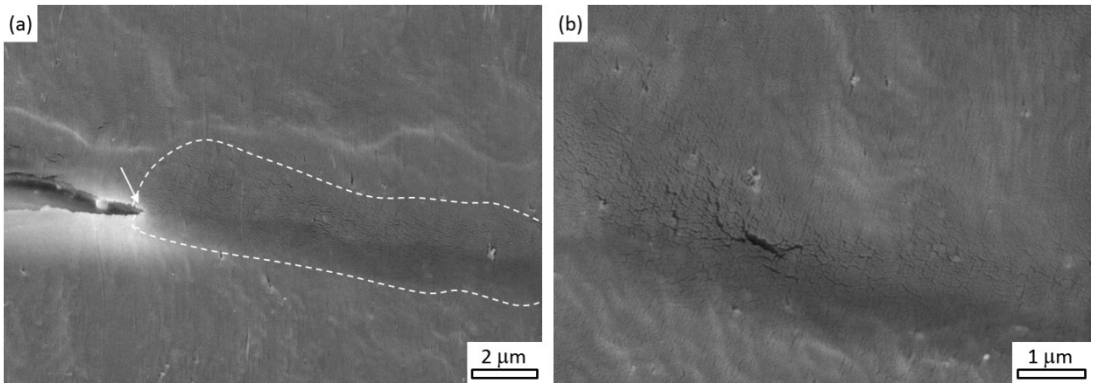

Figure 7.13: Micrographs obtained via scanning electron microscopy of the crack front of non-tested pressing specimens: (a) panoramic view, (b) detail of the damage ahead of the crack tip. The arrow points out the crack tip. The white dashed line circumvents the crack tip.

Figure 7.14 shows the crack front of the femtolaser samples, where the crack tip is surrounded by a small zone of white hue (delimited by arrows). This zone was formed by partially melted material produced by the pulses of the laser ablation process. In this case, the damage observed in the pressing or broaching samples (Figure 7.13) was not detected.

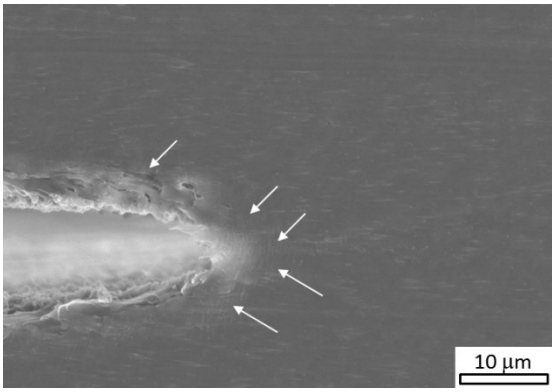

Figure 7.14: Micrograph obtained via scanning electron microscopy of the crack front of non-tested Femtolaser specimens. The damaged area beneath the crack tip is pointed out by arrows.

Despite fatigue notching technique being a non-contact procedure, damage ahead of the crack tip was clearly observable (Figure 7.15a), and extended around 100 µm in depth. In metals, fatigue and plastic zone and/or accumulated damage ahead of the crack tip are intimately related. This plastic zone, which progresses together with the fatigue crack, is responsible for the damage accumulation through which the crack grows [27]. These micromechanisms also seem to be accomplished in thermoplastic polymers such as PE100, for the damaged area (Figure 7.15b) beneath the crack tip can be considered as damage accumulation to be present in the fatigue process.

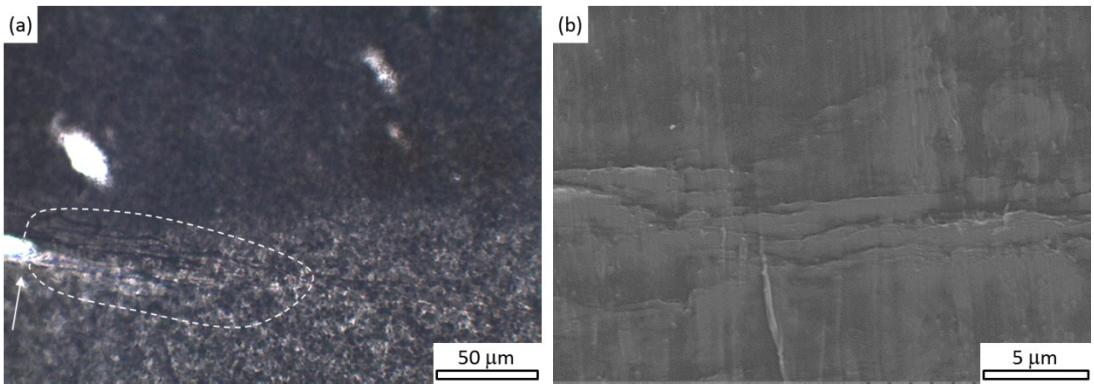

Figure 7.15: Crack front of non-tested fatigue specimens: (a) Micrograph obtained via transmitted light microscopy, (b) detail of the damage ahead of the crack tip inspected via scanning electron microscopy. The arrow points out the crack tip and the damaged area beneath the crack tip is indicated by white dashed lines.

According to the analysis of the crack front previously described, both the razor blade sharpened samples, pressing and broaching, as well as the specimens sharpened by the non-contact procedure such as fatigue presented some damage ahead of the crack tip but of very different origins. Moreover, the crack tip radii of both specimens sharpened with razor blades and specimens sharpened via fatigue were of the same order of magnitude, although the fatigue sharpened samples showed the smallest values (Table 7.4). This similarity of the crack front gave rise to similar fracture toughness values under LEFM approach (Table 7.2). However, the damage in the fatigue and razor blade sharpened specimens must be of a different

nature because of the remarkable differences found under EFPM conditions. As previously described, the fracture toughness of the razor blade sharpened specimens was 20% and 50% higher than that of the fatigue sharpened specimens at −60°C and 23°C, respectively (Table 7.3 and Figure 7.11). The reason why the differences between the fatigue notch sharpened samples and the set formed by the razor blade sharpened specimens are distinct at −60°C and 23°C is due to the stress state. While the fracture toughness values computed at −60°C were all in plane strain state, those determined at 23°C were not. The different nature of the damage is assessed with two experimental proofs: the profile of the sharp cracks introduced during the sharpening procedure and the presence of blunting in the fracture surfaces. During the fatigue process, the damage accumulates in the weak sites of the PE microstructure giving rise to an apparent morphology in form of fine microcracks which growth and finally coalescence into fatigue crack growth. This results in a tortuous and wavy sharp crack (Figure 7.12d), with no appearance of a blunting zone during the loading process in the fracture tests at −60°C (Figure 7.6d) and at 23°C (Figure 7.7d). On the other hand, when inserting the razor blade, the resulting sharp crack is the straight mark left after passing the razor blade and at the same time, damage is attained because the yield stress is surpassed locally and consequently, the crack initiation and subsequent propagation is controlled by a strain hardened area with mechanical properties distinct from those of the virgin material [2]. Besides, this type of damage in the razor blade samples favors the formation of blunting during the fracture process at −60°C (Figure 7.6a and b) and at 23°C (Figure 7.7a and b).

In turn, the reason why femtolaser sharpened samples presented identical fracture toughness values to those obtained in razor blade sharpened specimens is the big crack tip radii of the former. Although the femtolaser sharpened samples gave a minuscule zone affected by heat dissipation during the laser ablation, the crack tip radii were 4–5 times bigger than those of the pressing or broaching samples (Table 7.4). This accounts for the similarity in the fracture toughness values among the three types of sharpened specimens under both LEFM and EPFM conditions (Table 7.2 and Table 7.3 and Figure 7.11).

7.6. Conclusions

The effect of the notch sharpening technique on the fracture toughness of high density polyethylene, a semicrystalline thermoplastic, has been evaluated under LEFM and EPFM conditions. Fracture tests were carried out at −120°C, below the T_g of PE, for the application of the LEFM approach and at −60°C and 23°C, both above the T_g of PE, for the application of the EPFM approach. Contact notching procedures employing razor blades such as razor pressing and razor broaching and non-contact techniques such as femtolaser ablation and fatigue pre-cracking crack growth were investigated. For fatigue notch sharpening, the guidelines for fatigue notch pre-cracking in metals were followed and the loading conditions varied depending on the testing temperature for fracture characterization. Independent of testing temperature, the fracture toughnesses of specimens sharpened via the contact procedures were indistinguishable and secondly, the fracture toughness of the femtolaser sharpened specimens were similar to those obtained for the specimens sharpened via the applied contact procedures. The former is due to the similarity of the crack fronts of non-tested specimens after sharpening with razor blades and the latter is because the femtolaser sharpened specimens showed the highest crack tip radii.

At −120°C LEFM conditions, i.e. the size criteria for the plane strain state and the linearity criterion for the deformation, were satisfied and the fracture toughnesses of the four types of notch sharpened samples were practically the same, i.e. unaffected by the notch sharpening technique. At −60°C and 23°C the data analysis required EPFM for extensive plastic deformations. While at −60°C the LEFM size requirements for the plane strain state could still be met this was no longer the case at 23°C. The fracture toughness values obtained from the fatigue sharpened specimens were 20% and 50% smaller at −60°C and 23°C than those determined from specimens sharpened by razor pressing and razor broaching, respectively.

The analysis of the crack front revealed that samples sharpened by razor pressing, razor broaching and fatigue crack growth exhibited damage ahead of the crack tip and similar crack tip radii. The similarity of the crack front features for these three types of notch sharpened specimens accounted for the similarity of the fracture toughnesses evaluated using LEFM at −120°C. However, in the elastic plastic region of deformations the nature of the

damage is assumed to be completely different to explain the differences in toughness. This assumption was confirmed by analysis of the profiles of the sharp cracks and the fracture surfaces. The sharp cracks introduced via fatigue were wavy, indicating that the freely growing fatigue crack discovered the weakest sites in the microstructure and moved along their traces. This type of damage in fatigue precracked specimens obviously suppressed extensive blunting during the fracture process. On the other hand, in the razor blade sharpened specimens, the sharp crack was formed by the track left behind after broaching or pushing. During these processes, the yield strain was exceeded and a plastically deformed zone was created with voids in the vicinity of the notch tip. This situation will give rise to crack tip blunting when the fracture test is performed shifting the fracture toughness at crack initiation to higher values.

7.7. Acknowledgement

Authors are indebted to Ministerio de Economía y Competitividad of Spain for their financial support through projects MAT2012-37762-C02-2.

7.8. References

[1] A.B. Martínez, A. Segovia, J. Gámez-Pérez, M.L. Maspoch, Influence of femtolaser notch sharpening technique in the determination of essential work of fracture (EWF) parameters, Engng Fract Mech, 16 (2009), pp. 2604–2617

[2] A. Salazar, J. Rodríguez, A. Segovia, A.B. Martínez, Influence of the notch sharpening technique on the fracture toughness of bulk ethylene-propylene block copolymers, Polym Test, 29 (2010), pp. 49–59

[3] A. Salazar, A. Segovia, A.B. Martínez, J. Rodríguez, The role of notching damage on the fracture parameters of ethylene-propylene block copolymers, Polym Test, 29 (2010), pp. 824–831

[4] A. Salazar, J. Rodríguez, A. Segovia, A.B. Martínez, Relevance of the femtolaser notch sharpening to the fracture of ethylene-propylene block copolymers, Eur Polym J, 46 (2010), pp. 1896–1907

[5] A. Salazar, J. Rodríguez, A.B. Martínez, The role of notch sharpening on the J-fracture toughness of thermoplastic polymers, Engng Fract Mech, 101 (2013), pp. 10–22

[6] A.B. Martínez, D. Arencón, J. Rodríguez, A. Salazar, Influence of the notch sharpening on the impact fracture toughness of ethylene-propylene block copolymers, Polym Test, 36 (2014), pp. 75–81

[7] A.B. Martínez, N. León, D. Arencón, J. Rodríguez, A. Salazar, On the effect of the different notching techniques on the fracture toughness of PETG, Polym Test, 32 (2013), pp. 1244–1252

[8] A. Salazar, J. Rodríguez, A.B. Martínez, Fracture toughness reliability in polycarbonate: notch sharpening effects, Indian J Mater Sci (2013), p. 4 p. Article ID 187802

[9] Salazar A, Patel Y, William JG. Influence of crack sharpness on the fracture toughness of epoxy resins. In: 13th International conference on fracture, June 16–21, 2013, Beijing, China.

[10] B.N. Chichkov, C. Momma, S. Nolte, F. von Alvensleben, A. Tünnermann, Femtosecond, picoseconds and nanosecond laser ablation of solids, Appl Phys A-Mater, 63 (1996), pp. 109–115

[11] P. Moreno, C. Méndez, A. García, I. Arias, L. Roso, Femtosecond laser ablation of carbon reinforced polymers, Appl Surf Sci, 252 (2006), pp. 4110–4119

[12] J.G. Williams, KC and GC at slow speeds for polymes, D.R. Moore, A. Pavan, J.G. Williams (Eds.), Fracture mechanics testing methods for polymers, adhesives and composites, Elsevier Science Ltd. and ESIS, The Netherlands (2001), pp. 11–24

[13] G.E. Hale, F. Ramsteiner, J-fracture toughness of polymers at slow speed, D.R. Moore, A. Pavan, J.G. Williams (Eds.), Fracture mechanics testing methods for polymers, adhesives and composites, Elsevier Science Ltd. and ESIS, The Netherlands (2001), pp. 123–157

[14] E. Clutton, Essential work of fracture, D.R. Moore, A. Pavan, J.G. Williams (Eds.), Fracture mechanics testing methods for polymers,

adhesives and composites, Elsevier Science Ltd. and ESIS, The Netherlands (2001), pp. 177–195

[15] ISO 13586. Plastics – determination of fracture toughness (GIC and KIC) – Linear Elastic Fracture Mechanics (LEFM) approach; 2000.

[16] ASTM D5045-99. Standard test methods for plane-strain fracture toughness and strain energy release rate of plastic materials; 1999.

[17] ASTM D6068-96. Standard test method for determining J–R curves of plastics; 2002.

[18] ASTM E1820-06. Standard test method for measurements of fracture toughness. ASTM standards; 2007.

[19] ISO 3167. Plastics – multipurpose test specimens; 2014.

[20] ISO 527. Plastics – determination of tensile properties; 1997.

[21] ASTME E23-02. Standard test methods for notched bar impact testing of metallic materials; 2002.

[22] Frank A, Redhead A, Pinter G. The influence of test frequency and eccentric crack growth on cyclic CRB tests. ANTEC; 2012.

[23] L. Castellani, M. Rink, Fatigue crack growth of polymers, D.R. Moore, A. Pavan, J.G. Williams (Eds.), Fracture mechanics testing methods for polymers, adhesives and composites, Elsevier Science Ltd. and ESIS, The Netherlands (2001), pp. 91–116

[24] J.G. Williams, Introduction to elastic-plastic fracture mechanics, D.R. Moore, A. Pavan, J.G. Williams (Eds.), Fracture mechanics testing methods for polymers, adhesives and composites, Elsevier Science Ltd. and ESIS, The Netherlands (2001), pp. 119–122

[25] G. Pinter, M. Haager, W. Balika, R.W. Lang, Cyclic crack growth tests with CRB specimens for the evaluation of the long-term performance of PE pipe grades, Polym Test, 26 (2007), pp. 180–188

[26] R.A.C. Deblieck, D.J.M. van Beek, K. Remerie, I.M. Ward, Failure mechanisms in polyolefines: the role of crazing, shear yielding and the entanglement network, Polymer, 52 (2011), pp. 2979–2990

[27] T.L. Anderson, Fatigue crack propagation, Fracture mechanics: fundamentals and applications, CRC Press LLC, New York (1995), pp. 513–558

Part V.

Fatigue damage behaviour of polyolefin pipe grade materials

8. Introduction to Publications 3, 4 and 5

In order to shorten testing times for results needed to validate pipe material, behaviour cyclic tests have proven to be applicable (e.g. [1–8]). However, there is only little experience with fatigue behaviour of pipe grade polypropylene in literature. Literature mostly covers fatigue in reinforced PP [9–13] or injection grade materials [14]. Pipe grade PP material, which is usually characterized by high molecular weight (M_W) and corresponding low melt flow rate (MFR), is mostly characterized via impact tests [15,16] or rheology [17,18]. Both can give insights into material behaviour, but do not fully reflect on real application and long-term properties of PP material used in piping. A study by Jones and Lesser [19] in 1998 examined the fatigue behaviour of tough PP and showed promising results. However, even though they used quite tough PP (M_W around 330,000 and MFR = 0.7), materials used for piping still surpass these properties. Materials examined in the course of this work were found to have M_W > 500,000 and MFR < 0.3.

The cyclic CRB test has shown promising results in characterizing the long-term properties of tough PE-HD materials used for piping. Therefore, using this method for other tough pipe grade materials is a promising approach. The following chapter deals with the applicability, restrictions and limitations of the cyclic CRB test to different polymeric materials with a big focus on “quasi-brittle” failure of PP and the influence of its morphology on resulting properties.

Besides the publications shown in the following part, several more contributions have been made by the author in this field. In order to maintain the systematic focus of this thesis and not go too far beyond the scope, they have not been included directly, but are listed below for further inquiries:

Conference contribution: Arbeiter, F.; Pinter, G.; Frank, A.; “Comparison of long-term-properties of polyolefin pipe grades using linear elastic fracture mechanics”, Plastic Pipes Conference XVI, Barcelona, ES, 2012

Conference contribution: Arbeiter, F.; Schwab, M.; Pinter, G.; Frank, A.; “Damage propagation in reinforced pipe grade polypropylene under fatigue loads“, Poster at Frontiers in Polymer Science, Riva del Garda, IT, 2015

Conference contribution: Pinter, G.; Arbeiter, F.; Berer, M.; Schrittesser, B.; Frank, A.; “The Cyclic CRB Test – A Quick Test for Assessing Long-term Fracture Behaviour of Polymers”, Polymer Processing Society Conference - PPS2015”, Graz, AUT, 2015

8.1. References

[1] Frank A, Berger I, Arbeiter F, Pinter G. Characterization of crack initiation and slow crack growth resistance of PE 100 and PE 100 RC pipe grades with Cyclic Cracked Round Bar (CRB) Tests. In: Proceedings Plastic Pipes XVII 2014; 2014.

[2] Frank A, Redhead A, Kratochvilla T, Dragaun H, Pinter G. Accelerated Material Ranking with Cyclic CRB Tests. In: Proceedings Plastic Pipes XIV 2010; 2010.

[3] Pinter G, Haager M, Balika W, Lang RW. Cyclic crack growth tests with CRB specimens for the evaluation of the long-term performance of PE pipe grades. Polymer Testing 2007;26:180–8.

[4] Kratochvilla TR, Frank A, Pinter G. Determination of slow crack growth behaviour of polyethylene pressure pipes with cracked round bar test. Polymer Testing 2014;40:299–303.

[5] Hu Y, Summers J, Hiltner A, Baer E. Correlation of fatigue and creep crack growth in poly(vinyl chloride). Journal of Materials Science 2003;38:633–42.

[6] Nishimura H, Narisawa I. Fatigue behavior of medium-density polyethylene pipes. Polym. Eng. Sci. 1991;31:399–403.

[7] Parsons M, Stepanov EV, Hiltner A, Baer E. Correlation of stepwise fatigue and creep slow crack growth in high density polyethylene. Journal of Materials Science 1999;34:3315–26.

[8] Zhou Z, Hiltner A, Baer E. Predicting long-term creep failure of bimodal polyethylene pipe from short-term fatigue tests. J Mater Sci 2011;46:174–82.

[9] Karger-Kocsis J. Microstructural aspects of the fatigue crack growth in polypropylene and its chopped glass fibre reinforced composites. Journal of Polymer Engineering 1991:97–121.

[10] Karger-Kocsis J, Friedrich K, Bailey RS. Fatigue and Failure Behavior of Short and Long Glass Fiber Reinforced Injection-Molded Polypropylene. Science and Engineering of Composite Materials 1991;2.

[11] Pegoretti A, Ricco T. Fatigue crack propagation in polypropylene reinforced with short glass fibres. Composites Science and Technology 1999;59:1055–62.

[12] Trantina GG. Fatigue life prediction of filled polypropylene based on creep rupture. Polym. Eng. Sci. 1984;24:1180–4.

[13] Velasco JI, Saja JA, Martínez AB. FRACTURE BEHAVIOUR OF UNTREATED AND SILANE-TREATED TALC-FILLED POLYPROPYLENE COMPOSITES. [April 23, 2012].

[14] KARGERKOCSIS J, Friedrich K. Effect of skin-core morphology on fatigue crack propagation in injection moulded polypropylene homopolymer. International Journal of Fatigue 1989;11:161–8.

[15] Morath CC, Ward IM, Soliman M, Voets P, Kleppinger R. Biaxially oriented polypropylene pipes: implications for impact and hydrostatic pressure resistance. Plas. Rub. Compos 2006;35:447–54.

[16] Chen H, Karger-Kocsis J, Wu J, Varga J. Fracture toughness of α- and β-phase polypropylene homopolymers and random- and block-copolymers. Polymer 2002;43:6505–14.

[17] Yu L, Wu T, Chen T, Yang F, Xiang M. Polypropylene random copolymer in pipe application: Performance improvement with controlled molecular weight distribution. Thermochimica Acta 2014;578:43–52.

[18] McNally T, McShane P, Nally GM, Murphy WR, Cook M, Miller A. Rheology, phase morphology, mechanical, impact and thermal properties of polypropylene/metallocene catalysed ethylene 1-octene copolymer blends. Polymer 2002;43:3785–93.

[19] Jones NA, Lesser AJ. Morphological study of fatigue-induced damage in isotactic polypropylene. Journal of Polymer Science Part B: Polymer Physics 1998;36:2751–60.

.

9. Publication 3

9.1. Bibliographic information

- Title: Cyclic tests on cracked round bars as a quick tool to assess the long-term behaviour of thermoplastics and elastomers
- Authors and relevant contributions to this publication:
  - Florian ARBEITER[1]
    Experimental testing, microscopic investigations, data evaluation, preparation of the publication
  - Bernd SCHRITTESSER[2]
    Data for H-NBR, discussion of experimental results
  - Andreas FRANK[2]
    Data for PE, discussion of experimental results
  - Michael BERER[2]
    Data for POM, discussion of experimental results
  - Gerald PINTER[1,2]
    Discussion of experimental results
- Affiliations:
  1. Institute of Materials Science and Testing of Polymers, Montanuniversitaet Leoben, Otto Glöckel-Strasse 2, 8700 Leoben, Austria
  2. Polymer Competence Center Leoben GmbH, Roseggerstr. 12, 8700 Leoben, Austria
- Periodical: Polymer Testing

- DOI: 10.1016/j.polymertesting.2015.05.008

Statement with regard to this publication: The manuscript presented here is an adapted accepted manuscript in order to fit the formatting of the thesis and does not necessarily reflect exactly the actually published version.

9.2. Abstract

The aim of this work is to demonstrate the applicability of the cracked round bar test recently developed for PE-HD to other polymeric materials. The main advantage of this new test method are rather short testing times for PE-HD materials used in long-term applications such as piping. Therefore, this test is of high interest for other polymers used in similar applications. Five thermoplastic materials used for plumbing (PE-HD, PP-B, PB, PVC-U, PA12), a technical polymer (POM) and an elastomeric material (H-NBR) have been tested. Scanning electron microscopy has been applied to investigate fracture surfaces. Results show that the test method seems to be basically applicable to all tested materials. Most materials showed similar fracture behaviour as postulated in literature, despite the high acceleration factor of the cyclic CRB test.

9.3. Keywords:

CRB, PE, PP, PB, PVC, PA12, POM, H-NBR, Fatigue

9.4. Introduction & background

The cyclic cracked round bar test (CRB) has been developed to induce quasi-brittle failure in high density polyethylene (PE) used in pipe applications within a short amount of time [1-4]. Development of new, faster tests for this kind of material have been a key issue, since modern pipe grade materials cannot be tested within feasible times. Using established methods such as the Full Notched Creep Test or Notched Pipe Test it is not possible to distinguish between modern materials, since this kind of test is stopped if the materials pass 10,000 h of testing [5,6]. A further disadvantage of this sort of test is the use of chemicals and/or elevated temperatures to induce brittle failure. Therefore, testing conditions are quite far from actual application conditions. The CRB-test has shown promising results for the ranking of PE materials at room temperature [1] and for some polypropylene (PP) types at

elevated temperatures [7] within quite short times. The test has also recently been standardised for PE-HD materials under the Austrian ONorm [3] and ISO [8]. The CRB test is based on linear elastic fracture mechanics (LEFM). By applying a cyclic, instead of a static, load testing times can be immensely reduced while still inducing quasi-brittle failure. Requirements for applying LEFM to plastics are that the global loading situation is within the range of linear viscoelasticity and plastic deformations ahead of the crack tip are still limited to small areas [9]. When these requirements are met, several authors have found the failure mechanisms of PE in cyclic tests to be similar to those of the static case. Based on these findings, the CRB test has been found to be a valid tool to compare resistance against slow crack growth in PE. Due to its easy use, simple specimen geometry and high acceleration factor using fatigue, this test is predestined to be of high interest for different materials as well. Many materials used in engineering applications have to be examined with regard to their long-term behaviour. However, similar to PE, most materials cannot be tested within feasible times and are in need of new testing methods. Therefore, this work focuses on the applicability of the cyclic CRB test to different polymeric materials in order to induce quasi-brittle failure under fatigue load and gauge the validity of this test as a quick ranking tool. Failure behaviour of five thermoplastic materials used in various areas of piping (high density polyethylene (PE-HD), polypropylene block copolymer (PP-B), polybutylene (PB), polyvinylchloride (PVC) and polyamide 12 (PA12)), the technical polymer polyoxymethylene (POM) and an elastomer from oil-field applications (hydrogenated nitrile rubber (H-NBR)) has been investigated. The CRB test compares different materials by observing the load dependent failure times or cycles to failure. Similar to Wöhler fatigue curves, the different load levels and their respective failure cycles form a straight line in a fully logarithmic diagram. Thus, materials can not only be compared for a certain load level, but can also be used to assess changes in ranking in regard to the applied load level. For cyclic CRB tests, a circumferential razor blade notch is applied before testing. Therefore, scatter is vastly reduced and fewer specimens are required. Usually, three to four specimens at different load levels are sufficient to describe material behaviour in the quasi-brittle failure regime. More detailed information about stresses in tested materials can be identified by using the stress intensity factor K_I. The factor ($K_I = \sigma_I a^{0.5} Y$) describes the stress distribution in front of

the crack tip and is a function of global applied loading (σ), the crack length (a) and a parameter (Y), describing geometry dependency of K_I. The index of K describes the mode of the loading condition. Mode “I” refers to a pure crack opening load, and is the most relevant type for practical applications. When used to describe fatigue testing, K_I is often exchanged with ΔK_I which is the difference between K_{Imin} and K_{Imax} according to σ_{min} and σ_{max} during a load cycle. In the case of the cyclic CRB-test, the use of K_I also makes it possible to use specimens with different diameter and still get comparable results.

9.5. Materials

Materials used in this work were PE-HD, PP-B, PB, PVC-U, PA12, POM and H-NBR, as described below in respect of their main mechanical properties, areas of application and special characteristics.

Polyethylene is a very versatile polymer. Depending on its chemical structure and morphology it can be used for packaging, bottles or even for demanding applications such as gas and water pipes. When used for gas and water pipes, the material has to withstand crack growth for more than 50-100 years under a constant operating pressure of up to 16 bar. Chemical structure and composition of modern pipe grade polyethylene is optimized for high crack resistance. Therefore, it is quite challenging to get brittle failure in this material within short testing times. Nonetheless, for quality reassurance and further material development it is important to assess long-term behaviour.

Polypropylene, quite similar to PE, can also be used in very different fields. The PP-B tested in this work is a block-copolymer also used for pipe applications. One of its main uses is for nonpressurised sewer pipes which also have to last up to 100 years. Consequently, the material also exhibits high crack resistance which can lead to very long testing times using established methods. Furthermore, PP-B has a tendency to form rather large plastic zones when stress is applied. Thus, similar to PE, it is not possible to induce brittle failure without large scale plastic deformation within short testing times using common specimen types, as for example the compact tension (CT) specimen.

Polybutylene was developed in the 1950s and widely used for piping in the 1980s and 90s. The material combines good flexibility with strength at high temperatures. Therefore, PB is often used for hot-water transportation.

Polyvinylchloride finds its uses in several fields of application from piping, insulation of electric wires, to window frames and sills and clothing. For example, PVC is the dominating material worldwide, used for thermoplastic polymer pipes, even though its market share has reduced over recent few years, especially in Europe [10]. Due to its outstanding chemical and abrasion resistance [11] PVC is especially useful for sewer and drainage applications in aggressive environments. The PVC used in this study was a leadfree PVC-U type with a K-value of 67 used for non-pressure sewer pipe applications.

Polyamide is a technical polymer used especially for applications where a combination of high loads, temperature and media is involved. In combination with glass fibre reinforcement, different PA types are broadly used in automotive applications. The PA examined in this study was a non-reinforced PA12 type. It can be used for example in multi-layered pipes for oil transportation. Lately, it has also been considered for gas and water pressure pipes with higher pressure classes compared to PE-HD.

Polyoxymethylene is a technical polymer which exhibits good overall mechanical properties, high abrasion resistance, a low friction coefficient and high ductility down to several degrees below 0°C [12]. Therefore, it is often used in the fields of general engineering (e.g. cogwheels or sliding elements). The material used in this study falls within the latter category and has to withstand high constant loads, superimposed with several thousand loading cycles without fracture.

Hydrogenated nitrile rubber is a cross-linked, saturated copolymer made from acrylonitrile and butadiene. Due to its properties, H-NBR can be used as sealing and O-rings in the oil-field industry. Failure in this type of application can be very costly and particularly dangerous. Worst case result is a complete fragmentation of a cartridge seal which leads to a safety shutdown of the facility. Therefore, it is necessary to look for a cost efficient and fast ranking tools [13]. The H-NBR used is reinforced with carbon black and used

in oilfield applications. However, the remaining composition was not disclosed by the manufacturer.

9.6. Experimental work

To compare short term properties of all the materials, used, tensile tests based on ISO 527-1 and DIN 53504 were performed on a Z010 from Zwick (Ulm, GER). To determine Young's modulus of the thermoplastic materials, tests were performed at 1 mm/min, then testing speed was increased to 50 mm/min. The H-NBR material was tested according to DIN 53504 at 100 mm/min throughout the whole test. All fatigue experiments were carried out on fatigue machines under sinusoidal load control using cracked round bar specimens. Specimens were machined using a commercial lathe. A sharp circumferential initial notch was inserted into the specimens using an off-the-shelf razor blade (thickness = 0.1 mm, tip-radius < 5 mm) mounted on a lathe. All tests were carried out at room temperature (23°C, 50% r.h.). Specimens were tested with a loading ratio of $R = 0.1$ (F_{min}/F_{max}). Calculations of K_{Imax} and ΔK_I were carried out according to the Benthem and Koiter formula [14]. To affirm quasi-brittle failure of the specimens, scanning electron microscopy (SEM) was performed on fracture surfaces after testing. All fractographic pictures were taken with a Tescan-Vega-II from Tescan (Brno, CZ). To cope with vastly different material behaviour, standard parameters of the CRB test, like load range and frequency, have been modified to fit the new materials. To test H-NBR, specimen geometry had to be changed according to Figure 9.1.

Frequency was chosen at 10 Hz for PE, PVC and POM according to findings or experience in literature (PE [15], POM [16], PVC [17]). For PP [7], PB, PA12 and HNBR [13] testing frequency was reduced to 5 Hz to avoid excessive hysteretic heating. Polyamides are hygroscopic materials and drastically change properties depending on water content and level of saturation. The PA12 material was stored at 23°C and 50% rH for 8 weeks after processing. Whereas the duration of 8 weeks is not long enough to achieve equilibrium, properties are changing slowly compared to directly after processing. Experiments on PA12 in this work only focus on the applicability of the cyclic CRB test. The results are not intended to be used to compare between different PA grades. To actually rank PA materials amongst

themselves, equilibrium state should be achieved before testing, to avoid influences of physical ageing during fatigue tests. Further test parameters are summarized in Table 9.1. All specimens were examined under a light-microscope after testing to measure the real initial crack length on the fracture surface for correct K_{Imax} calculation.

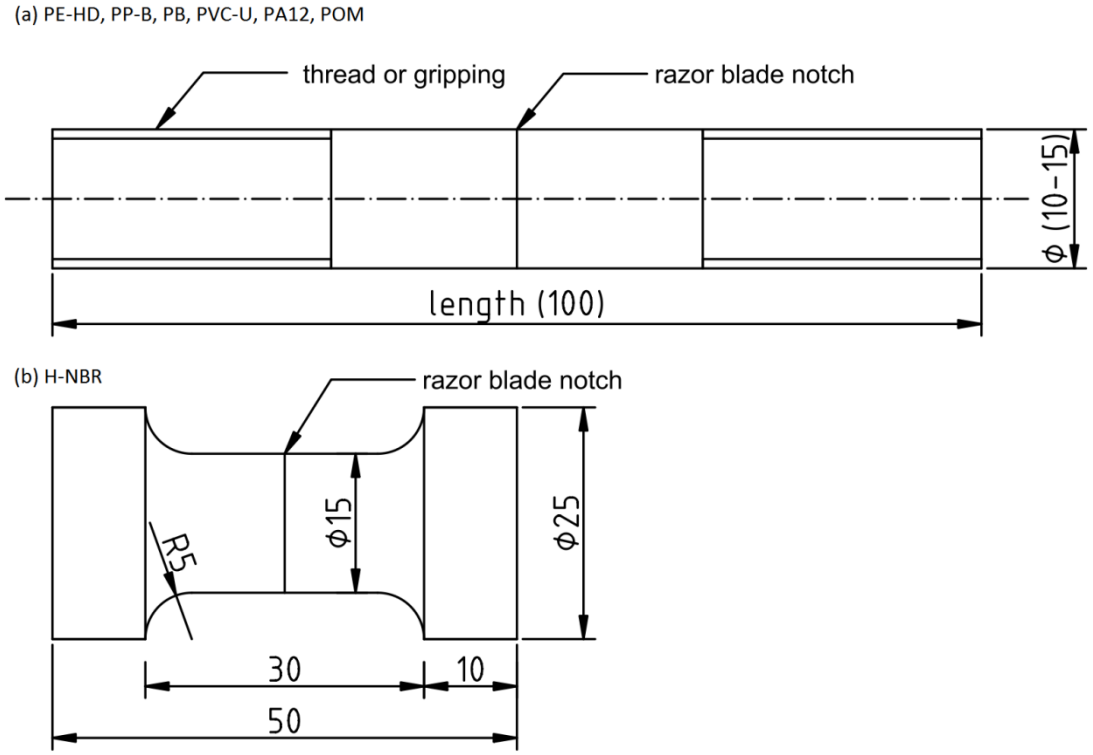

Figure 9.1: Geometries of used CRB-Specimens: (a) classical CRB-specimen ([8]); (b) CRB-specimen used for elastomers ([13]).

9.7. Results

Experiments can be divided into three parts, monotonic tensile tests, fatigue tests using CRB specimens and a comparison of fracture surfaces using SEM with crack opening displacement curves. Basic mechanical properties from monotonic tensile tests according to ISO 527 and DIN 53504 are shown in Table 9.2. For a better grasp of the differences in mechanical behaviour of the materials, averaged curves of five tests are shown in Figure 9.2 for each material.

Table 9.1: Testing parameters for the CRB fatigue tests

material	frequency [Hz]	diameter [mm]	target notch length [mm]	load-range [MPa]	load cell [kN]	machine type [-]
PE-HD	10	13.8	1.5	10 … 15	15	hydraulic$_1$
PP-B	5	15.0	1.5	13 … 16	15	hydraulic$_1$
PB	5	12.0	1.5	10 … 13	15	hydraulic$_1$
PVC-U	10	11.0	1.0	7.5 … 28	15	hydraulic$_1$
PA12	5	10.5	1.0	24 … 34	3	electrical$_2$
POM	10	10.0	1.0	26 … 44	15	hydraulic$_1$
H-NBR	5	15.0	1.5	1.8 … 2.3	3	Electrical$_3$

$_1$ MTS 858, MTS Systems GmbH (Eden Prairie, MN, USA)

$_2$ Acumen, MTS Systems GmbH (Eden Prairie, MN, USA)

$_3$ ElectroForce 3450, Bose Corporation (Eden Prairie, MN, USA)

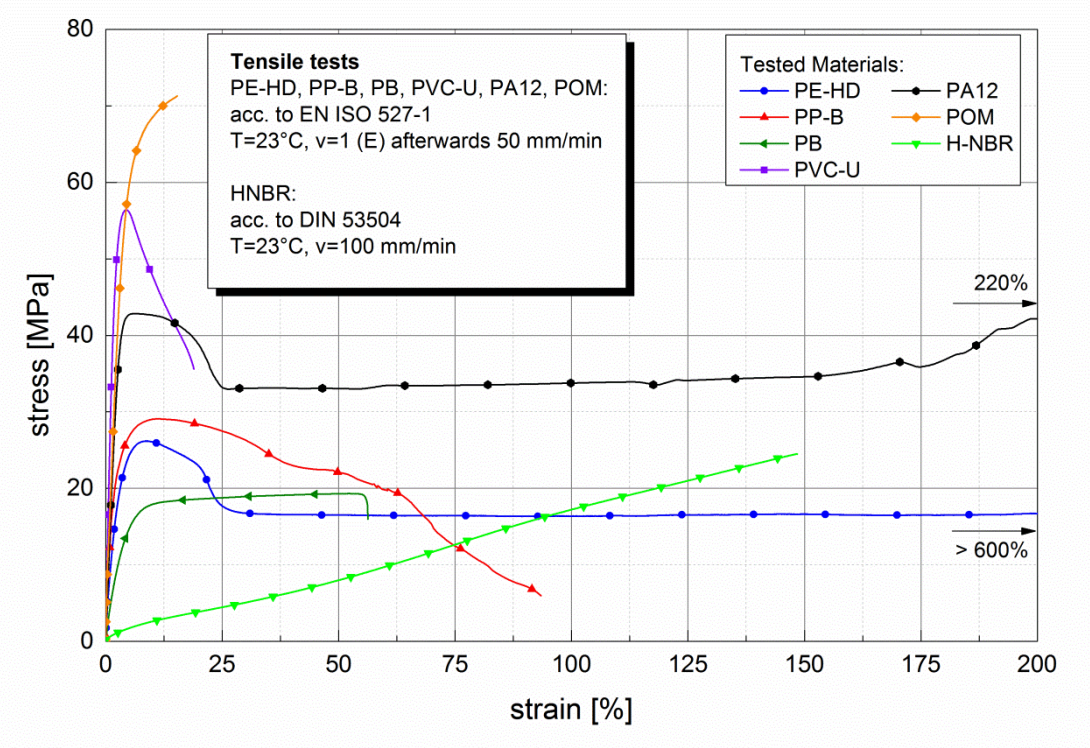

Figure 9.2: Comparison of tensile tests at room temperature for PE-HD, PP-B, PB, PVC-U, PA12, POM and H-NBR.

The second part of the results and main focus of this work are fatigue induced failure curves. An overview can be seen in Figure 9.3. All seven materials show a linear trend in a fully logarithmic diagram. Polyethylene, which is the material this test was developed for, could be fractured in quasi-brittle mode within $5 \cdot 10^5$ to $1.5 \cdot 10^6$ cycles, which corresponds to testing times of approx. 14-48 h.

The second commodity plastic, polypropylene, showed quasi-brittle failure at similar loading levels to polyethylene. However, testing times increased to $3 \cdot 10^6$ to $7 \cdot 10^6$ cycles, which corresponds to 7-14 days of testing. Higher loading levels lead to formation of large plastic zones during testing, and a failure mode mainly governed by large scale ductile deformation and tearing. The PB material fractured rather rapidly in comparison, between $3.0 \cdot 10^3$ and $3.0 \cdot 10^4$ cycles in the load range tested. PVC-U fractured between $5.0 \cdot 10^3$ and $4.0 \cdot 10^5$ cycles at ΔK_I values between 1.4 and 0.3 $MPam^{0.5}$. PA12 was tested between ΔK_I = 1.5 and 1.0 $MPam^{0.5}$. Since polyamides are prone to hysteretic heating during fatigue tests, temperature was measured using an IR-sensor close to the notch. The maximum temperature increase during testing was measured at ΔK_I = 1.5 $MPam^{0.5}$ and was approximately ΔT = 4.5°C. Below this ΔK_I value, temperature increase during tests was below ΔT = 2.0°C. Only towards the end of fatigue tests did temperature increase a little more due to higher local stresses in the vicinity of the crack tip. Specimens lasted between $1 \cdot 10^5$ and $1 \cdot 10^6$ cycles in this load range.

Polyoxymethylene could be tested at higher loading levels than polyethylene or polypropylene. Nevertheless, specimens fractured in a quasi-brittle mode within $2.8 \cdot 10^5$ to $3 \cdot 10^6$ cycles, or 8-83 h. Load levels of H-NBR were approximately one decade below those of PE and PP. Within a range of ΔK_I = 0.095 and 0.070 MPam0.5 specimens fractured within $1.5 \cdot 10^4$ and $3.5 \cdot 10^5$ cycles, which corresponds to 0.8 and 20 h of testing. It can be seen that all specimens fractured within comparatively quite short amounts of time, which could encourage using this test for comparisons of materials or ranking. However, for example, testing times for PP are quite high for fatigue tests. Therefore, higher temperatures could be used to decrease testing times, as proposed in Ref. [7]. However, due to different temperature dependence of polymeric materials there is no guarantee to get the same ranking at different temperatures.

Table 9.2: Basic properties of used materials:

Material	Young's Modulus [MPa]$_1$	Yield Stress [MPa]$_2$	Elongation at break [%]$_2$
PE	1150	27	>600
PP	1300	29	90
PB	480	19	56
PVC	3220	57	19
PA12	1470	43	215
POM	3100	71$_4$	15
H-NBR$_3$	17$_5$	23$_4$	150

$_1$ measured with 1 mm/min;

$_2$ measured with 50 mm/min;

$_3$ measured with 100 mm/min;

$_4$ ultimate tensile stress;

$_5$ stress at 100% strain acc. to DIN 53504

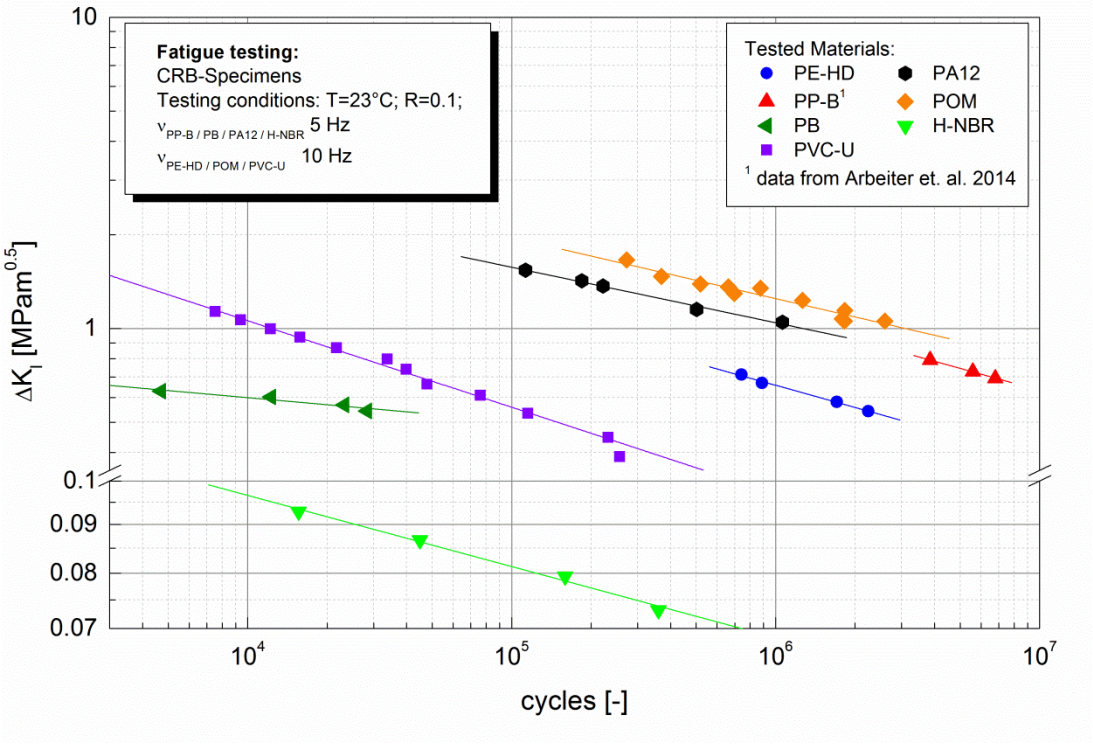

Figure 9.3: Results of fatigue testing via CRB-specimens: ΔK_I as a function of cycles to failure for all materials, tested at room temperature and a loading ratio of R=0.1. Data of PP-B taken from [7].

Interestingly, thermoplastic materials exhibit quite similar slopes, with the exception of PB, where the slope is not as steep and similar to the elastomeric H-NBR. The slopes in the fully logarithmic plot are as follows: PE-HD - 0.24; PP-B - 0.23; PB -0.08; PVC-U - 0.28; PA12 - 0.18; POM - 0.20; H-NBR - 0.07. Comparison of different materials is only possible if they fail in the same mode. A good tool to examine fracture behaviour is the use of SEM-fractography. Therefore, close attention has been paid to all fracture surfaces of the specimens. Figures 9.4-9.10 show the fracture patterns of all used materials at their initial applied stress intensity factor K_{Iini}. Similar to previous results of various authors (e.g. Ref. [18]),

PE shows three different stages of crack growth during a CRB fatigue test. The area close to the notch exhibits fine fibrillation, which is a classic appearance of both creep and fatigue crack growth in PE [2,19-24], consisting of discontinuous crack initiation and crack growth. The middle section of the specimen is dominated by ductile large scale tearing. In between is an area where the fine fibrillation of SCG changes to a coarser appearance, which is a classic sign of brittle - ductile transition. Furthermore, fine striations can be seen on the fracture surface, which are a clear indication of the former mentioned step-wise or discontinuous crack growth in fatigue testing of PE. The picture showing the area between transition and ductile tearing (Figure 9.4 top right) shows a rather flat surface with several grooves close to the large scale plastic deformations. This could be interpreted as a sign of plastic surface flow towards the large, highly stretched fibrils of final failure. Approximately 25-30% of the fracture surface can be attributed to the quasi-brittle failure mode.

The fracture surface of PP-B can also be roughly divided into three parts. The area close to the initial notch is again dominated by fine fibrillation, which grows coarser in the brittle - ductile transition area. In this area, fibrillations not only become coarser but are also drawn out in larger packages. The area in the middle of the specimen shows a rather smooth area compared to the middle area of PE. This could be an indication of large scale brittle failure, instead of ductile tearing.

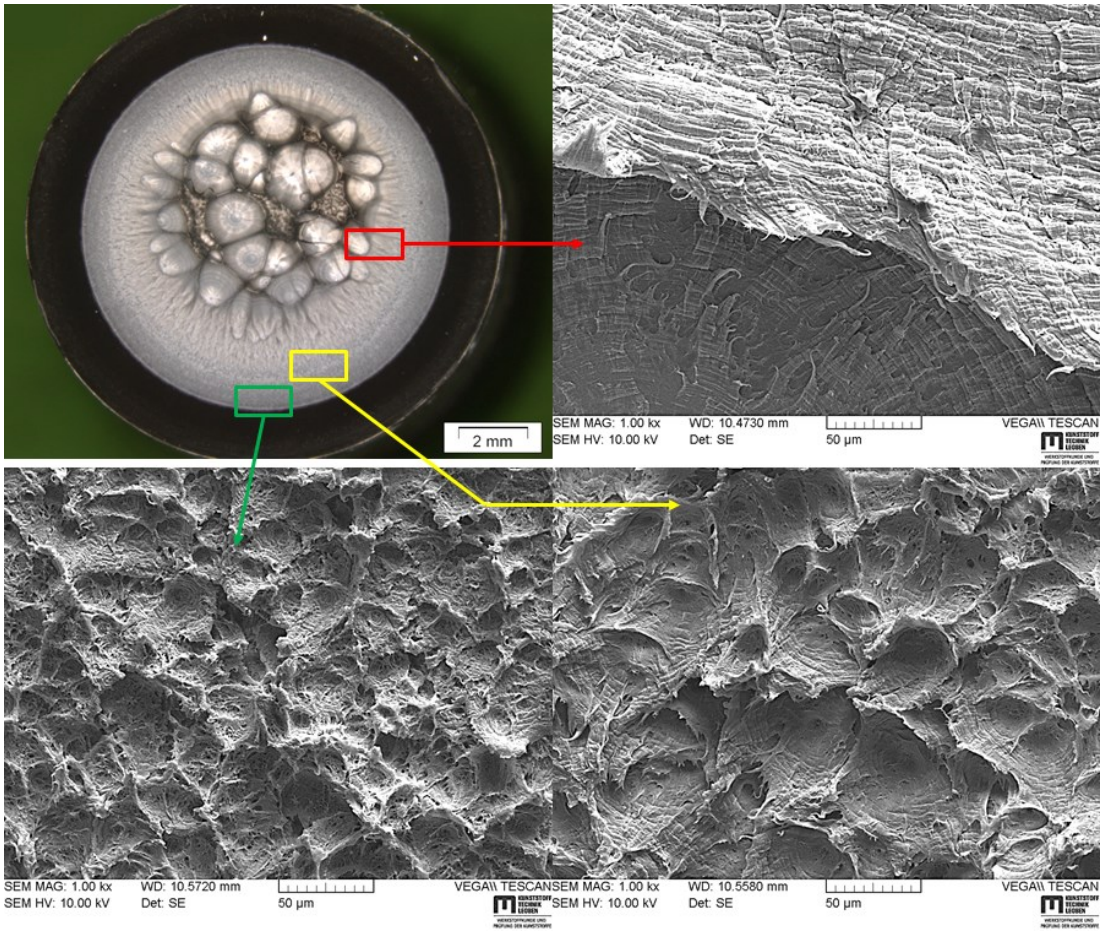

Figure 9.4: Areas of different crack growth mechanisms in PE CRB-specimen at K_{Iini} = 0.79 MPam$^{0.5}$.

Contrary to PE, there are no clear striations on the fracture surface. Previous work also shows that only a few steps in crack opening displacement signals can be found for this material [7]. The few steps compared to PE are also reflected in the fracture surface, where only about 10% can be attributed to a quasi-brittle failure mode. Scanning electron microscopy of the PB fracture surface showed the results depicted in Figure 9.6.

Close to the pre-notch the material showed formation of dimple-like structures with changing patterns of rather smooth areas and the formation of ductile deformed fibrils. This could be an indication of a step-wise crack growth, as indicated in Ref. [25]. Closer to the centre of the specimen the appearance changes into a rather smooth surface at the end of the last dimples with a sharp transition. The fracture of the residual specimen exhibits a very smooth surface without any signs of large scale deformation. The

dimple-like structure with fine fibrils covers around 20% of the fracture surface. Figure 9.7 shows the fracture surface of PVC-U at K_{Iini} = 0.823 MPam$^{0.5}$.

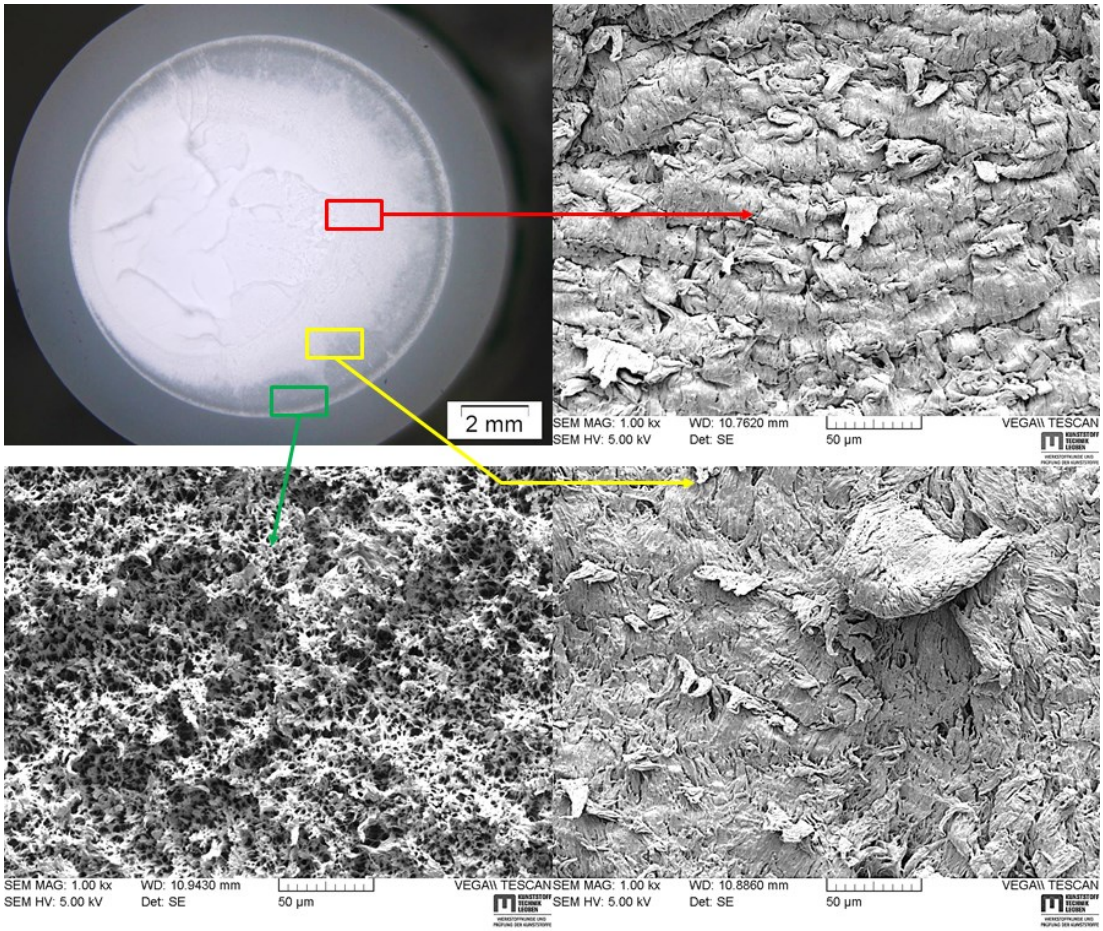

Figure 9.5: Areas of different crack growth mechanisms in PP-B CRB-specimen at K_{Iini} = 0.86 MPam$^{0.5}$.

Contrary to findings in literature (e.g. Refs. [17,26]), no clear fatigue induced striation-bands, or streak-like patterns can be seen on the fracture surface. However, compared to the SEM fractographs of fatigue induced PVC in Ref. [26], the coarse appearance without large plastic deformations seen on the bottom left of Figure 9.7 is quite comparable. Interestingly, close to the final failure the fracture surface still doesn't show formation of larger dimples, or rounded forms, which would be an indication of heat development close to the crack tip and/or a vibration induced creep fracture [26]. Therefore, it may be valid to speculate that the absence of typical fatigue striations is probably related to the steep slope of K_I as a function of crack length.

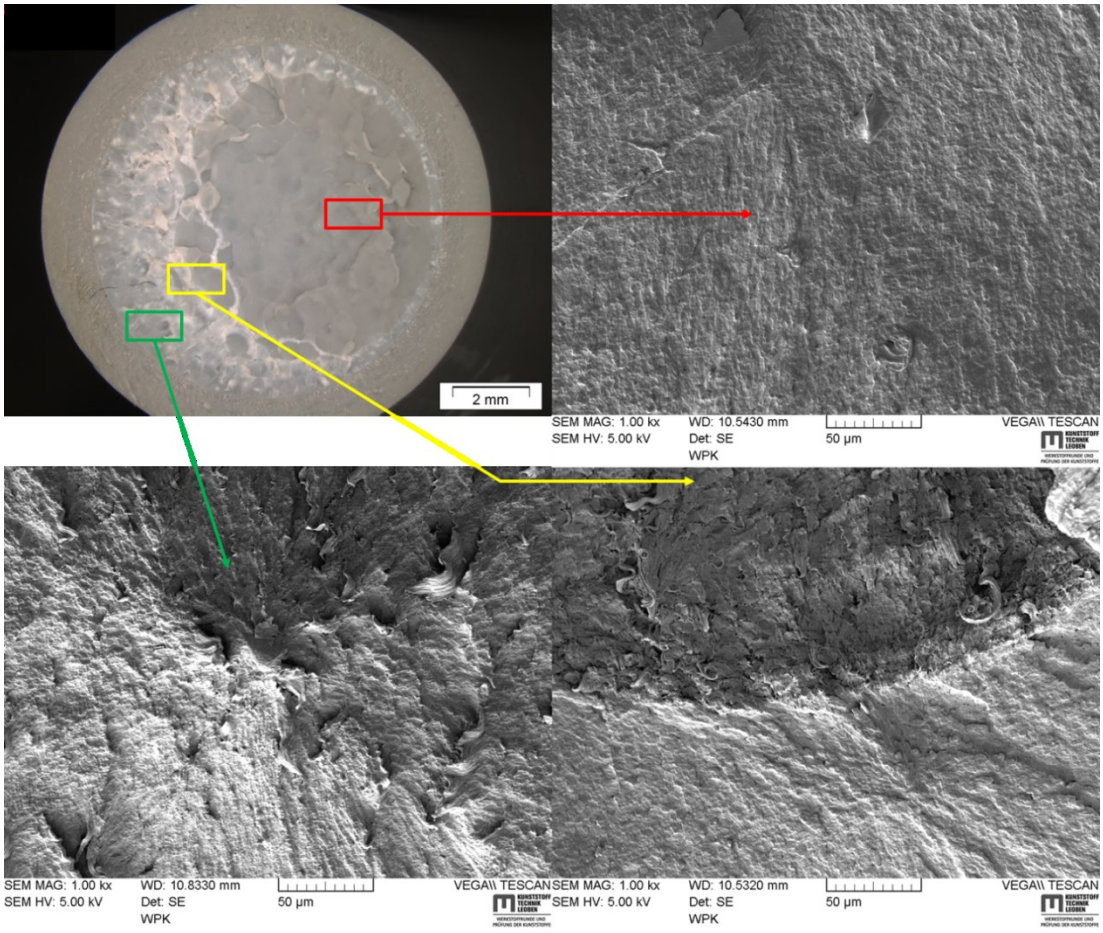

Figure 9.6: Areas of different crack growth mechanisms in PB CRB-specimen at K_{Iini} = 0.63 MPam$^{0.5}$.

Due to the rapid increase of K_I after crack initiation, there is not enough time for actual formation of striations, and the crack grows continuously through the material. Compared to the polyolefin materials tested before, the area before change in mode of fracture is significantly larger, at around 40 - 45%. Fracture surfaces of PA12 show a formation of several striations, number depending on load level, close to the pre-notch. Examination of these striations show fine ruptured fibrils, similar to PE (Figure 9.4). The appearance of this area is comparable to results found in Ref. [27] for PA12 grades suitable for laser sintering. With increasing crack length and higher local loads, fine ruptured fibrils are exchanged for larger dimples. The last area depicted at the top right shows a very smooth surface without signs of ductile deformation. For PA12, the area showing striations is only covering

around 5% of the fracture surface. The second area which still shows signs of ductile deformation covers an additional 35%.

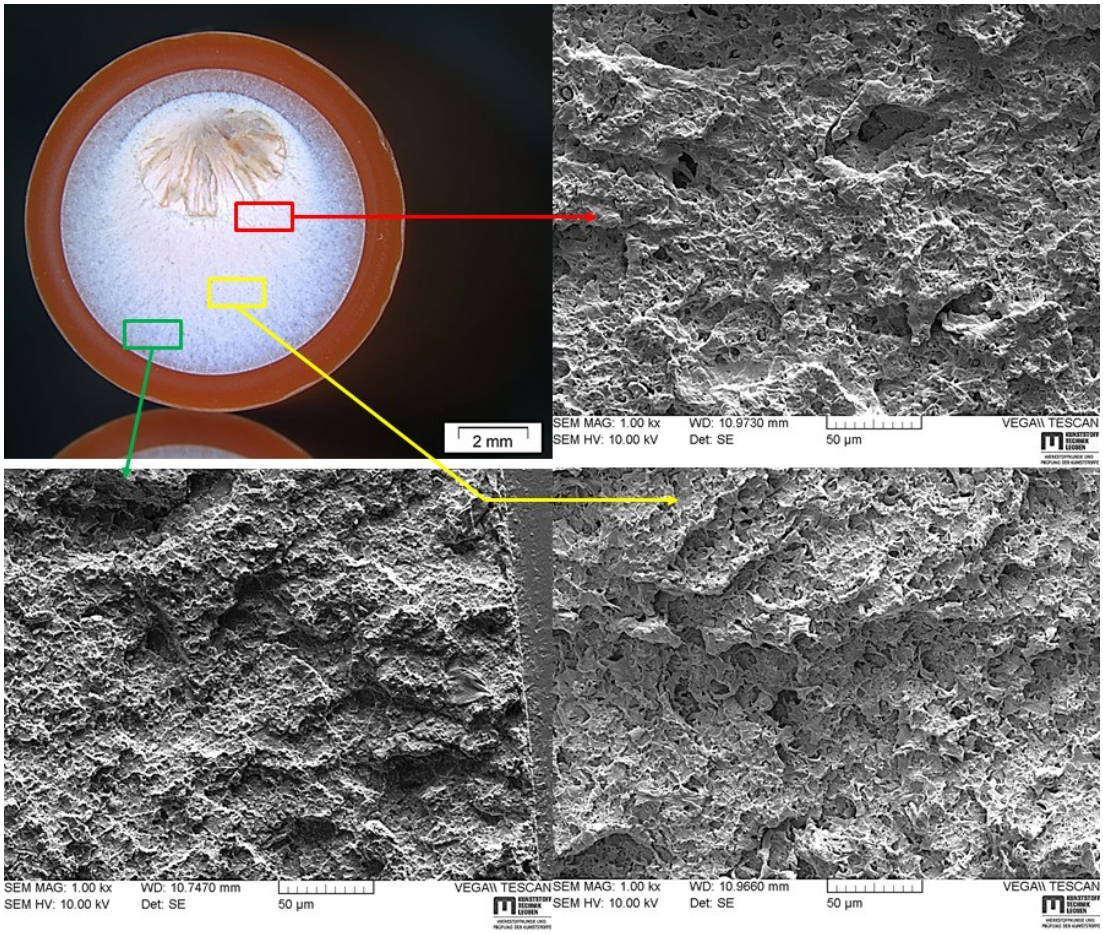

Figure 9.7: Areas of different crack growth mechanisms in PVC-U CRB-specimen at K_{Iini} = 0.83 MPam$^{0.5}$.

Compared to PE and PP, there are no areas with large fibrillations at the fracture surface of the POM (Figure 9.9). The area close to the notch is a rather plane surface with small flaky patterns, quite similar to fracture surfaces found in CT-specimen fatigue tests of the same material [16]. Following, is the transition area, where the surface is covered with small grooves, quite similar to the top right picture of Figure 9.4 for PE. This could again be an indication of plastic flow on the surface towards the final failure area in the middle of the specimen. The third area is again the fracture of the residual specimen area. Due to the rather high stress and low elongation at yield, this area has a rather coarse appearance, without big ductile

deformations. The area, which can be addressed to the quasi-brittle failure mode, is around 30% of the fracture surface.

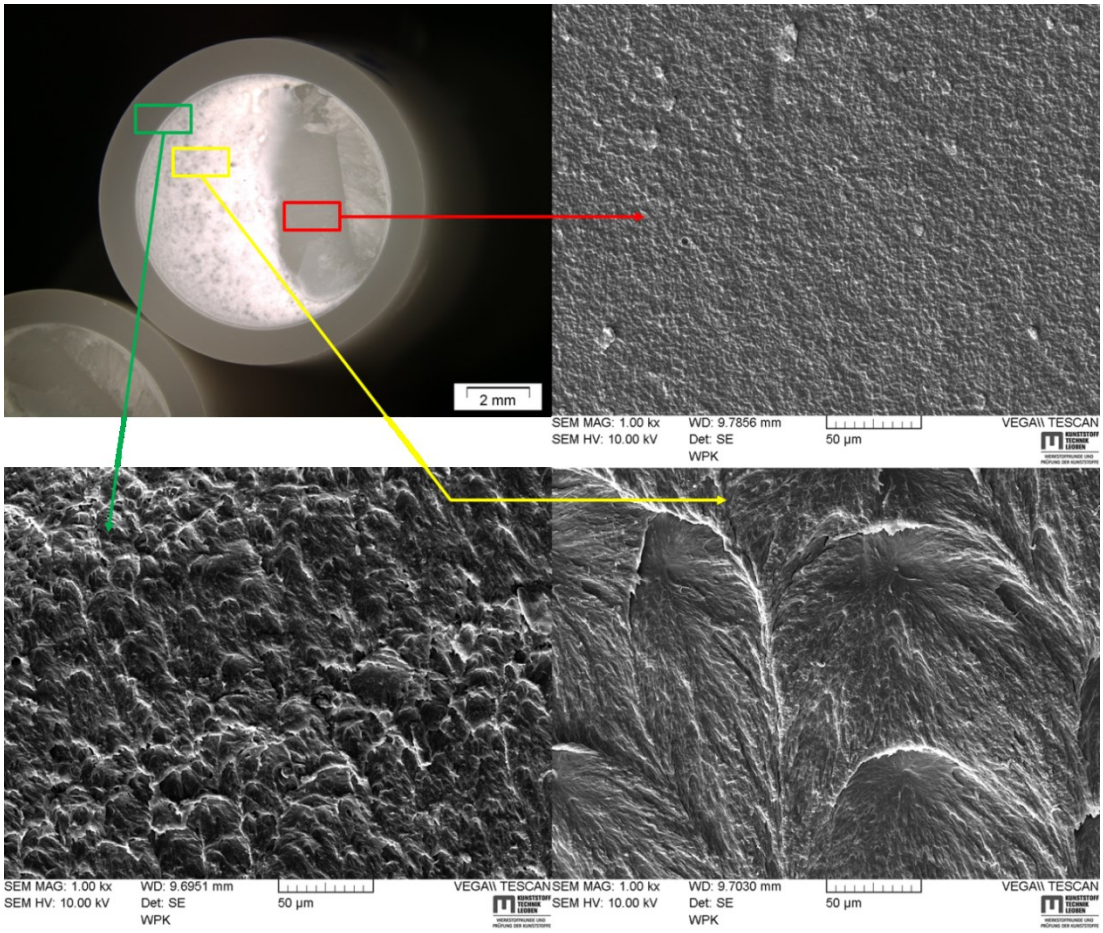

Figure 9.8: Areas of different crack growth mechanisms in PA12 CRB-specimen at K_{lini} = 1.37 MPam$^{0.5}$.

Compared with PE, PP, PVC and POM, H-NBR shows no classical signs of thermoplastic slow crack growth (e.g. fibrills). On the contrary, the fracture surface shows no clear signs of plastic deformation. This can of course be attributed to the chemical structure of the material. Compared to the other six materials, H-NBR is a crosslinked elastomer. Therefore, crack propagation does not occur, mainly due to disentanglement of molecule chains, like in PE [28], but more so due to the breaking of covalent bonds [29], resulting in more brittle failure (Figure 9.10).

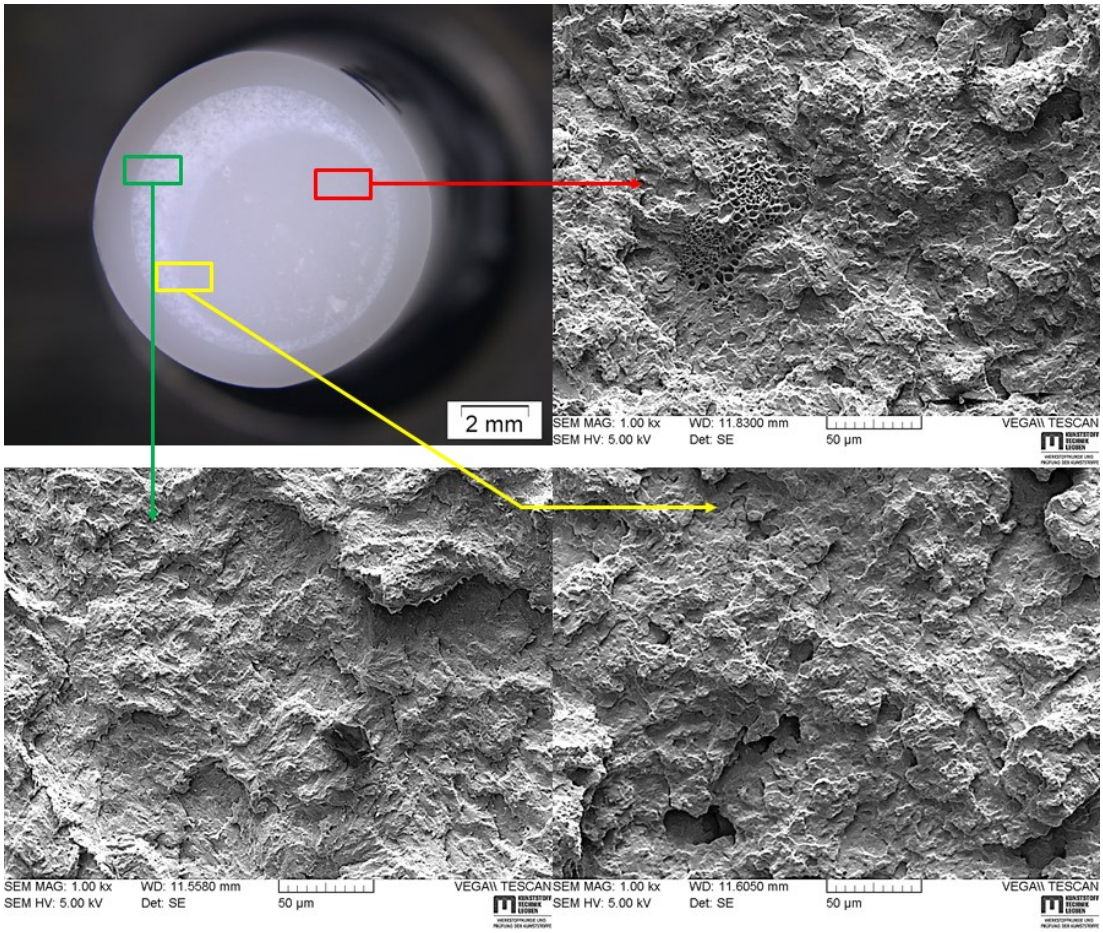

Figure 9.9: Areas of different crack growth mechanisms in POM CRB-specimen at K_{Iini} = 1.39 MPam$^{0.5}$.

For additional insight into the failure behaviour and differences in crack initiation and propagation times, crack opening displacement (COD) measured close to the notch can be used. In Figure 9.11, the difference between maximum and minimum crack opening during cycles is shown as ΔCOD. It is plotted as a function of test progress for all seven tested materials.

The ΔCOD signals shown in Figure 9.11 can be used to gain more information about the failure mechanisms of different tested materials. The trends shown are normalized to their initial values and can only be used as a qualitative comparison. Phenomena such as crack initiation can also be load dependent and change at a different loading level. The curves shown are only representative curves for one load level to show significant differences in the shape of the curves. In the case of PE-HD and PB, clear signs of step-

wise crack growth are shown, which correspond to fracture surface appearance. For the chosen load levels, initiation can be seen as a first shoulder in the signal at around 30% of the test progress. PP-B and PA12 show only indications of steps in the signals. For PP-B, the steps start to show around 80% of the testing time, which was already shown in Ref. [7]. The waves before this point can be attributed to small changes in ambient temperature ($\Delta T < 0.5°C$) during the test. Due to the testing temperature of 23°C, which is close to T_g, small changes are already visible in ΔCOD signals. Precise temperature control is necessary in order to avoid the danger of mistaking temperature influences for crack initiation. For PA12, it is not clearly distinguishable at which exact point crack initiation starts. Although there are striations visible on the fracture surfaces, they cannot easily be linked to changes in the signal. As predicted by facture surfaces, the PVC-U shows no step-wise crack growth in the ΔCOD signal, but a monotonic increase after an initial constant period of ca. 30%. Contrary to other materials tested, POM shows a decrease in ΔCOD after the first initial value, which then stays constant for an extended period of time. Afterwards, ΔCOD increases monotonically until final failure. H-NBR shows a steep increase at the beginning of the test, followed by a shallower but constant increase of the ΔCOD signal. Towards the end of the test, ΔCOD increases more rapidly again, leading to the final failure of the specimen.

9.8. Summary and outlook

The cyclic CRB test, which has been developed as a faster ranking method for PE-HD pipe grades, was successfully used to induce quasi-brittle failure in seven different polymers. This suggests the applicability in principle of this method to other materials. The materials used in this work range from commodity plastics (PE, PP, PB & PVC), to technical polymers (PA12 & POM) and elastomers (H-NBR). Although properties of the examined materials differ greatly, all showed a linear relationship within a fully logarithmic plot of applied ΔK_I and cycles to failure. The cyclic CRB test managed to induce fracture of specimens within several days of testing, which is a significant decrease in testing times, compared to classical tests.

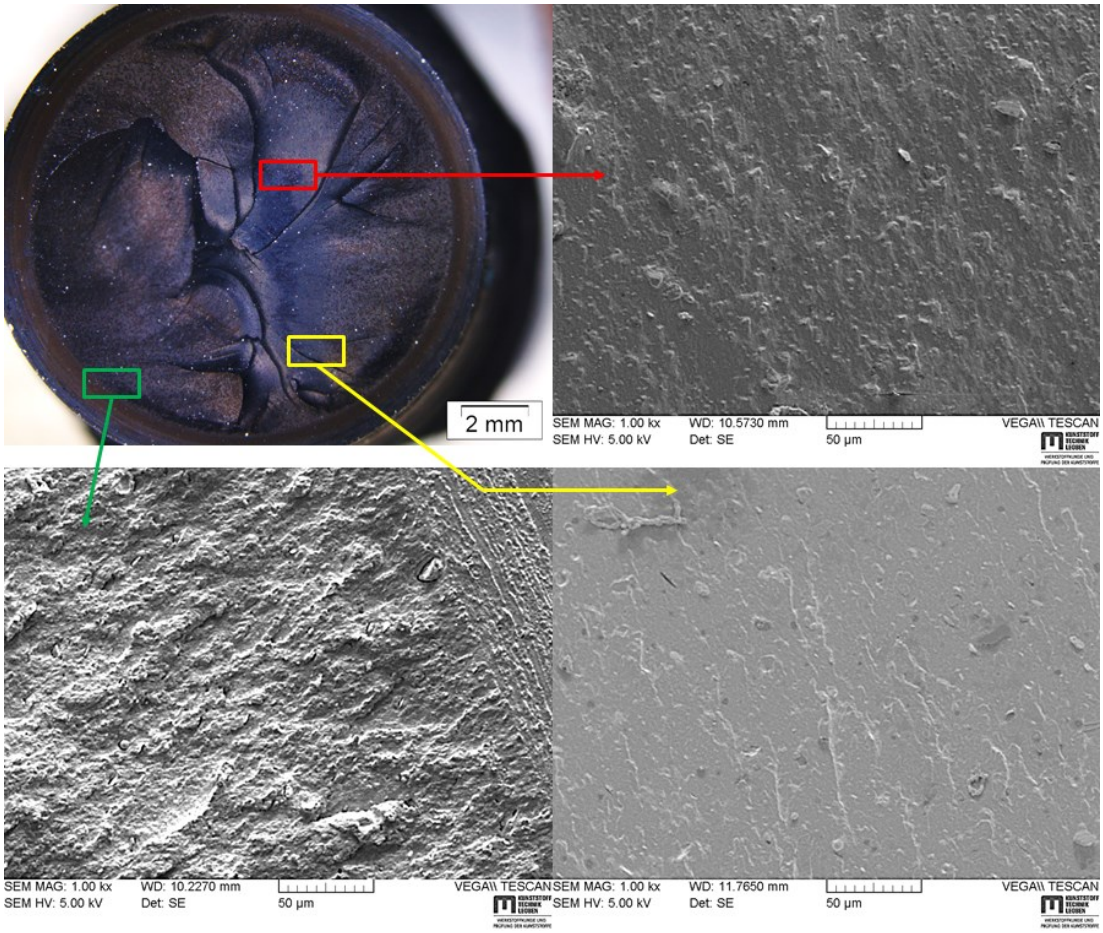

Figure 9.10: Areas of different crack growth mechanisms in H-NBR CRB-specimen at K_{Iini} = 0.09 MPam$^{0.5}$.

Fracture surfaces of the CRB specimens were examined using SEM. All seven materials were examined with regard to changes in fracture mechanisms during the test. PE and PP showed fracture surfaces comparable to literature (e.g. Refs. [30-32,21] for PE). PE-HD showed clear striations on the fracture surface, which is characteristic of step-wise crack growth. PP-B only showed one ring close to the pre-notch. Closer examination of this area revealed stretched and fractured fibrils, similar to PE. Decreasing the applied load to check for discernible step wise crack growth led to rather long testing times at 23°C and specimens did not fracture within $1 \cdot 10^7$ cycles. Further testing would be advisable, possibly at higher temperatures to decrease testing times, as suggested in Ref. [7].

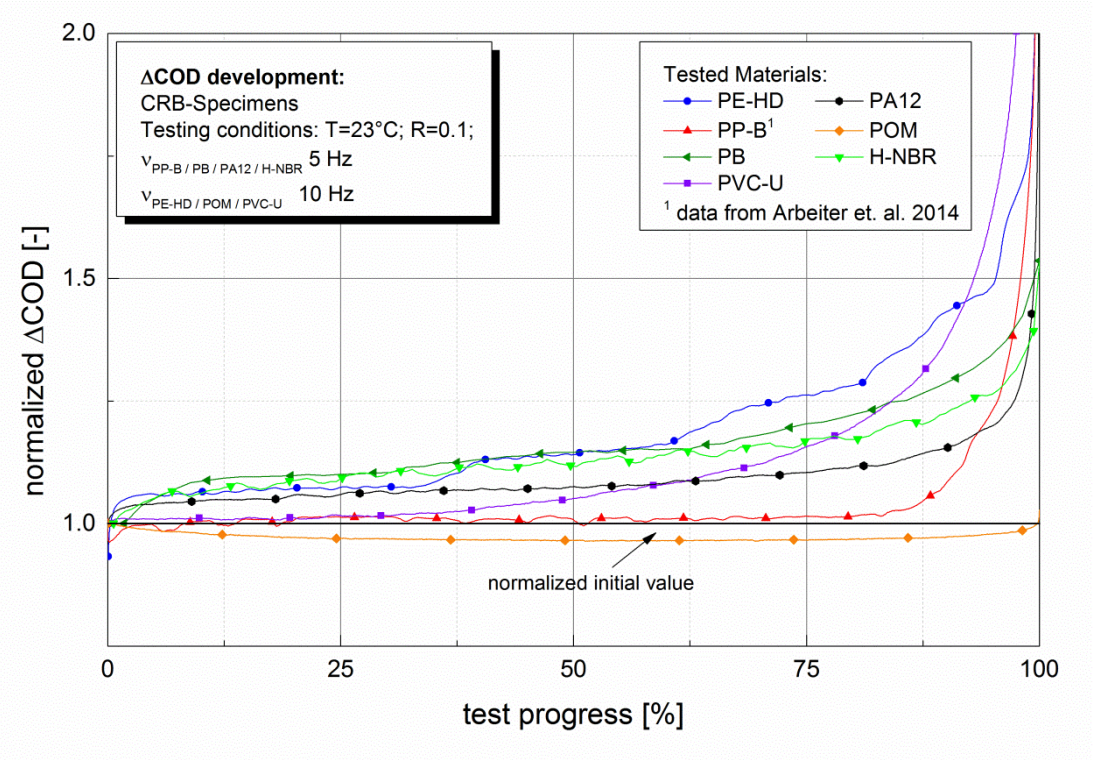

Figure 9.11: Differences in crack opening displacement trends of tested materials.

Polybutylene showed formation of a dimple-like structure close to the pre-notch. The surface of dimples alternated between micro-ductile and a rather smooth appearance, which might be an indication of a step-wise crack growth, as also suspected in Ref. [25]. Contrary to findings in literature, PVC-U showed no formation of discernible striations [17,33,34]. This may be attributed to the rapid increase of K_I as soon as a crack initiates. The linear relation between KI and cycles to failure could be measured over a large stress range between 7.5 and 28 MPa. The measured yield stress of this PVC was around 57 MPa. Therefore, the load level itself is probably not the cause of the absence of striations. The examined PA12 material showed some striations close to the pre-notch with ruptured fibrils. Closer to the centre a dimple-like pattern was dominant, before changing to a flat surface. POM also showed fracture surfaces similar to literature [16] without signs of ductile deformation, such as stretched fibrils, at a magnification of 1000-times. H-NBR also exhibits a rather smooth fracture surface. Contrary to the thermoplastic materials, there is apparently no drastic change in fracture

mechanisms throughout the test. The use of this test for a ranking of sealing materials has also recently been suggested in Ref. [13].

Observation of ΔCOD signals can also be used to get further insight into the fracture mechanisms of the respective material. It was found that, for PE-HD and PB as well as PP-B and PA12 to a certain amount, ΔCOD signals and fracture surfaces can be correlated. PVC-U, POM and H-NBR showed no signs of step-wise crack growth, but rather a continuous increase of ΔCOD until final failure. Research work for PE-HD has shown that the CRB method is not only usable as a faster ranking tool compared with classic methods, but can also be used for lifetime estimation of pipes made from PE [35-40]. It would be of high interest to further investigate the cyclic CRB test for the materials used in this work, since they are also used in long-term applications.

9.9. Acknowledgements

The research work of this publication was performed at the Institute of Materials Science and Testing of Polymers (Montanuniversitaet Leoben, Austria) within the framework of the FFG program of the Austrian Ministry of Traffic, Innovation and Technology and the Austrian Ministry of Economy, Family and Youth. Furthermore, work of this paper was also performed at the Polymer Competence Center Leoben GmbH (PCCL, Austria) within the framework of the COMET-Project of the Austrian Ministry of Traffic, Innovation and Technology.

9.10. References

[1] Frank A, Pinter G. Evaluation of the applicability of the cracked round bar test as standardized PE-pipe ranking tool. Polymer Testing 2014;33:161–71.

[2] Frank A, Lang RW, Pinter G. Accelerated Investigation of creep crack growth in polyethylene pipe grade materials by the use of fatigue tests on cracked round bar specimens: Proceedings Annual Technical Conference - ANTEC, Society of Plastics Engineers, Milwaukee, Wisconsin, USA 2008:2435–9.

[3] ONR. Determination of the resistance of slow crack growth of polyehtylene with cracked round bar (CRB) specimens(ONR 25194 (2011 10 01)); 2011.

[4] Frank A, Freimann W, Pinter G, Lang RW. A fracture mechanics concept for the accelerated characterization of creep crack growth in PE-HD pipe grades. Engineering Fracture Mechanics 2009;76:2780–7.

[5] ISO 16770. Plastics -- Determination of environmental stress cracking (ESC) of polyethylene -- Full-notch creep test (FNCT); 2004.

[6] ISO 13479. Polyolefin pipes for the conveyance of fluids -- Determination of resistance to crack propagation -- Test method for slow crack growth on notched pipes; 2009.

[7] Arbeiter F, Pinter G, Frank A. Characterisation of quasi-brittle fatigue crack growth in pipe grade polypropylene block copolymer. Polymer Testing 2014.

[8] ISO. Polyethylene (PE) materials for piping systems — Determination of resistance to slow crack growth under cyclic loading — Cracked Round Bar test method(18489); 2015.

[9] Lang RW. Applicability of linear elastic fracture mechanics to fatigue in polymers and short-fiber composites. Dissertation. Bethlehem, Pennsylvania; 1984.

[10] Ceresana Research. Market Study: Plastic Pipes; 2011.

[11] Uni-Bell PVC Pipe Association. Handbook of PVC pipe design and construction. 5th ed. New York, NY: Industrial Press; 2012, c2013.

[12] Domininghaus H, Eyerer P, Elsner P, Hirth T. DOMININGHAUS-Kunststoffe: Eigenschaften und Anwendungen: Springer; 2007.

[13] Schrittesser B. Performance of elastomers for high-pressure applications. Dissertation. Leoben; 2014.

[14] Benthem J, Koiter W (eds.). Method of Analysis and Solutions of Crack Problems. 3rd ed; 1973.

[15] Arbeiter F, Frank A, Pinter G. Impact of Single and Dual Pressure Butt-Welding Procedures on the Reliability of Pe 100 Pipe Welds. In:

Brown HL, Jones DH, editors. EUROTEC® 2013: Proceedings of the 2nd European Technical Conference & Exhibition; 2013, p. 466–471.

[16] Berer M, Pinter G, Feuchter M. Fracture mechanical analysis of two commercial polyoxymethylene homopolymer resins. J. Appl. Polym. Sci. 2014:n/a.

[17] Hertzberg RW, Manson JA. Micromechanisms of fatigue-crack advance in PVC. J Mater Sci 1973;8:1554–8.

[18] Pinter G, Haager M, Balika W, Lang RW. Cyclic crack growth tests with CRB specimens for the evaluation of the long-term performance of PE pipe grades. Polymer Testing 2007;26:180–8.

[19] Parsons M, Stepanov EV, Hiltner A, Baer E. Correlation of fatigue and creep slow crack growth in a medium density polyethylene pipe material. Journal of Materials Science 2000;35:2659–74.

[20] Brown N, Donofrio J, Lu X. The transition between ductile and slow-crack-growth failure in polyethylene. Polymer 1987;28:1326–30.

[21] Favier V, Giroud T, Strijko E, Hiver J, G'Sell C, Hellinckx S et al. Slow crack propagation in polyethylene under fatigue at controlled stress intensity. Polymer 2002;43:1375–82.

[22] Hamouda HBH, Simoes-betbeder M, Grillon F, Blouet P, Billon N, Piques R. Creep damage mechanisms in polyethylene gas pipes. Polymer 2001:5425–37.

[23] Pinter G, Balika W, Lang RW. A correlation of creep and fatigue crack growth in high density poly(ethylene) at various temperatures 2002;29:267–75.

[24] Pinter G, Lang RW. Creep Crack Growth in High Density Polyethylene. The Application of Fracture Mechanics to Polymers, Adhesives and Composites 2004:47–54.

[25] Andena L, Rink M, Frassine R, Corrieri R. A fracture mechanics approach for the prediction of the failure time of polybutene pipes. Engineering Fracture Mechanics 2009;76:2666–77.

[26] Ehrenstein GW. SEM of plastics failure: REM von Kunststoffschäden. Munich, Cincinnati: Carl Hanser Verlag; Hanser Publishers; ©2011.

[27] Salazar A, Rico A, Rodríguez J, Segurado Escudero J, Seltzer R, Martin de la Escalera Cutillas, F. Fatigue crack growth of SLS polyamide 12: Effect of reinforcement and temperature. Composites Part B: Engineering 2014;59:285–92.

[28] Huang Y, Brown N. Dependence of slow crack growth in polyethylene on butyl branch density: Morphology and theory. J. Polym. Sci. B Polym. Phys. 1991;29:129–37.

[29] Hamed GR. Molecular Aspects of the Fatigue and Fracture of Rubber. Rubber Chemistry and Technology 1994;67:529–36.

[30] Parsons M, Stepanov EV, Hiltner A, Baer E. Correlation of stepwise fatigue and creep slow crack growth in high density polyethylene. Journal of Materials Science 1999;34:3315–26.

[31] Shah A, Stepanov EV, Capaccio G, Hiltner A, Baer E. Stepwise fatigue crack propagation in polyethylene resins of different molecular structure. J. Polym. Sci. B Polym. Phys. 1998;36:2355–69.

[32] Zhou Z, Hiltner A, Baer E. Predicting long-term creep failure of bimodal polyethylene pipe from short-term fatigue tests. J Mater Sci 2011;46:174–82.

[33] Skibo MD, Manson JA, Hertzberg RW, Collins EA. Effects of molecular weight and plasticizer on fatigue crack propagation in PVC. J. of Macromolecular Sc., Part B 1977;14:525–43.

[34] Schinker MG, Könczöl L, Döll W. SEM observations of broken fibrils at fatigue fracture in PVC. J Mater Sci Lett 1982;1:475–8.

[35] Pinter G, Arbeiter F, Berger I, Frank A. Correlation of Fracture Mechanics Based Lifetime Prediction and Internal Pipe Pressure Tests. In: Proceedings Plastic Pipes XVII 2014; 2014.

[36] Frank A, Pinter G, Lang RW. Lifetime prediction of polyethylene pipes based on an accelerated extrapolation concept for creep crack growth with fatigue tests on cracked round bar specimens. In: Society of Plastics Engineers, editor. ANTEC; 2009, p. 2169–2174.

[37] Frank A, Pinter G, Lang RW. Fracture Mechanics Lifetime Prediction of PE 80 and PE 100 Pipes under Complex Loading Conditions. In Proceedings Plastics Pipes XV Vancouver (Cdn) 2010.

[38] Hutař P, Ševčík M, Náhlík L, Frank A, Kučera J, Pinter G. Numerical Lifetime Prediction of Polymer Pipes Taking into Account Residual Stress. KEM 2013;577-578:169–72.

[39] Hutař P, Ševčík M, Náhlík L, Pinter G, Frank A, Mitev I. A numerical methodology for lifetime estimation of HDPE pressure pipes. Engineering Fracture Mechanics 2011;78:3049–58.

[40] Frank A. Fracture Mechanics Based Lifetime Assessment and Long-term Failure Behavior of Polyethylene Pressure Pipes: Dissertation. Disseratation. Leoben, Austria; 2010.

10. Publication 4

10.1. Bibliographic information

- Title: Characterisation of quasi-brittle fatigue crack growth in pipe grade polypropylene block copolymer
- Authors and relevant contributions to this publication:
  - Florian ARBEITER[1]

    Experimental testing, data evaluation, preparation of the publication
  - Gerald PINTER[1,2]

    Discussion and scientific guidance
  - Andreas FRANK[2]

    Discussion and scientific guidance
- Affiliation:
  1. Institute of Materials Science and Testing of Polymers, Montanuniversitaet Leoben, Otto Glöckel-Strasse 2, 8700 Leoben, Austria
  2. Polymer Competence Center Leoben GmbH, Roseggerstr. 12, 8700 Leoben, Austria
- Periodical: Polymer Testing
- DOI: 10.1016/j.polymertesting.2014.05.016

Statement with regard to this publication: The manuscript presented here is an adapted manuscript in order to fit the formatting of the thesis and does not necessarily reflect exactly the actually accepted version.

10.2. Abstract

The aim of this work was to characterise quasi-brittle fatigue crack growth in a pipe grade polypropylene block copolymer. Cyclic cracked round bar specimen tests have been identified as a possible way to induce cyclic quasi-brittle crack growth within a reasonable amount of time. To ensure quasi-brittle failures, fracture surfaces have been examined using scanning electron microscopy. For further acceleration of the tests, higher temperatures with adapted load ranges have been applied. For 50°C and 80°C, a decrease in testing times of approx. 60% and 80% was achieved without significant changes in failure behaviour (e.g. cyclic crack opening displacement ($\Delta\delta$) curves or fracture surfaces) of the tested specimens. Relationships between applied load and testing times, as well as between crack initiation and failure have been examined. A change in ratio of crack initiation to total failure time was observed at higher temperatures. This has to be considered in future tests, especially when comparing different types of polypropylene at temperatures, differing from the real application.

Polypropylene is a widely used material in industrial applications. Besides extensive use as thin sheet (e.g. packaging) it has also been established for structural applications, such as pipes [1]. Therefore, the characterisation of long-term properties and failure and fracture modes is crucial. There is extensive literature on the fracture behaviour of various types of unfilled and filled polypropylene used for injection moulding, compression moulding, etc. using linear elastic [2,3], elastic plastic [2,4,5] or post-yield fracture mechanics [6]. However, most of this research focuses on polypropylene types not usable for structural applications such as pipes. For pipes, usually block- (PP-B), random- (PP-R), or homo polypropylene (PP-H) types with low melt flow rates (approx. 0.1 to 1 g/10 min) and high resistance against crack growth are used. Due to the ductile behaviour of the material, brittle facture tests are usually performed at either very low temperatures or high testing speed (e.g. impact testing [3]). When talking about structures that have to last at least 50 or even 100 years, slow crack growth (SCG) and/or fatigue failure always play important roles in engineering materials [7]. Impact or high speed tests are not adequate for describing this type of failure. Therefore, tests which describe SCG within reasonable amounts of times are needed. For high density polyethylene (PE-HD), several methods, such as the Full

Notched Creep Test [8], Pennsylvania Edge-Notch Test [9], Notched Pipe Test [10], internal pressure test [11] etc., to describe SCG are available. For polypropylene used in piping, there are fewer possibilities to characterise SCG. The main method to describe SCG in polypropylene pipe grades is the internal pressure test according to ISO 9080 [11] or ASTM D2837 [12]. However, testing modern polypropylene pipe grades takes extensive amounts of time when trying to achieve brittle failure. For example, authors in [13] have shown that, similar to PE-HD, brittle fractures in PP-R pipes under hydrostatic pressure only occur at either high temperatures (95°C) and/or after very long times (10.000 hours) of testing. Therefore, faster methods to characterise SCG in polypropylene pipe grades are needed. Test specimens which favour brittle failure is of high interest in the general field of engineering, since many failures in real structures are of this type. Fractures in brittle mode can be described using various methods, e.g. linear elastic fracture mechanics (LEFM). An advantage of this method is the principle of crack tip stress similitude, which allows transferring the stress distribution in front of a specified crack in a test specimen to a crack in an engineering structure. Therefore, LEFM parameters such as the applied stress intensity factor (K_I) or geometry independent critical stress intensity factor (K_{IC}) can be used to describe stresses, fracture or crack growth in applications without costly and time consuming component testing. The index “I” describes crack opening mode. All tests in this work are performed in this mode, which represents the most relevant loading mode [7]. LEFM has been used to describe long-term failure of engineering materials for several decades [7,14-17]. However, the disadvantage of this approach is that the restrictions on plastic zone formation and applicable load levels are quite high. Therefore, most of the standard tests and specimens used in LEFM cannot be applied to the rather ductile PP-B within feasible lengths of time. The application of a cracked round bar specimen (CRB) in fracture mechanics testing has been discussed for several years now [18-22]. This test shows promise in the endeavour to describe SCG in ductile piping materials. The CRB-test, as described in ONR 25194 [23], has been developed for the characterisation of SCG in tough high density polyethylene (PE-HD) materials used in piping applications by applying fatigue loads on the specimen [24-31]. Studies have shown that this type of loading can induce similar failure to SCG in real PE-HD pipes [27,32-39]. The advantage of this test is the circumferentially notch

around the specimen which promotes a plain strain state around the notch and decreases plastic zone sizes significantly compared to standard LEFM specimens (e.g. the Compact tension specimen). Another advantage is the steep slope of the K_I development inside the specimen as a function of crack length (a). Once crack growth initiates K_I increases rapidly, which again favours shorter testing times. Due to the high potential of this test to describe SCG in rather ductile polymers, it is used in this work to characterise SCG in PP-B. To gain further insight into the quasi-brittle crack growth of PP-B, to determine possible testing load ranges and to work out an optimum between testing time and the correct description of quasi-brittle crack growth, CRB-tests have been carried out at different temperatures.

10.3. Keywords:

Block polypropylene, Brittle fracture, Cracked round bar specimen, Fatigue

10.4. Background

For LEFM to be applicable to polymers there are two main preconditions. Applied loads have to be within the range of linear viscoelasticity and the plastic zone development at the crack tip has to be small in size [16]. Meeting these conditions, the method of the stress intensity factor, which describes the stress distribution (Equation 10.1, σ_I … applied global stress; a … crack length; Y … geometry factor) in front of a crack tip, can be applied [14].

$$K_I = \sigma_I \cdot \sqrt{a} \cdot Y \tag{10.1}$$

Aforementioned requirements for the application of LEFM are quite hard to meet with rather ductile polymers. Especially, the minimisation of plastic zone development poses serious difficulties. Therefore, the circumferentially notched CRB-specimens, which possess no free surfaces perpendicular to the notch tip, where usually plane stress instead of plane strain develops, provide an advantage. To decrease plastic zone sizes and decrease crack growth initiation and crack growth time, cyclic loading can be applied. To describe cyclic tests, often the difference between maximum and minimum applied stress intensity factor ΔK_I (Equation 10.2) during a cycle is used.

$$\Delta K_I = \Delta\sigma_I \cdot \sqrt{a} \cdot Y \tag{10.2}$$

Crack growth in polyolefin materials is mainly governed by the disentanglement and partially breakage of molecule-chains in front of the crack tip [32,40-42]. These failure mechanisms are dependent on the applied overall load, which leads to formation of high stress concentrations in front of a crack tip, according to Equations 10.1 and 10.2. Therefore, in order to not invalidate the application of LEFM or even transgress into ductile failure during testing, loads cannot be increased to further shorten testing times. Due to the high temperature dependence of disentanglement and chain breakage, higher temperatures should lead to shorter testing times [42,43]. Increasing the temperature is possible as long as no serious changes in failure mechanisms, by entering transition areas (e.g. glass transition (T_g) or the onset of melting temperature ($T_{m,on}$)), occur. Further details about failure processes in front of a crack tip in polyolefin materials are neatly summarised in [44]. Staying within the limitations of LEFM, the initiation of crack growth can be determined by use of crack opening displacement (δ), which is defined according to Equation 10.3 [15,45].

$$\delta = \alpha \cdot \frac{K_I{}^2}{\sigma_{ys} \cdot E} \tag{10.3}$$

It is mainly dependent on K_I, the Young's Modulus (E), σ_{ys} of the material and the geometry of the specimen. When dealing with polymeric materials, viscoelastic and temperature dependent behaviour has to be considered. This mean, that E and sys are now also a function of time (t) and temperature (T). Assuming the limitations of LEFM are met, all factors are only dependent on time (t), temperature (T) and, in the case of K_I, on the geometry (e.g. crack length a) of the specimen. Therefore, for both the upper and lower loading during test, the change of Young's Modulus and yield strength, according to time dependent material behaviour (e.g. creep or stress relaxation), compensate one another since they are only dependent on t and T but not the level of applied loading. The difference in crack opening displacement $\Delta\delta$ only changes when ΔK_I changes due to an increase in crack length (Equation 10.4).

$$\Delta\delta(t, T, a) = \alpha \cdot \left(\frac{K_{I1}(a)^2}{\sigma_{ys1}(t,T) \cdot E_1(t,T)} - \frac{K_{I2}(a)^2}{\sigma_{ys2}(t,T) \cdot E_2(t,T)}\right) \tag{10.4}$$

10.5. Material properties

Some basic material properties of the polypropylene material used are summarized in Table 10.1. The material is specifically designed for extrusion applications such as pipes or other long-term structural components.

Table 10.1: Basic material parameter of used polypropylene type from $[48]_1$ and own measurements$_2$

Material parameter	Testing conditions	value	unit
Melt Flow Rate $(MFR)_1$	[230°C/2.16 kg]	0.3	g/10 min
$Density_1$		900	kg/m³
Young's $Modulus_1$	[1 mm/min]	1300	MPa
Yield $Stress_1$	[50 mm/min]	28	MPa
Yield $Strain_1$	[50 mm/min]	6	%
Charpy Impact $Strength_1$	[notched, 23°C]	50	kJ/m²
Melting temperature $(Peak)_2 – T_m$	$[10K/min]_3$	165	°C
Melting temperature $(Onset)_2 – T_{m,on}$	$[10K/min]_3$	90	°C
Glass transition $(Peak)_2$ - T_g	$[1K/min]_4$	5	°C

$_3$ measured via DSC

$_4$ measured via DMA at 5 Hz

10.6. Experimental

In contrast to PE-HD extrusion types, the glass transition region of PP-B can be much closer to room temperature. Therefore, slight variations to the testing standard ONR 25194 [23], which describes the cyclic CRB-test for characterising quasi-brittle crack growth in PE-HD, were applied. In this test, round bar specimens with a circumferential, sharp pre-notch (approx. 10% of initial diameter) around the specimen are used. Then fatigue loads are applied in sinusoidal load control and a loading ratio of 0.1 to induce brittle failures within short testing times. Test frequency, which is usually 10 Hz, was decreased to 5 Hz to avoid excessive hysteretic heating above ΔT = 5°C. The applied loading range was adapted to fit the needs of the new material and different test temperatures. Calculation of K_I was performed with the formulation of Benthem and Koiter [18]. To gain information on the fracture behaviour of PP-B dependent on temperature as well as to shorten

testing times, tests were carried out at 23°C, as described in ONR 25194 [23], at 50°C and 80°C. The material was tested at three different load levels for all temperatures, with the exception of 50°C, where four specimens at different load levels were tested. Fatigue tests were carried out on servohydraulic machines from MTS (MTS 244.11S (15 kN load cell) and MTS table top 858 (15 kN load cell), MTS System Corporation, Berlin, GER). For tests at 50°C and 80°C, the MTS table top 858 was equipped with a heating chamber (651.05C-02, MTS System Corporation, Berlin, GER). To gather information on crack initiation strain gauges with an initial gauge length of 10mm (±1.5 mm, ISO 9513 Class 0.5) have been applied in equidistant 120° steps around the circumferential notch, according to [30]. The idea is to monitor the difference between maximum and minimum crack mouth opening displacement (Dd) as an indicator of crack initiation. Dynamic mechanical analysis (DMA) was performed on a Mettler DMA/SDTA86112N (Mettler-Toledo GmbH, Schwerzenbach, CH) with a displacement amplitude of 2 mm and a heating rate of 1 K/min from 30°C to 150°C. Since quasi-brittle crack growth in PE-HD pipe grades usually shows a macroscopically fibrillation on the fracture surface, specimens tested at 23°C, 50°C and 80°C were examined using a scanning electron microscope (SEM) (DSM 962, Carl Zeiss, Oberkochen, GER) in order to look for similar structures. Existence of such would confirm brittle crack growth. To determine Tm,on DSC analysis was performed on a DSC 1 (Mettler-Toledo GmbH, Schwerzenbach, CH) with a heating rate of 10 K/min.

10.7. Results and discussion

In Figure 10.1 the results for DMA analysis at frequencies between 1 and 20 Hz are shown. Fatigue tests were performed at a frequency of 5 Hz. Therefore, further discussion focuses on DMA results at 5 Hz. Via dampening behaviour (tan(δ)) T_g was evaluated. The peak of tan(δ) can be seen at approx. 5°C and the endset of the peak at approx. 30°C to 40°C. The loss-modulus (E''), which is an indicator for hysteretic heating [47,48], decreases from 60 MPa at 23°C to 35 MPa at 50°C and 30 MPa at 80°C. Therefore, tests performed at temperatures higher than 23°C should be less prone to hysteretic heating. The curves at 10 and 20 Hz show that at 50°C, and even more so at 80°C, E'' does not vastly increase with higher frequencies. Since hysteretic heating is also dependent on applied load and local stresses,

further tests were still performed at 5 Hz in order not to invalidate results by localized heating effects.

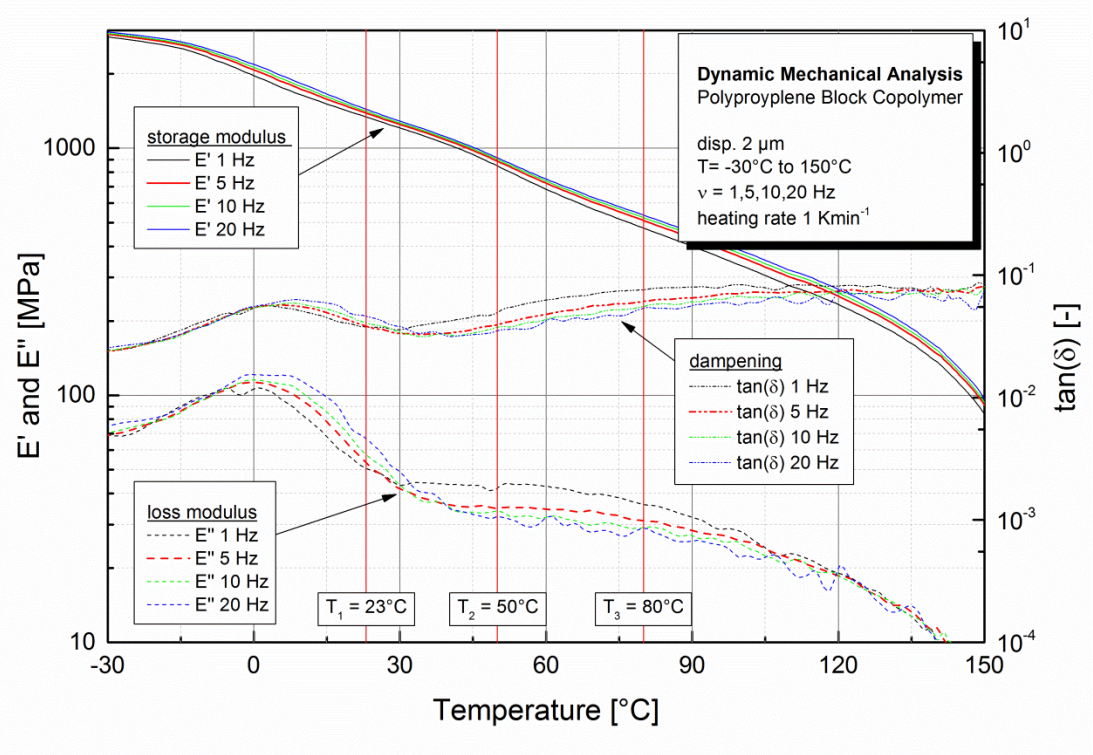

Figure 10.1: Storage modulus E', loss modulus E'' and loss factor tan(δ) at frequencies of 1, 5, 10 and 20 Hz.

To ensure the thermo-mechanical behaviour of the polymer remains unchanged, DSC runs have been performed to determine the onset of melting (Figure 10.2).

To evaluate $T_{m,on}$ the first heating run has been used. At approx. 80-90°C $T_{m,on}$ can be seen. Therefore, 80°C has been chosen as the third testing temperature for cyclic CRB tests. An overview of fatigue test results can be seen in Figure 10.3, where the cycles to fracture (N_f) are shown as a function of initial stress intensity factor (K_I). Similar to results from PE-HD, PP-B shows a linear trend between the applied load and log(N_f) for quasi-brittle failure in a double-logarithmic diagram. The accelerating effect of increased testing temperature, as indicated before, can be seen by the decreasing number of cycles until quasi-brittle fracture. However, test loads also have to be decreased to achieve a quasi-brittle mode of fracture. Cycles to failure, while achieving quasi-brittle failure, significantly decreases with higher

temperatures. While at 23°C it takes between two and seven million cycles to induce this type of failure, it takes between one and two million cycles at 50°C, and between 350.000 and 700.000 cycles at 80°C. This indicates an accelerating factor of approximately ten when comparing tests at room temperature and 80°C. The slope of cycles to failure to applied load in a double-logarithmic diagram seems to remain unchanged at higher temperatures.

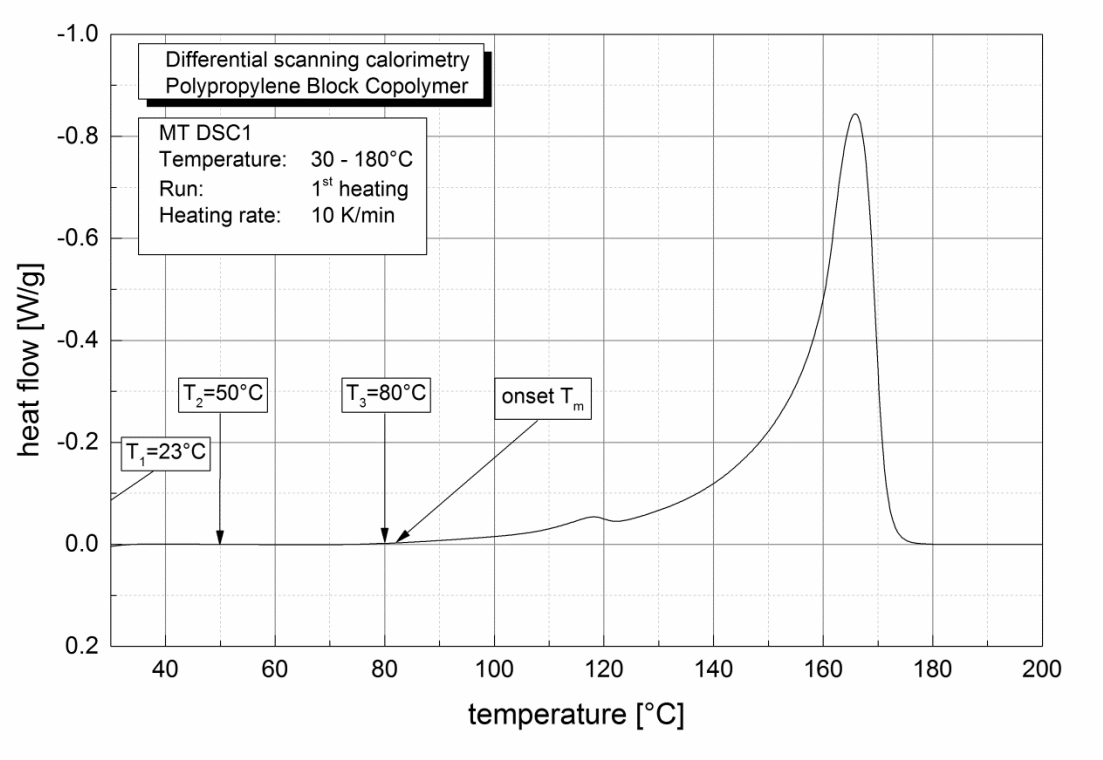

Figure 10.2: Thermal measurement via DSC to determine $T_{m,on}$ of PP-B as a limit for maximum testing temperature.

A further step in the characterisation of PP-B in regard to long-term brittle failure is to distinguish between crack initiation and crack growth. Therefore, the change in crack opening displacement ($\Delta\delta$) is monitored. As long as $\Delta\delta$ remains constant the crack has not started to grow. As soon as the crack starts to grow, $\Delta\delta$ changes according to the change in compliance. Additionally, it is very important that $\Delta\delta$ stays at a constant or as constant as possible value before crack initiation.

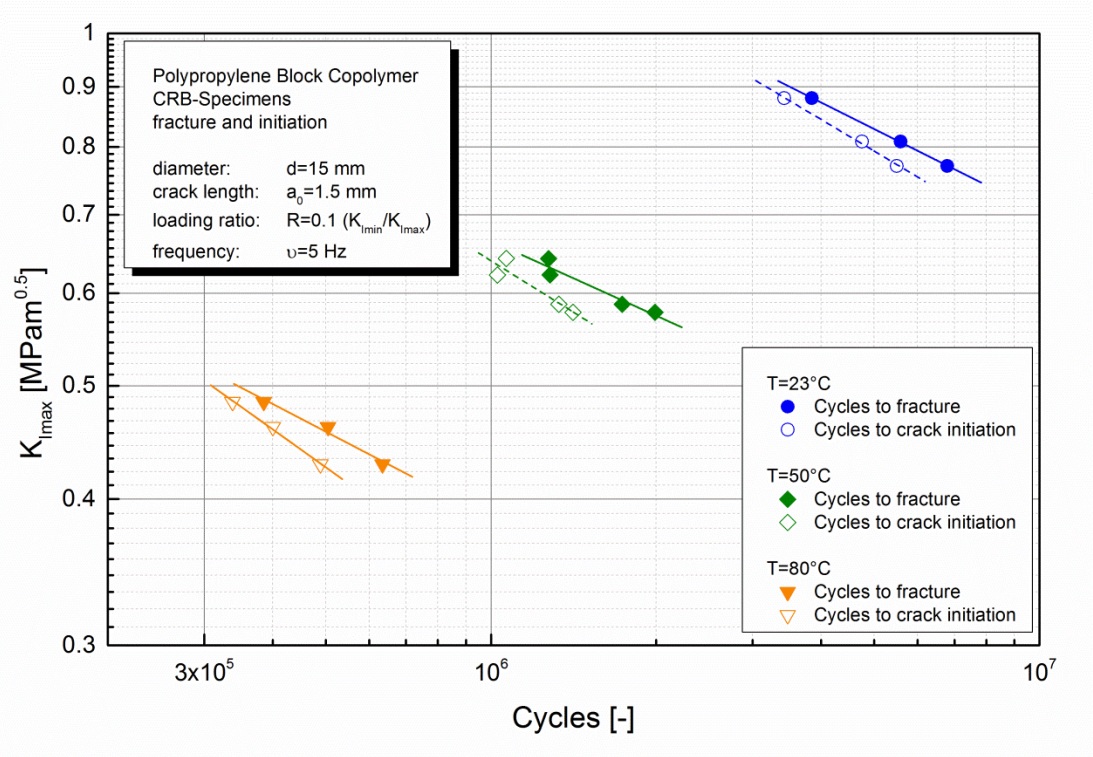

Figure 10.3: Failure behaviour of PP-B at various temperatures - cycles to failure and cycles to crack initiation as a function of initially applied K_I.

Otherwise the crack initiation point can be hidden and, more importantly, the limitations of neither LEFM nor linear viscoelasticity are met. The amount of crack initiation is also shown in Figure 10.3. Furthermore, $\Delta\delta$ curves which were used to detect crack initiation for PP-B at 23°C, 50°C and 80°C are shown in Figure 10.4. Crack initiation has been determined at the first clear deviation from the base line of constant $\Delta\delta$. The ratio of crack initiation to total cycles to failure is quite high for all tests at 23°C, 50°C and 80°C. Results can be seen in Figure 10.5 as a function of the applied load range. For the tests at 23°C, the ratio of crack initiation within the load range of tests is more than 80% of the total cycles to failure. At elevated temperatures of 50°C and 80°C, the minimum percentage decreases to about 70%. For comparison, the amount of crack initiation in PE-HD used for extrusion applications can go down to values like 30% (e.g. [30]).

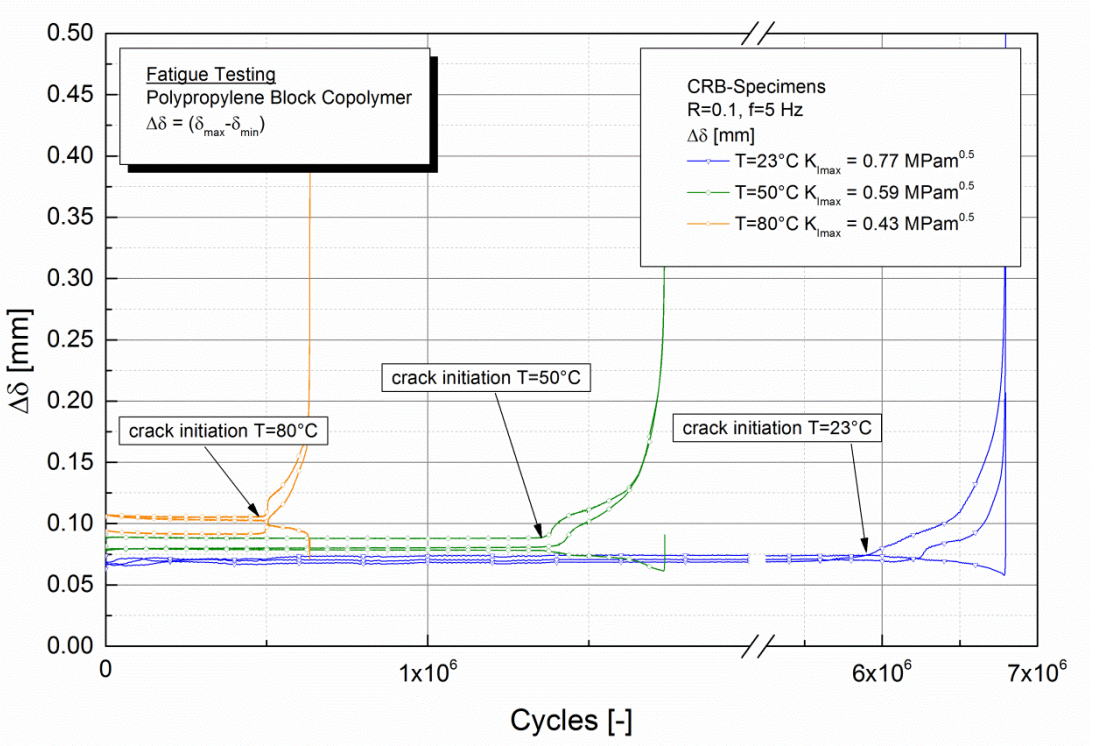

Figure 10.4: Strain gauge signals for PP-B at 23°C, 50°C and 80°C to determine crack initiation.

The exorbitant high amount of crack initiation in PP-B could be explained by the fact that this material is still prone to rather large plastic zone formation at the load levels applied to the specimens, even in CRB specimens. Therefore, cracks tend to be detained in rather large plastic zones for a long time before actual crack growth starts. Furthermore, Figure 10.5 shows that the amount of crack initiation to total failure time is dependent on the applied load. This trend can also be found in PE-HD [26] and is, similar to the above explanation, mainly governed by the formation and size of plastic zones. The slope of K_I-crack initiation ratio at 23°C is different to those at 50°C and 80°C, which could be explained by different dampening behaviour, as shown in DMA analysis. At 23°C the influence of T_g is still present, contrary to at 50°C and 80°C. Indications of stepwise crack growth, which can also be found in PE-HD, can be seen in the curve. Different to PE-HD, where usually several steps appear, PP-B only showed one or two distinguished steps before the end of the test. The fact, that this step also appears at 50°C and 80°C, where specimens are severed manually, indicates that this step does not belong to

the rupture of the specimen, but to either quasi-brittle crack growth, or the transition between quasi-brittle crack growth and end-failure behaviour. Although cycles to failure decrease drastically with increasing temperature, a comparison of the different temperatures in Figure 10.4 shows that the overall behaviour of the curves remains unchanged. Despite the accelerating effect, results can only be seen as valid if the failure occurs in a quasi-brittle mode.

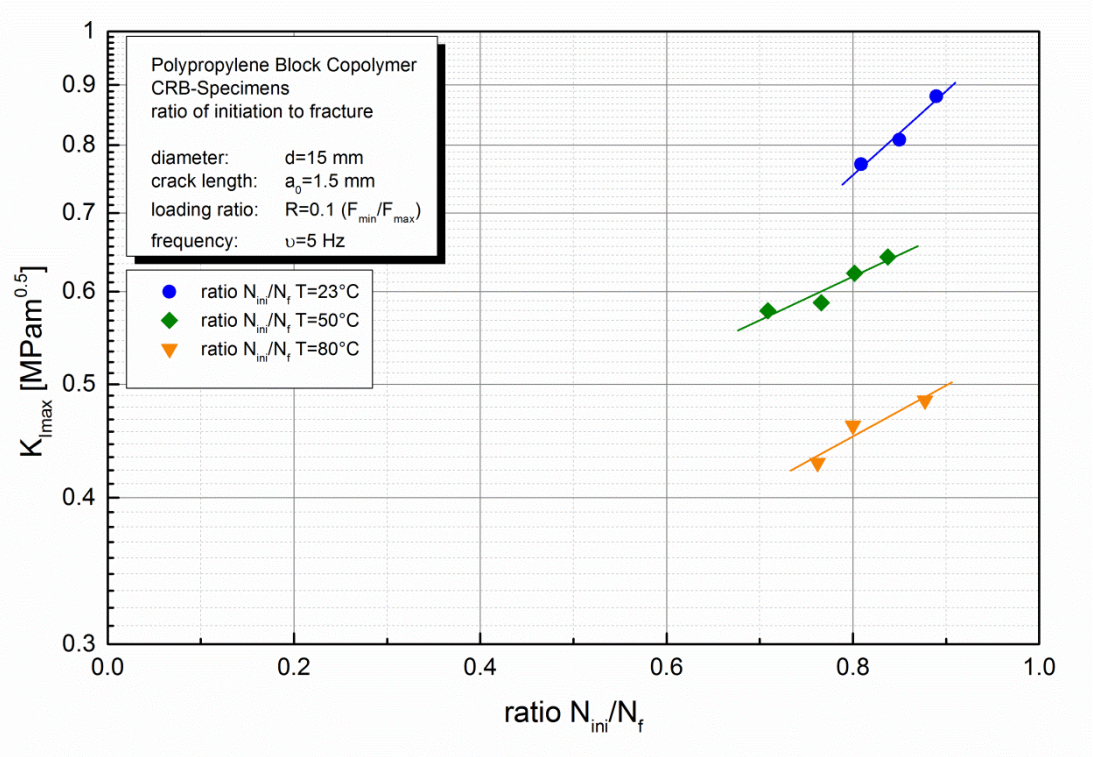

Figure 10.5: Comparison of K_{Imax} dependent crack initiation to total cycles to failure at 23°C, 50°C and 80°C.

To affirm assumption of this failure mode, fractographic analysis has been performed on the specimens using SEM. Figure 10.6 shows the results of tests at 23°C, 50°C and 80°C. All tested specimens show areas of brittle crack growth close to the pre-notch, followed by a transition area. In the area of quasi-brittle crack growth, macroscopically fibrillation quite similar to PE-HD can be seen [35,49-51]. In the area of transition, the fine strands of fibrillations change into coarser, drawn out packages of fibrillated areas. The ligament area, which is quite often characterised by global ductile tearing (e.g. PE-HD) exhibits a rather smooth surface at 23°C. At 50°C and 80°C the

remaining material after crack growth (Figure 10.6a) and transition (Figure 10.6b) has quite ductile behaviour due to the high temperatures. In order not to damage strain gauges by overstretching them, ligament areas had to be severed manually after the test and were not further examined. At 50°C and 80°C, appearance of both areas of crack propagation (a. and b.) remains similar. However, the size of macroscopically fibrillation in a. decreases with increasing temperature. This is explained by the fact that disentanglement and chain scission in crazed areas in front of a crack tip is a phenomenon mainly driven by thermal activation, strain rate [43] and applied stress intensity.

10.8. Summary and conclusions

Cyclic CRB-tests were examined as a possible tool to evaluate the long-term quasi-brittle failure of rather ductile polypropylene block copolymer. This test was developed to compare different PE-HD pipe materials at room temperature under fatigue load. For PE-HD, cyclic CRB-tests show similar fracture surfaces characteristics to real brittle failures in pipes from field failures or internal pipe pressure tests. Fine fibrillations, which are an indication of quasi-brittle crack growth in PE-HD, were also found on fracture surfaces of the tested polypropylene. Therefore, cyclic CRB-tests seem to meet the requirements for characterising quasi-brittle crack growth in this type of material. Observation of crack opening showed indications of stepwise crack growth. In contrast to PE-HD, where usually several of these steps can be found, only one to two steps were observed during testing polypropylene. Analogue to PE-HD, PP-B shows a linear relation between applied stress intensity factor and cycles to failure in a double-logarithmic ($\log(K_I)$- $\log(N_f)$) diagram.

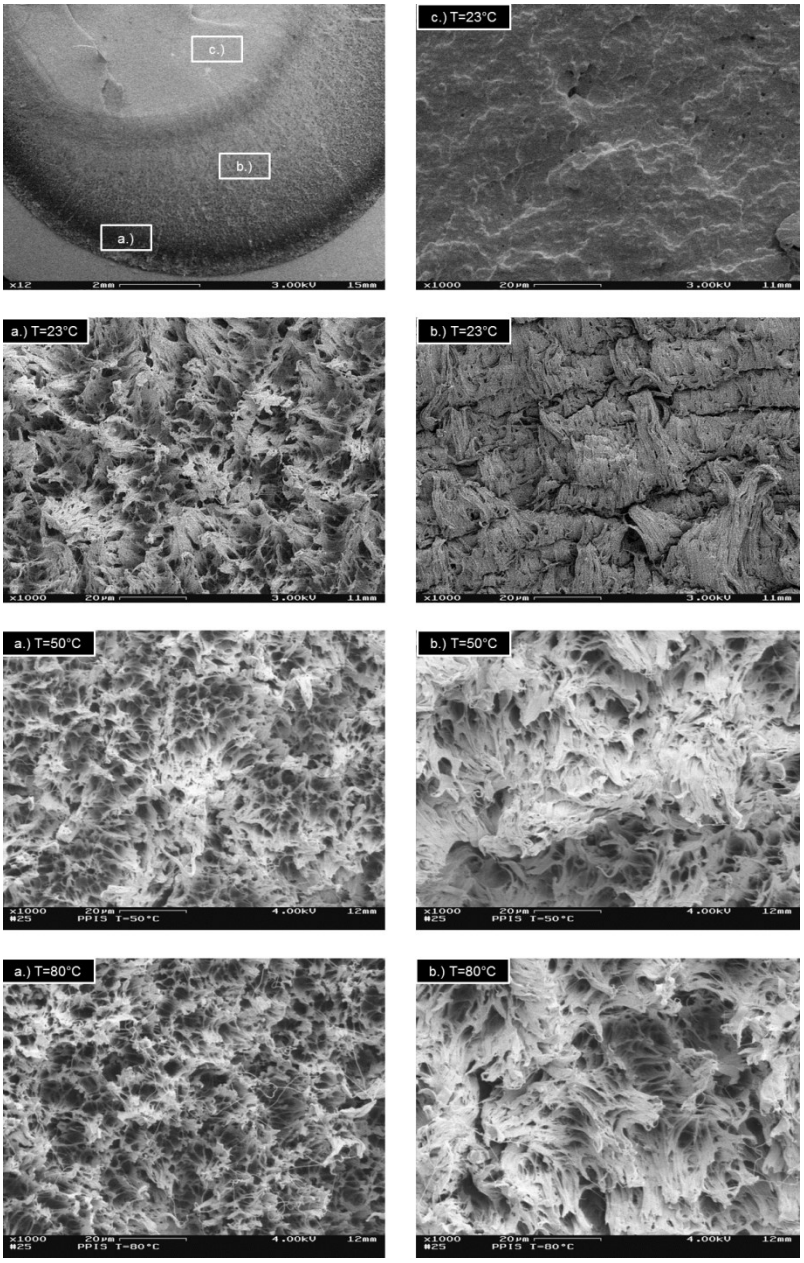

Figure 10.6: Fractographic analysis of the fracture surface of a specimen at K_{Imax} = 0.81 MPam$^{0.5}$ and 23°C, K_{Imax} = 0.64 MPam$^{0.5}$ and 50°C and K_{Imax} = 0.43 MPam$^{0.5}$ and 80°C using SEM.

To further decrease testing times, and gain deeper knowledge of the material, tests were not only performed at 23°C, as indicated in the Austrian standard ONR 25194, but also at 50°C and 80°C. 80°C was chosen as a maximum testing temperature in order to avoid big changes in thermo-mechanical behaviour with the onset of melting at about 80-90°C. For 50°C

and 80°C, finer macroscopically indications of fibrillations were found on the fracture surfaces. Crack opening also showed indications of stepwise crack growth like the tests at 23°C. Therefore, the overall failure behaviour remains mainly unchanged. The amount of crack initiation compared to the total failure cycles is rather high for the tested material. For the tested loading range it is approximately 80 to 90% at 23°C, and approximately 70 to 85% at 50°C and 80°C. Thus, crack initiation seems to be much more dominant in PP-B than it is in PE-HD. Slope of K_I-crack initiation ratio at 23°C is different to those at 50°C and 80°C. Experiments at higher temperatures showed significant decreases in testing times (about 60% for 50°C and 80% at 80°C), but can also change thermo-mechanical failure relationships such as K_I to crack growth initiation ratio, mainly due to the highly temperature dependent dampening behaviour. This effect has to be kept in mind when using this test to compare materials at temperatures which do not correspond to the real application temperature. According to loss-modulus from DMA-analysis, the possibility to test at higher frequencies than 5 Hz at 50°C and 80°C to further reduce testing times exists. Nevertheless, since hysteretic heating is not only dependent on frequency, but also on applied loading, further experiments to validate tests at higher frequencies are necessary.

10.9. Acknowledgement

The research work of this publication was performed at the Institute of Materials Science and Testing of Polymers (Montanuniversitaet Leoben, Austria) within the framework of the FFG program of the Austrian Ministry of Traffic, Innovation and Technology and the Austrian Ministry of Economy, Family and Youth with contributions of the Österreichisches Forschungsinstitut für Chemie und Technik (Austria), Martin-Luther-Universität Halle-Wittenberg (Germany) and the Polymer Competence Center Leoben GmbH (Austria).

10.10. References

[1] Cousins K. Polymers in building and construction: A Rapra Market Report. Shawbury, Shrewsbury, Shropshire, U.K: Rapra Technology Ltd; 2002.

[2] Nezbedova E, Pospisil V, Bohaty P, Vlach B. Fracture behaviour ofβ-polypropylene as a function of processing conditions. Macromol. Symp. 2001;170(1):349–57.

[3] Chen H, Karger-Kocsis J, Wu J, Varga J. Fracture toughness of α- and β-phase polypropylene homopolymers and random- and block-copolymers. Polymer 2002;43(24):6505–14.

[4] Pérez E, Alvarez V, Pérez C, Bernal C. A comparative study of the effect of different rigid fillers on the fracture and failure behavior of polypropylene based composites. Composites Part B: Engineering 2013;52:72–83.

[5] van der Wal A, Mulder JJ, Gaymans RJ. Fracture of polypropylene: 2. The effect of crystallinity. Polymer;1998(39 (22)):5477–81.

[6] Karger-Kocsis J. How does "phase transformation toughening" work in semicrystalline polymers? Polym. Eng. Sci. 1996;36(2):203–10.

[7] Hertzberg RW. Deformation and fracture mechanics of engineering materials. 4th ed. New York: J. Wiley & Sons; 1996.

[8] ISO 16770. Plastics -- Determination of environmental stress cracking (ESC) of polyethylene -- Full-notch creep test (FNCT); 2004.

[9] ISO 16241. Notch tensile test to measure the resistance to slow crack growth of polyethylene materials for pipe and fitting products; 2005.

[10] ISO 13479. Polyolefin pipes for the conveyance of fluids -- Determination of resistance to crack propagation -- Test method for slow crack growth on notched pipes; 2009.

[11] EN ISO 9080. Plastics piping and ducting systems - Determination of the long-term hydrostatic strength of thermoplastics materials in pipe form by extrapolation; 2003.

[12] ASTM. Standard Test Method for Obtaining Hydrostatic Design Basis for Thermoplastic Pipe Materials or Pressure Design Basis for Thermoplastic Pipe Products; 2011.

[13] Litvinov V, Soliman M. The effect of storage of poly(propylene) pipes under hydrostatic pressure and elevated temperatures on the

morphology, molecular mobility and failure behaviour. Polymer 2005;46(9):3077–89.

[14] Irwin GR. Analysis of stresses and strains near the end of a crack traversing a plate. J. Appl. Mech. 1957(24):361–4.

[15] Broek D. Elementary engineering fracture mechanics. 3rd ed. The Hague ;, Boston, Hingham, Mass: Martinus Nijhoff; Distributed by Kluwer Boston; 1982.

[16] Lang RW. Applicability of linear elastic fracture mechanics to fatigue in polymers and short-fiber composites; 1984.

[17] Anderson TL. Fracture mechanics: Fundamentals and applications. 3rd ed. Boca Raton [u.a.]: CRC, Taylor & Francis; 2005.

[18] Benthem J, Koiter W (eds.). Method of Analysis and Solutions of Crack Problems. 3rd ed; 1973.

[19] Nakamura T, Shih C, Freund L. Elastic-plastic analysis of a dynamically loaded circumferentially notched round bar. Engineering Fracture Mechanics 1985;22(3):437–52.

[20] Itoh Y, Murakami T, Kashiwaya H. Approximate formulae for estimating the of a circumferentially cracked round bar under tension or torsion. Engineering Fracture Mechanics 1988;31(6):967–75.

[21] Ule B, Leskovšek V, Tuma B. Estimation of plain strain fracture toughness of AISI M2 steel from precracked round-bar specimens. Engineering Fracture Mechanics 2000;65(5):559–72.

[22] Scibetta M, Chaouadi R, van Walle E. Fracture toughness analysis of circumferentially-cracked round bars. International Journal of Fracture 2000(104):145–68.

[23] ONR 25194. Determination of the resistance of slow crack growth of polyehtylene with cracked round bar (CRB) specimens; 2011.

[24] Haager M. Bruchmechanische Methoden zur beschleunigten Charakterisierung des langsamen Risswachstums von Polyethylen-Rohrwerkstoffen. Dissertation. Leoben, Austria; 2006.

[25] Haager M, Zhou W, Pinter G, Chudnovsky A. Studies of Creep and Fatigue Crack Growth in HD-PE pipe materials.

[26] Frank A. Fracture Mechanics Based Lifetime Assessment and Long-term Failure Behavior of Polyethylene Pressure Pipes: Dissertation. Disseratation. Leoben, Austria.

[27] Pinter G, Haager M, Balika W, Lang RW. Cyclic crack growth tests with CRB specimens for the evaluation of the long-term performance of PE pipe grades. Polymer Testing 2007;26(2):180–8.

[28] Pinter G, Haager M, Lang RW. Lifetime and safety assessment of PE pressure pipes based on fracture mechanics fatigue tests. Proceedings of Antec;2007:2921–5.

[29] Frank A, Lang RW, Pinter G (eds.). Accelerated Investigation of creep crack growth in polyethylene pipe grade materials by the use of fatigue tests on cracked round bar specimens: Proceedings Annual Technical Conference - ANTEC, Society of Plastics Engineers, Milwaukee, Wisconsin, USA; 2008;2435-2439.

[30] Frank A, Freimann W, Pinter G, Lang RW. A fracture mechanics concept for the accelerated characterization of creep crack growth in PE-HD pipe grades. Engineering Fracture Mechanics 2009;76(18):2780–7.

[31] Frank A, Pinter G, Lang RW. Prediction of the remaining lifetime of polyethylene pipes after up to 30 years in use. Polymer Testing 2009;28(7):737–45.

[32] Barker MB, Bowman J, Bevis M. The performance and causes of failure of polyethylene pipes subjected to constant and fluctuating internal pressure loadings. J Mater Sci 1983;18(4):1095–118.

[33] Chudnovsky A, Moet A, Bankert RJ, Takemori MT. Effect of damage dissemination on crack propagation in polypropylene. J. Appl. Phys. 1983;54(10):5562.

[34] SHAH A, Stepanov E, Hiltner A, Baer E, Klein M. Correlation of fatigue crack propagation in polyethylene pipe specimens of different geometries. International Journal of Fracture 1997;84(2):159–73.

[35] Parsons M, Stepanov EV, Hiltner A, Baer E. Correlation of fatigue and creep slow crack growth in a medium density polyethylene pipe material. Journal of Materials Science 2000;35(11):2659–74.

[36] Parsons M, Stepanov EV, Hiltner A, Baer E. Effect of strain rate on stepwise fatigue and creep slow crack growth in high density polyethylene. Journal of Materials Science 2000;35(8):1857–66.

[37] Pinter G, Balika W, Lang RW. A correlation of creep and fatigue crack growth in high density poly(ethylene) at various temperatures. In: Temperature-Fatigue Interaction, editor. International Conference on Temperature-Fatigue Interaction, p. 267–275.

[38] Balika W, Pinter G, Lang RW. Systematic investigations of fatigue crack growth behavior of a PE-HD pipe grade in through-thickness direction. J. Appl. Polym. Sci 2007;103(3):1745–58.

[39] Frank A, Pinter G. Evaluation of the applicability of the cracked round bar test as standardized PE-pipe ranking tool. Polymer Testing 2014;33:161–71.

[40] Lustiger A, Ishikawa N. An analytical technique for measuring relative tie-molecule concentration in polyethylene. J. Polym. Sci. B Polym. Phys. 1991;29(9):1047–55.

[41] Brown N, Lu X, Huang Y. The fundamental material parameters that govern slow crack growth in linear polyethylene. Plastics, Rubber and Composites Processing and Applications 1992(17):255–8.

[42] Kausch H (ed.). Intrinsic Molecular Mobility and Toughness of Polymers I. Berlin/Heidelberg: Springer-Verlag; 2005.

[43] Kausch HH (ed.). Crazing in Polymers Vol. 2. Berlin, Heidelberg: Springer Berlin Heidelberg; 1990.

[44] Deblieck RA, van Beek D, Remerie K, Ward IM. Failure mechanisms in polyolefines: The role of crazing, shear yielding and the entanglement network. Polymer 2011;52(14):2979–90.

[45] Burdekin FM, Stone DEW. The crack opening displacement approach to fracture mechanics in yielding materials. The Journal of Strain Analysis for Engineering Design 1966;1(2):145–53.

[46] Borealis AG. Data Sheet - BA202E: Polypropylene Block Copolymer for Non-Pressure Pipes; Available from:

http://www.borealisgroup.com/datasheets/10017403, accessed Feb. 2014;.

[47] DIN EN ISO 6721-1. Bestimmung dynamisch-mechanischer Eigenschaften - Allgemeine Grundlagen; 1996.

[48] Ehrenstein GW, Riedel G, Trawiel P. Praxis der thermischen Analyse von Kunststoffen. 2nd ed. München: Hanser; 2003.

[49] Pinter G. Rißwachstumsverhalten von PE-HD unter statischer Belastung. Dissertation. Leoben, Austria; 1999.

[50] Hamouda HBH, Simoes-betbeder M, Grillon F, Blouet P, Billon N, Piques R. Creep damage mechanisms in polyethylene gas pipes. Polymer 2001(42):5425–37.

[51] Pinter G, Haager M, Balika W, Lang RW. Fatigue crack growth in PE-HD pipe grades. Plas. Rub. Compos 2005;34(1):25–33.

11. Publication 5

11.1. Bibliographic information

- Title: Influence of molecular structure and reinforcement on fatigue behaviour of tough polypropylene materials
- Authors and relevant contributions to this publication:
  - Florian ARBEITER[1]
    Experimental testing, preparation of the publication
  - Gerald PINTER[1,2]
    Discussion and scientific guidance
  - Andreas FRANK[2]
  - Discussion and scientific guidance
- Affiliation:
  1. Institute of Materials Science and Testing of Polymers, Montanuniversitaet Leoben, Otto Glöckel-Strasse 2, 8700 Leoben, Austria
  2. Polymer Competence Center Leoben GmbH, Roseggerstr. 12, 8700 Leoben, Austria
- Periodical: Polymer
- Status: Submitted

Statement with regard to this publication: The manuscript presented here is a present-day manuscript and does not necessarily reflect exactly the version published later on.

11.2. Abstract

Molecular structure and reinforcement heavily influence the fatigue performance of polypropylene materials. Aim of this study is to investigate the fatigue behaviour of different unreinforced and reinforced tough polypropylene materials used for piping applications. Due to high resistance against crack growth, these materials usually can't be fatigued in quasi-brittle failure mode within feasible amounts of times. However, this is the important failure mode for pipe materials. Therefore, the new cyclic cracked round bar (CRB) test, developed for tough polyethylene materials, has been used to determine fatigue behaviour of homo-, random- and reinforced polypropylene at elevated temperature.

Differences between the materials were characterized via dynamic mechanical analysis, differential scanning calorimetry and molecular mass distribution, before conducting fatigue tests. Even though molecular mass distribution was similar for unreinforced materials, fatigue lifetimes differed greatly. The mismatch of molecular mass and fatigue lifetime was mainly attributed to the different buildup and morphology of the base polymer. Reinforcement of materials (talcum and wollastonite) revealed big influences in fatigue behaviour as well.

11.3. Keywords

Polypropylene, Fracture, Fatigue, CRB, Talcum, Wollastonite

11.4. Introduction

Polypropylene (PP) is a widely spread material, used for several applications. The PP materials examined in this study are used for structural applications, such as piping. Due to performance requirements, these materials are optimized for high crack resistance over a long period of time. To assure safety and long lifetimes, it is necessary to be able to characterize the crack growth behavior and compare materials with regard to failure behavior in the quasi-brittle failure regime. However, classical test methods used in piping industry do not yield results within months or even years of testing. With modern PP grades, especially those optimized for pressurized applications, the quasi-brittle failure cannot be reached within even several thousand hours of testing. According to EN ISO 15874-2 [1], which regulates testing of

long-term properties of pipes made from PP, Random- (PP-R) and Homopolymers (PP-H) are expected to show no quasi-brittle fracture below 50°C for over 100 years. Therefore, faster methods are needed for comparison between materials.

So far, different polypropylene types and blends have mostly been compared in regard to fracture properties (e.g. toughness) via elastic plastic (e.g. [2–4]), post yield fracture mechanics like EWF (e.g. [5–8]) or at high velocities and/or low temperatures (e.g. [3,9–11]), which does not necessarily coincide with application conditions or mode of failure in actual pipe applications. Another possibility to accelerate testing is the use of fatigue loads instead of static, which has also shown promising results for polyethylene (PE) materials used under similar conditions.

11.5. Background

Fatigue behaviour of polypropylene, similar to most polymers, can be mainly divided into two different stages [12–14]. At high stress levels and frequencies, specimens fracture due to high loads within very short testing times. This can mainly be attributed to either hysteretic heating, or too high applied stress levels close to or even above the yielding point of the material. At reduced stress and frequency, the failure mode changes to the second region, the so called quasi-brittle failure mode. In this mode failure times are significantly longer. The mode changes from either large scale deformation due to yielding, thermally dominated failure or unstable crack growth to a failure mode, where lifetime of the material is associated with the nucleation and growth of flaws [12].

The main aim of this work is to investigate the fatigue behavior of different PP materials with regard to aforementioned modes of failure. For pipe materials, the second mode of failure is critical with regards to expected lifetime. Hence a big focus of this work is on this failure mode. A new and rather promising test for faster characterization of this failure mode for PE and other pipe materials is the cyclic cracked round bar (CRB) test (e.g. [15–19]). The CRB-test is a fatigue test on cylindrical, circumferentially notched specimens. By introducing fatigue loads, instead of a static one, initiation and propagation of cracks can be highly accelerated [17]. Even though the loading situation is different in fatigue compared to a static test, authors have thoroughly shown

that damage mechanisms are comparable for PE [20,21]. Another big advantage of specimen geometry in CRB tests is the notch without any free surfaces perpendicular to it. At free surfaces plane stress condition is dominating [22], which promotes larger plastic zone sizes. Since plane stress condition and its resulting plastic zones hinder crack initiation and growth, they have to be avoided as much as possible in order to shorten testing times. The cyclic CRB test can also be used to go into actual lifetime calculation, using a linear elastic fracture mechanics approach, if failure occurs in quasi-brittle failure mode [23–25]. First testing results on a PP pipe material also demonstrate the potential of fatigue induced loading using CRB specimens for polypropylene [18].

Polypropylene materials used for long-term applications exhibit vastly different material properties, depending on their molecular structure and, if present, reinforcements. For this study a representative for each of the three main groups of PP used for structural applications, namely PP-homopolymer (PP-H), PP-random copolymer (PP-R) and PP-block copolymer (PP-B), were tested. The co-monomer incorporated in the investigated materials was PE. Tacticity and morphology [9,26–30] of PP materials, which can also influence the resulting properties, are not a subject of the study at hand.

11.6. Experimental

11.6.1. Materials

The materials used for experiments are listed in Table 11.1 below. Material data was taken from data-sheets published by the producer [31–33] or from experiments. All materials are currently used in industry for pressurized (PP-R) and non-pressure pipe systems (PP-H, PP-B and PP-Blends). They have proven to be highly dependable materials. More specifically, the used PP-H is intended for sheets, profiles and industrial non-pressure pipes. The PP-R type is intended for heating, plumbing, domestic water and relining. The blended materials with mineral reinforcement are used as sewage pipes. Based on areas of application the materials have to exhibit quite different mechanical properties to perform as desired.

Table 11.1: Description of used materials [31–33]

Material	Young's Modulus, 23°C [MPa]	Yield Stress, 23°C [MPa]	Density, 23°C [kg/m³]	MFR 230°C/2.16 kg [g/10min]
PP-B	1300	28	900	0.30
PP-H	1650	36	905	0.30
PP-R	900	25	905	0.25
PP-B & Talcum (50 wt%)	3970	28	1320	< 0.20
PP-B & Wollastonite (20 wt%)	2560	31	1070	< 0.20

11.6.2. Dynamic-mechanical analysis

Similar to previous work [18] dynamic-mechanical analysis (DMA) measurements have been performed before fatigue testing, to examine material behavior at elevated testing temperature. Measurements have been performed on a Mettler DMA/SDTA861 40N (Mettler-Toledo GmbH, Schwerzenbach, CH). The parameters for the tests were a displacement of 2 µm during oscillation, frequencies from 1 to 20 Hz and a heating rate of 1 $Kmin^{-1}$ in tensile loading mode. To compare materials, storage- (E') and loss-modulus (E'') and dampening behavior (tan(δ)) have been evaluated.

11.6.3. Differential scanning calorimetry

For comparison of the melting behavior of the unreinforced materials differential scanning calorimetry (DSC) analysis has been used. To determine melting onset and melting peak temperatures, a run with a heating rate of 10 K/min under nitrogen atmosphere (50 ml/min) has been performed between 25 and 200°C. Experiments were performed on a DSC 1 (Mettler-Toledo GmbH, Schwerzenbach, CH).

11.6.4. Molecular mass distribution

The molecular mass distribution of the tested unreinforced PP materials has been measured using size exclusion chromatography (SEC). The measurements were performed after a dissolution time of 150 minutes with a column temperature of 160°C and an analysis time of 35 to 40 minutes.

11.6.5. Cracked Round Bar-tests

Fatigue tests of pure PP-H and PP-R have been performed on an ElectroForce 3450 (Bose Corporation, Eden Prairie, MN, USA) and a testing temperature of 80°C. The temperature was fixed at 80°C as an averaged middle compared to various testing standards, where PP pipe materials are tested at temperatures up to 110°C and to be able to compare results to previous work of PP-B [18]. A temperature sensor was positioned close to the specimen to monitor the actual temperature within the chamber. Tests for reinforced materials were conducted on a 15 kN MTS 858 TableTop system (MTS, Eden Prairie, MN, USA) at 23°C and again on an ElectroForce 3450 for 80°C. Specimen preparation was performed according to ISO DIS 18489 [15] and machined from compression molded plaques with a thickness of 16 mm for PP-H and PP-R. Reinforced materials were directly cut from thick walled pipes. The diameter of the cylindrical specimens was 15 mm and the initial notch depth 10% of diameter. Contrary to ISO DIS 18489, the frequency of the test was chosen at 5 Hz instead of 10 Hz to avoid excessive hysteretic heating. The tests were performed with a loading ratio (applied minimum to maximum load: $R=F_{min}/F_{max}$) of 0.1. The range of applied initial stresses was approx. 9.5 – 15.5 MPa for PP-H, 9.5 to 12 MPa for PP-R and 13 to 16 MPa for reinforced PP at 23°C and between 5.5 to 8 MPa at 80°C. After testing, actual initial notch length was measured via optical microscopy and stresses adapted accordingly. The microscope used for optical measurements was an Olympus SZX12 (Olympus Corporation, Tokyo, JP). Due to the higher compliance at 80°C, especially for PP-R, it was possible to observe the shape of notch and crack tip of the specimens via travelling microscope. The specimen compliance was evaluated as the ratio of difference between maximum and minimum piston movement and maximum and minimum applied load ($\Delta C=\Delta disp./\Delta F$). Afterwards data was normalized using the initial value to show the load dependent development more clearly.

Scanning electron microscopy

For more information on the failure behavior of tested materials, fracture surfaces of CRB-specimens have been examined via scanning electron microscope (SEM – DSM 962, Carl Zeiss, Oberkochen, GER). Special attention is put on the examination of plastic deformation mechanisms, such as formation and breakdown of crazes.

11.7. Results and Discussion

The following chapter shows the main experimental findings of this work. For a better understanding the results are divided into examination of the materials and fatigue experiments. The first part is consisting of DMA-analysis, DSC and SEC. Fatigue testing includes the fracture curves of all five materials at a testing temperature of 80°C and additionally at 23°C for reinforced PP. Furthermore, analysis of fracture surfaces and a closer examination of compliance development during testing are shown.

11.7.1. Examination of materials

Before mechanical testing, DMA-analysis was performed, to determine the behavior at the actual testing temperature. In Figure 11.1 the results for PP-B [18], PP-R, PP-H, Talcum and Wollastonite reinforced PP are shown. Storage modulus E' at the target testing temperature is around 700 MPa for PP-H, 500 MPa for PP-B and 250 MPa for PP-R. Damping behaviour of PP-H and PP-B are rather similar at 80°C, whereas PP-R has a slightly higher level. It can also be seen, that at 80°C and above, properties change more significantly for PP-R, compared to the other two materials. Glass transition peak-temperature of PP-H and PP-B are around 5-10°C, and -5 to 0°C for PP-R. For reinforced materials storage and loss modulus are higher, compared to the unfilled materials. Due to the high content of mineral reinforcement, PP-talcum has a comparable high modulus for PP. Around 23°C it is around 4,000 MPa and drops to roughly 2,000 MPa at 80°C. Wollastonite reinforced PP starts with around 2,800 MPa at 23°C and drops to 1,200 MPa at 80°C. Glass transition peak-temperature is around 10°C for both materials. However, peaks are broader than and not as pronounced as for the pure materials.

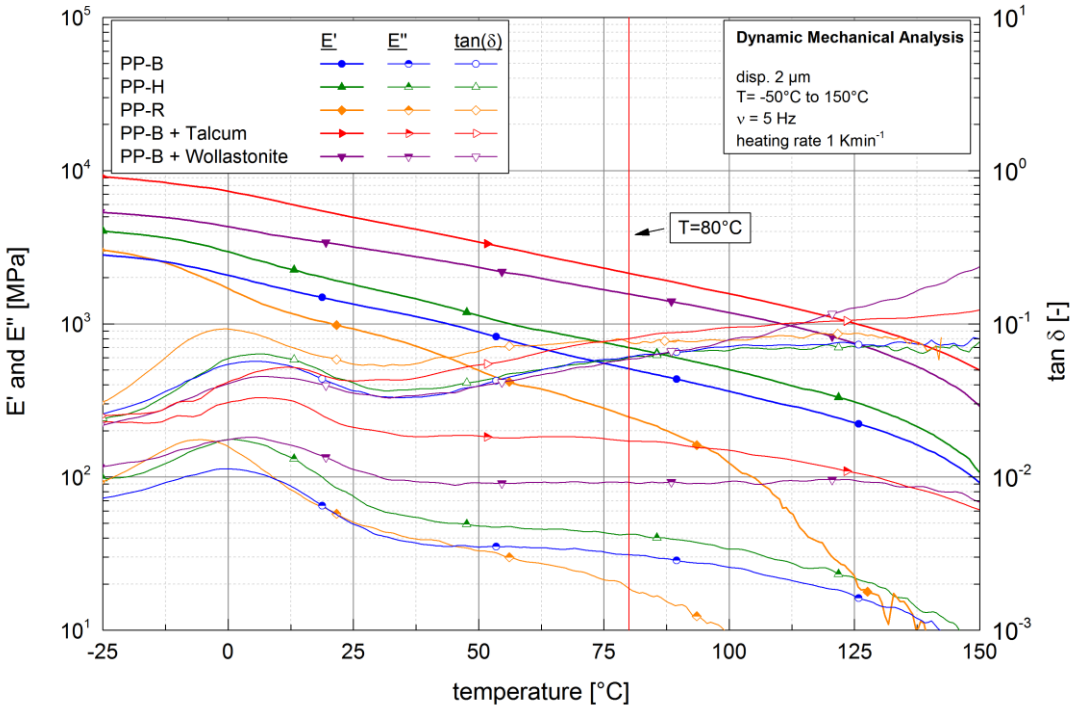

Figure 11.1: Dynamic mechanical analysis of the examined materials: PP-H, PP-R and PP-B [18], PP and Talcum and PP and Wollastonite.

To gain further insight, into the differences of the examined base materials, DSC and SEC experiments were carried out. Figure 11.2 shows the results of DSC analysis for the first heating run. Both PP-H and PP-B show similar melting peak temperatures between 165 and 170°C. However, PP-B additionally shows the expected second peak of the PE-copolymer material around 120°C. The melting peak temperature of PP-R is lower compared to the other two materials, around 145°C. This can be explained by the formation of γ-modification, which is reported to affect the equilibrium melting temperature of PP-R due to changes of the specific enthalpy and /or entropy of melting [34]. The shape of the melting peak of PP-R is also not as sharp and pronounced. Furthermore, PP-H and PP-B show first signs of a melting onset in DSC-measurements around 85 to 90°C. The onset for PP-R shows much earlier around 70°C.

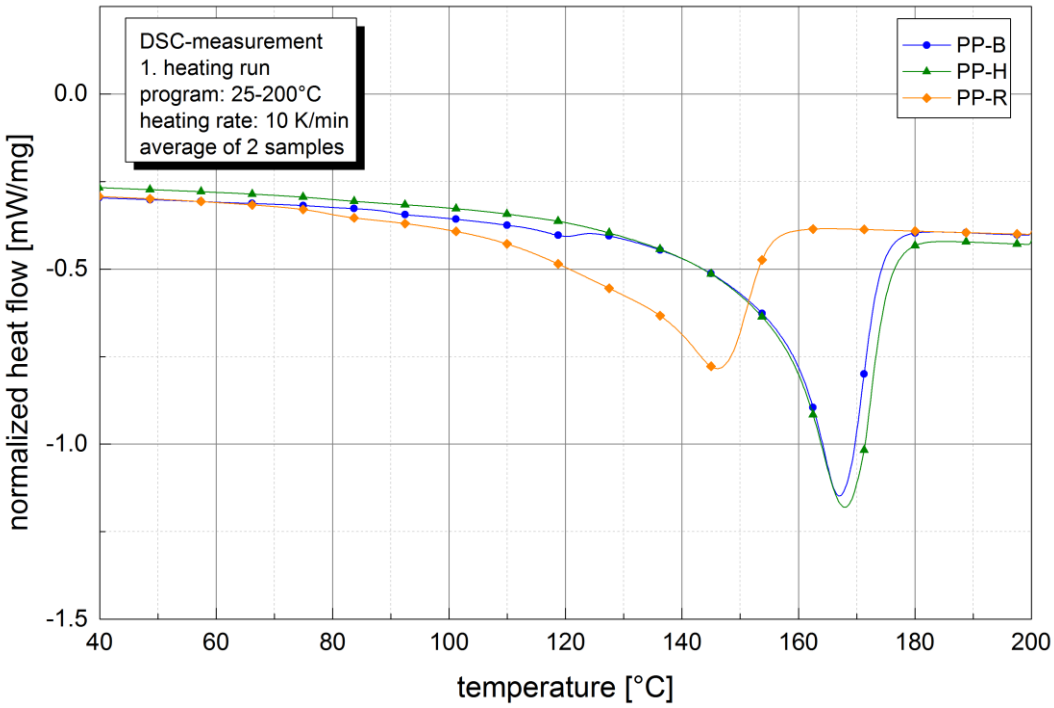

Figure 2: Differential scanning calorimetry of PP-H, PP-R and PP-B.

In Figure 11.3a comparison of PP-B, PP-H and PP-R microtome slices is shown. Slices of 20 µm were taken from the middle of untested fatigue samples. Morphology was investigated using polarized light microscopy and a magnification of 500x. The Picture of PP-B shows dispersed black dots which are presumably the incorporated ethylene-blocks. Similar dispersion of ethylene blocks was found in literature via SEM on fractured specimen surfaces after impact testing [26] and on cryo-fractured and etched PP-B [35]. The second picture (Figure 11.3b.) shows the morphology of PP-H. Expectedly it shows formation of α-modification. Even though spherulites are not as pronounced as after isothermal cooling, several structures with sizes up to 40 µm can be found. The third picture (Figure 11.3c.) shows the morphology of PP-R. According to literature, PP-R has a tendency to form γ-modification which hinders overall crystallization and decreases spherulitic growth speed [36]. In combination with a higher amount of crystallization nuclei, this might explain the formation of a more cross-hatched overall appearance, compared to PP-H.

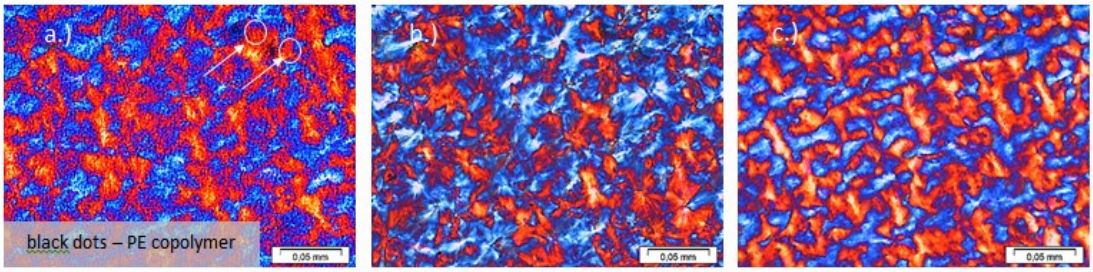

Figure 11.3: Comparison of the morphology of PP-B (a), PP-H (b) and PP-R (c) at a magnification of 500 under polarized light. Samples taken as 20 µm slices from the middle of CRB specimens.

In Figure 11.4 the molecular mass distribution of the base materials are shown. The materials were measured for a PP- equivalent. It was found, that PP-B has the lowest number average molar mass of the three examined materials, around 89,000, compared to 91,300 of PP-R and 111,000 of PP-H. However, the mass average molar mass was the highest around 605,000, compared to 538,000 of PP-R and 557,000 of PP-H. Therefore, PP-B shows the highest dispersity of 6.8 (5.9 for PP-R and 5.0 for PP-H). However, the overall shape of the curves is quite comparable for all three materials.

11.7.2. Fatigue tests

Results of fatigue tests on notched specimens are shown in Figure 11.5 for unreinforced materials at 80°C and Figure 11.10 for the reinforced materials for 23 and 80°C in a fully-logarithmic plot of cycles to failure and applied nominal stress. The PP-homopolymer was tested between 15.5 and 9.5 MPa. Between 15.5 and around 14 MPa the specimens fractured within 24 hours of testing. Fracture surfaces showed signs of unstable crack growth at the highest load levels. Decreasing the applied load led to large-scale whitening on the surfaces. Below 13 MPa, the failure mode changed. As shown in Figure 11.7 fracture surfaces showed signs of quasi-brittle crack growth in the form of very small ruptured fibrils close to the pre-notch. Furthermore, the slope in the diagram changed drastically, similar to results found for PE-materials.

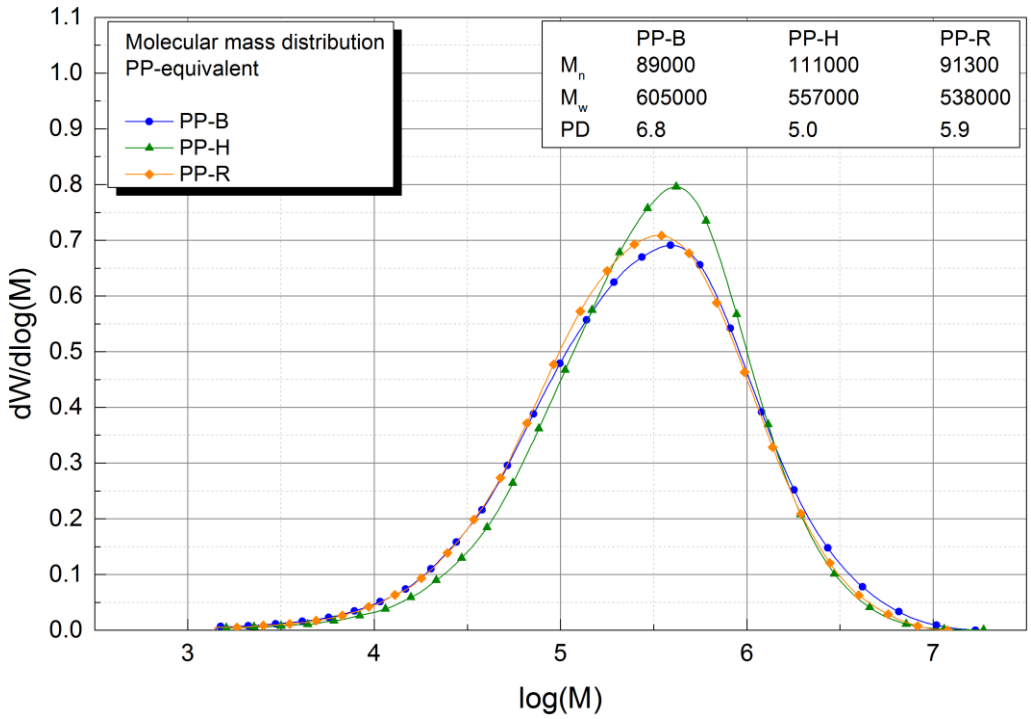

Figure 11.4: Molar mass distribution of PP-H, PP-R and PP-B, measured for a PP-equivalent.

Data of quasi-brittle failure for PP-B was taken from former work [18] and added for comparison. The block copolymer shows a rather similar behavior to PP-H with regards to the slopes of the different areas in the diagram. However, load levels and cycles to failure are significantly different. The tested load levels were between 12.5 and 7.5 MPa. The change of failure mode showed around 11 MPa. Similar to PP-H different stages of failure were detected. At the highest load levels, signs of unstable crack growth were visible on the fracture surfaces. At lower loads, again stress whitening appeared. Below 11 MPa, signs of quasi-brittle failure showed close to the pre notch in the form of ruptured fibrils, as shown in Figure 11.9 [18]. Random PP was tested between 11.5 and 9.5 MPa. It can already be seen, that the range of applied stresses is significantly smaller compared to PP-H and PP-B. Between 11.5 and 10 MPa PP-R fractured below 4.10^4 cycles, showing signs of unstable crack growth in the middle and stress whitening close to the pre notch. The last test, performed at 9.5 MPa, lasted more than 9.10^6 cycles (≈21 days at 5 Hz). Besides the significant increase in cycles to

failure, also the appearance of the fracture surface changed at this load level. Whereas at higher load levels the fracture surface showed a combination of unstable crack growth and stress whitening, now almost the whole specimen shows stress whitening. However, close to the pre-notch, the fracture surface shows a different look (compare Figure 11.8). Due to extensive testing times of several million cycles no further experiments were carried out below 9.5 MPa. A comparison of fracture surfaces is shown in Figure 11.6 to show described changes in failure mode. To determine whether or not PP-R switches to another failure mode at this stress level, different evaluation of obtained data is required.

Nevertheless, depending on the intended application, fatigue results offer a good possibility for material ranking. For higher loads and shorter times PP-H shows a better performance than PP-B and PP-R, mainly due to a higher yield stress. However, going to lower loads, which are often the more practical relevant loading cases in structural applications, such as pipes, PP-R shows a superior long-term performance compared to PP-H and PP-B.

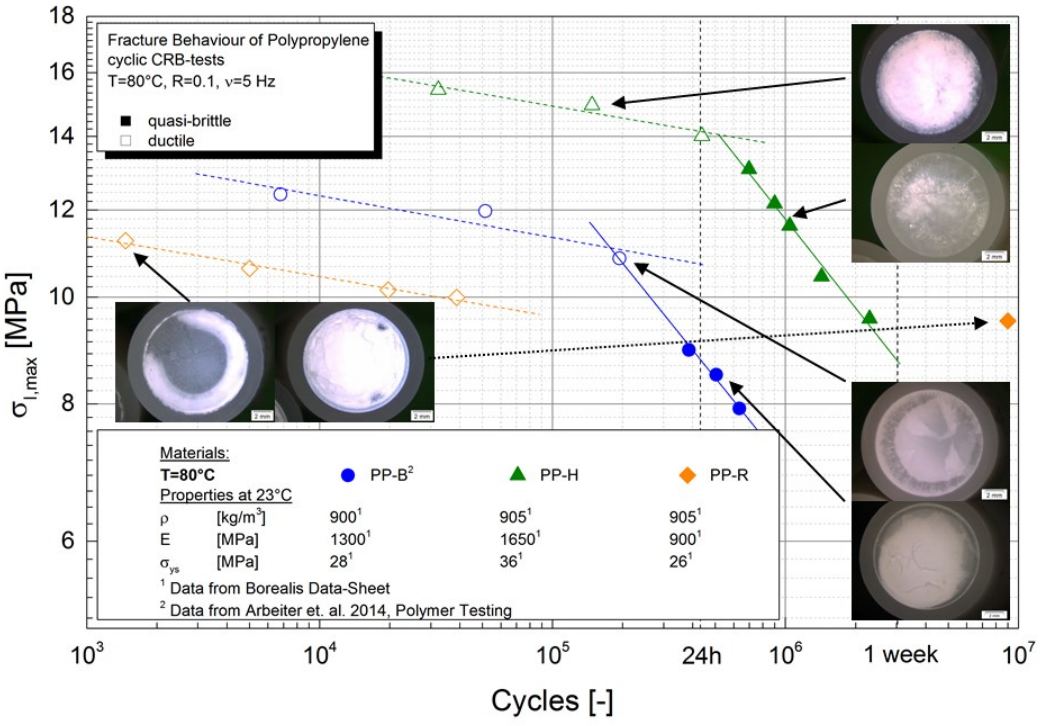

Figure 11.5: Fracture curves of the unreinforced materials PP-H, PP-R and PP-B [18] for different areas of fracture behaviour.

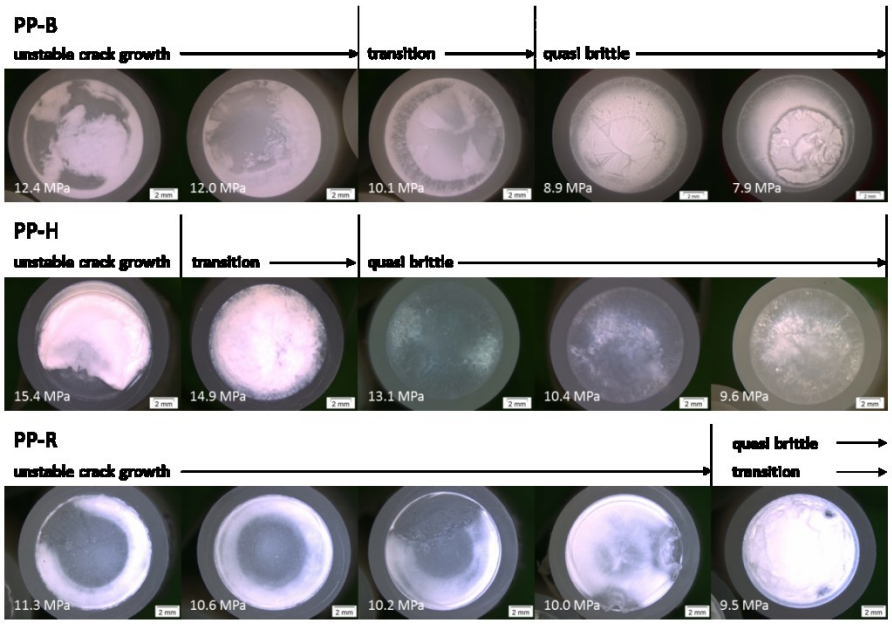

Figure 11.6: Comparison of fracture surfaces for PP-H, PP-R and PP-B at different stress levels.

To gain further information in regard to the long-term performance in the quasi-brittle failure regime, SEM analysis was performed. Pictures of PP-H in the quasi-brittle failure mode are shown in Figure 11.7. There was no macroscopically plastic deformation, or large scale formation of fibrils. The area close to the razor-blade pre-notch showed some warping of the plane of fracture and small areas of ruptured fibrillation (top right). The fibrillation occurred not as single strands, but in packages of several branched strands. The warping, as well as the ruptured fibrils might be an indication of a failure due to formation and breakdown of multiple crazes and small scale yielding, as shown in [37] for impact testing of PP at moderate speed. The area right beside (bottom right) still shows some warping but no fibrillation, correlating well with the testing at higher testing speeds in [37]. The final area of the tested specimen (bottom left) shows a mixture of smooth areas and out of plane fracture. This could signify unstable crack growth as found in [37] for very high testing speeds. This similarity of changing failure modes between impact and fatigue tests might be explained by the fact, that specimens in load controlled fatigue tests also experience different strain rates, depending on load level and progression of the test.

Figure 11.8 shows the fractographs of the PP-R specimen at 9.5 MPa, which is suspected to be in the transition area between mode 1 and quasi-brittle failure. The area of different appearance can be seen quite clearly in the overview-picture as a ring next to the initial pre-notch (dashed lines). In this area several different appearances of the fracture surface can be found. Nevertheless, traces of the formation and breakdown of fibrils due to fatigue damage could be found (top right). Similar to PP-H above, this might be a sign of failure due to small scale yielding and multiple crazing. In the transition area (bottom right), the fracture surface shows a smoother appearance besides several visible grooves in the direction of crack growth. This might indicate failure due to multiple crazing, without small scale yielding, due to higher loads and strain rates. The surface area of the residual fracture (bottom left) is again very smooth with light warping in arbitrary direction and several spherical holes, indicating failure due to unstable crack growth.

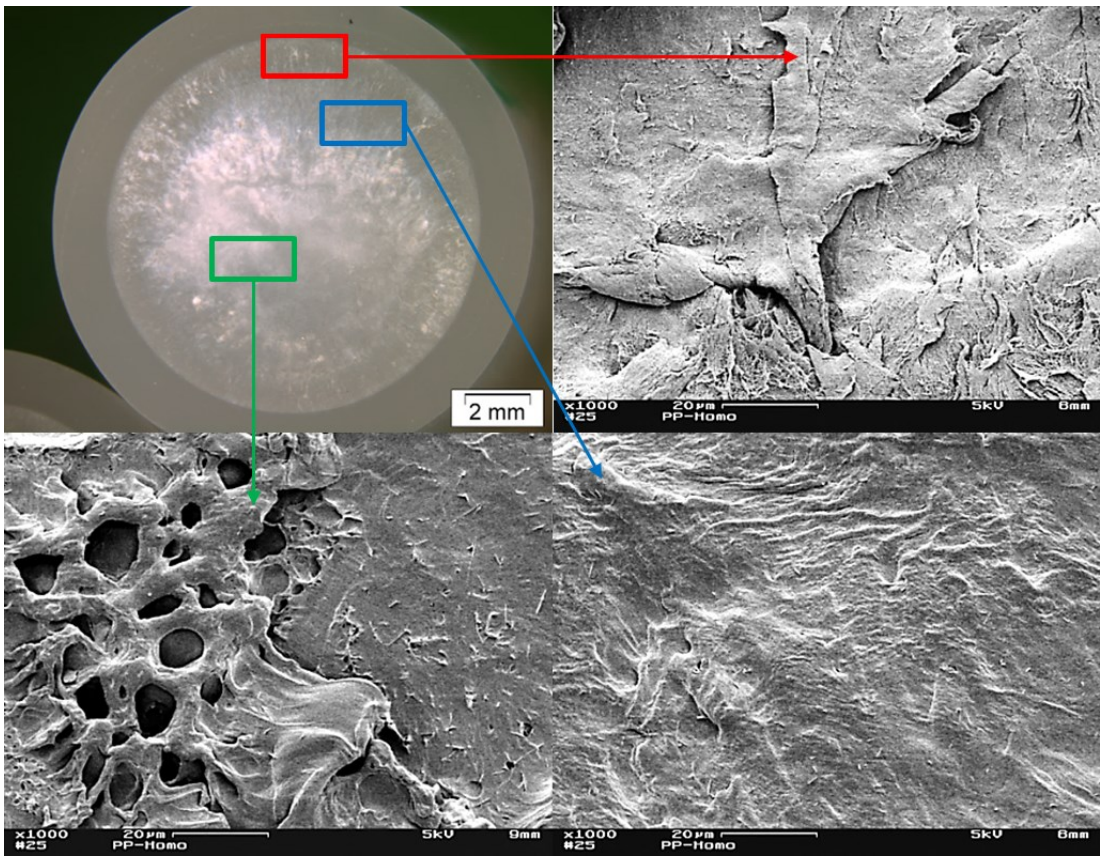

Figure 11.7: Fracture surface analysis of PP-H, tested at 80°C and 12 MPa using SEM at a magnification of 1000x.

The area with signs of fibrillation close to the pre-notch is a further indication of a change in fracture mode for PP-R at this load level, besides the significant increase of cycles to failure. The overall stress whitened appearance might also be an explanation, why PP-R shows a better performance in this failure region. Compared to PP-H, where the damage propagates through the material without showing large areas of yielding, energy might be dissipated in PP-R due to the formation of ductile deformation mechanisms. For comparison, the fracture surface of PP-B [18] has been added below in Figure 11.9.

Compared to PP-H and PP-R, larger ruptured craze fibrils were found on the fracture surface. Also the transition area shows signs of packages of drawn fibrils. Contrary to PP-H and PP-R the residual area in the middle of the specimen, showed a very ductile behaviour at 80°C [18], more similar to PE-HD than PP-H and PP-R above. Interestingly, a clear differentiation between PP matrix and PE inclusions is not possible anymore (compare Figure 11.3).

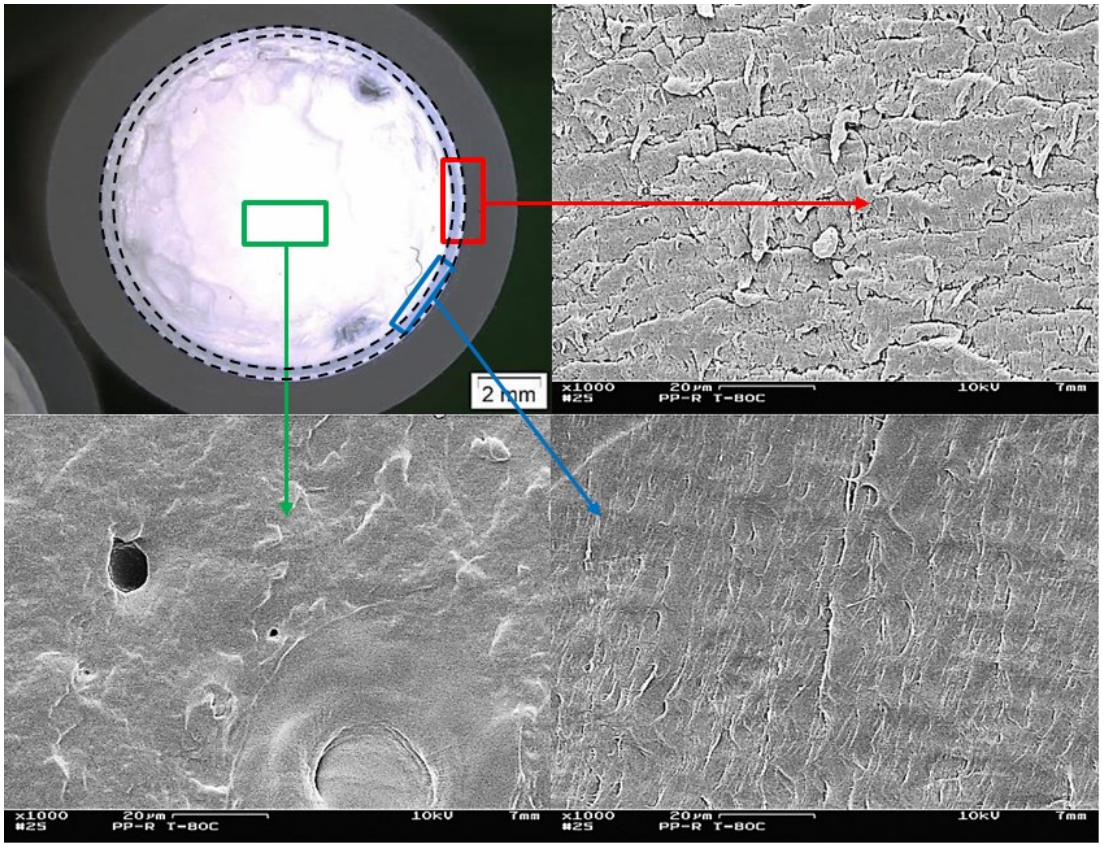

Figure 11.8: Fracture surface analysis of PP-R, tested at 80°C and 9.5 MPa using SEM at a magnification of 1000x.

A reason for the lower fatigue resistance in the quasi-brittle region at 80°C, compared to PP-H, might be due to several reasons. Polyethylene shows an overall lower Young's Modulus compared to the PP matrix material. Therefore, the effective load bearing area is decreased compared to pure PP material. Furthermore, if PE segments are not sufficiently bonded to the PP matrix as found in [26] for blended PP/PE materials, the holes might act as notches which decrease fatigue lifetime.

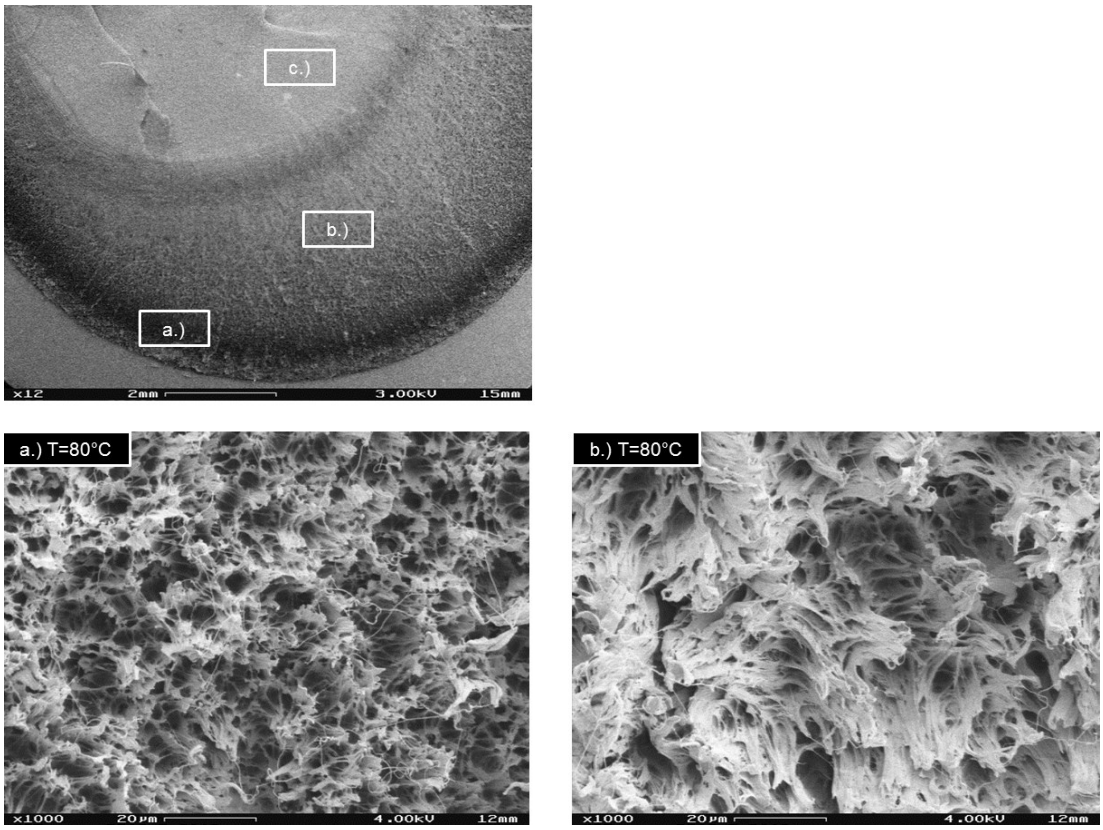

Figure 11.9: Fracture surface analysis of PP-B, tested at 80°C and 8 MPa using SEM at a magnification of 1000x [18].

Fatigue results of the reinforced materials at 23 and 80°C are shown in Figure 11.10. Materials were tested at 80°C as a comparison to the unreinforced materials and at 23°C for an estimation of the fatigue behaviour close to actual application temperature. Both materials were tested between 13 and 15 MPa at 23°C and between 6 and 8 MPa at 80°C. At 23°C PP & wollastonite and PP & talcum show similar slopes in the fully logarithmic plot. The material with almost 50% talcum reinforcement endures higher loads for similar failure cycles compared to the material with 20% wollastonite. At 80°C

the slopes of both materials change. This may be due to the fact, that 80°C is far from any transition region, whereas at 23°C the influence of T_g is still present (compare). Furthermore, slopes at 80°C of the reinforced materials are less steep compared to the unreinforced materials. Again, ranking of materials depends on the intended application and load levels. However, for the purpose of structural long-term applications used at rather low loads (below approx. 11 MPa at 23°C and 6.5 MPa at 80°C), reinforced materials show superior fatigue resistance due to shallower slopes. The talcum reinforced material exhibits a better performance compared to the wollastonite reinforced material. However, differences in reinforcement percentage (50 and 20%) lessen the validity of direct comparison.

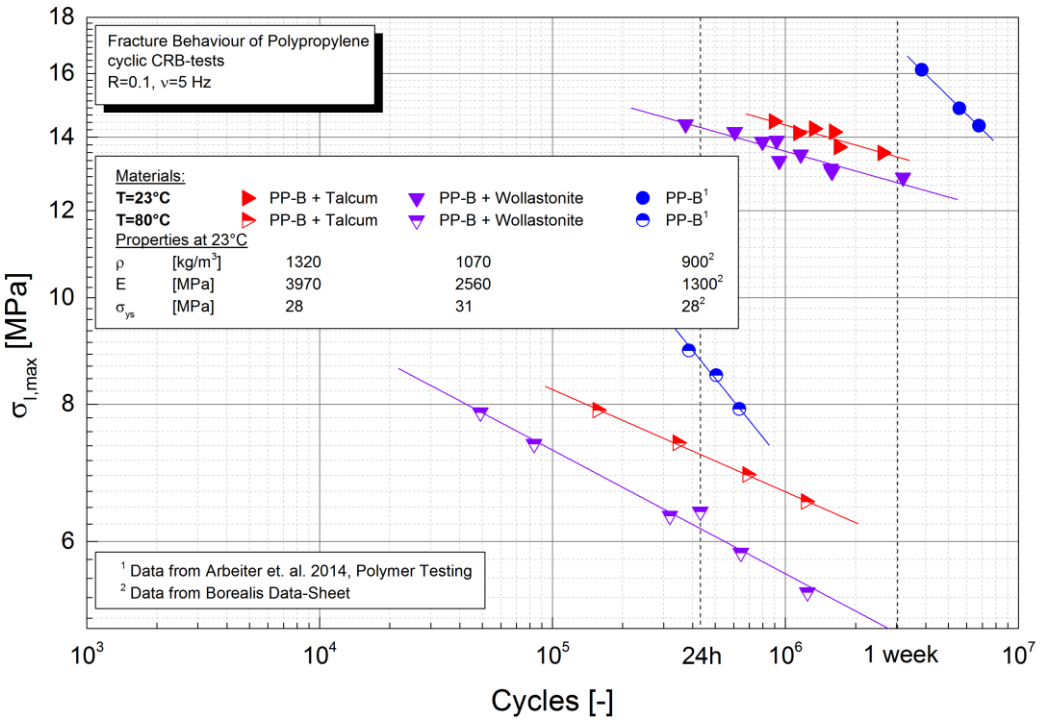

Figure 11.10: Fracture curves of the reinforced materials PP-B & talcum and PP-blend & wollastonite at 23 and 80°C with pure PP-B from [18] for comparison.

Figure 11.11 and Figure 11.12 show the fracture surface of the PP-blend with wollastonite and PP-B with talcum in three regions of the specimen. The specimens were tested at 23°C. Both reinforced materials show three distinctive regions on the fracture surface. Close to the pre-notch, there is

formation and breakdown of fine fibrils, with wollastonite needles and talcum plates in between. Adjacent is a region of transition, where signs of broken down fibrils are visible but they are stretched in packages, rather than single strands. Closer to the center, the wollastonite reinforced material shows a very smooth and brittle surface with signs of broken and pulled out needles. This failure behaviour is very similar to unreinforced PP-B at 23°C [18]. Due to the high crack velocity and strain rates in the center of the specimen towards the end of the test, talcum plates and material around them have no time for rearrangement or deformation before fracture. Therefore, the material shows a rock-like fracture surface with a rather brittle failure of PP matrix material and talcum sticking out of the surface. Fracture surfaces of specimens tested at 80°C showed the same different areas. Only the size and number of fibrils in the first area changed, similar to pure PP-B, as shown in [18]. Interestingly, the failure of the residual area of the reinforced PP-B material remained rather brittle, compared to the unreinforced PP-B. This might be attributed to the overall stiffer material behaviour and embrittlement due to the reinforcement (compare to Figure 11.10 and Table 11.1).

For comparison, all tested PP types are compared in Figure 11.13 at 80°C. It can be seen, that reinforcement with minerals tilts fracture curves towards a shallower slope. For low stress applications this can lead to an improvement of long-term performance of the materials. However, at high stress applications, such as pressurized pipes, where applied stress is closer to the transition between failure modes, unreinforced materials could be a saver choice.

Development of specimen compliance has been investigated as a possible additional method for distinguishing between different failure-modes. In Figure 11.14 and Figure 11.15 are the results shown for PP-H and PP-R in a semi-logarithmic plot. Specimen compliance was normalized to the first value for a better visibility of the trends at different initial stress levels.

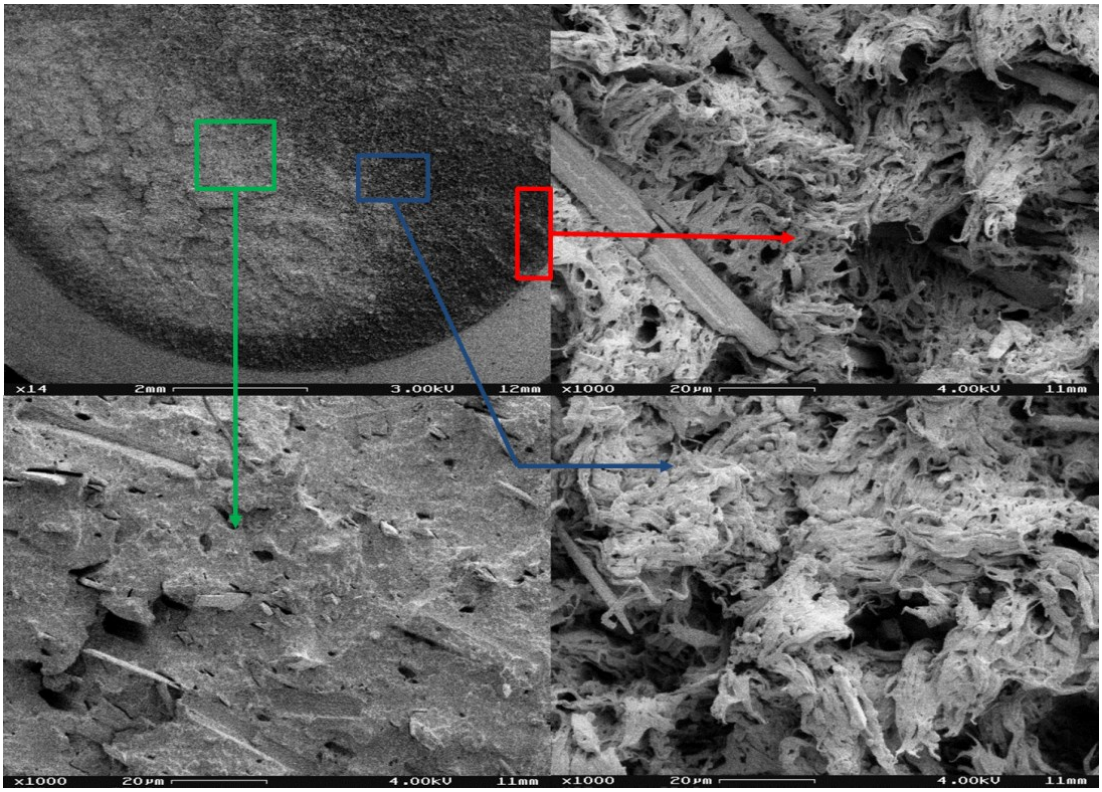

Figure 11.11: Fracture surface analysis of PP-blend & wollastonite, tested at 23°C and 13 MPa using SEM at a magnification of 1000x.

The trends of PP-H in Figure 11.14 show, that specimens which failed in the first failure region show a different behaviour than the specimens which failed in the second failure region. The specimens at the highest two stress levels show a monotonic increase of specimen compliance over the course of testing. The specimen tested at 14 MPa which is very close the transition between both regions shows first signs of a constant specimen compliance level during the test. Below 14 MPa of testing all compliance curves show a clear stagnation of the value after an initial increase or even a decrease during the test, which might be in relation to a local strain hardening effect in front of the crack tip, as reported for other polymers under fatigue load [13,38,39]. The specimen tested at the lowest stress level even showed a first sign of a step-like development of specimen compliance towards the end.

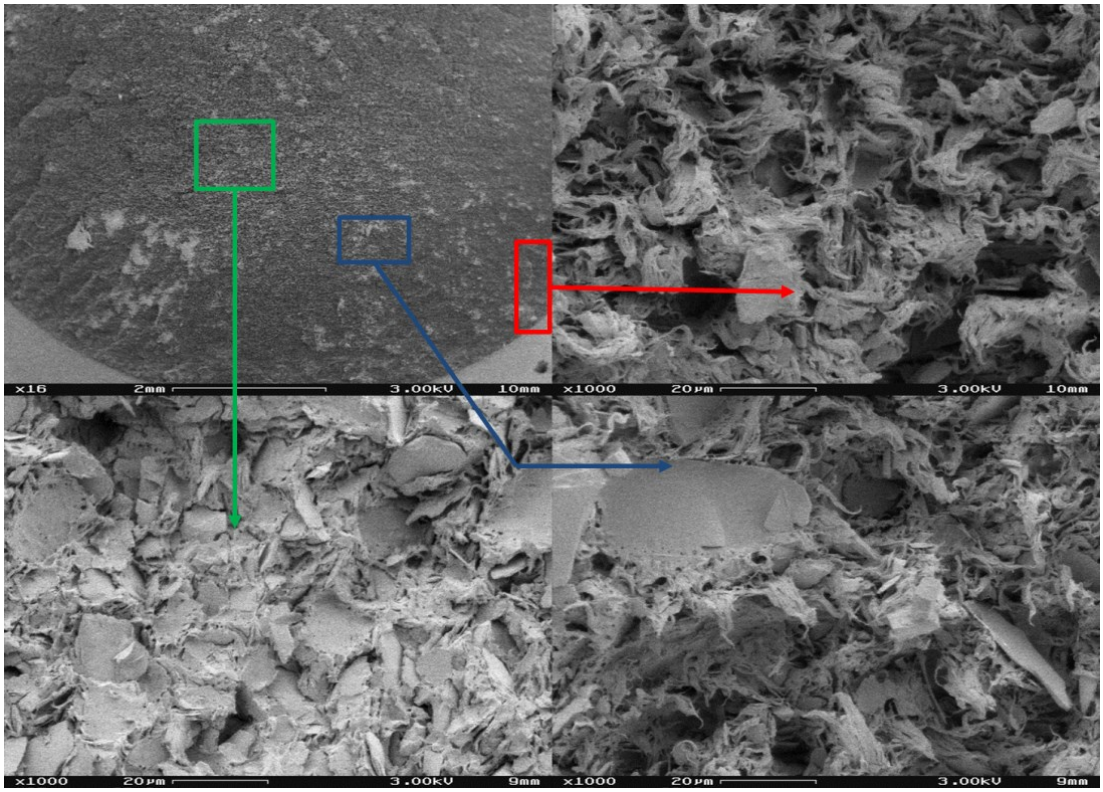

Figure 11.12: Fracture surface analysis of PP-B & talcum, tested at 23°C and 13 MPa using SEM at a magnification of 1000x.

In Figure 11.15 the same analysis was done for PP-R. For this material, where the second failure region has not been clearly investigated yet, compliance analysis delivers valuable additional information. Similar to PP-H, the tests which failed in the first failure mode, normalized specimen compliance increased continuously over the whole test. The last test, performed at 9.5 MPa shows a similar trend compared to the test at 10 MPa in the beginning. After a few thousand cycles, when the compliance of the test at 10 MPa continued to increase further, it stagnated at 9.5 MPa and even decreased later on. Between 4 and 9 million cycles, the test showed a similar behaviour to the test of PP-H at the lowest stress level. Towards the end of the test first indications of step-wise compliance increase could be detected. Observation of the crack tip using a travelling microscope during the test showed that the step in normalized compliance was accompanied with an increase in crack length. However, before another step could be formed, stress in the ligament area lead to final failure of the specimen.

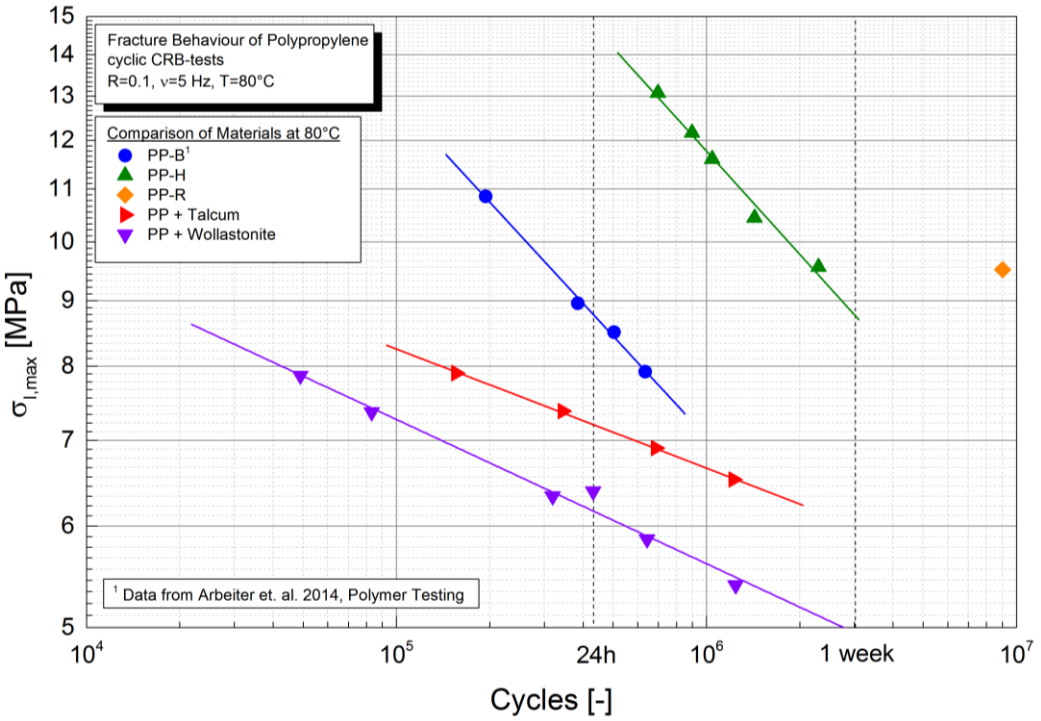

Figure 11.13: Comparison of all five tested materials at 80°C in quasi-brittle failure mode.

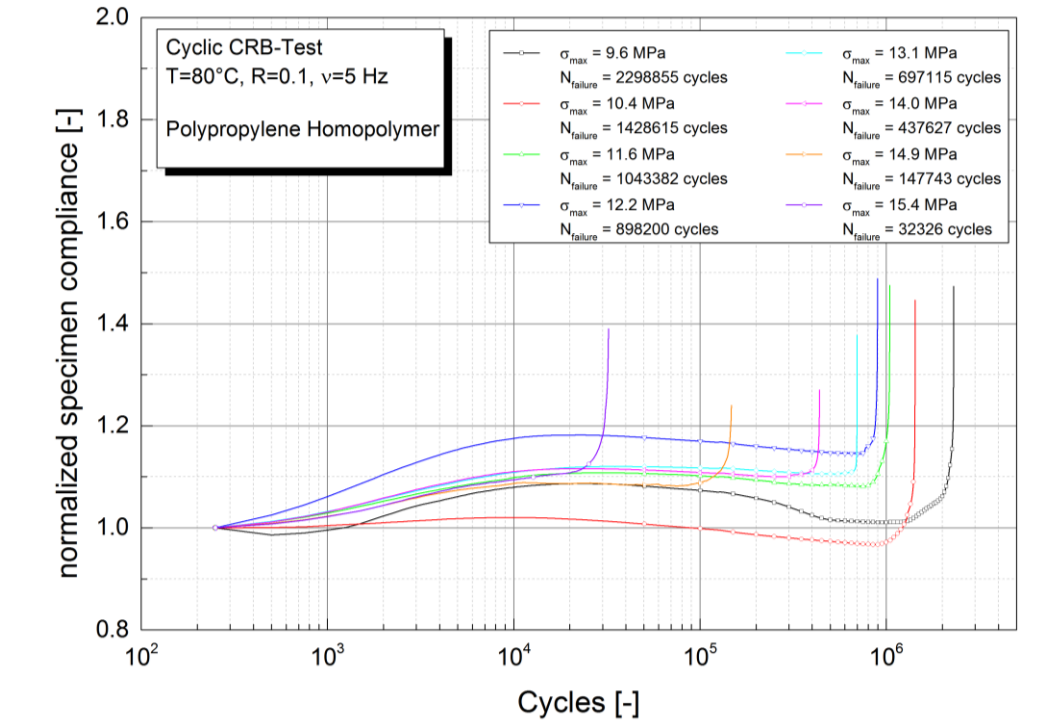

Figure 11.14: Development of normalized specimen compliance of PP-H as a function of applied stress level.

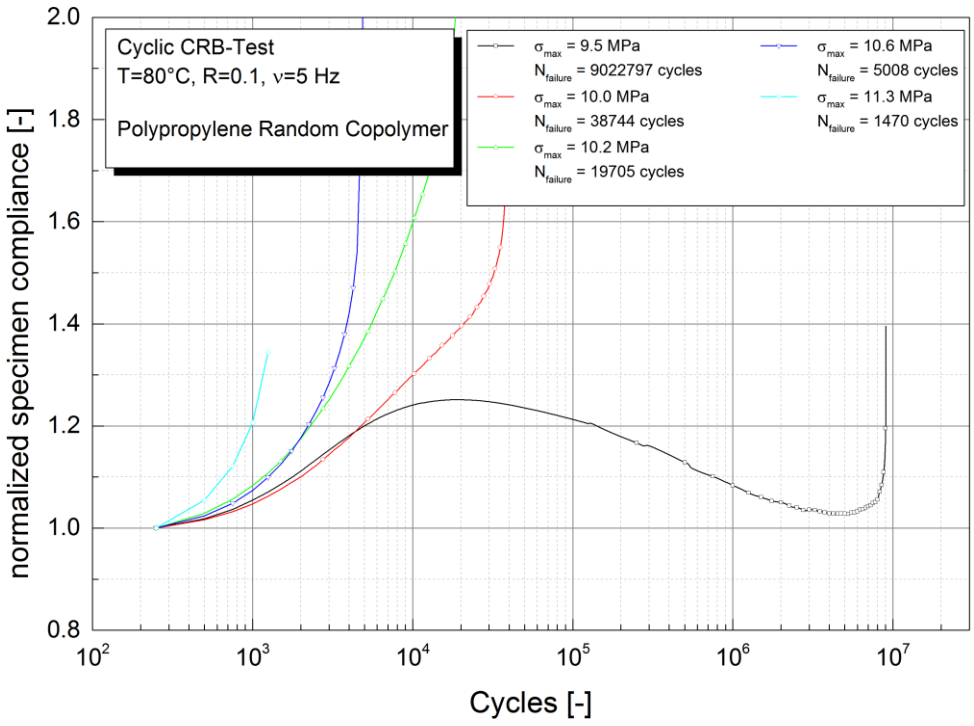

Figure 11.15: Development of normalized specimen compliance of PP-R as a function of applied stress level.

To further investigate the failure mode of PP-R at the stress level around 9.5 MPa, hysteresis analysis has been performed. In Figure 11.16 the development of the hysteresis is shown for a test above 10 MPa and the test at 9.5 MPa. Interestingly, also this analysis shows a clear difference between the two stress levels. Above 10 MPa the hysteresis changes in form and slope over the course of testing, indicating a fast damage progression and maybe even hysteretic heating [40,41]. At 9.5 MPa, the hysteresis' slope and shape stay rather constant until failure. This indicates a vastly decreased damage progression speed, compared to tests above 10 MPa. In both cases, hysteresis shift towards higher strains due to creeping. This change in hysteresis behaviour is a further indication, that the mode of failure changes around 9.5 MPa towards quasi-brittle.

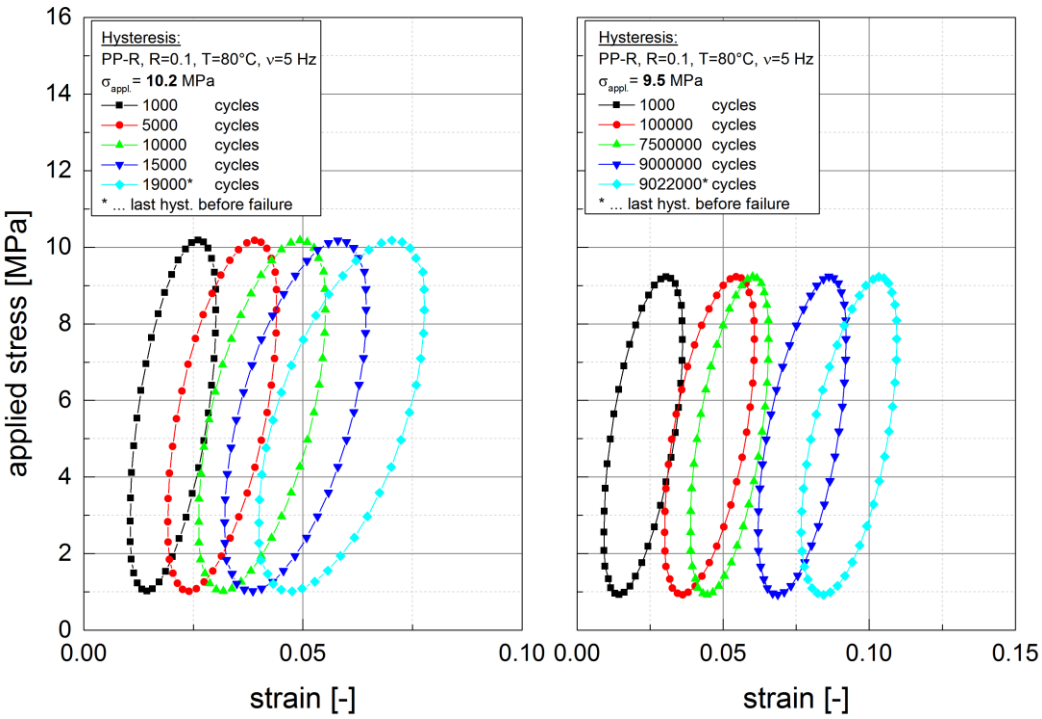

Figure 11.16: Development of hysteresis in PP-R: Comparison of region one failure (10.2 MPa) and the transition area (9.5 MPa).

Even though failure modes can be quiet easily distinguished for PP-H in the fracture curve, the same analysis has been performed on PP-H as a comparison. The results for PP-H are shown in Figure 11.17. The same trends as for PP-R can be seen, even though differences are not as pronounced. At the higher load, in failure region one, hysteresis slightly tilts towards the end of the test and also the shape changes. At the lower load level in quasi-brittle failure region form and slope remain mostly unchanged until final failure. Due to the shorter testing time and higher mechanical properties at a similar load level in quasi-brittle failure mode, the overall strain of PP-H is much smaller compared to PP-R.

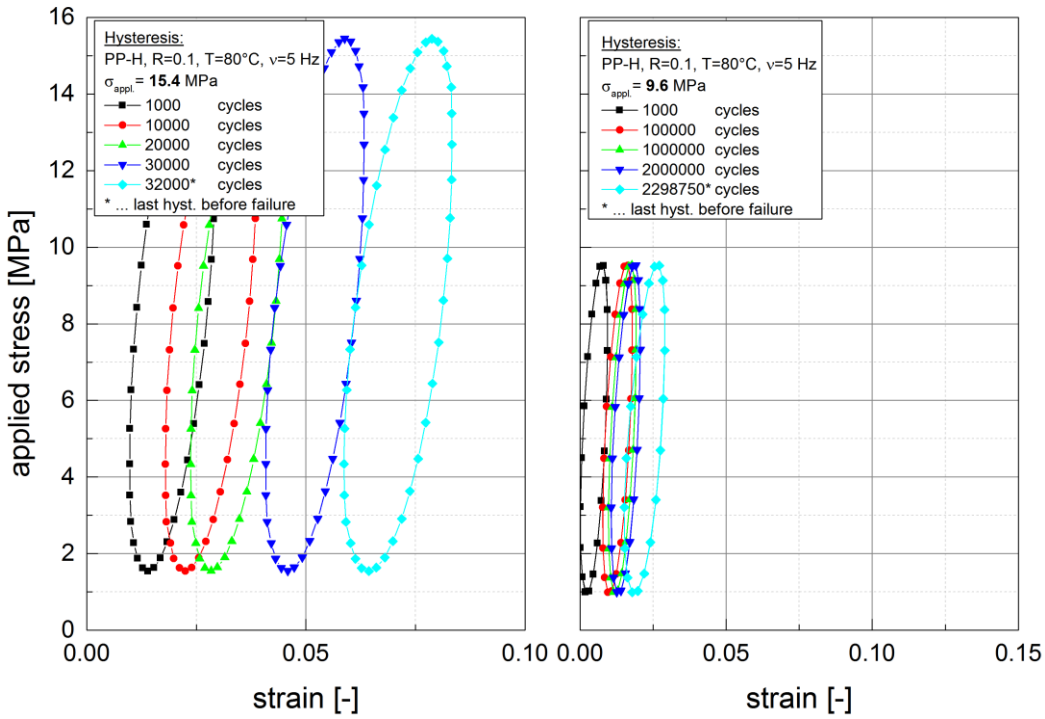

Figure 11.17: Development of hysteresis in PP-H: Comparison of region one failure (15.4 MPa) and the transition area (9.6 MPa).

11.8. Conclusions

Using DMA and DSC analysis, it was possible to show the differences in thermal and mechanical behaviour over a wide range of temperatures. The properties of PP-R were not only the lowest, but also decreased much earlier compared to the other materials. This might be explained by the formation of γ-modification in PP-R, which decreases crystallization speeds, lowers the equilibrium melting temperature and leads to an overall decreased crystallinity [34,36]. Molecular mass distribution of the unreinforced materials showed a rather similar curve for all three materials. Nevertheless, fatigue testing at 80°C using CRB specimens revealed tremendous differences between PP-H, PP-B and PP-R. This highlights the fact, that fatigue performance is not only influenced by MWD and morphology, as shown in [42], but is additionally also highly dependent on the presence of co-monomer in the main chain. Similar results for quasi-static properties, such as flexural modulus or impact properties have been reported previously [37,36,43]. Similar to PE-HD pipe materials, unreinforced PP Materials

showed two different areas of failure. These areas are often referred to as ductile and quasi-brittle failure regime for PE-HD pipe materials [44,45]. However, the definition of the first failure mode is not quite fitting for the tested PP-H and PP-R materials in fatigue, seeing that this region seems to be dominated by unstable crack growth accompanied with very smooth fracture surfaces. In contrast, PP-B shows behaviour more similar to findings in PE-HD.

Regarding a ranking of the materials, it can be said, that in the first failure region PP-H shows better performance than PP-B and PP-R. This can mainly be addressed to differences in yield stress and crystallinity. In the second failure region, PP-R shows a better performance below 10 MPa, compared to PP-H and PP-B. In this failure mode PP-B showed the lowest fatigue resistance. Incorporated PE blocks seem to weaken the material with regard to fatigue, compared to pure PP-H. Comparing fracture surfaces, PP-R appears to have a higher tendency towards formation of plastic deformation mechanisms (stress whitened fracture surfaces, blunted crack tips, etc.) than PP-H. Plastic deformation usually dissipates a lot of energy, which might explain the better performance of PP-R. Observation of the crack tip via travelling microscope during the test also showed blunting of the notch tip which decreases local stress concentrations. Contrary to CRB tests on PE-HD no clear crack growth was observed until final failure of the specimen. It can be speculated, that the specimen failed due to formation and coalescence of crazes, as discussed in [12]. Interestingly, the changes in failure mode and appearance of fracture surfaces seem to correlate to trends found for impact tests on PP at different loading rates [37]. Tests at high stress levels and accompanied strain rates in fatigue showed a similar failure mode to tests at high speeds in impact tests, namely unstable crack growth with very smooth fracture surfaces. By decreasing the stress level in fatigue, or velocity in impact tests, warping of fracture surfaces can be found. This was explained in [37] by the formation and breakdown of multiple crazes. Further decreasing test parameters, fracture surfaces additionally showed signs of formation and breakdown of fibrils, which can be explained by small scale yielding and multiple craze formation. As mentioned above, the last failure mode of large scale yielding, was not experienced during fatigue tests. Hysteresis and compliance analysis was found to deliver additional insights

into material behaviour during fatigue tests. Especially for PP-R, where the second failure mode could not be clearly established, these methods can be used to distinguish between failure modes.

Additionally to the unreinforced materials, which already exhibited vastly different fatigue properties, also two reinforced materials were tested. Due to their actual application temperature, and overall more brittle behaviour, both materials were tested not only at 80°C, but also at 23°C. At both temperatures, the 50 wt% talcum reinforced material showed superior fatigue properties, compared to the wollastonite 20 wt% reinforced material. Fractographic analysis of failed specimens showed clear formation of fibrils between mineral reinforcement (compare Figure 11.11 and Figure 11.12), which can be addressed to the matrix material of PP-B [18]. The first region failure for this material has not been examined, due to the area of real-life application of these materials. When comparing to the pure PP-B, it can be seen, that the reinforcement changes the failure behaviour significantly. Quasi-brittle failure shows a shallower slope, compared to the unreinforced material.

As a conclusion, testing via cyclic CRB tests at elevated temperature appears to be a suitable method for PP-H and reinforced PP materials. Both failure regions of interest can be reached within several hours of testing. Testing of PP-R is possible, albeit only in the first failure region, or with the downside of rather long testing times. Testing at other temperatures could provide remedy, although the thermo-mechanical changes have to be considered, due to the rather low melting temperature onset. As a next step, testing the applicability of lifetime estimation concepts, as developed for PE pipe materials [23–25,46,47], to the tested PP materials would be of high interest.

11.9. Acknowledgement

The research work of this publication was performed at the Institute of Materials Science and Testing of Polymers (Montanuniversitaet Leoben, Austria) within the framework of the FFG program of the Austrian Ministry of Traffic, Innovation and Technology and the Austrian Ministry of Economy, Family and Youth with contributions of the Österreichisches Forschungsinstitut für Chemie und Technik (Austria), Martin-Luther-

Universität Halle-Wittenberg (Germany) and the Polymer Competence Center Leoben GmbH (Austria). PP-H and PP-R material used for this publication was kindly provided by Borealis AG.

11.10. References

[1] ISO. Plastics piping systems for hot and cold water installations -- Polypropylene (PP) -- Part 2: Pipes(15874-2); 2013.

[2] Grellmann W, Che M. Assessment of temperature-dependent fracture behavior with different fracture mechanics concepts on examples of unoriented and cold-rolled polypropylene. Journal of Applied Polymer Science 1998:1237–49.

[3] Salazar A, Frontini PM, Rodríguez J. Determination of fracture toughness of propylene polymers at different operating temperatures. Engineering Fracture Mechanics 2014;126:87–107.

[4] Morhain C, Velasco JI. Determination of J-R curve of polypropylene copolymers using the normalization method. Journal of Materials Science 2001;36:1487–99.

[5] Turcsán T, Mészáros L, Khumalo VM, Thomann R, Karger-Kocsis J. Fracture behavior of boehmite-filled polypropylene block copolymer nanocomposites as assessed by the essential work of fracture concept. J. Appl. Polym. Sci. 2014;131:n/a.

[6] Karger-Kocsis J, Khumalo VM, Bárány T, Mészáros L, Pegoretti A. On the toughness of thermoplastic polymer nanocomposites as assessed by the essential work of fracture (EWF) approach. Composite Interfaces 2013;20:395–404.

[7] Karger-Kocsis J, Barany T. Plane-stress fracture behavior of syndiotactic polypropylenes of various crystallinity as assessed by the essential work of fracture method. Polym. Eng. Sci. 2002;42:1410–9.

[8] Saminathan K, Selvakumar P, Bhatnagar N. Fracture studies of polypropylene/nanoclay composite. Part I: Effect of loading rates on essential work of fracture. Polymer Testing 2008;27:296–307.

[9] Chen H, Karger-Kocsis J, Wu J, Varga J. Fracture toughness of α- and β-phase polypropylene homopolymers and random- and block-copolymers. Polymer 2002;43:6505–14.

[10] Kausch H, Gensler R, Grein C, Plummer, C. J. G., Scaramuzzino P. Crazing in semicrystalline thermoplastics. Journal of Macromolecular Science, Part B 1999;38:803–15.

[11] Gahleitner M, Bernreitner K, Neiβl W, Paulik C, Ratajski E. Influence of molecular structure on crystallization behaviour and mechanical properties of polypropylene. Polymer Testing 1995;14:173–87.

[12] Jones NA, Lesser AJ. Morphological study of fatigue-induced damage in isotactic polypropylene. Journal of Polymer Science Part B: Polymer Physics 1998;36:2751–60.

[13] Lesser AJ. Changes in mechanical behavior during fatigue of semicrystalline thermoplastics. J. Appl. Polym. Sci. 1995;58:869–79.

[14] Constable I, Williams JG, Burns DJ. Fatigue and cyclic thermal softening of thermoplastics. ARCHIVE: Journal of Mechanical Engineering Science 1959-1982 (vols 1-23) 1970;12:20–9.

[15] ISO. Polyethylene (PE) materials for piping systems - Determination of resistance to slow crack growth under cyclic loading - Cracked Round Bar test method(18489); 2015.

[16] Frank A, Pinter G. Evaluation of the applicability of the cracked round bar test as standardized PE-pipe ranking tool. Polymer Testing 2014;33:161–71.

[17] Frank A, Lang RW, Pinter G. Accelerated Investigation of creep crack growth in polyethylene pipe grade materials by the use of fatigue tests on cracked round bar specimens: Proceedings Annual Technical Conference - ANTEC, Society of Plastics Engineers, Milwaukee, Wisconsin, USA 2008:2435–9.

[18] Arbeiter F, Pinter G, Frank A. Characterisation of quasi-brittle fatigue crack growth in pipe grade polypropylene block copolymer. Polymer Testing 2014.

[19] Arbeiter F, Schrittesser B, Frank A, Berer M, Pinter G. Cyclic tests on cracked round bars as a quick tool to assess the long-term behaviour of thermoplastics and elastomers. Polymer Testing 2015;45:83–92.

[20] Pinter G. Slow crack growth in PE-HD under static and cyclic loads. Habilitation. Leoben; 2008.

[21] Parsons M, Stepanov EV, Hiltner A, Baer E. Correlation of fatigue and creep slow crack growth in a medium density polyethylene pipe material. Journal of Materials Science 2000;35:2659–74.

[22] Broek D. Elementary engineering fracture mechanics. 3rd ed. The Hague, Boston, Hingham, Mass: Martinus Nijhoff; Distributed by Kluwer Boston; 1982.

[23] Frank A, Pinter G, Lang RW. Lifetime prediction of polyethylene pipes based on an accelerated extrapolation concept for creep crack growth with fatigue tests on cracked round bar specimens. In: Society of Plastics Engineers, editor. ANTEC; 2009, p. 2169–2174.

[24] Pinter G, Arbeiter F, Berger I, Frank A. Correlation of Fracture Mechanics Based Lifetime Prediction and Internal Pipe Pressure Tests. In: Proceedings Plastic Pipes XVII 2014; 2014.

[25] Frank A, Pinter G, Lang RW. Fracture Mechanics Lifetime Prediction of PE 80 and PE 100 Pipes under Complex Loading Conditions. In Proceedings Plastics Pipes XV Vancouver (Cdn) 2010.

[26] Grein C, Bernreitner K, Hauer A, Gahleitner M, Neißl W. Impact modified isotatic polypropylene with controlled rubber intrinsic viscosities: Some new aspects about morphology and fracture. Journal of Applied Polymer Science 2003;2003:1702–12.

[27] Karger-Kocsis J. Toward understanding the morphology-related crack initiation and propagation behavior in polypropylene systems as assessed by the essential work of fracture approach. Journal of Macromolecular Science, Part B 2006;38:635–46.

[28] Kotter I, Grellmann W, Koch T, Seidler S. Morphology–toughness correlation of polypropylene/ethylene–propylene rubber blends. J. Appl. Polym. Sci. 2006;100:3364–71.

[29] Bai H, Wang Y, Zhang Z, Han L, Li Y, Liu L et al. Influence of Annealing on Microstructure and Mechanical Properties of Isotactic Polypropylene with β-Phase Nucleating Agent. Macromolecules 2009;42:6647–55.

[30] Rosa C de, Auriemma F, Paolillo M, Resconi L, Camurati I. Crystallization Behavior and Mechanical Properties of Regiodefective, Highly Stereoregular Isotactic Polypropylene: Effect of Regiodefects versus Stereodefects and Influence of the Molecular Mass. Macromolecules 2005;38:9143–54.

[31] Borealis AG. Product Data Sheet: BE50; 2014.

[32] Borealis AG. Product Data Sheet: RA130E; 2014.

[33] Borealis AG. Data Sheet - BA202E: Polypropylene Block Copolymer for Non-Pressure Pipes; Available from: http://www.borealisgroup.com/datasheets/10017403.

[34] Mileva D, Androsch R, Radusch H. Effect of cooling rate on melt-crystallization of random propylene-ethylene and propylene-1-butene copolymers. Polym. Bull. 2008;61:643–54.

[35] Rungswang W, Saendee P, Thitisuk B, Pathaweeisariyakul T, Cheevasrirungruang W. Role of crystalline ethylene-propylene copolymer on mechanical properties of impact polypropylene copolymer. J. Appl. Polym. Sci. 2013;128:3131–40.

[36] Gahleitner M, Jääskeläinen P, Ratajski E, Paulik C, Reussner J, Wolfschwenger J et al. Propylene-ethylene random copolymers: Comonomer effects on crystallinity and application properties. J. Appl. Polym. Sci. 2005;95:1073–81.

[37] Gensler R, Plummer C, Grein C, Kausch H. Influence of the loading rate on the fracture resistance of isotactic polypropylene and impact modified isotactic polypropylene. Polymer 2000;41:3809–19.

[38] Berer M, Major Z, Pinter G, Constantinescu DM, Marsavina L. Investigation of the dynamic mechanical behavior of polyetheretherketone (PEEK) in the high stress tensile regime. Mech Time-Depend Mater 2013.

[39] Hertzberg RW, Manson JA. Fatigue of engineering plastics. New York: Academic Press; 1980.

[40] Altstädt V. Hysteresismessungen zur Charakterisierung der mechanisch-dynamischen Eigenschaften von R-SMC Zusammenhang von Struktur u. Eigenschaften; 1987.

[41] Zahnt B. Ermüdungsverhalten von diskontinuierlichen glasfaserverstärkten Kunststoffen: Charakterisierungsmethoden, Werkstoffgesetze und Struktur-Eigenschafts-Beziehungen. Dissertation. Leoben, Austria; 2003.

[42] Karger-Kocsis J. Dependence of the fracture and fatigue performance of polyolefins and related blends and composites on microstructural and molecular characteristics. Macromol. Symp. 1999;143:185–205.

[43] Kock C, Aust N, Grein C, Gahleitner M. Polypropylene/polyethylene blends as models for high-impact propylene-ethylene copolymers, part 2: Relation between composition and mechanical performance. J. Appl. Polym. Sci. 2013;130:287–96.

[44] Lang RW, Stern A, Dörner GF. Applicability and limitations of current lifetime prediction models for thermoplastics pipes under internal pressure. Die Angewandte Makromolekulare Chemie 1997:131–45.

[45] Pinter G, Haager M, Balika W, Lang RW. Fatigue crack growth in PE-HD pipe grades. Plas. Rub. Compos 2005;34:25–33.

[46] Lang RW, Pinter G, Balika W, Haager M. A Novel Qualification Concept for Lifetime and Safety Assessment of PE Pressure Pipes for Arbitrary Installation Conditions. In: Proceedings Plastic Pipes XIII; 2006.

[47] Frank A, Hartl AM, Pinter G, Lang RW. Validation of an accelerated fracture mechanics extrapolation tool for lifetime prediction of PE pressure pipes. In: Society of Plastics Engineers, editor. ANTEC; 2010, p. 1638–1643.

Part VI.

Influence of thermal ageing on the performance of reinforced pipe grade polypropylene

12. Introduction to Publications 6

Besides failure of pipelines due to crack growth or other mechanically driven damage, there is also the question of material ageing and its interaction with aforementioned mechanisms. Ageing of polymeric materials can be divided into physical and chemical ageing. Whereas physical ageing can influence “Stage I” and “Stage II” failure of pipes, chemical ageing can have a big impact on “Stage II” and “Stage III” failures. Therefore, it is necessary to characterize both types of ageing and its influence in order to cover the whole lifetime-spectrum of pipes.

When focusing especially on long-term properties of pipes, chemical ageing can pose a severe threat to lifetimes of polymeric pipes, by decreasing the time necessary before the onset of “Stage III” type failure. In order to avoid “Stage III” failure of pipe systems sufficient stabilization of polymeric materials is imperative. This type of failure can additionally be accelerated drastically for example by media [1–4], thermal ageing [5,6], or a combination thereof.

Similar to the previous chapters, it is impractical to wait for naturally aged pipes, especially since studies on excavated pipes have shown that even after 30 years of use pipes are still in good condition without significant chemical ageing [7]. To ensure pipe safety and examine material degradation, accelerated testing procedures are necessary. As mentioned above, thermal activation of otherwise slow processes is one possibility to accelerate ageing. However, accelerated ageing procedures can lead to false results, if they change otherwise unaffected properties. Even if it is the aim to characterize only the influence of chemical ageing and corresponding changes in “Stage II” or “Stage III” failures, it is important to observe other possible changes, e.g. due to physical ageing, as well. Otherwise, the danger of misinterpretation of changes in properties is imminent.

The typical processes of thermo-oxidative degradation envisaged for polypropylene have been described by Gugumus [8] as following:

Initiation / Branching:

$POOH + PH \rightarrow PO^* + H_2O + P^*$

$POOH + PH \rightarrow P = O + H_2O + PH$

$POOH + POOH \rightarrow PO_2^* + H_2O + PO^*$

$POOH + POOH \rightarrow POOH + P = O + H_2O$

Propagation:

$PO^* + PH \rightarrow POH + P^*$

$PO^* \rightarrow (P = O)_{methyl\text{-}ketone} + P^*$

$P^* + O_2 \rightarrow PO_2^*$

$PO_2^* + PH \rightarrow POOH + P^*$

Termination:

$PO_2^* + PO_2^* \rightarrow P = O + POH$

$PO_2^* + PO_2^* \rightarrow POOP + O_2$

Regardless of the exact chemical processes, it is clear that thermo-oxidative degradation leads to a reduction of average molecular mass and embrittlement of the material. In order to avoid, or at least delay these mechanisms, which would significantly decrease lifetimes of pipes, usually a combination of primary and secondary antioxidants is used. Primary antioxidants are generally hydrogen-donors or radical scavengers, which terminate chemical reactions that would otherwise lead to chain scission (compare “Propagation”). They are responsible for the long-term stabilization of polymers. Classic examples of this type of stabilizers are hindered phenols. Secondary antioxidants (e.g. phosphorus compounds) react with hydro peroxides (compare “Initiation / Branching”) and also protect primary antioxidants during processing.

Besides the publication shown in the following part, another contribution has been made by the author in this field. In order to maintain the systematic focus of this thesis and not go too far beyond the scope, they have not been included directly, but are listed below for further inquiries:

Conference contribution: Pappler, U.; Arbeiter, F.; Pinter, G.; “Life time prediction of coextruded multilayer polypropylene pipes”; Plastics Piping System Congress / 57th CEN/TC 155 meeting, Vienna, AUT, 2015

12.1. References

[1] Devilliers C, Fayolle B, Laiarinandrasana L, Oberti S, Gaudichet-Maurin E. Kinetics of chlorine-induced polyethylene degradation in water pipes. Polymer Degradation and Stability 2011;96:1361–8.

[2] Choi B, Chudnovsky A, Paradkar R, Michie W, Zhou Z, Cham P. Experimental and theoretical investigation of stress corrosion crack (SCC) growth of polyethylene pipes. Polymer Degradation and Stability 2009;94:859–67.

[3] Lundbäck M, Hassinen J, Andersson U, Fujiwara T, Gedde UW. Polybutene-1 pipes exposed to pressurized chlorinated water: Lifetime and antioxidant consumption. Polymer Degradation and Stability 2006;91:842–7.

[4] Richaud E, Farcas F, Fayolle B, Audouin L, Verdu J. Accelerated ageing of polypropylene stabilized by phenolic antioxidants under high oxygen pressure. J. Appl. Polym. Sci. 2008;110:3313–21.

[5] Weon J. Effects of thermal ageing on mechanical and thermal behaviors of linear low density polyethylene pipe. Polymer Degradation and Stability 2010;95:14–20.

[6] Pinter G, Lang RW. fracture mechanics characterisation of effects of stabilisers on creep crack growth in polyehtylene pipes. Plas. Rub. Compos 2001:94–100.

[7] Frank A, Pinter G, Lang RW. Prediction of the remaining lifetime of polyethylene pipes after up to 30 years in use. Polymer Testing 2009;28:737–45.

[8] Gugumus F. Thermooxidative degradation of polyolefins in the solid state: 6. Kinetics of thermal oxidation of polypropylene. Polymer Degradation and Stability 1998:235–43.

13. Publication 6

13.1. Bibliographic information

- Title: Influence of accelerated ageing on mechanical and fracture mechanical properties of talcum reinforced polypropylene pipe material
- Authors and relevant contributions to this publication:
  - Florian ARBEITER[1]

    Experimental testing, data evaluation, preparation of the publication
  - Ralf LACH[2]

    Experimental testing, data evaluation, discussion of results
  - Udo PAPPLER[3]

    Discussion of results
  - Erwin MAYRBÄURL[4]

    Experimental testing, data evaluation, discussion of results
  - Wolfgang GRELLMANN[2]

    Discussion of results
  - Gerald PINTER[1]

    Discussion of results
  - Andreas FRANK[5]

    Discussion of results

- Affiliation:
  1. Institute of Materials Science and Testing of Polymers, Montanuniversitaet Leoben, Otto Glöckel-Strasse 2, 8700 Leoben, Austria
  2. Polymer Service GmbH Merseburg, 06217 Merseburg, Germany
  3. OFI Technologie & Innovation GmbH, 1030 Vienne, Austria
  4. Poloplast GmbH & Co. KG, 4060 Leonding, Austria
  5. Polymer Competence Center Leoben GmbH, Roseggerstr. 12, 8700 Leoben, Austria

- Periodical: Polymer Degradation and Stability
- Status: Submitted

Statement with regard to this publication: The manuscript presented here is a present-day manuscript and does not necessarily reflect exactly the version published later on.

13.2. Abstract

Polymer materials are widely used for infrastructural applications such as piping nowadays. Since service lifetime is always an issue with suchlike applications, ageing behaviour of respective materials plays a vital role. Expected lifetimes of more than a hundred years in pipe applications make it necessary to use accelerated ageing procedures, such as storing at higher temperatures.

In this study a polypropylene material used with talcum reinforcement for sewer pipes has been subjected to accelerated ageing at 80°C in air for a time period of 18 months. Examination of the material showed no significant changes due to physical or chemical ageing within this period of time, using established thermic or mechanical tests. Stabilizer concentrations decreased, but were still present after 18 months. However, accelerated ageing by conditioning at 80°C led to annealing of residual stress from the extrusion process. Due to decreased effective stress, samples lasted longer during fatigue tests. This indicates that accelerated ageing of pipe materials via conditioning at higher temperatures heavily impacts lifetime estimations. If not considered, annealing of samples at higher temperatures could lead to significant overestimation of lifetimes later on.

13.3. Keywords

physical ageing, chemical ageing, polypropylene, residual stress, pipe

13.4. Introduction

To provide the high living standard of our modern society, polymeric materials are widely used in infrastructural constructions. Pipes for gas, water and heat supply or for sewage disposal, cable coatings for communication or power supply, lining of modern zero-energy and energy-plus buildings or geomembranes for waterproofing of tunnels or waste disposal sites are only a few examples in which polyolefin materials like polyethylene (PE) or polypropylene (PP) are frequently used in long-term applications. Especially in the field of sewage or drainage pipes PP has shown high reliability and potential. However, due to the extraordinary long required service time of typically 50 years and to reliably achieve or even excess the typical design operation times, knowledge about the ageing behaviour of the particular material is of essential importance. Depending on its origin, ageing in polymers can occur due to physical, chemical or a combination of both processes. Lifetime calculation of pipes is often performed via fracture mechanical approaches, using information like crack initiation or propagation rates. However, so far calculations were mostly performed using fracture mechanical values from virgin materials without considering physical or chemical ageing. Seeing that both types of ageing cannot be ruled out over the course of service lifetimes of 50 to 100 years, it is essential to identify the impact of both on fracture mechanical values used for calculations.

13.5. Background

While in service, several different internal and external influences as well as different failure modes must be considered with respect to the lifetime assessment of pipes. The failure characteristics of pipes are usually divided into three different regions with distinctive failure appearance. In Figure 13.1 these regions are illustrated for internally pressurized polyethylene (PE) pipes [1,2]. Within the first region (“Stage I”), too high loads are responsible for a relatively early ductile failure. Within this region high stress provokes large scale plastic deformation which finally leads to a typical “fish-mouth” fracture. Resistance against this type of failure is usually determined by the yield stress of the material [3]. Physical ageing (e.g. crystallization, changes in density etc.) can influence the yield stress of a polymeric material. Therefore, performance of pipes in “Stage I” can also change, depending on physical ageing processes. In the second region (“Stage II”), often referred to

as “quasi-brittle”, a combination of crack initiation and creep crack growth propagation results in a failure by slow crack growth (SCG). It usually occurs at lower loads and after long service times. Complex micro-mechanical mechanisms of craze formation, macromolecular chain disentanglement and craze breakdown [4–8] as well as chain rupture [9,10] have been confirmed to be responsible for SCG. Local crack tip aging due to chemical processes has been reported to influence failure in “Stage II” [11–13]. Additionally, similar to “Stage I” physical ageing can also influence crack initiation and propagation rates, for example via changes in density or annealing processes. For pressurized pipes “Stage II” has shown to be the most critical one in terms of lifetime [14]. Therefore, pipe grade materials for pressurized applications are usually optimized with regard to this failure mode. Finally, the third region (“Stage III”) is characterized by material degradation as a result of thermo-oxidative aging. This mechanism of chemical aging becomes important after very long service times and leads to a general large-scale embrittlement of the material followed by an almost load-independent fracture of the pipe. To prevent the material from this type of failure and shift lifetimes towards higher values, suitable stabilizer systems are used to retard the chemical reactions responsible for thermo-oxidative degradation.

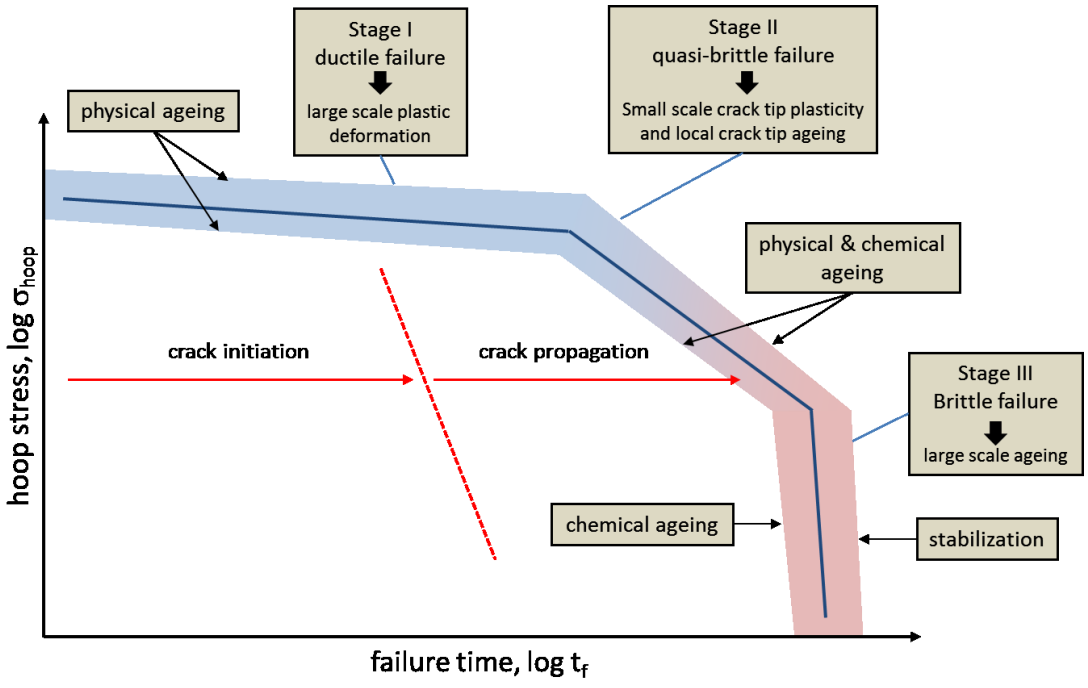

Figure 13.1: Characteristic failure regions of Polyethylene pipes under hydrostatic pressure (in reference to [1,2]).

For estimation of pipe lifetime under internal pressure, usually the internal pressure is the most critical load. Additionally, soil loads or point loads can be

taken into consideration to refine lifetime calculations [15]. Due to the lack of internal pressure, unpressurized pipes usually don't experience the "Stage I" failure as described above. The decisive stress in unpressurized pipes usually stems from external soil loads and, in case of bad trenching, external point loads. Therefore, "Stage I" failure for unpressurized pipes changes from the "fish-mouth" fracture to buckling. Nevertheless, the failure region is still essentially influenced by the yield stress (σ_{ys}) and additionally the creep modulus (E_{cr}) of the pipe material. Buckling of pipes, as described for "Stage I" failure in non-pressure pipes usually occurs within rather short times. Therefore, mechanical short-term properties are important. After settlement and solidification of the soil around the pipe, this failure mode is usually not the most critical anymore. The big exception to this case is, if the soil around the pipe is disturbed later on. Excavation work in close proximity can loosen the soil again, making "Stage I" type failures possible again. Therefore, mechanical properties also have to be known even after longer service times.

Similarly to pressurized pipes, the "Stage II" failure for non-pressure pipes is determined by crack initiation and SCG. In contrast to pressurized pipes, where load distribution is often assumed to be uniform due to the internal load, stress distribution in non-pressure pipes can be highly asymmetrical, which has to be taken into consideration [16]. Failure in "Stage II" is generally the critical one for buried pipes, since they can appear even after decades of operation without prior indication. To ensure safety in this region, usually long-term tests (e.g. internal pressure tests acc. to ISO 9080 [17]) are performed. Besides classical standardized test methods, resistance against crack initiation and SCG can be examined using test methods, based on linear elastic (LEFM), or elastic plastic fracture mechanics (EPFM). The advantage of these methods is, that using a combination of material data and finite element analysis, long-term behaviour of pipes can be examined not only under internal pressure, but also under the consideration of additional factors such as soil-, traffic- and point loads, as well as residual stress in the pipe wall itself.

In "Stage III", where failure of the pipe is considered to be almost independent from the applied loading situation, pressurized and unpressurized pipes are quite comparable. Due to accompanying material degradation, mechanical properties diminish rapidly, leading to large-scale embrittlement and global micro-crack formation. This mechanism can mainly be influenced or postponed by using sufficient stabilizers and additives for the respective needs of application.

Whereas the influence of ageing on “Stage I” can be examined within a rather short timescale, the influence on “Stage II” and “Stage III” would require samples aged for decades at application temperature. To keep this study within a manageable timeframe, samples were artificially aged using higher temperatures and shifted towards application temperature using the Arrhenius approach. While this procedure is widely discussed in literature and demands caution due to possible nonlinear-Arrhenius like behaviour [18,19], it can still be used as a rough estimation for a technological approach.

13.6. Experimental

The experimental program was built on the thermic and chemical analytical test methods Differential Scanning Calorimetry (DSC), Oxidation Induction Time (OIT), Fourier Transformed Infrared (FTIR) Spectroscopy and High Pressure Liquid Chromatography (HPLC). To focus on mechanical properties tensile tests were conducted and residual stress in the pipe wall was determined. The resistance against SCG was characterized using elastic plastic fracture mechanics (EPFM) using monotonic and linear elastic fracture mechanics (LEFM) using fatigue tests.

13.6.1. Material selection

The material examined in this work was a reinforced polypropylene block copolymer (PP-B) as it is typically used for the load bearing layer in multi-layer sewer pipes. The base polymer was reinforced with approx. 50 wt% talcum and chalk to increase mechanical properties. To prevent thermo-oxidative material aging during processing and service of the pipe, typical commercially available processing stabilizers as well as long-term stabilizers based on phenols and on phosphate have been added to attain a material similar to actual industrial applications. For the purpose of confidentiality no further information about the exact stabilizer system can be provided within this work.

13.6.2. Specimen Preparation

Several studies on accelerated ageing of PP were summarized in [19]. Interestingly, for most PP materials a change in activation energy was observed around 83°C. Therefore, samples were stored below this temperature at 80°C to achieve maximum ageing acceleration while maintaining approx. the same activation energy compared to application temperature. Assuming activation energy around 30-50 kJ/mol [20–22], as

reported in literature for various PP materials, ageing for 18 months (~13.000 h) should induce similar ageing as 50-100 years at 20°C.

For this study mono-layer pipes with a diameter of 160 mm and a wall thickness of 19 mm were extruded on a commercial pipe extrusion line. To induce artificially accelerated ageing, pipe ring segments were stored in air at 80°C for time periods of 0, 6, 12 and 18 months. Specimens for material characterization were taken directly from the pipe walls after conditioning. During specimen machining special attention was given on the prevention of additional heat treatment

13.6.3. Thermic and chemical testing

Differential Scanning Calorimetry

To examine changes in degree of crystallinity (α_{cr}) and in the melt temperature (peak-value T_{mp}) DSC has been performed according to ISO 11357-3 [23] on a device of the type DSC1 (Mettler Toledo, Columbus, OH, USA). Samples in the range of 6 to 7 mg have been taken from pipe walls from the surface and the centre. To estimate influence of physical ageing α_{cr} the first heating run (30°C to 200°C with a rate of 10 K/min) was evaluated between 80°C and 180°C and normalized to the wt% of the polymer matrix. Changes in T_{mp} were also evaluated. Results of α_{cr} and T_{mp} on the second run were examined for possible indication of material deterioration due to chemical ageing.

Oxidation Induction Time

Results from OIT have been found to correlate well with stabilizer concentration in polyolefins (e.g. [24,25]). In this context, specimens of 15±2 mg were tested according to the Austrian pipe standard ONORM EN 728 [26]. With a device of the type DSC1 (Mettler Toledo, Columbus, OH, USA), samples were heated up to 210°C under nitrogen atmosphere (50 ml/min). Afterwards the temperature was held and the atmosphere switched to oxygen (50 ml/min) to induce oxidation. The time until the onset of degradation was determined.

Fourier Transformed Infrared Spectroscopy

Analysis via FTIR Spectroscopy has been used to examine the aged material with regards to the formation of oxidation products, such as carbonyl or carboxyl groups. The pipe material was investigated with a device of the type Vertex 70 (Bruker, Billerica, USA) via attenuated total reflection (ATR) on the outer pipe wall surface. After baseline correction, spectra have been

normalised using the peak at 1375 cm^{-1}, which is characteristic for the methyl group (-CH_3) in PP. Close attention has been paid to the formation of clear bands which are associated with the formation of thermally induced degradation products, such as carboxyl or carbonyl groups.

High Performance Liquid Chromatography

High performance liquid chromatography has been used to detect the stabilizer concentration in the polymer as a function of ageing time. Therefore additives were extracted from the polymer at temperatures <40°C to prevent the samples from thermal influence. A device of the type 1260 Infinity LC System (Agilent, Santa Clara, CA, USA) was used for analysing the type and amount of stabilizers.

13.6.4. Mechanical Tests

Tensile tests

For classic mechanical properties tensile tests have been performed. To gain data directly comparable to other tests in this work, Cylindrical Dumbbell Specimens and Multipurpose Test Specimens (e.g. ISO 3167 [27] and ISO 527 [28]) have been used. Dumbbell specimens used were made from the same specimens as for cyclic CRB tests. The exact shape of this Cylindrical Dumbbell Specimens can be seen in Figure 13.2. For Evaluation of Young's Modulus (E) three contact extensometers of the type 632.13F from MTS (MTS, Eden Prairie, MN, USA; gauge length 10 mm) have been mounted around the specimen in 120° steps to check for asymmetric deformation in the round specimen. Only specimens with symmetric deformation were evaluated, using the average of all three signals. Testing speed was chosen at 1 mm/min throughout the whole test. Specimens were milled from the pipe walls in axial direction. Elastic modulus (E), yield stress (σ_{ys}) and strain at break (ε_{br}) were compared for different ageing times. Multipurpose specimens were measured according to ISO 527 [28]. All tensile tests were conducted on a device of the type Zwick Z010 (Zwick/Roell GmbH & Co. KG, Ulm, GER).

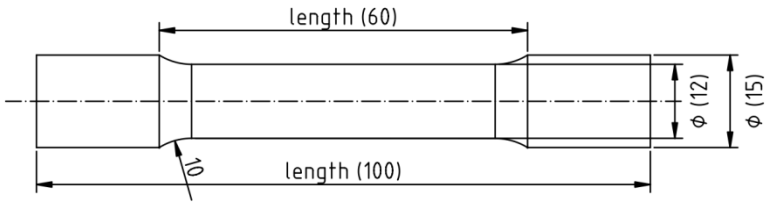

Figure 13.2: Specimen geometry used for tensile testing.

Determination of residual stresses

Residual stresses in the pipe walls, which stem from the extrusion process, where the pipes are cooled from the outside, can also heavily influence the overall behaviour of the material. Therefore, residual stress analysis for the pipe walls has been performed according to ring deformation tests [29,30]. For this analysis, ring segments with a thickness of approx. 15 mm have been cut from the pipes after conditioning. From these rings, a 120° segment has been cut out and the deformation of the remaining pipe segment was measured as a function of time over the period of 8 weeks. Afterwards the segment was deformed back into its original shape, and residual stress of the aged pipe segments were calculated from the force necessary. A correction for thick walled pipes was considered [29].

13.6.5. Fracture-mechanical Tests

J-Integral

Stable crack initiation and crack propagation behaviour can be quantified by the concept of J-Integral calculation and the determination of crack resistance (R) curves [31]. Primarily developed for metals, this concept has also been frequently applied to polymers [32–34]. Within the current study, single edge notched bending (SENB) specimens were subjected to three-point bending at a testing speed of 10 mm/min at room temperature. The tests were conducted on a device of the type Zwicki (Zwick/Roell, Ulm, GER). The applied maximum force was varied in regular steps and the deformation work (A_G) was calculated from measured force-displacement curves. After the tests, specimens were cooled in liquid nitrogen and fractured at high loading rates. The amount of stable crack growth Δa was measured with an optical microscope. Data was evaluated according to the procedure described in [35–38] to determine crack resistance (R) curves (shown in Figure 13.3). For determination of J-integral values Equations 13.1 and 13.2 with the geometry factor $\Gamma(\frac{a}{W})$ = 2 for SENB specimens were used. Plotting

calculated J-integral values as a function of crack extension Δa gives the R-curve of the examined material which can be used to compare the different ageing conditions.

$$J_0 = \frac{A_G}{B(W-a)}\Gamma\left(\frac{a}{W}\right) \quad (13.1)$$

$$J = J_0\left(1 - \frac{\Delta a\left(0.75\,\Gamma\left(\frac{a}{W}\right)-1\right)}{W-a}\right. \quad (13.2)$$

The R-curve, which shows the development of J as a function of Δa was fitted using an exponential fit as shown in Equation 13.3 [37,38], where C1 and C2 are constants of the fit.

$$J = C1\Delta a^{C2} \quad (13.3)$$

Using this fitted curve both resistance against short-term crack initiation $J_{0.2}$ (measured at Δa=0.2 mm) and resistance against crack propagation dJ/d(Δa) (slope at Δa=0.2 mm) were evaluated.

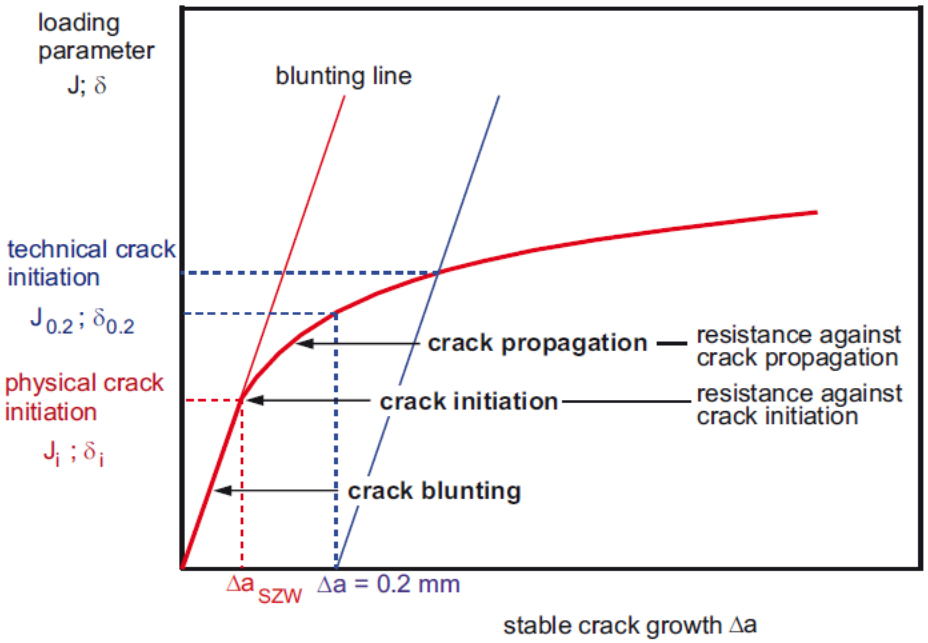

Figure 13.3: Explanation of R-curve for estimation of resistance against crack initiation and propagation [38].

Cyclic Cracked Round Bar Test

To determine resistance against SCG in tough pipe grade polymers, Cyclic CRB Tests have proven to be a powerful tool. Initially developed over the last decade for faster evaluation of PE pipe grade material performance [39–46],

cyclic CRB tests have shown promise to be used for different materials, such as PP, as well [47–49]. The Cyclic CRB Test is a LEFM based fatigue test on circumferentially notched round bar specimens. Recently the Cyclic CRB Tests has also be standardized within ISO 18489 [50] as a quick ranking tool for modern PE pipe grades. Even though the loading situation is different from real application, various authors have shown the comparability to real pipes [46,51–55]. All Cyclic CRB Tests were conducted on a 15 kN servo-hydraulic testing machine from MTS (MTS, Eden Prairie, MN, USA). Calculation of applied stress intensity factor (K_I) was performed according to Benthem and Koiter [56], which has proven to be very accurate for CRB specimens [57–59]. The applied load ratio ($R = P_{min}/P_{max}$) was chosen at 0.1, which provides fast results. To avoid excessive hysteretic heating the tests were conducted with a frequency of 5 Hz. Specimen diameter was 15 mm with an initial crack length of the circumferential notch of a_{ini}=1.5 mm. Testing environment was air at 23°C and 50% rh. To evaluate CRB tests, applied load (e.g. as K_I, ΔK_I (= K_{Imax}-K_{Imin} during a load cycle) or corresponding nominal stresses σ_0 or $\Delta\sigma_0$) is plotted as a function of cycles to failure (N_f) in a log-log-diagram. Specimens failing in the same failure mode build a straight line in this diagram (compare Figure 13.4). Materials can be compared, by observing the position of the failure curve in the diagram, where materials with higher N_f at the same applied load usually possesses a higher resistance against SCG. A change in failure mode, e.g. “Stage I” instead of “Stage II”, can be seen as a clear change in slope, similar to internally pressurized pipes Figure 13.1.

13.7. Results and discussion

13.7.1. Thermic and chemical testing

To validate the influence of thermal treatment on tested pipe materials, thermic and chemical tests were performed in a first step.

Differential Scanning Calorimetry

Judging from the values for the degree of crystallinity (α_{cr}) of the first run in Figure 13.5 there seems to be no significant change due to physical ageing within 18 months of thermal conditioning. Also the melting temperature evaluated at the peak of the melting curve (T_{mp}) does not change significantly. The only difference between surface and centre of the pipe wall is a slightly lower T_{mp} on the surface for the unaged pipe. Excessive physical ageing would be notable by an increase of α_{cr} or maybe even a shift of T_{mp} towards higher temperatures.

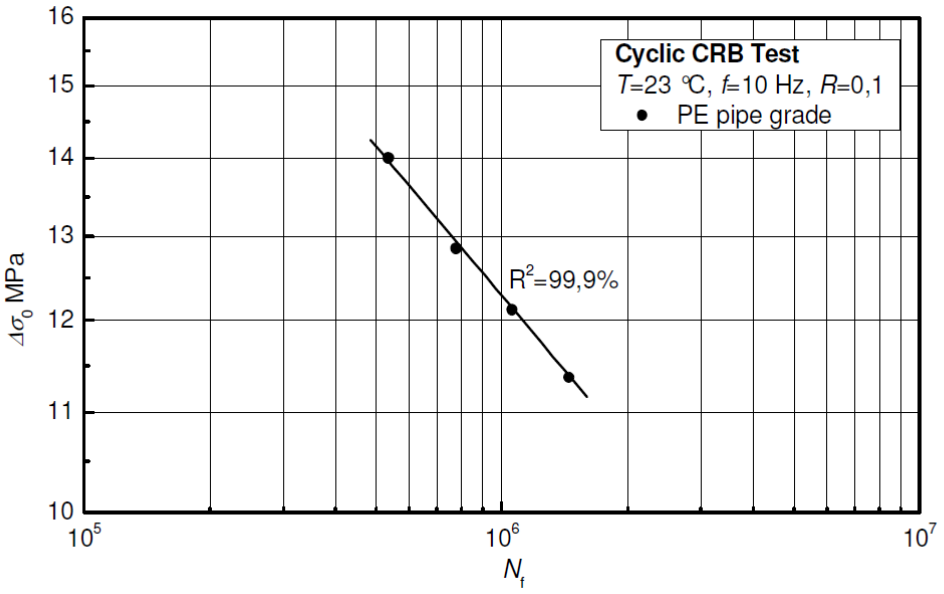

Figure 13.4: Evaluation of cyclic CRB test according to ISO 18489 [50].

Both could be accompanied by a change of lamellar thickness and distribution [60], which could influence fracture mechanical properties in "Stage I" and "Stage II" failures [61]. The second run also showed no significant decrease of T_{mp} which would be an indication of material degradation due to chemical ageing, which in turn heavily influences "Stage II" and "Stage III" failures of pipes. It can be assumed that conditioning at 80°C is sufficiently below the melt transition range so that even after continuing conditioning no significant physical ageing processes are noticed via DSC. Mineral fillers can act as heterogeneous nucleation agents which accelerate crystallization (e.g. [62–64]). In combination with rather slow cooling times inside the pipe wall during extrusion and due to bad thermal conductivity, crystallinity could have almost reached an equilibrium state for these conditions before thermal conditioning. Furthermore, incorporated talcum and chalk reinforcement of approx. 50 wt% could also hinder further crystallization processes at 80°C. Going by these results, also no severe chemical ageing is expected at this stage.

Oxidation Induction Time

In contrast to the DSC results, the determined OIT-values show a clear decrease from >40 minutes at 210°C down to approx. 9 minutes after 18 months in the centre of the specimens. The decrease confirms a consumption or depletion of stabilizers during thermal conditioning.

Nevertheless, even after 18 months of testing, OIT times are still measureable, which means stabilizers are still actively inhibiting chemical ageing of the polymer. This not only explains the lack of change of DSC results, but also indicates that fracture mechanical values should not degrade due to chemical ageing. For comparison, OIT was also compared to stabilizer depletion in Figure 13.7.

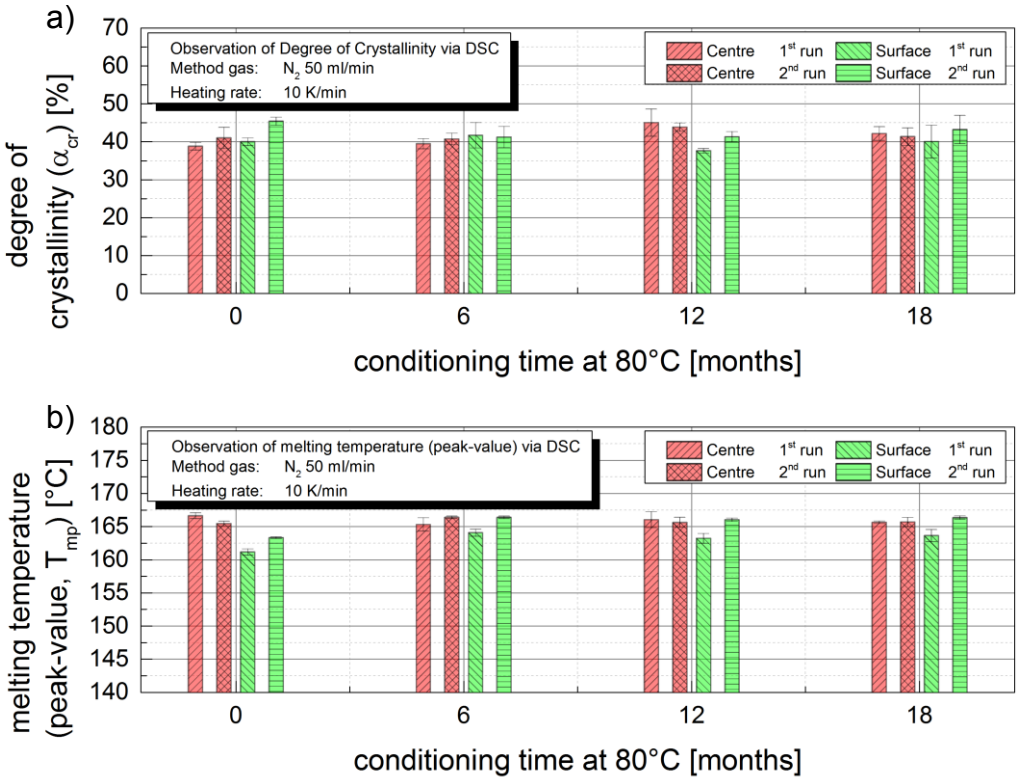

Figure 13.5: Results of DSC analysis – changes in (a) α_{cr} and (b) T_{mp} depending on conditioning time and pipe wall position of sample.

Fourier Transformed Infrared Spectroscopy

To affirm results from OIT, characteristically spectrograms were determined with FTIR Spectroscopy to detect degradation of the polymer matrix. The results for different ageing times are shown in Figure 13.6. In contrast to ageing studies performed on non-stabilized PP [65,66], no clear indications of ageing could be found. Thermo-oxidative ageing of PP is usually quite similar to that of PE. The first stage of degradation of PP is limited by the peroxide radical decomposition, whereas later on the mode of degradation switches to random chain scission [67]. So the indication of the first stage ageing process would be the formation of bands between 1700-1800 cm^{-1}

which are linked with the formation of carbonyl groups [68–70]. Antioxidants can be seen quite clearly between 1500 and 1700 cm^{-1} [39,71].

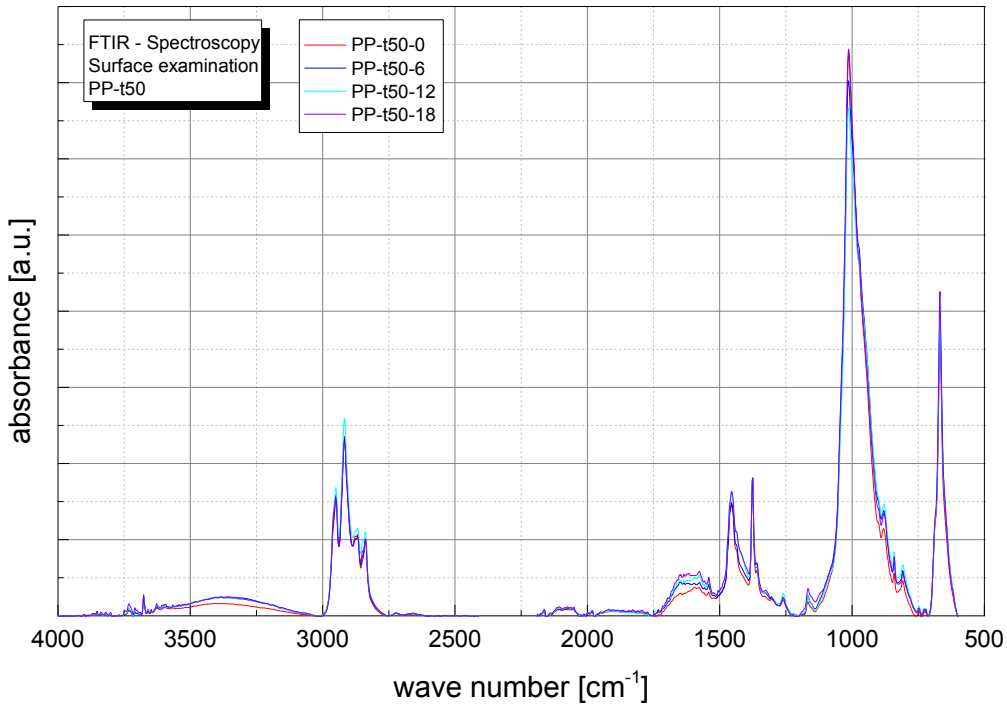

Figure 13.6: Results of FTIR Spectroscopy to observe the possible formation of bands linked to degradation of PP.

High Performance Liquid Chromatography

To validate results from FTIR and OIT measurements, HPLC analysis of stabilizer concentrations were performed additionally. Three different types of stabilizers, two based on phenols and one on phosphate, used in the material have been observed with HPLC. The results in Figure 13.7 show the development of stabilizer concentrations as a function of ageing time. Results have been normalized to the initial value before ageing. It can be seen, that the phenolic primary antioxidant is no longer detectable after six months of conditioning. The remaining two stabilizers clearly deplete with progressing ageing time, which corresponds well with results from OIT. After 18 months of ageing at 80°C the two stabilizers are still detectable. Whereas the trend remains unchanged, values of the surface samples are lower compared to the centre. Analysis via HPLC confirms that two of the stabilizers are still active and protect the polymer from degradation after 18 months. Nevertheless, thermo-oxidative processes deplete stabilizers on the surface faster compared to the centre. Still active stabilizers also explain the lack of

FTIR bands which would indicate severe thermo-oxidative chemical ageing of the material itself. Both methods to determine remaining stabilisation of the material, normalized OIT and cumulative stabilizer concentration, correlate quite nicely with $R^2 \geq 0.998$ in a linear fit, similar to results in literature for polyolefin materials [24,25].

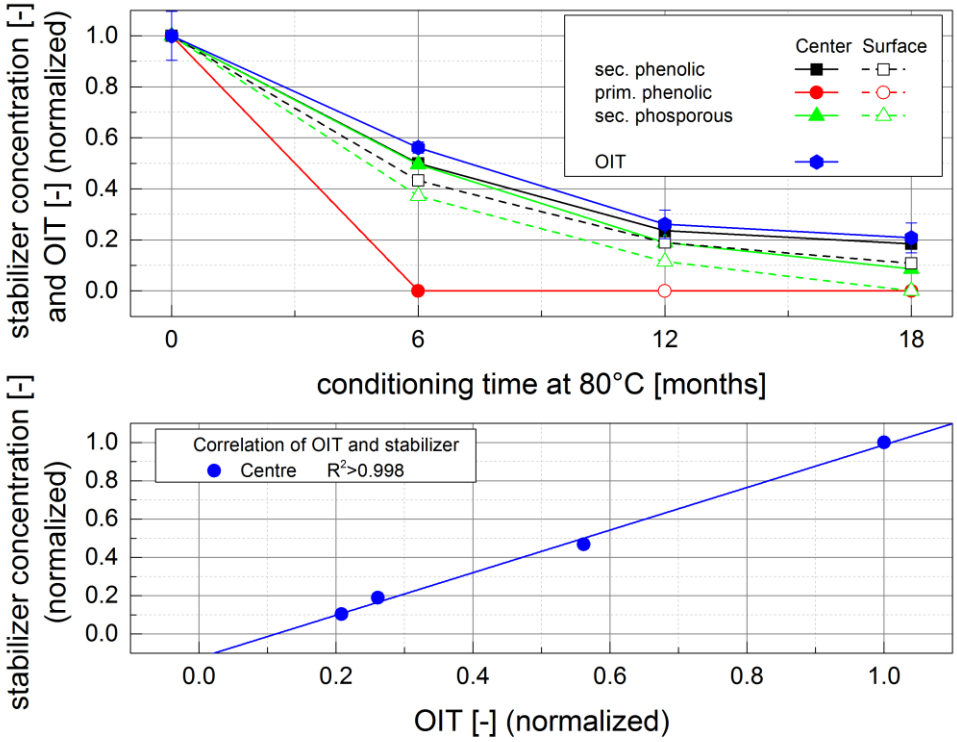

Figure 13.7: Normalized stabilizer concentrations in centre and surface and OIT as a function of conditioning time at 80°C and correlation between stabilizer and OIT.

13.7.2. Mechanical Tests

To validate possible influences due to physical or chemical ageing, classical values such as E, σ_{ys} and ε_{br} were measured. Additionally, the development of residual stress in pipe walls was observed.

Tensile tests

Physical ageing, such as an increase in the degree of crystallinity, is usually observable by changing properties such as E or σ_{ys} whereas chemical ageing is typically observed via ε_{br}. Since FTIR, DSC and OIT already showed no influence of physical or chemical ageing, significant changes in properties are not expected. To detect chemical ageing due to thermo-oxidative ageing specimens with a maximum of surface/volume ratio would be advisable. To

detect physical ageing processes, such as changes in crystallinity or free volume, which are volume effects, a lower ratio is advisable. Both, Cylindrical Dumbbell Specimens (CDS) and Multipurpose Testing Specimens were used to examine possible changes. Both specimen geometries showed similar results and trends. In Figure 13.8 results of mechanical properties, as measured via CDS, are shown. It is easily recognizable, that all three properties do not change over the course of 18 months of conditioning at 80°C. Both, E and σ_{ys} which are usually sensitive to changes in crystallinity increase only about 2-3%, which is still within the range of testing uncertainty and standard deviation. Strain at break is quite often used to characterize embrittlement due to chemical ageing in polymers (e.g. [72,73]). Results for strain at break also show no clear trend, which speaks for little to no chemical ageing, as indicated by the results of OIT and HPLC. However, scatter of results is quite significant, compared to E and σ_{ys}, which is a general problem with this property and is certainly amplified by the fact that the material is reinforced with minerals. Results from quasi-static tests coincide nicely with results from tests above. As predicted by analysis via DSC, OIT, FTIR and HPLC, there seems to be no chemical or physical ageing after 18 months at 80°C.

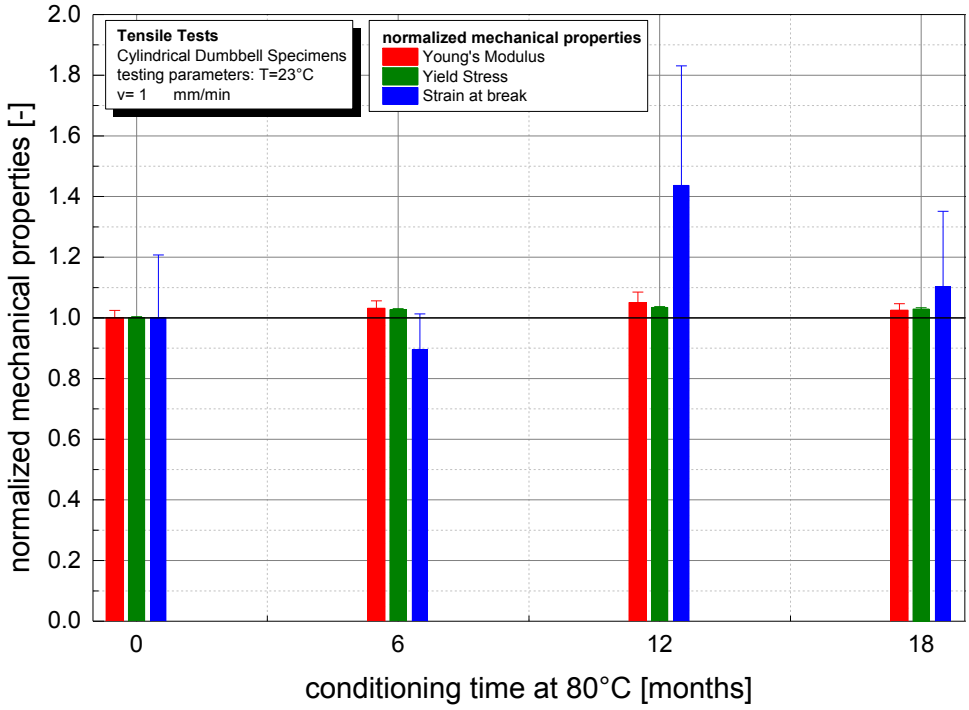

Figure 13.8: Normalized mechanical properties as a function of ageing time at 80°C.

Determination of residual stresses

Another important aspect with regard to long-term properties of pipe grade materials are residual stresses in the pipe wall. Studies have shown that such stresses in polymer pipe walls can amount up to around 2-5 MPa [3,30,74–76]. Considering, that polymer pipes are often subjected to stress levels around 8-12 MPa in long-term applications, and that SCG is a stress driven mechanisms, residual stresses can significantly influence expected service times [77,78]. Studies on excavated old pipes have shown that even after up to 30 years of operation, residual stress of up to 4 MPa can still be found in the pipe walls [79]. The results for the residual stress for the pipe of the current study as a function of thermal ageing can be seen in Figure 13.9. The data show that the residual stress decreased significantly during the first phase of thermal conditioning. Whereas in the initial condition a value of approx. 4.3 MPa was determined, the magnitude decreased to 2.2 MPa after 6 and 2.0 MPa after 12 and 18 months.

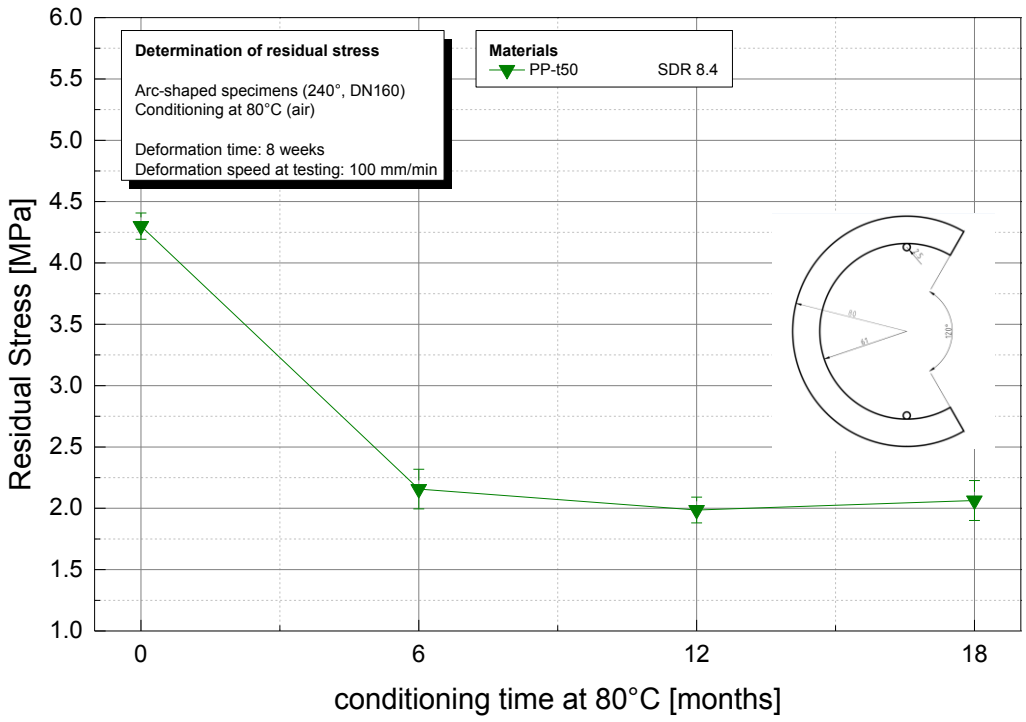

Figure 13.9: Development of residual stress as a function of conditioning time at 80°C.

This indicates significant physical ageing via annealing, which reduces the residual stress, although no changes in crystallinity could be detected. This definite influence of physical ageing, due to annealing at 80°C, which does

not occur in real application [79], has to be kept in mind, when comparing fracture mechanical properties later on.

13.7.3. Fracture-mechanical Tests

The following chapters show the influence of thermal treatment on crack initiation and crack propagation due to physical or chemical ageing of the examined material. Both types of ageing are essential to expected lifetime performance of pipes and have to be integrated in estimations.

J-Integral

In Figure 13.10, results for resistance against crack initiation ($J_{0.2}$) and crack propagation ($dJ/d(\Delta a)$) measured via EPFM are shown. It can be seen, that both values increase slightly with ageing time. However, compared to other studies where changes in fracture toughness could be directly linked to crystallinity [80], there seems to be a different underlying reason here. Most likely, decreasing residual stress, as shown above, influences the macroscopically response of the material.

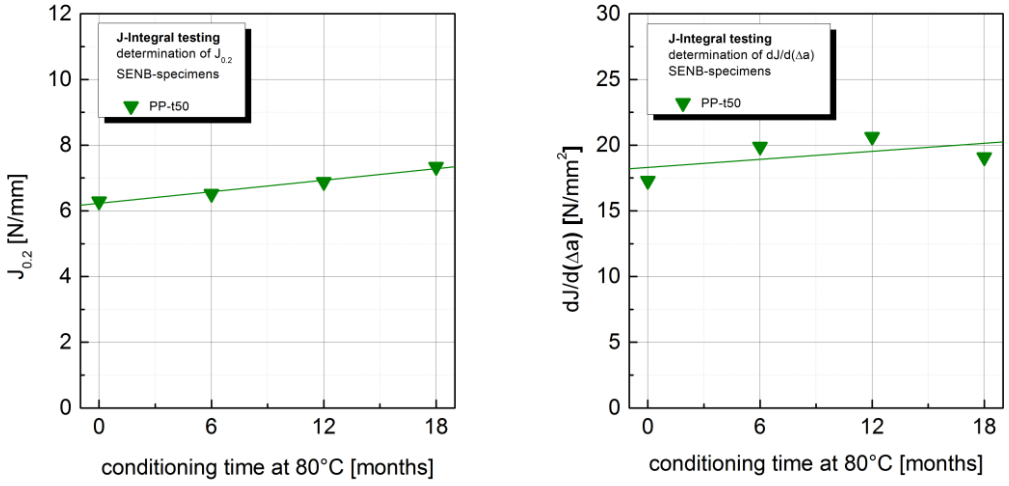

Figure 13.10: Changes in resistance against crack initiation ($J_{0.2}$) and crack propagation ($dJ/d(\Delta a)$) measured via J-Integral as a function of conditioning time at 80°C.

Cyclic Cracked Round Bar Test

A similar trend to the increase in fracture toughness via J-integral could also be found in the data of the Cyclic CRB Tests. The failure cycle numbers at different stress intensity factors as a function of the aging time are summarized in Figure 13.11 and the data show an increase for annealed

samples. Especially at lower applied stress levels and respective higher cycles to failure the difference between untreated and annealed specimens is significant. Since no changes in mechanical properties or crystallinity which could explain differences in results were found, changes in resistance against fatigue can most likely be attributed to the reduction of residual stress due to annealing at 80°C. Residual stress in pipewalls usually shows a distribution of stress levels, from compressive stress on the outer surface and tensile stress on the inner surface. While compressive stress effectively decreases the applied K_I, tensile stresses increase the effective applied load during a fatigue test. This asymmetry in stress over the specimen cannot only lead to a faster crack initiation at the position of tensile stress in the pipe wall, but in worst case also lead to asymmetric crack growth in the round specimen. It is also shown in Figure 13.11 that the superposition of the respective stress intensity factors due to applied testing load (K_n) and the sum of applied testing load and additional load due to residual stress ($K_{c,res}$) leads to a significant reduction of scatter at high cycle numbers. This indicates that the difference of unaged and aged specimens is most likely a phenomenological artefact due to neglecting of different internal stress levels after ageing. To further confirm no significant changes in failure behaviour due to thermal treatment, fracture surfaces were examined using scanning electron microscopy (SEM). Figure 13.12 shows the area of quasi-brittle failure at similar applied K_I for ageing times of 0 to 18 months. It can be seen, that no significant changes in actual fracture mechanism occur.

13.8. Summary

To determine the effect of thermal treatment on ageing of stabilized talcum reinforced PP pipe grade material, samples have been subjected to conditioning at 80°C in air for 18 months. The material has been investigated with respect to physical and chemical ageing. Analysis via DSC showed no significant changes due to physical or chemical ageing. Using OIT and HPLC stabilizer reduction could be detected. Nevertheless, both OIT and stabilizer concentrations were still good enough to further inhibit chemical ageing. Both, OIT and stabilizer concentration could also be correlated using a linear fit. Results were also confirmed by FTIR spectroscopy, where no formation of peaks, typical for chemical ageing was observed.

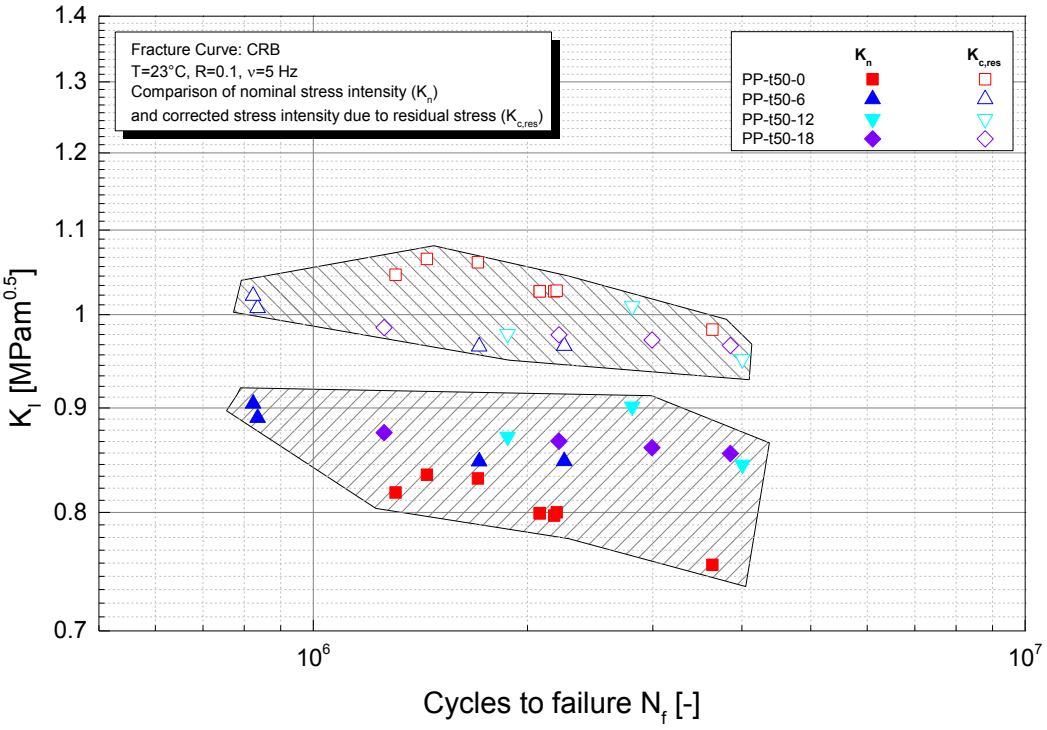

Figure 13.11: Results from cyclic CRB tests as a function of conditioning time at 80°C with applied K_I (full symbols, K_n) and superposition of applied K_I and K_I due to residual stress (open symbols, $K_{c,res}$).

Mechanical testing affirmed the assumptions of DSC and FTIR analysis. Significant changes could not be detected, neither due to physical nor chemical ageing. However, fracture mechanical properties determined via EPFM and LEFM showed an improvement of the material due to conditioning at 80°C. This can most likely be addressed to annealing processes, which led to a decrease in residual stress in the samples. Regarding lifetime estimation and extrapolation procedures this has to be kept in mind, since similar annealing processes do not occur in real applications under normal circumstances. Overall, the examined pipe material which was subjected to thermal conditioning at 80°C in air showed no significant deterioration even after 18 months. Although stabilizer concentration is decreasing with conditioning time this suggests sufficient stabilization for approx. 100 years in real application.

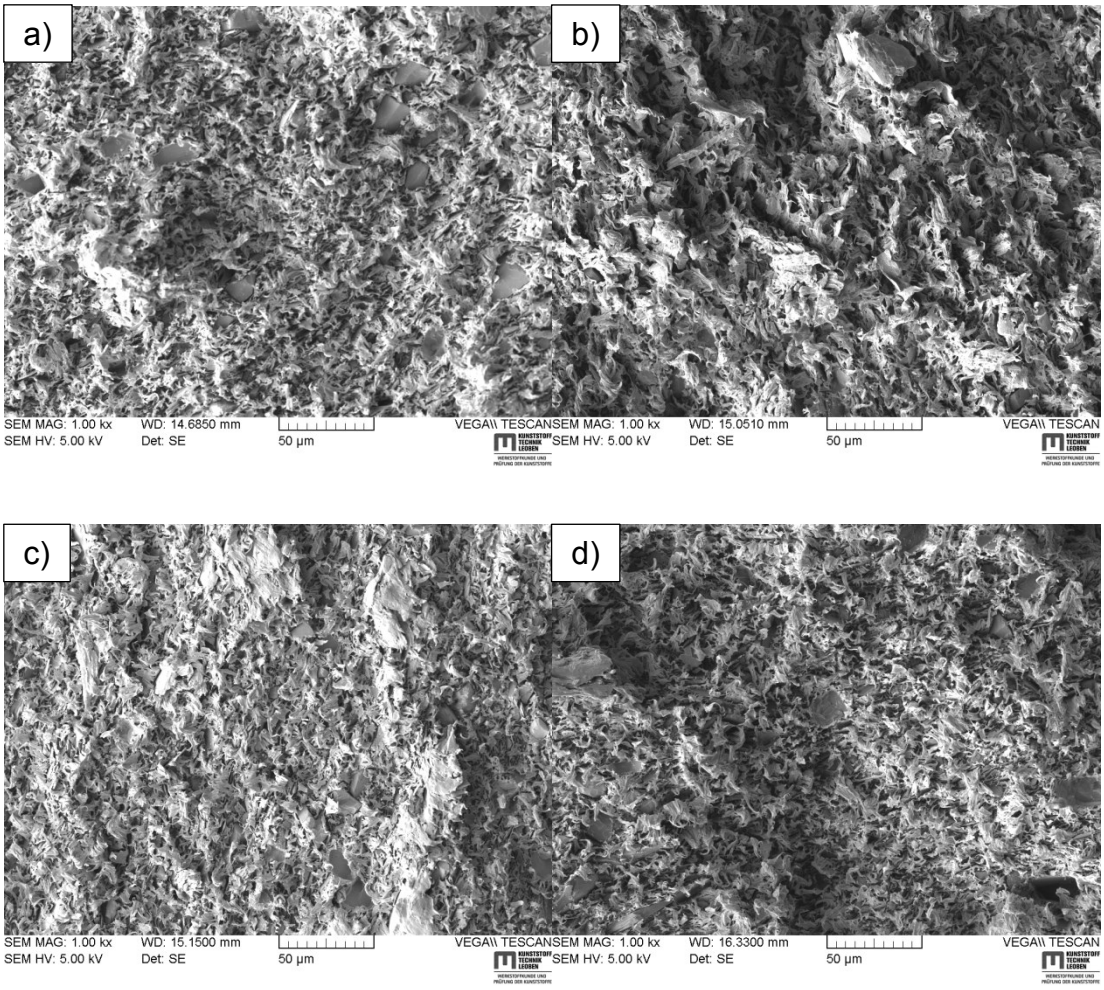

Figure 13.12: Comparison of fracture surfaces of CRB-specimens after (a) 0 months of thermal treatment and K_I=0.83 MPam$^{0.5}$, (b) 6 months of thermal treatment and K_I=0.84 MPam$^{0.5}$, (c) 12 months of thermal treatment and K_I=0.84 MPam$^{0.5}$, (d) 18 months of thermal treatment and K_I=0.86 MPam$^{0.5}$.

13.9. Acknowledgement

The research work of this publication was performed at the Institute of Materials Science and Testing of Polymers (Montanuniversitaet Leoben, Austria) within the framework of the FFG program of the Austrian Ministry of Traffic, Innovation and Technology and the Austrian Ministry of Economy, Family and Youth with contributions of the Österreichisches Forschungsinstitut für Chemie und Technik (Austria), Martin-Luther-Universität Halle-Wittenberg (Germany) and the Polymer Competence Center Leoben GmbH (Austria).

13.10. References

[1] Lang RW, Pinter G, Balika W. Konzept zur Nachweisführung für Nutzungsdauer und Sicherheit von PE-Druckrohren bei beliebiger Einbausituation. 3R International 2005:32–41.

[2] Richard K, Gaube E, Diedrich G. Trinkwasserrohre aus Niederdruckpolyäthylen. Kunststoffe;1959:516–25.

[3] Krishnaswamy RK. Analysis of ductile and brittle failures from creep rupture testing of high-density polyethylene (HDPE) pipes. Polymer 2005;46:11664–72.

[4] Dugdale D. Yielding of steel sheets containing slits. Journal of the Mechanics and Physics of Solids 1960;8:100–4.

[5] Barenblatt GI. The mathematical theory of equilibrium cracks in brittle fracture. Advances in applied mechanics 1962;7:55–129.

[6] Friedrich K. Crazes and shear bands in semi-crystalline thermoplastics. In: Crazing in Polymers: Springer; 1983, p. 225–274.

[7] Lustiger A. Environmental stress cracking: the phenomenon and its utility. Carl Hanser Verlag, Failure of Plastics 1986:305–29.

[8] Kausch H, Gensler R, Grein C, Plummer, C. J. G., Scaramuzzino P. Crazing in semicrystalline thermoplastics. Journal of Macromolecular Science, Part B 1999;38:803–15.

[9] Hans-Henning K. Polymer Fracture. 2nd ed. Berlin, Heidelberg: Springer; 1987.

[10] Lustiger A, Ishikawa N. An analytical technique for measuring relative tie-molecule concentration in polyethylene. J. Polym. Sci. B Polym. Phys. 1991;29:1047–55.

[11] Lang RW, Stern A, Dörner GF. Applicability and limitations of current lifetime prediction models for thermoplastics pipes under internal pressure. Die Angewandte Makromolekulare Chemie 1997:131–45.

[12] Pinter G, Lang RW. Effect of stabilization on creep crack growth in high-density polyethylene. Journal of Applied Polymer Science 2003:3191–207.

[13] Pinter G, Haager M, Wolf C, Lang RW. Thermo-Oxidative Degradation during Creep Crack Growth of PE-HD Grades as Assessed by FT-IR Spectroscopy. Macromol. Symp. 2004;217:307–16.

[14] Barker MB, Bowman J, Bevis M. The performance and causes of failure of polyethylene pipes subjected to constant and fluctuating internal pressure loadings. J Mater Sci 1983;18:1095–118.

[15] Frank A, Hutař P, Pinter G. Numerical Assessment of PE 80 and PE 100 Pipe Lifetime Based on Paris-Erdogan Equation. Macromol. Symp. 2012;311:112–21.
[16] Ševčík M, Arbeiter F, Hutař P, Pinter G, Náhlík L. The Effect of Soil Load on Fracture Behaviour of Three-Layer Polymer Pipe for Non-Pressurised Applications. KEM 2014;627:197–200.
[17] EN ISO 9080. Plastics piping and ducting systems - Determination of the long-term hydrostatic strength of thermoplastics materials in pipe form by extrapolation; 2003.
[18] Gray RL. Accelerated testing methods for evaluating polyolefin stability. ASTM Special Technical Publication 1990:57–74.
[19] Celina M, Gillen KT, Assink RA. Accelerated aging and lifetime prediction: Review of non-Arrhenius behaviour due to two competing processes. Polymer Degradation and Stability 2005;90:395–404.
[20] Richters P. Initiation process in the oxidation of polypropylene. Macromolecules 1970:262–4.
[21] Gugumus F. Effect of temperature on the lifetime of stabilized and unstabilized PP films. Polymer Degradation and Stability 1999;63:41–52.
[22] Gijsman P, Hennekens J, Vincent J. The influence of temperature and catalyst residues on the degradation of unstabilized polypropylene. Polymer Degradation and Stability 1993;39:271–7.
[23] DIN. Kunststoffe Dynamische Differenz-Thermoanalyse (DSC)(11357).
[24] Marshall DI, George EJ, Turnipseed JM, Glenn JL. Measurement of oxidation stability of polyolefins by thermal analysis. Polym. Eng. Sci. 1973;13:415–21.
[25] Foster GN. Analytical methods applied to the testing of oxidation inhibition. In: Pospisil J, Klemchuk P, editors. Oxidation inhibition in organic materials. 2nd ed. Boca Raton, Florida: CRC Press Inc; 1990, p. 299–342.
[26] ÖNORM. Kunststoff-Rohrleitungs- und Schutzrohrsysteme - Rohre und Formstücke aus Polyolefinen - Bestimmung der Oxidations-Induktionszeit(ÖNORM EN 728 (1997-11-01)); 1997.
[27] ISO. Plastics - Multipurpose test specimens (ISO 3167:2014)(3167); 2014.
[28] ISO 527. Plastics - Determination of tensile properties.

[29] Williams JG, Hodgkinson JM, Gray A. The determination of residual stresses in plastic pipe and their role in fracture. Polym. Eng. Sci. 1981;21:822–8.

[30] Pilz G. Viskoelastische Eigenschaften polymerer Werkstoffe für Rohranwendungen. Leoben, Montanuniv., Diss., 2001; 2001.

[31] Cherepanov GP. Crack propagation in continuous media. Journal of Applied Mathematics and Mechanics 1967;31:503–12.

[32] Lach R, Seidler S, Grellmann W. Crack propagation kinetics of polymers at quasistatic and moderate impact loading. Abstract book // ICF XI, 11th International Conference on Fracture 2005:5360,1-6.

[33] Grellmann W, Lach R, Seidler S. Experimental determination of geometry-independent fracture mechanics values J, CTOD and K for polymers. International Journal of Fracture 2002;118:9–14.

[34] Lach R, Krolopp T, Hutař P, Grellmann W. Influence of the Interface and the Additional Layer on the Stable Crack Propagation through Polyolefin Bilayered Structures. Procedia Materials Science 2014;3:867–72.

[35] Grellmann W, Seidler S, Hesse W. Procedure for Determining the Crack Resistance Behaviour Using the Instrumented Charpy Impact Test. In: Grellmann W, Seidler S, editors. Deformation and Fracture Behaviour of Polymers. Berlin, Heidelberg: Springer Berlin Heidelberg; 2001, p. 71–86.

[36] Grellmann W, Seidler S, Jung K, Che M, Kotter I. Influence of Specimen Geometry and Loading Conditions on the Crack Resistance Behviour of Poly(vinyl chloride) and Polypropylene. In: Grellmann W, Seidler S, editors. Deformation and Fracture Behaviour of Polymers. Berlin, Heidelberg: Springer Berlin Heidelberg; 2001, p. 51–70.

[37] ESIS TC4. A Testing Protocol for Conducting J-Crack Resistance Curve Test on Plastics; 2001.

[38] Grellmann W, Seidler S. Polymer testing. 2nd ed. München [u.a.]: Hanser; 2013.

[39] Frank A. Fracture Mechanics Based Lifetime Assessment and Long-term Failure Behavior of Polyethylene Pressure Pipes: Dissertation. Disseratation. Leoben, Austria; 2010.

[40] Frank A, Berger I, Arbeiter F, Pinter G. Characterization of crack initiation and slow crack growth resistance of PE 100 and PE 100 RC pipe grades with Cyclic Cracked Round Bar (CRB) Tests. In: Proceedings Plastic Pipes XVII 2014; 2014.

[41] Frank A, Redhead A, Kratochvilla T, Dragaun H, Pinter G. Accelerated Material Ranking with Cyclic CRB Tests. In: Proceedings Plastic Pipes XIV 2010; 2010.
[42] Pinter G, Haager M, Balika W, Lang RW. Cyclic crack growth tests with CRB specimens for the evaluation of the long-term performance of PE pipe grades. Polymer Testing 2007;26:180–8.
[43] ONR. Determination of the resistance of slow crack growth of polyehtylene with cracked round bar (CRB) specimens(ONR 25194 (2011 10 01)); 2011.
[44] Kratochvilla TR, Frank A, Pinter G. Determination of slow crack growth behaviour of polyethylene pressure pipes with cracked round bar test. Polymer Testing 2014;40:299–303.
[45] Frank A, Pinter G. Evaluation of the applicability of the cracked round bar test as standardized PE-pipe ranking tool. Polymer Testing 2014;33:161–71.
[46] Frank A, Lang RW, Pinter G. Accelerated Investigation of creep crack growth in polyethylene pipe grade materials by the use of fatigue tests on cracked round bar specimens: Proceedings Annual Technical Conference - ANTEC, Society of Plastics Engineers, Milwaukee, Wisconsin, USA 2008:2435–9.
[47] Arbeiter F, Pinter G, Frank A. Characterisation of quasi-brittle fatigue crack growth in pipe grade polypropylene block copolymer. Polymer Testing 2014.
[48] Arbeiter F, Schrittesser B, Frank A, Berer M, Pinter G. Cyclic tests on cracked round bars as a quick tool to assess the long term behaviour of thermoplastics and elastomers. Polymer Testing 2015;45:83–92.
[49] Schoeffl PF, Lang RW. Effect of liquid oilfield-related media on slow crack growth behavior in polyethylene pipe grade materials. International Journal of Fatigue 2015;72:90–101.
[50] ISO. Polyethylene (PE) materials for piping systems — Determination of resistance to slow crack growth under cyclic loading — Cracked Round Bar test method(18489); 2015.
[51] Frank A, Pinter G, Lang RW. Lifetime prediction of polyethylene pipes based on an accelerated extrapolation concept for creep crack growth with fatigue tests on cracked round bar specimens. In: Society of Plastics Engineers, editor. ANTEC; 2009, p. 2169–2174.
[52] Parsons M, Stepanov EV, Hiltner A, Baer E. Correlation of stepwise fatigue and creep slow crack growth in high density polyethylene. Journal of Materials Science 1999;34:3315–26.

[53] Zhou Z, Hiltner A, Baer E. Predicting long-term creep failure of bimodal polyethylene pipe from short-term fatigue tests. J Mater Sci 2011;46:174–82.

[54] Parsons M, Stepanov EV, Hiltner A, Baer E. Correlation of fatigue and creep slow crack growth in a medium density polyethylene pipe material. Journal of Materials Science 2000;35:2659–74.

[55] Pinter G, Balika W, Lang RW. A correlation of creep and fatigue crack growth in high density poly(ethylene) at various temperatures 2002;29:267–75.

[56] Benthem J, Koiter W (eds.). Method of Analysis and Solutions of Crack Problems. 3rd ed; 1973.

[57] Murakami Y. Stress intensity factors handbook. Oxford: Pergamon Pr; 1990.

[58] Scibetta M, Chaouadi R, van Walle E. Fracture toughness analysis of circumferentially-cracked round bars. International Journal of Fracture 2000:145–68.

[59] Haager M. Bruchmechanische Methoden zur beschleunigten Charakterisierung des langsamen Risswachstums von Polyethylen-Rohrwerkstoffen. Dissertation. enLeoben, Austria; 2006.

[60] Ehrenstein GW, Riedel G, Trawiel P. Praxis der thermischen Analyse von Kunststoffen. 2nd ed. München: Hanser; 2003.

[61] Brown N, Lu X, Huang Y. The fundamental material parameters that govern slow crack growth in linear polyethylene. Plastics, Rubber and Composites Processing and Applications 1992:255–8.

[62] McGenity PM, Hooper JJ, Paynter CD, Riley AM, Nutbeem C, Elton NJ et al. Nucleation and crystallization of polypropylene by mineral fillers: relationship to impact strength. Polymer 1992;33:5215–24.

[63] Castillo LA, Barbosa SE, Capiati NJ. Influence of talc genesis and particle surface on the crystallization kinetics of polypropylene/talc composites. J. Appl. Polym. Sci. 2012;126:1763–72.

[64] Hadal R, Dasari A, Rohrmann J, Misra R. Effect of wollastonite and talc on the micromechanisms of tensile deformation in polypropylene composites. Materials Science and Engineering: A 2004;372:296–315.

[65] Delprat P, Duteurtre X, Gardette J. Photooxidation of unstabilized and HALS-stabilized polyphasic ethylene-propylene polymers. Polymer Degradation and Stability 1995;50:1–12.

[66] Gugumus F. Thermooxidative degradation of polyolefins in the solid state: Part 1. Experimental kinetics of functional group formation. Polymer Degradation and Stability 1996;52:131–44.

[67] Peterson JD, Vyazovkin S, Wight CA. Kinetics of the thermal and thermo-oxidative degradation of polystyrene, polyethylene and poly (propylene). Macromolecular chemistry and physics 2001;202:775–84.

[68] Fayolle B, Audouin L, Verdu J. Initial steps and embrittlement in the thermal oxidation of stabilised polypropylene films. Polymer Degradation and Stability 2002;75:123–9.

[69] Richaud E, Farcas F, Fayolle B, Audouin L, Verdu J. Accelerated ageing of polypropylene stabilized by phenolic antioxidants under high oxygen pressure. J. Appl. Polym. Sci. 2008;110:3313–21.

[70] Fayolle B, Audouin L, Verdu J. A critical molar mass separating the ductile and brittle regimes as revealed by thermal oxidation in polypropylene. Polymer 2004;45:4323–30.

[71] Allen NS, Hoang E, Liauw CM, Edge M, Fontan E. Influence of processing aids on the thermal and photostabilisation of HDPE with antioxidant blends. Polymer Degradation and Stability 2001;72:367–76.

[72] Oreski G, Wallner GM. Aging mechanisms of polymeric films for PV encapsulation. Solar Energy 2005;79:612–7.

[73] van Melick H, Govaert LE, Raas B, Nauta WJ, Meijer H. Kinetics of ageing and re-embrittlement of mechanically rejuvenated polystyrene. Polymer 2003;44:1171–9.

[74] Hutař P, Ševčík M, Zouhar M, Náhlík L, Kučera J. The effect of residual stresses on crack shape in polymer pipes. In: Carpinteri A, editor. Proceedings of the 4th International conference on Crack paths (CP 2012), Gaeta (Italy), 19-21 September, 2012. [Gaeta: s. n.]; 2012, p. 489–496.

[75] Poduška J, Kučera J, Hutař P, Ševčík M, Křivánek J, Sadílek J et al. Residual stress distribution in extruded polypropylene pipes. Polymer Testing 2014;40:88–98.

[76] Kazakov A. An automated method for the measurement of residual stress in melt-extruded plastic pipes. Polymer Testing 1998;17:443–50.

[77] Hutař P, Ševčík M, Náhlík L, Frank A, Kučera J, Pinter G. Numerical Lifetime Prediction of Polymer Pipes Taking into Account Residual Stress. KEM 2013;577-578:169–72.

[78] Hutař P, Ševčík M, Frank A, Náhlík L, Kučera J, Pinter G. The effect of residual stress on polymer pipe lifetime. Engineering Fracture Mechanics 2013;108:98–108.

[79] Frank A, Pinter G, Lang RW. Prediction of the remaining lifetime of polyethylene pipes after up to 30 years in use. Polymer Testing 2009;28:737–45.

[80] Frontini PM, Fave A. The effect of annealing temperature on the fracture performance of isotactic polypropylene. J Mater Sci 1995;30:2446–54.

Part VII.

Summary, Conclusions and Outlook

Summary

Pipes made from polymeric materials have proven to be reliable and efficient solutions for modern society's infrastructural needs. However, while materials steadily improve, quality assurance is and will always be still an issue. To satisfy the need for more selective and faster screening methods new test procedures are on the march. Studies have shown that various short-term tests can be used to characterize the long-term behaviour of polyethylene pipe materials in real application. Especially methods based on fracture mechanics seem very promising in this endeavour and have been pursued for over 30 years now. While improving material properties are pushing these methods also to their limits, remedy was found recently by applying different specimen geometries. For example the cracked round bar specimen, which favours plane strain state, has shown excellent consensus between fast screening tests and real application. Of course there are still several open questions like the influence of specimen preparation, which is always an issue with fracture mechanical specimens.

To address this issue, the influence of different notching techniques on fracture mechanical values, such as a critical stress intensity factor or results from J-integral testing was investigated in Publication 2. For this reason a very tough polyethylene pressure pipe grade material was examined above and below glass transition temperature. Below the transition temperature, no big differences could be found between the investigated notching techniques (razor pressing, broaching, femtolaser and fatigue). At 23°C which is quite close to actual application, differences between different procedures became apparent. Not only different notch shapes and amounts of pre-damage in front of the crack tip were found, but also fracture properties, such as R-curves via J-integral were different. This indicates that tests used later on for

lifetime estimation could very well be affected by the notching procedure itself.

Nevertheless, tools are available which can be used to measure, extrapolate and calculate lifetimes of pipes made from polyethylene (compare Publication 1). Other polymeric materials for piping are lagging behind in this regard. Materials, such as polypropylene, are still mainly characterized via internal pressure tests, which take more than a year to perform and do not give a further differentiation between materials when passed. However, clear differentiation between grades is important not only for quality reasons, but also to deliver necessary input towards further material improvements.

Therefore, it was a clear further aim of this thesis, to find methods that are applicable to polypropylene and other pipe materials and can be used as a tool to further differentiate between materials. Review of the state of art of available testing methods hinted towards several methods which might be applicable. Ultimately, the cyclic cracked round bar test was selected as the method of choice.

In a first screening of pipe grade materials, PE, PP, PB, PVC, PA and even polymers for other technical applications, such as POM and H-NBR were tested. All of the seven materials could be fractured in the desired mode of failure within days of testing. Compared to classical test methods which take more than a year, the test shows promising results within only days of testing. Fracture surface analysis via scanning electron microscope was performed for further investigation of failure mechanisms. For PE, PP and also PA clear striations, which are directly linked to temporary stopped cracks during step-wise crack growth, could be found on the fracture surfaces. PB, POM and PVC showed macroscopically smoother surfaces, with small scale yielding at closer inspection. The tested rubber showed a very smooth surface as expected of a cross-linked elastomeric material.

To further investigate the applicability of this test method and to increase feasibility, tests were also performed at different temperatures. It showed, that testing at the elevated temperature of 80°C, which is also the standard testing temperature in other pipe material standards, decreased testing times immensely for PP, while maintaining the same overall fracture behaviour.

Depending on its application, PP homopolymer, block copolymer or random copolymer are used in industry. While homopolymer and block copolymer are usually used in unpressurized applications, such as sewer or drainage pipes, random copolymers are also used for heated and pressurized pipes, e.g. heated floor pipes. It was found, that the chemical structure and morphology of different PP pipe grade materials influences the results from cyclic cracked round bar tests immensely, which corresponds well with results from classical methods. While block copolymer material could be tested at 23°C, 50°C and 80°C, homo- and random copolymer were only tested at 80°C to keep testing times within a feasible time frame. Also failure mechanisms differed greatly for the three types. Whereas block copolymer showed similar failure mechanisms as PE (e.g. striations and strands of ruptured craze fibrils), homo- and random copolymer fracture surfaces were much smoother. Respective load dependent failure mechanisms in fatigue tests were found to be roughly comparable with velocity controlled mechanisms of impact tests in literature.

For block- and homopolymer, the two failure modes of “Stage I” and “Stage II” could be identified via fracture curves, where the transition in between is clearly visible as a kink in the slope. For the very tough random copolymer, only Stage I was directly measurably. The transition to the quasi-brittle failure could be estimated by using different methods of evaluating fatigue tests. Close inspection of hysteresis and compliance development during the test showed clear signs of a change in failure mode at the lowest tested load level. Also the fracture surface at this load level showed patterns and signs of different failure mechanisms.

Another important aspect of this thesis was the characterization of the influence of accelerated artificial ageing on long-term properties of PP. A disadvantage of highly accelerated tests is that the naturally occurring ageing mechanisms of polymers in real long-term applications are neglected. For example, whereas fast test methods can characterize the quasi-brittle failure mode of a pipe grade material, they do not account for chemical or physical ageing of the polymer over the course of a real service lifetime of more than 50 or even 100 years. To further investigate this problem, talcum reinforced PP pipe material used for sewer pipe applications has been artificially aged

for 18 months at 80°C in air, which induces similar ageing to 50+ years at 20°C in real application. Conditioning at elevated temperatures accelerates chemical processes, which was used to estimate stabilizer depletion and degradation of material properties over long periods of times within feasible testing times. Several properties which are directly related to physical or chemical ageing, such as mechanical and fracture mechanical properties, as well as degree of crystallinity, melting temperature and stabilizer depletion were monitored. It was found, that stabilization of material was sufficient, to avoid any large scale chemical degradation of the material in question. Whereas mechanical properties were found to stay at a constant level even after 18 months, fracture mechanical properties, such as J-integral or results from fatigue tests were found to improve. However, enhancement of these values could be directly linked with a decrease of residual stress in the pipe walls due to temperature induced annealing, which usually does not occur in real application, with the exception of PP used at similar elevated temperatures. This change in properties due to the accelerated ageing procedure, instead of naturally occurring ageing has to be considered when performing lifetime estimations. Otherwise, calculations could lead to non-conservative results.

Conclusions and Outlook

Results presented in this thesis showed the principle applicability of the cyclic cracked round bar test as an accelerated testing method for polymer pipe grade materials besides PE and revealed the most important influences during testing. Seeing that this test just passed ISO-standardization for PE pipe materials and is discussed for other materials in pipe industry as well, data of this thesis could provide vital information for future steps in this area. Furthermore, results can be used for additional information when assessing influence of ageing on materials. However, to use the test to go into a real lifetime calculation of pipe systems made from PP, further research is necessary.

Another interesting factor would be the closer examination of the influence of specimen preparation. Similar to the study done in publication 2, where the influence of different methods has been already investigated for monotonic testing, the influence of the notching procedure on fatigue crack growth or crack growth under static loading has to be examined.

Fatigue data of different very tough PP types has been acquired in quasi-brittle failure mode which was hitherto hardly possible. Also a relationship between morphological aspects and fatigue properties could be established for unreinforced PP materials. To fully understand the failure mechanisms of various materials tested in this thesis it is advisable to further invest in an in-depth study of micromechanical processes, which occur during fracture. A clear differentiation between damage/crack initiation period and actual propagation can increase precision of estimated lifetimes. A temperature and load level dependency of the ratio of initiation and propagation was found for unreinforced PP-B during this thesis. For a clear differentiation of both

mechanisms for other unreinforced and reinforced PP materials more empirical data is still necessary to affirm results found in this thesis.

To actually calculate lifetimes based on fracture mechanical methods it is important to further characterize not only the actual fracture of the specimens, but also the exact crack kinetics which lead up to it. For unreinforced materials it should be possible to use a compliance calibration approach, similar to the procedure for PE. For highly reinforced PP, as examined in two of the publications of this thesis, it has shown that changes in compliance may not suffice to correlate with actual changes in crack length. The reason being, that even though damage is propagating through the material, compliance changes only marginally before final failure, which cannot be perceived with certainty using contact extensometers. It may be advisable to develop an additional method of characterizing damage propagation for comparison and to perform lifetime calculations.

Another important aspect which has to be addressed in the future is the exact loading situation of pipe systems. Contrary to pressurized pipes made from PE, where the main load stems from internal pressure which can roughly be seen as uniform, unpressurized pipes are primarily subjected to asymmetric loading scenarios due to soil and traffic load. This asymmetric loading situation has to be considered via finite element analysis in the future, when performing calculations. First models to combine asymmetric loading conditions and even multi-layer build ups have been developed during this thesis as well, but are still unpublished. Furthermore, statistical models would be advisable, to account for the probability of initial defects at the locations of most critical stress in asymmetric pipe loading. Besides number and location of initial defects their size is important as well. Depending on material, reinforcement and processing, initial defect sizes may vary drastically. Seeing that most existing lifetime models treat initial defect sizes as input parameters for calculations, inquiries for the different materials are almost imperative for future work.

Interesting for both industry and scientific community would also be to perform further studies with regards to mode of operation and necessary amounts of stabilizers in pipe materials. This could be done by using methods established in this thesis in combination with longer ageing times or

reduced amounts of stabilizers. In consideration of harsh price politics in pipe industry, being able to lower prices by reducing the applied amount of stabilizer whilst maintaining quality could gain a serious advantage.

Appendix

Symbols

Designation	Unit	Description
σ_{hoop}	[MPa]	Hoop stress in pipe wall
K_I	[MPam$^{0.5}$]	Stress intensity factor in mode I
t_f	[s]	Time to failure
da	[m]	Crack extension
dt	[s]	Difference in time
σ_I	[MPa]	Applied stress in mode I
a	[m]	Crack length
W	[m]	Specimen length
t_{SCG}	[s]	Time due to slow crack growth
t_{ini}	[s]	Crack initiation time
a_{ini}	[m]	Initial crack length
a_f	[m]	Final crack length
σ_{min}	[MPa]	Applied min. stress
σ_{max}	[MPa]	Applied max. stress
R	[-]	Stress ratio of $\sigma_{min}/\sigma_{max}$
ΔT	[K]	Hyteretic heating
ΔK_I	[MPam$^{0.5}$]	Difference in applied K_I during a fatigue cycle
$wt\%$	[%]	Weight percent

K_{Imax}	[MPam$^{0.5}$]	Maximum applied K_I during a fatigue cycle
r_p	[m]	Radius of plastic zone
σ_{ys}	[MPa]	Yield Stress
m	[-]	Plastic constraint factor
b		
ΔC	[N/mm]	Difference in compliance
a_c	[m]	Crack length for compliance calibration
SDR	[-]	Standard dimension ratio
$tan(\delta)$	[-]	Dampening
T_g	[°C]	Glass transition temperature
E	[MPa]	Young's Modulus
v	[-]	Poisson's ratio
J_{IC}	[N/mm]	Critical J-Integral in mode I
$J_{0.2}$	[N/mm]	J-Integral at 0.2 mm crack extension
$Pmin$	[N]	Applied minimum load
$Pmax$	[N]	Applied maximum load
K_{max}	[MPam$^{0.5}$]	Applied maximum stress intensity factor K
σ_Y^f	[MPa]	Yield stress during fatigue prenotching
σ_Y^t	[MPa]	Yield stress during testing
K_{IC}	[MPam$^{0.5}$]	Critical stress intensity factor in mode I
B	[m]	Specimen breadth
B_N	[m]	Specimen breadth after side grooving

P	[N]	Force
COD	[m]	Crack opening displacement
a_0	[m]	Crack length after notching
$P_{5\%}$	[N]	Force at intersection of adjusted initial slope for K_{IC} testing
G_{IC}	[N/mm]	Critical energy release rate in mode I
C		Coefficient for R-curve fitting
N		Exponent for R-curve fitting
$W\text{-}a$	[m]	Ligament length
M_W	[g/mol]	Molar mass weight average
MFR	[g/10min]	Melt flow rate
Y	[-]	Geometry factor for K_I specimens
K_{Iini}	[MPam$^{0.5}$]	Initial applied K_I
ΔCOD, $\Delta\delta$	[m]	Difference in crack opening displacement
ν	[1/s]	Frequency
$T_{m,on}$	[°C]	Melting onset temperature
T_m, T_{mp}	[°C]	Melting temperature (peak value)
δ	[m]	Crack opening displacement
α	[-]	Crack blunting shape coefficient
E'	[MPa]	Storage modulus
E''	[MPa]	Loss modulus
N_f	[-]	Cycle number at failure
$\Delta disp$	[mm]	Difference in displacement
M_N	[g/mol]	Molar mass number average
PD	[-]	Polydispersity
$\sigma_{I,max}$	[MPa]	Applied maximum stress in mode I

ρ	[kg/m^3]	Density
E_{cr}	[MPa]	Creep modulus
ε_{br}	[%]	Strain at break
A_G	[Nmm]	Deformation work
J_0	[N/mm]	J-Integral
J	[N/mm]	J-Integral incl. geometry change
Δa	[m]	Stable crack extension
K_n	[MPam$^{0.5}$]	Nominal applied K
$K_{c,res}$	[MPam$^{0.5}$]	K after superimposing residual stress